FORMULATION OF REACTIVE OXYGEN DELIVERY SYSTEMS

by

THOMAS JON HALL

A thesis submitted to the
University of Birmingham
for the degree of
DOCTOR OF PHILOSOPHY

Biochemical Engineering
School of Chemical Engineering
College of Engineering and Physical Sciences
University of Birmingham
December 2019

UNIVERSITY OF
BIRMINGHAM

University of Birmingham Research Archive

e-theses repository

This unpublished thesis/dissertation is copyright of the author and/or third parties. The intellectual property rights of the author or third parties in respect of this work are as defined by The Copyright Designs and Patents Act 1988 or as modified by any successor legislation.

Any use made of information contained in this thesis/dissertation must be in accordance with that legislation and must be properly acknowledged. Further distribution or reproduction in any format is prohibited without the permission of the copyright holder.

ABSTRACT

Antibiotics are vital to modern medicine, helping to protect patients from infection. However, antimicrobial resistance (AMR) is growing at an unprecedented rate, with 10 million people predicted to die annually from resistant infections by 2050.

Honey has been used for thousands of years for topical wound care applications. However, delivering natural honey as an antimicrobial can see its effects differ greatly from batch to batch. Herein, a bioengineered antimicrobial honey (SurgihoneyRO™ - SHRO) with promising antimicrobial activity was used to circumvent such issues and enable consistent dosing. The antimicrobial properties elicited from SHRO are predominantly owed to the production of reactive oxygen species (ROS), such as hydrogen peroxide (H_2O_2), by means of a water-sensitive enzymatic reaction. Much like honey, SHRO is an adherent, highly viscous product, limiting clinical use and application. This thesis aims to overcome these issues by developing a fundamental understanding of SHRO and engineering novel delivery systems that ease application, allow for *in situ* activation of ROS and maintain antimicrobial efficacy.

This work demonstrates three systems that are capable of locally delivering efficacious doses of ROS to a wound site. These systems include: 1) the formulation of ROS producing emulsions which have the ability to trigger the therapeutic generation of H_2O_2 (0.7 – 4.2 μmol g^{-1}), over 24 hour and display viscosities between 1.4 and 60.7 Pa · s at a shear rate of 4.1 s^{-1} by varying dispersed phase volumes (30-60%) and adding thickening agents. This flexibility allows for the tailoring of specific applicational mechanisms, such as that of a spray or a cream. 2) the formulation of ROS producing superabsorbent powders with a capacity to absorb up to 120.7 mL g^{-1} of water and generate 3.1-5.2 μmol g^{-1} of H_2O_2 in a 24 hour period. In addition to tackling topical infections this system also has the potential to simultaneously provide a protective environment and stimulate wound healing. 3) the formulation of an implantable ROS producing calcium sulphate bone cement capable of generating up to 0.7 μmol g^{-1} of H_2O_2 over 24 hours. In addition, this system demonstrates compressive strengths comparable to trabecular bone (32.2 MPa), highlighting it's *in vivo* suitability. Each of these formulations has been tested *in vitro* against clinically relevant, World Health Organisation priority pathogens, namely *Staphylococcus aureus, Escherichia coli* and *Pseudomonas aeruginosa.* Overall this thesis demonstrates the potential to reduce reliance on traditional antibiotics by exploiting formulation engineering to aid society in the fight against AMR.

DEDICATION

I would like to dedicate this thesis to my parents, Diane and Christopher Hall. Without whose tireless, unconditional support and delicious packed lunches, this would not have been possible. Thank you for everything you have done and continue to do, you give me the encouragement to be whoever I want to be, to do what I want to do and to pursue the endeavours I enjoy. Words alone simply cannot explain how much it has all meant to me. I truly would not be where I am today without you, I hope I have done you proud.

ACKNOWLEDGMENTS

First and foremost, I would like to thank my supervisors Dr Sophie C. Cox and Professor Liam M. Grover to whom I owe a huge debt of gratitude. I would like to thank them for their time, patience and encouragement, as well as providing me with the opportunity to pursue my interests in science. Sophie, you have always pushed me to be the best I possibly could be, you were the voice of reason, logic and understanding. Thank you for your patience and support, I will forever be grateful. Furthermore, I would like to thank the EPSRC, Matoke Holdings Ltd. and the Formulation Engineering CDT for funding this research.

I am incredibly lucky to be part of a fantastic research group, TRAILab. You are all amazing, extremely competitive and I could not have done it without you. Tom Robinson and Erik Hughes thank you for keeping me sane over the years, providing help, guidance and when needed, a distraction from science. Long live fish and chip Fridays! I would also like to thank the friends that have supported me throughout this journey. James, Nicole, Robert and Eve you have been amazing. Thank you for always understanding, making time and most importantly putting up with me. I cannot wait for our next R6 adventure.

Penultimately I would like to thank my family, my parents, grandparents, my brother and Ollie. Your unwavering support and belief in what I could achieve was incredible. I could not have asked for anymore, you're all fantastic.

My final thanks are reserved for Hannah Vaughan, you are my rock. You encouraged me to be my best, to always keep on going and not give up. You have helped me achieve something I never thought possible, you believed in me when I did not always believe in myself, you were there no matter the hour. I could not have done this without you.

CONTENTS

LIST OF FIGURES

LIST OF TABLES

LIST OF ABBREVIATIONS

AMR	Antimicrobial resistance
ATP	Adenosine triphosphate
BMP	Bone morphogenic protein
BSE	Back scattered electrons
CD	Cyclodextrin
CPC	Calcium phosphate cement
CPI	Catastrophic phase inversion
CSC	Calcium sulphate cement
CSH	Calcium sulphate hemihydrate
D:H	Diameter by height
DI	Deionised water
DMEM	Dulbecco's modified eagle medium
DNA	Deoxyribonucleic acid
E. coli	Escherichia coli
ELISA	Enzyme-linked immunosorbent assay
ePTFE	Polytetrafluoroethylene
FTIR	Fourier-transform infrared spectroscopy
G6PDH	Glucose-6-phosphate dehydrogenase
GOx	Glucose oxidase
HCD	(2-hydroxypropyl)-b-cyclodextrin
HDF	Human dermal fibroblasts
HGT	Horizontal gene transfer
HK	Hexokinase
HLB	Hydrophilic-lipophilic balance

IFT	Interfacial tension
L:P	Liquid to powder ratio
LB	Luria-Bertani broth
LVR	Linear viscoelastic region
MCD	Methylated-β-cyclodextrin
MRSA	Methicillin-resistance Staphylococcus aureus
NAD	Nicotinamide adenine dinucleotide
NADH	Nicotinamide adenine dinucleotide + hydrogen
o-DDH	o-dianisidine dihydrochloride
O/W	Oil in water
O/W/O	Oil in water in oil
P. aeruginosa	Pseudomonas aeruginosa
PBS	Phosphate buffered saline
PDGF	Platelet derived growth factor
PFA	Paraformaldehyde
PGPR	Polyglycerol polyricinoleate
PLLA	Polylactic acid
PMMA	Polymethyl methacrylate
POD	Peroxidase
RI	Refractive Index
RNA	Ribonucleic acid
ROS	Reactive oxygen species
S. aureus	Staphylococcus aureus
SE	Secondary electrons
SEM	Scanning electron microscope

SHRO	SurgihoneyRO™
SMEs	Small-medium enterprises
SPA	Sodium polyacrylate
SPAN 80	Sorbitan monooleate 80
TGF	Transforming growth factor
W/O	Water in oil
W/O/W	Water in oil in water
WHO	World health organisation
XG	Xanthan gum
XRD	X-ray diffraction

PEER-REVIEWED JOURNAL PUBLICATIONS

M.S. Dryden, J. Cooke, R.J. Salib, R.E. Holding, T. Biggs, A.A. Salamat, R.N. Allan, R.S. Newby, F. Halstead, B. Oppenheim, **T. Hall**, S.C. Cox, L.M. Grover, Z. Al-hindi, L. Novak-Frazer, M.D. Richardson, Reactive oxygen: A novel antimicrobial mechanism for targeting biofilm-associated infection, J. Glob. Antimicrob. Resist. 8 (2017) 186–191. doi:10.1016/j.jgar.2016.12.006.

E.A.B. Hughes, S.C. Cox, M.E. Cooke, O.G. Davies, R.L. Williams, **T.J. Hall**, L.M. Grover, Interfacial Mineral Fusion and Tubule Entanglement as a Means to Harden a Bone Augmentation Material, Adv. Healthc. Mater. (2018) 1–9. doi:10.1002/adhm.201701166.

T.J. Hall, J.M.A. Blair, R.J.A. Moakes, E.G. Pelan, L.M. Grover, S.C. Cox, Antimicrobial emulsions: Formulation of a triggered release reactive oxygen delivery system, Mater. Sci. Eng. C. 103 (2019) 1–10. doi:10.1016/j.msec.2019.05.020.

E.A.B. Hughes, M. Chipara, **T.J. Hall**, R.L. Williams, L.M. Grover, Chemobrionic structures in tissue engineering: self-assembling calcium phosphate tubes as cellular scaffolds, Biomater. Sci. (2020). doi:10.1039/C9BM01010F.

LIST OF PUBLISHED PATENTS (INVENTOR)

Matoke Holdings Ltd. (2018). Dual dispenser containing water and antimicrobial composition. WO 2018/091890A.

Matoke Holdings Ltd. (2018). Antimicrobial compositions. WO 2018/065608A1.

Matoke Holdings Ltd. (2019). Antimicrobial compositions and formulations releasing hydrogen peroxide. CN107847566A.

CHAPTER ONE

1. INTRODUCTION

Antimicrobials have been used for millennia in the treatment of microbial infections. There is well documented evidence of topical wound management having taken place in ancient civilisations from across the globe, including China, Egypt and Greece [1–3]. Nevertheless, infections now seen as simple and straightforward to treat, such as gastroenteritis and pneumonia, were once the number one cause of death worldwide [4,5]. Infections caused by a simple cut or transmitted through a cough or a sneeze were also often fatal. Notably in the 19th century tuberculosis, a bacterial infection that mainly affects the lungs, was solely responsible for 25% of all deaths in Europe [6].

Despite infections being a major cause of death in humans, it was not until 1676 that the existence of bacteria and microorganisms were discovered by a textile merchant, Antonie Van Leeuwenhoek, where he observed what he called 'Animalcules' through a single lensed microscope [7,8]. The conclusive link between microorganisms and infection, however remained undetected until Louis Pasteur's research into Germ theory in the mid 19th century [9]. This work laid the foundation for German physician Paul Ehrlich who noted that certain chemical dyes would stain some bacterial cells but not others [10]. With this principle in mind he concluded that substances could be developed to selectively kill bacteria without harming other cells [11]. In 1909 this led to the discovery of arsphenamine, which although difficult to deliver and highly unstable in air, was successfully used to treat *Treponema pallidum*, the bacterial

infection responsible for causing syphilis [12–14]. Arsphenamine is now regarded as the first modern chemotherapy agent [15].

Following on from the key concept of compound specificity developed in the previous century, the first antibiotic, penicillin, was discovered by Sir Alexander Fleming in 1928 [16–19]. However, as with arsphenamine, stabilisation and mass production limited early antibiotic use and it was not until the 1940's that these challenges were overcome [20–22]. At which point penicillin, '*the wonder drug*', was rolled out worldwide, changing the face of modern medicine and saving millions of lives [23,24]. Unfortunately, the euphoria surrounding this antibiotic was short lived, as by the 1950's bacterial resistance had become a significant clinical issue [25]. The discovery and deployment of beta-lactam antibiotics restored confidence and hope in medicine, however again this was short lived with resistance rapidly emerging, resulting in the first case of methicillin-resistant *Staphylococcus aureus* (MRSA) [1,26,27]. Between the late 1950's and the early 1980's there was a huge rise in the discovery and development of new antimicrobials, introducing nearly 60% of all antibiotic classes to market, in a bid to solve the problem of resistance [28]. However, with only two new classes discovered since that period, the antibiotic pipeline is beginning to dry up, and resistance is once again on the rise [29,30].

Antimicrobials are starting to fail, in what is fast becoming a global problem. Scientists in every continent on earth, including Antarctica, have reported the detection of resistant microbes [31,32]. The UK government reports estimate that by 2050, 10 million people will die annually around the globe as a direct result of antimicrobial resistance (AMR), which is more deaths than from cancer and diabetes combined [33,34]. Further worsening of the AMR crisis could have significant consequences for surgical procedures and cancer chemotherapy as it becomes too hazardous to undertake [35].

It has been demonstrated throughout history that nature has a remarkable propensity to adapt and survive. As such, observations of the natural world often serve as inspiration for scientific innovation. With the majority of current antimicrobials found in or derived from nature, and with the benefit of billions of years of evolution, it seems only logical that this approach warrants further investigation. One such area of interest is the use of reactive oxygen species (ROS) as a treatment for infection [36,37]. The antimicrobial properties of ROS are widely exploited in nature, including as part of the human body's defence system [38]. Production of ROS has even been identified as the predominant mechanism of action for certain types of antimicrobial honey [39,40]. Interestingly, the use of honey for wound care dates back to 3000 BC, and promisingly, to date no honey-resistant phenotypes have been observed in bacteria for both ROS producing honey or manuka [41]. However, being a natural product, the efficacy of honey can vary widely, this high degree of variability does not conform with the reproducibility requirements of modern day medicine [42]. Therefore, in order to harness the antimicrobial efficacy of honey, an approach to enable consistent ROS production is needed. This prompted the development of an engineered honey (SurgihoneyRO™ - SHRO) capable of generating tailorable amounts of ROS through the enzymatic oxidisation of glucose [43,44].

This thesis for the first time aims to utilise ROS produced from a bioengineered honey and formulate efficacious delivery systems for the treatment of topical infections. To achieve this, it was firstly important to understand and characterise the novel engineered honey, SHRO (Chapter 3). The knowledge developed in Chapter 3 was then used as a foundation to guide the engineering a number of systems capable of controllably releasing ROS. As seen in work by both Ehrlich and Fleming, the delivery of an antimicrobial can be a significant challenge, one which must be overcome in order to maximise the effect on society. This case is no

different, much like commercially available honey, SHRO is highly viscous and adherent, which so far has limited clinical usability and thus uptake, despite its promising efficacy. Chapters 4 – 6 are focused on engineering three distinctive SHRO delivery systems with the following objectives:

- To enhance clinically usability and expand applicational areas by enabling easy administration, such as that produced by a spray, cream, powder or injectable system.
- To ensuring that processing conditions did not reduce antimicrobial efficacy of the active SHRO.
- To add additional functionality with the aim of creating an environment that also improves wound healing.

CHAPTER TWO

2. LITERATURE REVIEW

2.1 Infection and Treatment

Infections occur due to foreign disease causing microorganisms invading host tissues, these microorganisms are commonly referred to as pathogens [45,46]. Not all microorganisms cause disease, known as probiotics these flora provide an advantageous environment necessary for human health, assisting processes such as digestion and pathogenic defence [47,48]. It is worth noting that the terms "infection" and "disease" are not synonymous; infection is the consequence of a pathogen invading a host and beginning to grow, whereas disease only occurs once an invading pathogen has impaired tissue function [49]. For disease to occur, pathogens must first gain access, invade, colonise, and cause damage to host tissues. Access is normally achieved through either natural orifices, such as the mouth or nose, or breaches in the skin that may result from a wound [50].

2.1.1 Pathogens

There are six main types of pathogens: bacteria, protozoa, fungi, helminths, viruses, and prions [51–53]. Bacteria exist as unicellular prokaryotic microorganisms, absent of membranous internal organelles such as nuclei, mitochondria or lysosomes. Genomes within bacteria are circular in nature and DNA is double stranded, replicating by means of binary fission [49]. There are a number of different types of bacteria morphology, the three most common are bacillus (rod), coccus (spherical), and spirillum (helical) [54,55]. These bacteria are then frequently categorised based on Gram staining results, which is influenced by the

structural composition of the cell wall [56]. Gram positive bacteria have a cell wall that consists of a thick layer of peptidoglycan, which helps to support the cell membrane. This peptidoglycan layer is responsible for retaining the crystal violet dye used during Gram staining, causing this type of bacteria to appear purple in colour [57]. In contrast, the cell wall of Gram negative bacteria comprises of a thin peptidoglycan layer sandwiched between an outer and an inner membrane. This thinner layer does not retain the crystal violet dye during Gram staining and therefore does not appear purple. It does however stain pink due to the use of a counterstain, such as Safranin, during the process [58].

Protozoa, like bacteria are unicellular, however differ in that they are eukaryotic in nature and do not possess cell walls [59]. Fungi are also eukaryotic organisms with rigid cellulose or chitin based cell walls and reproduce by forming spores. However, the majority of fungi are multicellular with a few exceptions, such as yeast which is unicellular [60]. Like fungi, helminths are also multicellular and are simple invertebrates with reproductive cycles including multiple stages and often requiring a host [61]. Treatment of helminth infections can be difficult since like human physiology, it is made up of differentiated tissues meaning that the drugs used in treatment are often also toxic to human cells [49,62].

In contrast to bacteria, protozoa, fungi and helminths, viruses are not actually organisms due to the fact that, they have no inherent metabolism and cannot reproduce independently [63]. Viruses contain a nucleic acid genome consisting of genetic material organised as either double stranded DNA or single stranded RNA [64]. This is then surrounded by protein and referred to as a capsid. Viruses are also often encapsulated in a lipid envelope acquired from the host cell [65]. Similarly, prions are also not classed as organisms since they are composed entirely of protein. These proteinaceous particles are normally either inherited

or transferred through infected tissue. As with other pathogens, viruses and prions cause disease by means of disrupting the normal functions of the host cell [66].

2.1.2 Pathogenic Immune Response

Not all infections require treatment as the human body's immune response is often able to detect and neutralise pathogens [67,68]. Antigens, usually proteins on the surface of the cell, stimulate the response of lymphocytes and phagocytes [69]. Lymphocytes are types of white blood cell and consist of T and B lymphocytes. T-lymphocytes attack and destroy pathogens in a specific manner while B-lymphocytes produce specific antibodies for the encountered antigen whilst also enabling memory cells to trigger a secondary immune response if encountered again [70,71]. Phagocytes destroy pathogens by means of phagocytosis, a fundamental process of the body's innate immune system that engulfs and digests foreign particles [72,73]. In contrast to lymphocytes that generate a pathogen specific immune response, phagocytes respond in the same manner irrespective of the pathogen [74]. Notably, both of these cell types utilise the production of ROS to stimulate and drive the immune response to the target site, where hydrogen peroxide is used for cell signalling (0.1-10 μM) and as an antimicrobial agent (>25 μM) [75–77].

2.1.3 Antimicrobials

Pathogens have the ability to compromise, overwhelm or evade a body's defences causing disease, this may necessitate medical intervention to prevent permanent damage, including loss of tissue function and death [78]. Antimicrobials are a group of agents with the ability to kill or inhibit the growth of microorganisms. Commonly known agents include antibacterials, antifungals, and antiparasitics. Each has the capacity to target specific microorganisms, i.e. antibacterials are only effective against bacteria [79]. Antibiotics form a

subgroup of the broader category, antibacterials, and differ by definition in regard to their source of origin. Antibiotics, originally defined as substances produced by one microorganism for the selective inhibition or eradication of another, now includes synthetically produced molecules. Synthetically produced antibiotics mimic substances formed by microorganisms in nature for the inhibition or eradication of bacteria [80,81].

2.2 Antimicrobial Resistance

Modern medicine is highly reliant on the use of efficacious antimicrobials, especially antibacterials and antibiotics [82]. However, microorganisms through mutations in chromosomal genes and by gene transfer, have rapidly developed resistance mechanisms to antimicrobials and are able to resist and, in some cases survive treatment (Antimicrobial resistance - AMR) [83]. The emergence of AMR, specifically that due to drug or multi-drug resistant bacteria, was responsible for 50% of all deaths associated with clinical infections in Europe in 2008 [84]. Given this worrying statistic, the focus of the remainder of this chapter will be largely on antibacterial and antibiotic resistant bacteria.

2.2.1 Resistance Development and Mechanisms of Action

In general, antibacterials can be delivered topically, parenterally, orally or as a suppository with dosing dependent upon route of administration and age. Antibacterials work by inhibiting cellular processes, pathways and functions, specifically antibiotics have modes of action that precisely targets one aspect of a cell's ability to survive, as can be seen in Table 2.1 [85]. Other antimicrobials, such as metal ions (silver, copper etc.) and honey, have a number of mechanisms of action affecting multiple pathways [86]. This is likely why resistance development to these types of antimicrobials is less common.

Table 2.1. The mechanism of action of common antibiotic classes. *Adapted from *Alanis.,* [87].

Mechanism of Action	Antibiotic Classes
Inhibition of cell wall synthesis	Beta-lactams
	Glycopeptides
	Cyclic lipopeptides
Inhibition of protein synthesis	Tetracyclines
	Aminoglycosides
	Oxazolidinones
	Streptogramins
	Ketolides
	Macrolides
	Lincosamides
Inhibition of DNA synthesis	Fluoroquinolones
Inhibition of RNA Synthesis	Rifampin
Inhibition of folic acid synthesis	Sulphonamides
	Trimethoprim
Disorganisation of the cell membrane	Polymyxins

Resistance to antimicrobials is a naturally occurring phenomenon and can either occur due to intrinsic characteristics of the species being treated or develop due to antimicrobial exposure. Resistance plasmids (R-factors) have even been found to be present in microbes within a pristine environment, one with no record of any previous contact with antibiotics [88]. The effects of AMR, however have been exacerbated by human intervention and is largely associated with the excessive use and misuse of antimicrobials in both healthcare environments and agriculture [89]. Every year in the USA an average of 3 million kilograms of antibiotics

are administered to patients, 13 million kilograms of antibiotics are administered to animals, and the environment as a whole is exposed to a further 15 million kilograms of antibiotics [90,91]. Exposing microbes to a multitude of antimicrobials at varying doses, promotes natural adaptation and the development of resistance.

Intrinsic resistance is a microorganisms natural ability to resist the mechanism of action of a particular antimicrobial. This could be due to inherent structures or functional characteristics of the cell [92]. An example of intrinsic resistance is observed during the use of the antibacterial triclosan, which has broad efficacy against both Gram positive and Gram negative bacteria. However, due to the additional coding of the enzyme *enoyl-ACP reductase* in members of the genus *Pseudomonas,* the mechanism of action of triclosan is inhibited [93]. Other examples of intrinsic resistance can be found in Gram negative species of bacteria. For example, the antibiotics daptomycin and vancomycin are both highly effective against Gram positive bacteria but have a reduced ability to cross the outer membrane of Gram negative bacteria, severely reducing efficacy [94,95].

In addition to fundamental intrinsic differences, microbes can also develop resistance at two different stages; at a planktonic phase and at community level [96]. Cellular resistance can occur due to gene mutation or by horizontal gene transfer (HGT) [97]. HGT is where DNA is acquired from another resistant organism not passed down as a product of reproduction [98]. This can occur by an organism up taking free DNA (transformation), plasma-mediated transfer (conjugation) or phage-mediated transfer (transduction) [99]. Community level bacterium can develop resistance to tolerate far greater stress than an individual cell. This is exemplified by a microorganism's ability to form biofilms resulting in up to a 1000 fold increase in antibiotic resistance [100]. Furthermore, planktonic and community level resistance can

become synergistic, increasing and enhancing the overall AMR of the microbes [101]. Specific mechanisms of resistance can be found in Table 2.2 and visualised in Figure 2.1.

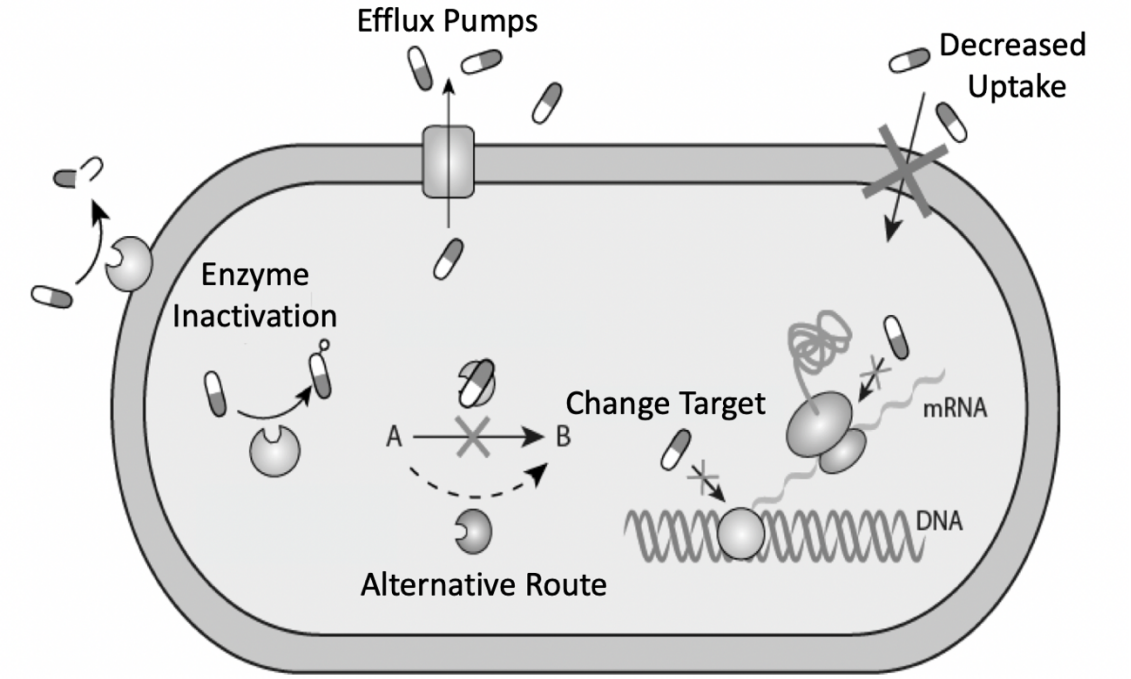

Figure 2.1. Mechanisms attributed to antibiotic resistance *Adapted from ReAct., [102].

Table 2.2. Antimicrobial resistance mechanisms.

Mechanisms of Cellular Resistance	References
Inactivation by hydrolysis or drug modification	[103,104]
Reduction of drug binding affinity by means of target alteration of target bypass	[105]
Decreasing drug permeability through the membrane	[106]
Use of efflux pumps to expel drugs from within the cell	[107]
Transfer of resistance determinants from other organisms by means of horizontal gene transfer	[108]
Mechanisms of Community Resistance	
Development of a biofilm matrix	[109–111]
Development of persister cells which are slow growing to reduce effect from antimicrobials which target bacteria which are dividing	[112]
Starvation induced stringent response as a result of limited nutrients in the biofilm also reduces the effect from antimicrobials which target bacteria which are dividing	[113,114]
Synergistic Mechanisms	
Enhanced mutation rate in biofilms	[115]
Extracellular DNA present within the biofilm encourages horizontal gene transfer	[116–119]
Low concentration of antimicrobial provides sympathetic conditions for increased mutation rates and horizontal gene transfer	[120,121]
Higher expression of cellular resistance mechanisms	[122]

Hospital acquired infections (HAI) are a major safety concern worldwide, increasing morbidity, mortality, costs and length of treatment [123]. A recent study within the European Union identified on average around 2.61 million new patients contract a HAI, while in the USA HAI's cost $28-48 billion dollars and 90,000 lives annually [124,125]. It has been shown that only 17 different microorganisms, which prevalently include *Staphylococcus aureus*, *Pseudomonas aeruginosa* and *Escherichia coli*, account for up to 87% of all HAI, of which 20% display drug or multidrug resistant phenotypes [126,127]. With resistance to antimicrobials ever increasing and the development of new antibiotics grinding to a halt, to help drive and guide development, in 2017 the World Health Organisation (WHO) published a list of 12 priority pathogens (Table 2.3) [128]. These are the pathogens most likely to cause a significant impact on human health if resistance continues to develop on its present trajectory. The pathogens are graded from critical to medium with those in the critical category resistant to multiple antimicrobials, including carbapenem a 'last resort' antibiotic, posing an imminent threat to health [128,129].

Table 2.3. World Health Organisation priority pathogens. *Derived from WHO., [128].

Critical
Acinetobacter baumannii – carbapenem resistant
Pseudomonas aeruginosa – carbapenem resistant
Enterobacteriaceae – carbapenem resistant, extended-spectrum beta-lactamase producing (ESBL)
High
Enterococcus faecium – vancomycin resistant
Staphylococcus aureus – methicillin resistant, vancomycin intermediate and resistant
Helicobacter pylori – clarithromycin resistant
Campylobacter spp. – fluoroquinolone resistant
Salmonellae - fluoroquinolone resistant
Neisseria gonorrhoeae – cephalosporin resistant, fluoroquinolone resistant
Medium
Streptococcus pneumoniae – penicillin non susceptible
Haemophilus influenzae – ampicillin resistant
Shigella spp. – fluoroquinolone resistant

2.3 Use and Development of Novel Antimicrobials

According to The Pew Trust, as of June 2019 approximately 42 new antibiotics are in Phases 1-3 of development, appearing to suggest that the drug development pipeline has been reinvigorated amid the growing concern surrounding AMR [130]. However, historic data suggests that fewer than 1 in 3 new antibiotics at this stage make it to market reducing the number of viable antibiotic treatments to approximately 14 [131]. Furthermore, no new novel mechanisms of action are currently in the pipeline with all developments being derived from or combined with existing products [132]. Analysis by The Pew Trust also suggests that many of these drugs do not target the critical priority pathogens as identified by the WHO [130,131].

The development of new antibiotics comes with inherent challenges especially in contrast to other therapeutic fields. This is mainly due to the fact that the "low hanging fruit" in the production of antimicrobial derivations and combinations has mostly been tapped, leaving only the complex, costly task of discovering novel antimicrobial mechanisms [133–135]. This expense is what has caused many large pharmaceutical companies to exit the antimicrobial market and instead focus on more profitable therapeutics [136]. To put this into perspective, a study by the London School of Economics has indicated that the typical net present value of an antibiotic is in the region of -$50 million and this is in comparison to the development and marketing of drugs for musculoskeletal conditions, which produces a net present value of $1.15 billion [137]. To further compound the problem, in order to maintain the efficacy of antimicrobial treatment and to ensure that there is always an option available, it would be necessary to develop novel mechanisms but not enter them into the market until necessary. This strategy would prevent disease causing microbes from coming into contact with the newly developed antimicrobials stopping the development of resistance towards them. However, this means creating products and essentially leaving them on a shelf, reducing profits

and eating into a products patent life span [138]. Only 4 large pharmaceutical companies (Merck & Co., Roche, GlaxoSmithKline and Pfizer) still have active antibiotic programmes leaving small-medium sized enterprises (SMEs) to fill the void in the development of new antimicrobials [139]. Popular avenues of exploration have included the re-examination of metallic ions such as silver and other natural antimicrobial compounds, including honey as a means of treating infections. These antimicrobial products have historically been critical in wound care but were superseded by the discovery and development of antibiotics. However, the emergence of antibiotic resistance has forced the re-evaluation of such compounds as both a means of treatment and the development of novel antimicrobial technologies.

2.3.1 Honey

One specific area of interest for SMEs is to exploit and develop existing antimicrobial sources to their full potential, such as that of ROS and honey [36,37]. For millennia specific types of honey have been used as a topical wound treatment without the development of AMR [140]. The composition of honey in nature is highly dependent on floral source, weather conditions, temperature, geological location and storage time but is mainly composed of three components, fructose (≈38%), glucose (≈31%) and water (≈17%) [141,142]. The remaining constituents are other sugars, acids, proteins, vitamins and minerals [143]. Inherently, endogenous water within the honey structure is bound to sugar molecules and is low in concentration, providing many of the systems physicochemical characteristics (e.g. viscosity), and inducing a high degree of osmolarity [40,144]. Being osmotic allows the honey to draw water away from organisms causing dehydration and produce an environment non-conducive to cellular activity [145]. In addition, the presence of gluconic acid further increases the antimicrobial hostility of the system, creating an environment that typically has a pH between 3.2 and 4.5 [40].

The antimicrobial effects of honey are not only due to the levels of acidity and osmolarity but also the presence of peroxide or non-peroxide components [146,147]. Non-peroxide honeys, such as Manuka are monofloral and dependant on one source of nectar, in this case from the Manuka tree [148]. Manuka honey contains compounds, such as catalase, that affect the production and accumulation of hydrogen peroxide. However, increased levels of methylsyringate, methylglyoxal and bee defensin-1 are found within the honey, which result in a strong antimicrobial effect [42,149,150]. Manuka honey is widely used in wound care with uses such as the formulation of antimicrobial biomimetic meshes as is demonstrated by Mancuso. *et al.*, [151].

More commonly within a honey system is the formation of hydrogen peroxide, which arguably provides honey with its most potent antimicrobial effect [152]. Hydrogen peroxide and other ROS are produced upon dilution of unbound water by the enzyme mediated (glucose oxidase – GOx) oxidation of glucose (Eq. 2.1) [36]. As aforementioned (section 2.1.2), in addition to its direct antimicrobial effects the presence of ROS in a wound can stimulate the immune system to respond to infective pathogens [153,154]. This immune response occurs at ROS concentrations between 5 - 250 μM [155]. Furthermore, ROS has also been found to support wound healing between 0.1 – 10 μM, specifically the processes of proliferation, differentiation, migration, angiogenesis and act as an anti-inflammatory [155–157].

$$C_6H_{12}O_6 + H_2O + O_2 \xrightarrow{GOx} C_6H_{12}O_7 + H_2O_2 \qquad \text{(Eq. 2.1)[42]}$$

2.4 Use of Reactive Oxygen Species in Wound Care

As a natural product the antimicrobial activity of honey can vary greatly. Such irregularity is not conducive to modern day medicine and one of the reasons that clinical uptake and use of honey or honey based products is limited [157,158]. Notably, neat hydrogen peroxide (H_2O_2) has previously been used in wound care to treat and prevent infection, but its use is also limited due to its fast reactivity. As such high, often cytotoxic doses (≥3%) are used in order to keep the ROS concentration above the microbicidal level for a longer, therapeutically relevant, period of time [159–161]. In contrast endogenous macrophages generate much lower local concentrations of ROS of between 10 - 1000 µM. Hyslop. *et al.,* [77] further indicates that ROS concentrations of 25 – 50 µM are sufficient to induce bacteriostasis however concentrations of up to 500 µM may be necessary to observe bacterial cell death in some organisms [162]. A review by Zhu. *et al.*, [163] therefore concluded that it would be beneficial to deliver these, lower, tailored doses of ROS and maintain these concentrations at the site of infection.

2.4.1 SHRO

In order to realise the potential use of honey as a viable antimicrobial treatment it must be capable of delivering specific and controlled amounts of ROS over a clinically relevant period of time. A novel engineered medical grade honey, SHRO, meets this realisation. SHRO is a bioengineered honey processed to enhance and deliver a specific and consistent antimicrobial effect [164]. Key *in vitro* and *in vivo* studies by Dryden, Halstead and Cooke., [165], Dryden, Milward and Saeed., [164], and Dryden. *et al.*, [166] found SHRO to be a powerful antimicrobial agent, effective at treating wounds and ulcers. SHRO has been shown to eradicate both Gram positive and Gram negative bacteria, including *Staphylococcus aureus* (*S. aureus*), *Pseudomonas aeruginosa* (*P. aeruginosa*) and *Escherichia coli* (*E. coli*). In addition, SHRO has

also been shown to be strongly efficacious against World Health Organisation priority pathogens, namely, MRSA and vancomycin-resistant *Enterococcus faecium* [43,44,167–171]. Furthermore, Halstead. *et al.,* [168] discovered that SHRO prevented the formation and reduced the seeding of biofilms.

Clinically, SHRO demonstrated an ability to prevent and treat surgical site infections as well as Hickman and vascular line infections. In all cases the use of SHRO prevented the need for the administration of antibiotics [166,172]. As aforementioned, SHRO is an engineered honey, this allows the potency to be tailored as required. This property permitted SHRO to outperform other medical grade honeys, such as Activon and Medihoney and two of the most commonly used antimicrobials in wound dressings; silver and iodine [43].

2.4.2 Mode of Action

Hydrogen peroxide and other ROS are produced from SHRO by means of an enzymatic reaction as shown in Eq. 2.1 [42]. The kinetics of this reaction can be mathematically described using the Michaelis-Menten equation (Eq. 2.2), which states that the reaction rate (V) is equal to the maximum rate achieved (V_{max}) multiplied by the concentration of the substrate [S] divided by that of the Michaelis constant (K_M) plus the concentration of the substrate [173]. As with any novel healthcare technology it is prevalent that the pharmacokinetics and mode of action are well documented [167,174]. Understanding the kinetics of the system will allow for quantification of ROS over time along with determination of production rates.

$$V = \frac{V_{max}[S]}{K_M + [S]} \qquad \text{(Eq. 2.2)[173]}$$

Molecular oxygen (O_2) is essential in the mitochondrial production of adenosine triphosphate (ATP), which provides energy. An increase in the ATP yield is necessary for the greater demand of energy required to repair tissues [39]. If that O_2 molecule has been reduced by the addition of electrons it is referred to as a ROS. Examples of ROS include the hydroxyl ion (OH^-) and radical ($\cdot OH$), the superoxide anion ($\cdot O_2^-$), peroxide ($\cdot O_2^{-2}$), and hydrogen peroxide (H_2O_2) [36].

The production of ROS at concentrations > 25 μM provides SHRO with its potent antimicrobial activity, with multiple mechanisms of action [162]. Dryden. *et al.,* [167] indicates that ROS elicits its antimicrobial action through reactions with thiol groups found in enzymes, proteins and DNA, inhibiting function. Additionally, Wang. *et al.*, [175] demonstrates that ROS can oxidise bacterial cell walls and membranes preventing transport and compromising how vital molecules interact, leading to cellular death. Furthermore, it has been shown that ROS can inhibit protein synthesis in ribosomes and disrupt electron transport (Figure 2.2) [176–178].

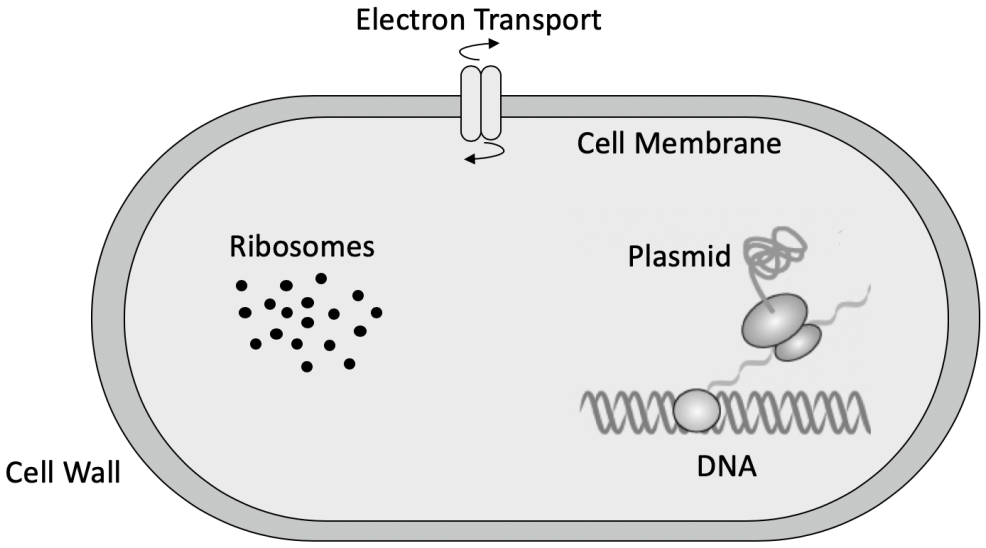

Figure 2.2. Bacterial structures and processes affected by treatment with ROS

2.5 Delivery Systems

SHRO somewhat realises the potential use of honey as a viable antimicrobial treatment. It is capable of delivering specific and controlled amounts of ROS providing, repeatable, consistent, efficacious, results and eliminates the variability associated with that of natural honey [164]. As illustrated in work by both Ehrlich and Fleming, the delivery of an antimicrobial can be a significant challenge, one which must be overcome in order to maximise the effect on society [12–14,20–22]. Much like commercially available honey, SHRO is an adherent and highly viscous product that produces ROS as a result of an enzymatic, water-initiated reaction [42], limiting its clinical usability and uptake, despite its promising efficacy.

To maximise the impact of SHRO on infection treatment, usage and clinical uptake needs to be increased. Within the healthcare setting the most prominent sites of infection are topical. The skin acts as one of the first lines of defence, breaches caused by either an accident (e.g. trauma) or from an intentional act (e.g. surgical incision) allows for the incursion of pathogens and is the leading cause of infection [179]. Topical antimicrobials therefore are commonly used both to treat infections and to act as a prophylactic [180,181]. Delivering an antimicrobial topically can offer a number of advantages to that of systemic administration, including localised, targeted delivery of antimicrobials to the specific site, which minimises systemic toxicity [179]. Common topical approaches to deliver antimicrobials or more broadly other actives, include the development of emulsions, creams and powders.

Another identified area for which the development of a SHRO delivery system could make an impact is that of implants and implantable devices. Currently 45% of all nosocomial infections are associated with the insertion of implants, of which a high proportion are resistant to treatment and extremely persistent. This can result in additional surgery and the removal of

the implant [182]. In addition to research into inherent methodologies to make the implant itself antimicrobial, auxiliary materials used in implant fixation can also be functionalised, for example antimicrobial bone cements.

To enable easy delivery of SHRO, there is a need to create alternative physical formulations with a reduction in the adhesive characteristics of SHRO. The formulation should also be able to exhibit a controllable release profile, with the aim of producing efficacious amounts of ROS (> 25 μM) for up to or in excess of 24 hours to achieve a therapeutically relevant treatment period. When designing such systems, it is important to consider the underlying mechanisms of action. In the case of SHRO, the oxidation of glucose to produce ROS is a reaction that requires water (Eq 2.1). SHRO contains 16-20% water, which is bound to sugars and is therefore not free to react [183]. As a consequence, to avoid premature production of ROS before clinical application formulations must be designed to utilise a non-aqueous vehicle. Such a formulation would enable the efficacy of the product to be maintained during storage with the aim of activating the formulation *in situ*. Furthermore, glucose oxidase denatures at temperatures greater than 55°C, therefore adding a temperature limitation to the formulation process [151].

2.5.1 Emulsions and Emulsion Formulation

Colloids are a class of soft matter materials, which incorporates multiphase systems, including emulsions [184]. An emulsion can be defined specifically as a mixture of two or more liquids that are ordinarily considered immiscible, this sees one liquid (dispersed phase) become dispersed in another (continuous phase) to form a homogenous mixture [185]. Emulsions are used widely in a diverse range of industries, including food, firefighting, polymer manufacture, photography and drug delivery [186,187].

There are two types of basic emulsions that can be formed; the first is that of an oil in water emulsion (O/W), whereby the oil forms the dispersed phase and the water is the continuous phase. The second type of emulsion is a water in oil (W/O) emulsion, in which the water is dispersed within the continuous oil phase [188]. More complex emulsions, such as multiple emulsions can also be formed, for example double emulsions that include water in oil in water emulsions (W/O/W) and oil in water in oil emulsions (O/W/O) [189,190]. It is worth noting however, that although basic notation describes an emulsion as water in oil or oil in water, it is not bound by these two compounds as it is in fact describing the lyophilic (oil) or hydrophilic (water) tendencies of that phase [191]. Such would be the case in an emulsion where SHRO forms the polar (hydrophilic) component within the system.

Emulsion Stability

Emulsions are inherently thermodynamically unstable and as a result they do not tend to form spontaneously [192,193]. In order to form an emulsion, there is an energy requirement that is normally delivered to the system through methodologies such as shaking, stirring and homogenisation [194]. Over time emulsions will phase separate in order to reduce the unfavourably high energy states associated with interfacial tension [195]. The stability of an emulsion is characterised by its ability to resist a change in properties over a period of time [196].

There are five main instability mechanisms associated with emulsions, these are; sedimentation or creaming, coalescence, flocculation, Ostwald ripening and phase inversion (Figure 2.3) [197–199]. Sedimentation, most commonly observed in W/O emulsions, occurs when the dispersed phase is denser than that of the continuous phase. Gravitational forces then

act upon the dispersed droplets forcing them to settle at the bottom of the emulsion [200]. Creaming is the opposite phenomenon to that of sedimentation; droplets rise to the top of the emulsion due to buoyancy of the dispersed phase [201]. The occurrence of sedimentation and creaming can both be described by Stokes law, a mathematical expression describing how resistive forces in viscous fluids influence the way in which a dispersed particle moves and, in such cases, the maximum velocity that can be achieved. In detail, the equation directly relates particle radius (r) to sedimentation and creaming velocities (v). Whilst also accounting for any difference between the droplet density (ρ_1), the density of the continuous phase (ρ_2) and the bulk density (η) under the effect of gravity (g) (Eq. 2.3) [202].

$$v = \frac{2r^2(\rho_2-\rho_1)g}{9\eta} \qquad \text{(Eq. 2.3)[202]}$$

Merging of two dispersed droplets to form one larger droplet is described as coalescence. This occurs due to the disruption of the interfacial film caused by the interaction of two droplets [203], which are more likely to interact when in close proximity, such as in sedimentation or creaming layers. Coalescence may also occur due to droplet collision during Brownian diffusion and over time this can greatly impact emulsion stability [203,204]. Instability can also occur due to the presence of attractive forces between droplets, referred to as flocculation. These forces may result in the droplets forming flocs (groupings of droplets), increasing the probability of coalescence but may also contribute to maintenance of droplet structure [205,206]. The development of flocculation can lead to a change in emulsion flow behaviour, which may impact delivery and dosing [207]. Ostwald ripening occurs when solids in solution crystallise, over time smaller crystals deposit onto larger crystals, which leads to a decrease in homogeneity and a destabilisation of the emulsion [208,209]. The fifth instability mechanism, phase inversion is a phenomenon that occurs when the dispersed phase of an

emulsion becomes the continuous phase or vice versa [210]. Phase inversion is widely used to formulate emulsions, with many manufacturers using this process in order to create products with increased stability and a small size distribution of droplets within a continuous phase [211]. It can occur due to the introduction of particular flows (shear induced), changing temperature, alterations in phase volumes (catastrophic phase inversion – CPI), change in pH or the addition of salts [212].

In order to increase the stability of emulsions, molecules known as surfactants or emulsifiers are used. Surfactants orientate at the interface between the two emulsion phases and reduce the interfacial tension (Figure 2.4a-b) There are four types of surfactants; non-ionic, anionic, cationic and zwitterionic (Figure 2.4c) [213]. These compounds typically have a polar (hydrophilic) head and non-polar (lipophilic/hydrophobic) tail. [199,214]. Emulsifier configurations vary, meaning they can exhibit different levels of polarity and charge. Non-ionic surfactants carry no net charge in the head group, anionic and cationic surfactants carry negative and positive charges in the head groups respectively, and zwitterionic surfactants carry both a negative and a positive charge in the head group [215,216]. With regards to topical and medical applications it is generalised that anionic and cationic surfactants produce a potent irritancy as a result of surface active properties interacting with bio-membranes and intracellular processes. Non-ionic surfactants have the lowest irritant effect and are widely used in cosmetics and medicine [217,218].

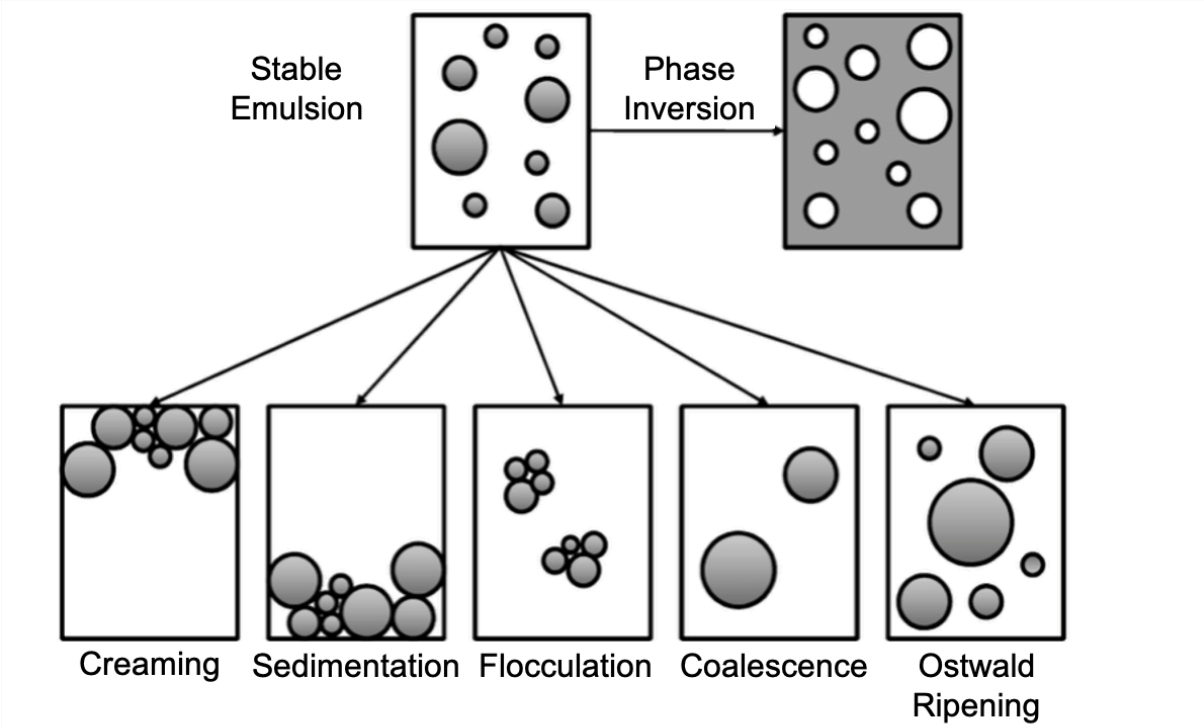

Figure 2.3. Instability mechanisms associated with emulsions * Adapted from McClements., [197].

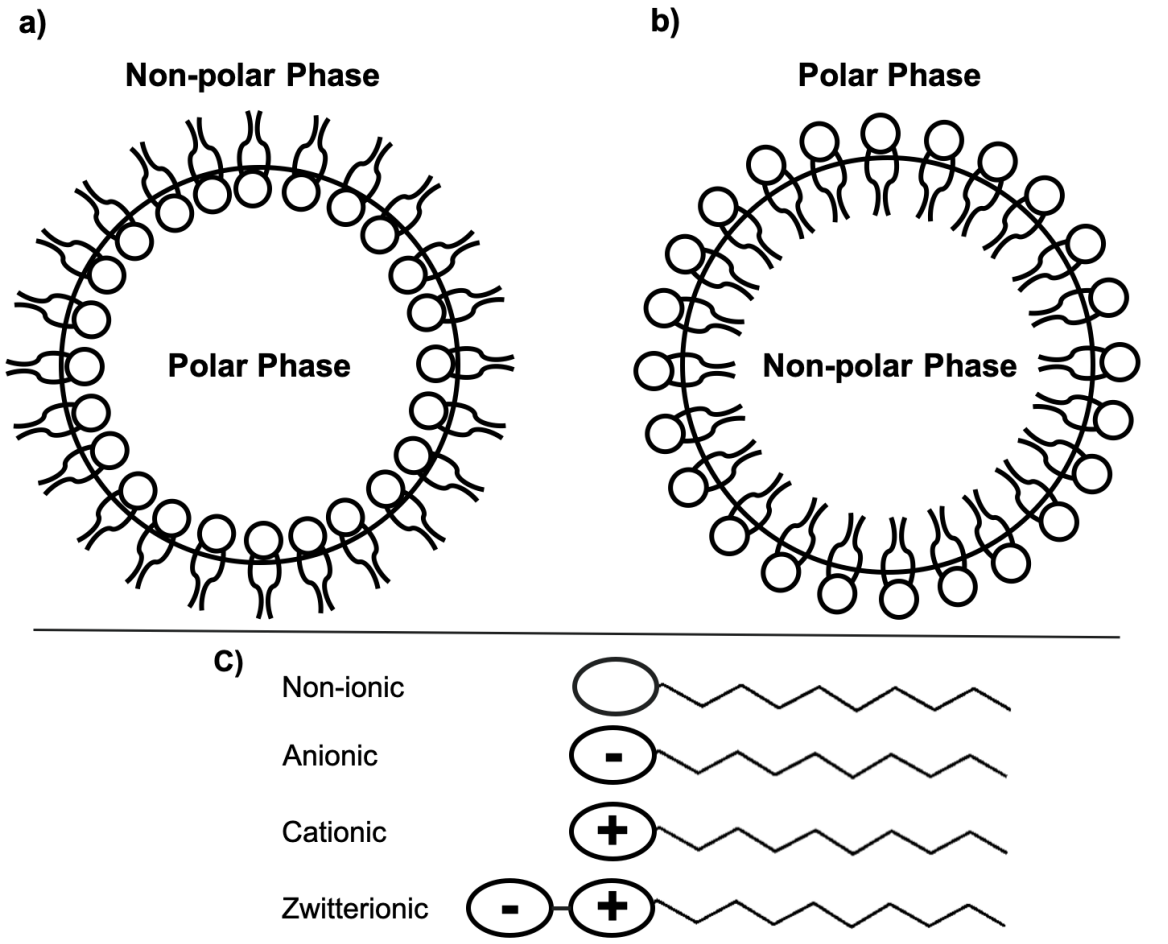

Figure 2.4. Orientation of surfactants in O/W (a) , W/O emulsions (b) and different types of surfactants (c).

The exact mechanism of a surfactant is dependent upon the type of film that is formed (Figure 2.5) [219]. Monomolecular films produce a monolayer at the interface, capable of repelling nearby droplets and preventing coalescence. Multimolecular films form multiple layers around the droplet and much like the monomolecular films provides resistance to coalescence through repulsion [199]. In addition, multimolecular films have the ability to swell, which can increase the overall viscosity of the system further reducing the likelihood of droplets merging [219]. Solid particle films can also be formed by utilising materials that can be wetted by both the polar and non-polar phase. This property results in the particles concentrating around the interface of the phases and produces a mechanical barrier to prevent coalescence [199,219].

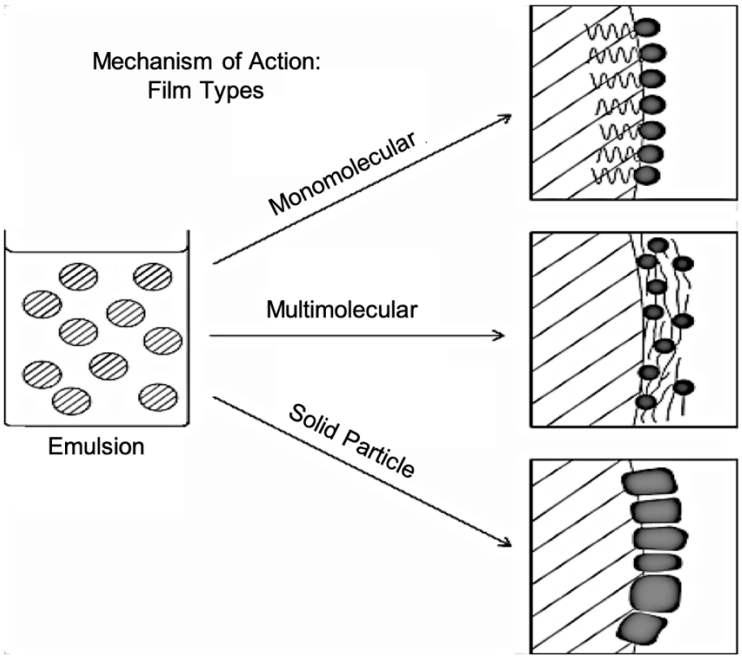

Figure 2.5. Different mechanisms of action for surfactants dependent upon type of film formed. *Adapted from Madaan. *et al.*, [219].

The overall polarity of a surfactant also varies between compounds, this variance is measured on a scale known as the hydrophilic-lipophilic balance (HLB) [220]. HLB values can range from 0 – 20 with values <10 indicative of a molecule that has greater lipophilic tendencies. HLB values >10 indicate a higher degree of polarity. Emulsifiers that have a greater polarity (HLB value >10) will in general form O/W emulsions, conversely those that are more lipophilic will produce W/O emulsions (HLB value <10) [221]. As HLB values are additive, desired HLB values can be achieved by combining surfactants. The final HLB of the mixture (HLB_m) can be calculated using Eq. 2.4 whereby $\%_A$ and $\%_B$ represent the percentage of the two surfactants in the final mixture and HLB_A and HLB_B signify the HLB values of both surfactants [222,223].

$$HLB_m = (\%_A \times HLB_A) + (\%_B \times HLB_B) \quad \text{(Eq. 2.4)[222]}$$

With regards to the formulation of a SHRO emulsion it would be advantageous to form a SHRO in oil emulsion in order to protect the SHRO from atmospheric water in storage, preventing premature ROS activation and a reduction in its antimicrobial efficacy prior to application. In order to achieve this a non-ionic surfactant, with an HLB value conducive of W/O emulsion formation should be used.

Common types of oil used in medicine and the formulation of emulsions include but are not limited to: paraffin oil, vegetable oil, olive oil and corn oil [224–226]. Paraffin oil is the by-product of petroleum distillation and has a number of medical and cosmetic applications, such as drug delivery and cream formulation [224]. Unlike most oils used in emulsion formation paraffin oil is highly refined and is made up of exclusively long, higher chain alkanes [227]. Vegetable, olive and corn oil on the other hand are composed of varying blends of different triglyceride esters and fatty acids [228]. In terms of common surfactants, as previously mentioned non-ionic surfactants have the lowest irritant effect [217,218]. As such non-ionic surfactants, including polyglycerol polyricinoleate (PGPR) and Sorbitan monooleate 80 (SPAN 80) are amongst the most commonly used surfactants in food and healthcare applications. The HLB values of PGPR and SPAN80 are 1.5 and 4.3 respectively, meaning they are both used to formulate W/O emulsions [229–232].

Emulsion Processing Variables

The formulation of a stable emulsion is crucial for both efficient storage and for the reproducible production of the final applied therapeutic and efficacious dose. However, this stability requirement is driven by a number of factors including mechanism of instability and length of time the product must remain stable for in order to maintain efficacy. Processing

parameters that can influence emulsion stability include stirring intensity, mixing time, emulsifier concentration and formulation temperature [199,233].

Emulsions are formulated through the application of mechanical energy. This energy deforms the interface between the two phases creating droplets of one phase within another [234]. The size of the droplets created is relative to the energy input into the system, with higher energies forming smaller droplets and increasing stability [235]. Examples of equipment used to deliver this mechanical energy include shakers or agitators, propeller mixers, turbine mixers, homogenisers and sonicators [199].

In addition to the amount of mechanical energy delivered to the system, another key parameter is the mixing time. According to Khan. *et al.,* [199] droplet diameter within the emulsion decreases with stirring speed and time. However, it is also noted that prolonged mixing may cause the surfactant to drop out of the interface between the two phases, due to the exerted shear forces [233].

The most efficient surfactant concentration is dependent upon both the emulsion being formed and the type of surfactant. In general, there is a concentration window for which a surfactant is effective [233]. Outside of this range the stability of the final emulsion significantly diminishes. Low concentrations of surfactant produce an unstable emulsion as droplets have a tendency to agglomerate. High concentrations of surfactant also have an adverse effect on emulsion stability [236]. This is due to an increased time for the interfacial film between the two colliding droplets to drain of the continuous phase and this leads to interfacial deformation with a greater propensity for droplets to coalesce [237,238].

Preparing stable emulsions at low temperatures is possible, however as the surface tension of most liquids decreases with an increase in temperature, more stable emulsions can often be created at higher temperatures [199]. Systems exposed to higher kinetic energies also have a greater ability to overcome the attractive forces of the continuous phase, the temperature at which this occurs is known as the critical temperature value [233].

Cream Formulation

Simply, a cream is an emulsion that contains approximately equal volumes of water and oil. Typically, creams have a thickening agent added to the emulsion in order to achieve particular rheological and sensory properties, appropriate to the target application [239]. Creams usually display non-Newtonian viscoelastic behaviour with an elastic microstructure, which pertains to a shear thinning and low yield stress response to allow for good spreadability. Upon the removal of shear forces the microstructure transiently regenerates and returns to its original viscosity [240].

Emulsion Characterisation

The evaluation of an emulsion, its properties and its characteristics can be determined by various methods (Table 2.4). These include but are not limited to methodologies that identify the emulsion type, quantify interfacial tension, determine the droplet size, characterise stability and assess the rheological properties [241].

Table 2.4. Key Emulsion Characterisation Techniques

Characteristic Assessed	Test/Methods
Type of Emulsion	Dilution Test
	Addition of Hydrophilic or Lipophilic Dyes
	Conductivity
Interfacial Tension	Tensiometer
Droplet Size	Microscopy
	Laser Diffraction
Instability Mechanisms	Visual Measurements
	Accelerated Conditions:
	Centrifuge
	Temperature
Flow	Rheology

A dilution test works on the principle that addition of supplementary continuous phase will not have an adverse effect on the emulsion. For example, diluting an O/W emulsion with water will not result in a stability change, however the addition of water to a W/O emulsion will cause the emulsion to break [242]. Dyes could also be used to determine the type of emulsion, by utilising either a lipophilic or hydrophilic dye and analysing the results under a microscope, the type of emulsion can be determined by the location of the dye [195]. Alternatively, the type of emulsion may also be assessed by measuring the conductivity. As oil is a poor conductor, an oil continuous emulsion will not allow a current to pass. The inverse is true if the emulsion that has been formed is water continuous as a current is allowed to flow [219].

Interfacial tension is a contractive property that allows the surface of a liquid to resist an external force and can be measured using a tensiometer [243]. There are different types of tensiometers such as: a goniometer that measures the interfacial tension using a pendant or sessile drop technique [244,245], a Du Noüy ring tensiometer, which pulls a submersed platinum ring out of the liquid in order to measure the surface tension [246], a Wilhelmy plate tensiometer which places a plate perpendicular to the interface and measures the force that is

exerted onto it, and a bubble pressure tensiometer that exploits the pressure generated from gas or air bubbles in the measuring liquid using a capillary of a known size [247,248].

The determination of droplet size can be commonly achieved by either microscopic examination or by laser diffraction methodology [219]. Droplet size can offer insight into the stability of the emulsion, with smaller droplets providing greater stability. However, if droplet size is found to increase over time it could indicate the occurrence of coalescence [199,219]. In addition to droplet size, stability can also be assessed by measuring sedimentation or creaming. The rate at which the dispersed phase sediments, creams or coalesces can be examined visually either under storage or accelerated storage conditions [196,249]. Accelerated conditions are often used to predict long term stability, with emulsions commonly exposed to environments such as centrifugation or an increase in storage temperature [199]. Centrifugation increases the rate of gravitational phase separation due to a difference in density. Exposing an emulsion to 15400 *g* for five hours is equivalent to the predicted annual gravitational effect the emulsion would be subjected to in storage [250]. Alternatively, stability can be assessed by increasing the storage temperature. This has a number of effects on the emulsion, however arguably the most influential is that it can decrease the viscosity of the phases and increase sedimentation rates [199,250]. Additionally, higher temperatures provide the system with a greater kinetic energy resulting in more droplet collisions and increasing the likelihood of coalescence. Both methodologies allow for long term stability predictions to be made [187].

Rheology can be used to assess the flow characteristics of an emulsion, which may be an important indicator for how easy the formulation may be to deliver or be retained once it has been applied topically. Specifically, oscillatory rheology can be used to assess the emulsions ability to store energy elastically and the viscous shear response, which allows energy dissipation

through heat [251]. These properties are known as the storage (G') and loss modulus (G") of the emulsion and they can be further analysed by means of a frequency sweep in order to describe the time dependant behaviour of the emulsion [252]. This was concluded to be an important assessment of emulsion stability by Tadros [253]. The viscosity profile of emulsions investigates the dependency of G' and G" on frequency and the effect of energy dissipation within droplets [254]. Relative values of G' and G" are known to be indicative of a change in fluid structure [255].

2.5.2 Powder Formulation

Powders are widely used in medicine to deliver therapeutic compounds, be that as tablet precursors intended for internal use or in its particulate form for external, topical, application [256]. In addition, powders can often offer greater stability than that of liquids, are more convenient and easier to apply, can be blended with other medical applications and may increase the speed of the therapeutic effect due to the large surface area [257–259]. A powder delivery system however can provide issues with storage, especially if the formulated powder is hydroscopic or has a tendency to dissolve in a humid environment, such as SHRO [260,261]. In order to achieve a powder, it is necessary to remove liquid components such as water from the system. Three methods of water separation include; solvent extraction, evaporation or freeze drying [262–264].

Solvent Extraction

Solvent extraction otherwise known as liquid-liquid extraction separates compounds based upon their relative phase solubility in polar or non-polar (organic) solvents [265,266]. There is then a net mass transfer between the two immiscible phases, usually in the direction of water (polar) to organic solvent. This process is governed by the chemical potential of the

system and a fundamental drive to adopt a state of lowest free energy [262]. The two immiscible liquids can then be isolated using a separation funnel and processed [266]. Often volatile solvents are used in order for the organic or less polar solvent to evaporate leaving behind the dry solute [267].

The process of solvent extraction has been utilised a number of times on honey such as work by Rezić. *et al.,* [268] and Jiménez. *et al.,* [269] for the extraction, separation and determination of pesticide residues within the matrix. However, Hatt. *et al.,* [270] highlights that this methodology could be problematic for the extraction of water for the purposes of creating a dry honey powder. The first issue is that of the complexity of the compositional make-up of honey, which contains lots of different compounds such as water, sugars, enzymes and minerals all with varying polarities [142,143]. This would make extraction and separation of just water difficult as some compounds may have a higher affinity to the water phase than that of the solvent. In addition to this, this methodology often utilises volatile solvents and this could pose both an issue with regards to enzyme stability, which as described in Wiggers. *et al.*, [271] can be inhibited. Furthermore, it is well known that volatile solvents are often associated with health risks ranging from topical irritation to cancer [272].

Evaporation

Another method for the removal of water could simply be to increase the temperature and force the water to evaporate. This could be achieved by the utilisation of a conventional oven or by a method known as spray drying [273], which forces liquids through a nozzle, creating droplets between 10 and 500 μm depending on the nozzle type [274] that are then sprayed into a hot chamber (typically >100°C) forcing the water to evaporate. The formation

of small droplets maximises heat transfer and therefore, the rate at which the water evaporates. The solid particles are then collected in a powder drum [275,276].

Both oven and spray drying are routinely used in formulation of honey powder for use as a sweetener or an additive in the culinary sector [277–279]. Whilst maintaining flavour, the high temperature that honey is exposed to during these procedures could fundamentally disrupt the conformity of the enzyme resulting in an inability to produce ROS [151,280]. In addition, exposure to heat may reduce the sugars in the honey to hydroxymethylfurfural [281].

Freeze Drying

In contrast to spray drying other dehydration techniques do not require high temperatures to remove water. Freeze drying, a synonymous technique to lyophilisation, is able to maintain structure and functionality by using low temperatures and low pressures to remove ice from a material by means of sublimation [282–284]. At atmospheric pressure most compounds exist in three temperature dependant phases (solid, liquid, gas), however sublimation is an endothermic process by which a compound can directly transition from solid to gaseous phase, without transitioning through the intermediary liquid phase [285,286]. This phenomenon occurs at a distinct region of a materials phase diagram, known as the triple point and identifies the maximum pressure (6.12 mbar) and temperature (0.01°C) threshold required for sublimation to occur. If these values are exceeded ice will melt into water and will transition through its liquid phase prior to vaporisation (Figure 2.6) [287].

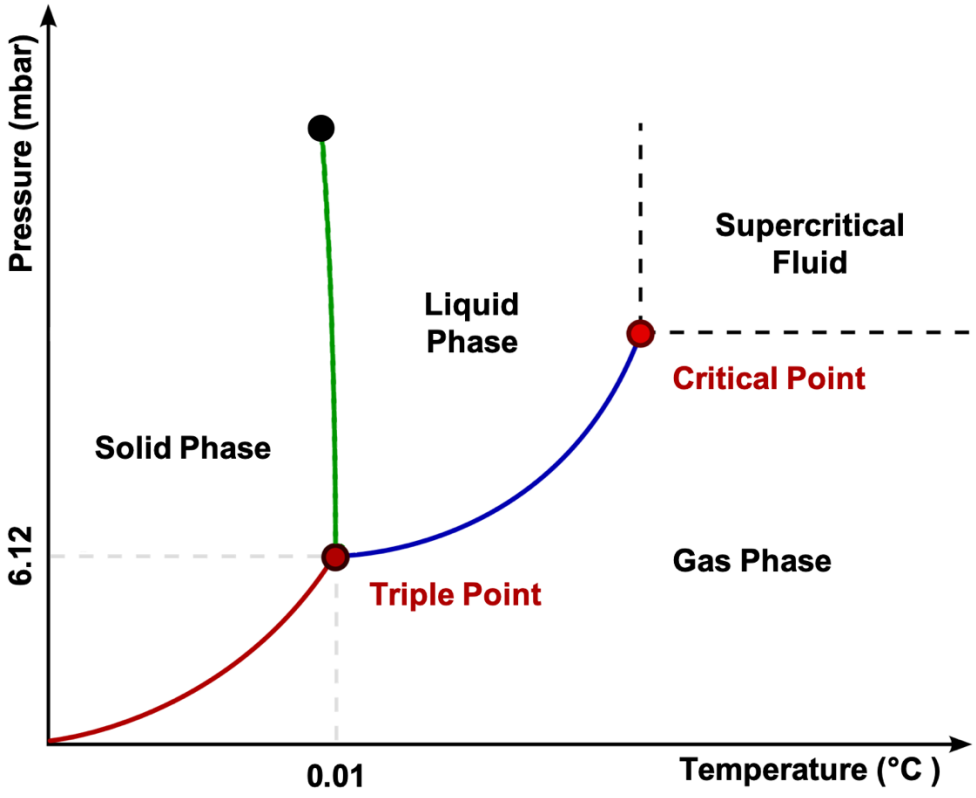

Figure 2.6. Phase diagram of water illustrating the triple point associated with sublimation.

The process of freeze drying can occur in up to four main stages; pre-treatment, sample freezing, primary drying and secondary drying [288,289]. At the pre-treatment stage the sample is prepared for freeze drying, which may involve concentrating the product or adding components to improve processing, such as drying agents to increase glass transition temperature [264].

The glass transition of a material describes the transformation from an amorphous "glassy" state into a viscous state or *vice-versa* [290]. In the context of honey, the highly concentrated sugars and organic acids produces a product characterised by low glass transition temperatures (T_g), often reported below -50°C, which provides an inherent challenge to the freeze drying process [291–294]. If the temperature of the drying chamber is higher than that

of the T_g of honey it will adhere to the chamber surface, preventing the drying process [295–297]. Due to the low T_g of honey drying agents such as starch, maltodextrin or gum Arabic are typically added in order to increase the T_g of the honey, ensuring that the T_g is not crossed within the chamber, keeping the material in it amorphous state [298]. Drying agents increase the T_g by reducing particle to particle cohesion, which reduces the water-holding capacity of the material, enabling the water content of the honey to be removed, the drying process to proceed and a powder to be formed [299–301].

When freezing the sample for drying it is important that the material is cooled below that of its triple point, to ensure that sublimation occurs in preference to instigating the melting process [302]. The speed of freezing is also a factor to consider, slow freezing forms larger crystals that allows a product to dry faster, but ice crystals can damage sensitive structures, such as enzymes. In order to prevent the formation of larger ice crystals, materials can be frozen quickly with common methods, including using a -80°C freezer or the use of liquid nitrogen [303].

Once the material is frozen, the pressure within the freeze dryer is then lowered through the application of a vacuum to initiate the primary drying phase [304]. With small amounts of heat provided, usually through conduction or radiation, the ice in the material sublimates removing up to 95% of the endogenous water [305]. This phase can often last for a number of days to ensure heating is minimised, which is particularly important for temperature sensitive formulations. Vaporised water is then condensed in a condensing chamber and allowed to solidify [264,306].

If further drying is required a secondary drying phase can be performed, this aims to remove any remaining water in the material [307]. During this phase the temperature is increased higher than that in the primary phase and the pressure is lowered further, this helps to break any physicochemical interactions that may be present, allowing any remaining water to be vaporised and removed. Following the secondary drying phase, a typical material will have a final residual water content between 1 and 4% [305].

Added Hydrogel Functionality

With the rise of chronic wounds and the morbidity associated with them, wound care is becoming increasingly important. A number of wound dressings have been developed with the aim of both protecting the wound from developing infection and also to aid the wound healing process (Table 2.5). Simply, wounds can be classified as either being dry or wet with treatments varying depending upon type. A dry wound would benefit from a moist environment in order to support the inflammatory phase and increase the rate of epithelisation [308]. In contrast a wet wound would benefit from having the amount of exudate limited to allow for autolytic debridement which further promotes successful wound healing [309].

Table 2.5 Commercially available wound dressings [309].

Dressing Type	Commercially Available Products	Characteristics
Gauze	Curity, Vaseline Gause, Xeroform	Can Dry Wounds
Films	Bioclusive, Blisterfilm, Cutifilm, Flecigrid, OpSite, Tegaderm	Retains Moisture
Hydrocolloids	Aquacel, Comfeel, DuoDERM, Granuflex, Tegasorb	Traps Fluid
Hydrogels	Carrasyn, Curagel, Nu-gel, Purilon, Restore, SAF-gel, XCell	Rehydrates Wound
Foams	3M Adhesive Foam, Allevyn, Lyofoam, Tielle	Moderately Absorbent
Alginates	Algisite, Kaltostat, Sorbsan, Tegagen	Highly Absorbent, Acts as a Haemostatic agent.
Hydrofibers	Aquacel Hydrofiber	Highly Absorbent
Skin Substitutes	Alloderm, Apligraf, Biobrane, Bioseed, Dermagraft, Epicel, EZ Derm, Hyalograft, Integra omnigraft, Laserskin, Myskin, TransCyte	Provides Growth Factors and Cytokines

As aforementioned one of the benefits of forming a powder delivery system is that it can be blended with other materials to add functionality. Given the known benefits of using hydrogels in wound care, the incorporation of a superabsorbent to facilitate *in situ* gelation may enhance treatment [310]. Hydrogels are formed of complex, hydrophilic, polymer networks with a capacity to contain and absorb large quantities of water, such as that found within biological fluids [311]. The high water content and porosity of hydrogels provides a close resemblance to that of native tissue and thus provides a foundation for the process of wound healing [312,313]. Specifically, it has been shown that the moist environment provided by a hydrogel dressing simplifies healing phases such as granulation, the repair of the epidermis, and the removal of dead tissue [314–317].

Polymers commonly used to make hydrogels include alginate, gellan gum, agar, polyvinyl pyrrolidone and polyethylene glycol, however these require crosslinking in solution to form hydrogels [318]. Crosslinking is achieved with the action of various gel specific stimuli, which can include the use of radiation, heat, pressure or chemicals [319]. Therefore, hydrogels

are often delivered hydrated for efficiency. This approach, however, is less feasible if the formulation incorporates a water-sensitive compound, such as SHRO since it would be activated and a reduction in efficacy observed prior to application.

In order to control the gelation rate of a hydrogel within a powder system, superabsorbent polymers may be exploited to rapidly draw in water. One of the most well-known superabsorbent polymers is sodium polyacrylate (SPA) [319], which is supplied as a granular solid. SPA has the capacity to absorb between 100-1000 times its own mass of water, hence its pseudonym, waterlock [320,321]. The mechanism behind SPA's preeminent ability to absorb and retain water is twofold. Firstly, SPA is a long, randomly coiled polymer formed of a backbone containing carboxylic acid groups (COOH), which are hydrophilic and thus draw water into the structure [322]. This water displaces sodium ions and this causes the coiled polymer to unravel [323]. Next, hydrogen bonds form between the COOH groups and water molecules, retaining and incorporating the H_2O molecules into its structure (Figure 2.7)[319].

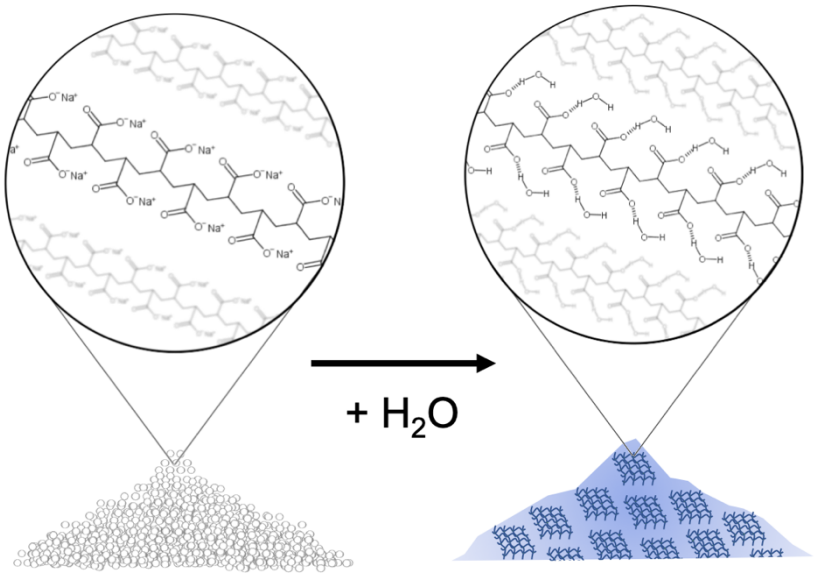

Figure 2.7. The formation of hydrogen bonds between carboxylic acid groups and water molecules on the backbone of sodium polyacrylate, which results in the formation of a hydrogel.

Characterisation of Powders

The evaluation of a powder, its properties and its characteristics can be determined by various methods (Table 2.6). These include but are not limited to methodologies that identify the morphology, size and flow of the powder particulates [324,325].

Table 2.6. Key Powder Characterisation Techniques

Characteristic Assessed	Test/Methods
Morphology/Size	Microscopy (Inc. Light and SEM)
	Laser Diffraction
	Dynamic Image Analysis
Flow	Shear Cell Rheology
	Angle of Repose
	Carr's Compressibility Index
	Hausner Ratio

There are a number of methods used to determine the morphology and size of powder particles, commonly these parameters are characterised and analysed by means of microscopy, laser diffraction and use of dynamic image analysis techniques [326–328].

Visualisation of particles can be achieved simply by use of a light microscope, however for a more detailed analysis an instrument such as a scanning electron microscope (SEM) may be used. A SEM uses an electron beam scanned in a raster pattern across the surface of the material [329]. These electrons interact with atoms on the surface and detectors then identify either secondary electrons that are emitted from excited atoms (SE) or electrons are back scattered from the electron beam (BSE), providing information relating to topography and composition [330]. A SEM microscope is capable of resolving and measuring particles down to 1 nm in size [331].

Laser diffraction methods can also be used in order to determine the size distribution of particles. This technique analyses the "halo" produced by diffracted laser light as the beam passes through a particle dispersion [332]. The angle by which the laser is diffracted is indicative of size, with the relative angle increasing with decreasing particle size. Mie theory is used in order to calculate the size distribution of the particles with the reported sizes given as the diameter of a volume equivalent sphere [325,333].

An alternative to using a laser diffraction technique is to use dynamic image analysis. In contrast to laser diffraction techniques, dynamic image analysis assesses each individual particle recording characteristic, such as sphericity and size [334,335]. Dynamic image analysis works on the principle that a camera containing specialised optics is capable of obtaining images at a rate of 500 frames per second with an exposure time of sub-nanosecond, thus capturing images of individual particles within a single frame [334]. Particles are continuously feed past the camera until a significant number have been imaged. Control over the particle flow and concentration prevents the overlap of particles within the image. The images of the particles are then analysed and evaluated using software [328,336].

The flow of a powder is also another important parameter to characterise as it is influential in the application of the product. Methodologies associated with the determination of powder flow are numerous, however shear cell rheology and the calculation of the angle of repose, Carr's compressibility index or Hausner ratio are amongst the most common methods [337].

Shear cell rheology allows for the analysis of particle cohesion within the bulk powder [338]. Instruments such as the Schulze shear cell measures the yield strength of the powder as

it begins to flow as a function of the applied stress. The flow property of the powder is then expressed and can be compared to other materials [339,340]. Other empirical measures of flow include the determination of the angle of repose [324]. This angle can be calculated using a number of methodologies such as; the tilting box method, cylinder removal method or more commonly the fixed funnel method [341,342]. The fixed funnel method allows for a known quantity of material to be added to a closed or blocked funnel. The funnel is then opened at a set height and a powder pile is formed. The angle that is formed between the horizontal plane and the sloping face of the powder is the angle of repose and can be calculated by using trigonometry [341,343]. This angle is related to the density, surface area and coefficient of friction exhibited by the powder. Materials forming a low angle of repose and, thus a flatter pile, indicate a greater propensity to flow than that which form a tall pile and hence display a high angle of repose [341]. Alternatively to the angle of repose, powder flow can be assessed by means of calculating Carr's compressibility index (CI) (Eq. 2.5) or the Hausner ratio (H) (Eq. 2.6) [343–345]. This is achieved by adding a known quantity of powder into a graduated measuring cylinder with care not to compact the powder, taking note of the volume. A mechanical tap, or method by which to reduce the interparticulate voids is then applied and the final tapped volume is measured [324]. Materials that flow poorly are characterised by the presence of large interparticle interactions and results with greater differences between the bulk and tapped densities [344,346].

$$CI = \frac{v_i - v_f}{v_i} \times 100 \qquad \text{(Eq.2.5) [343]}$$

$$H = \frac{v_i}{v_f} \qquad \text{(Eq.2.6) [344]}$$

Whereby v_i is the initial, freely settled, bulk volume and v_f is the final, compressed, tapped volume.

2.5.3 Bone Cements

Bone tissue infections, otherwise known as osteomyelitis, are a serious complication that can arise from surgery or trauma [347]. Nearly half (45%) of all nosocomial infections are associated with the insertion of implants or implantable devices, of which a high proportion are resistant to treatment and extremely persistent [182,348]. Not only can the development of osteomyelitis present a risk to life but it can also result in additional surgery and the failure or removal of the implant [347].

In addition to functionalising implants with antimicrobials, there is a need to also consider materials used for fixation of these devices since they directly interface with surrounding tissue. Bone cement is widely used to fix prosthetics into place and also to augment bone defects [349,350]. It is essential that these cements are biocompatible, resorbed at a rate that matches bone formation, cost-effective, easily stored and easy to apply within the clinical setting [351]. The three most common bone cements include; polymethyl methacrylate (PMMA), calcium phosphate (CPC) and calcium sulphate (CSC) [352,353]. PMMA cements set by means of an exothermic reaction, which can reach temperatures up to 120°C [354]. This setting mechanism limits antimicrobial loading to compounds that are thermally stable, such as gentamicin, erythromycin or vancomycin, and would not be suitable for the incorporation of SHRO [355,356]. A number of calcium salt based cement systems have emerged in recent decades providing orthopaedic surgeons with a practical substitute to that of autogenous bone grafting with the most prominent being CPC and CSC [357]. Both of these calcium cements set at lower temperatures than PMMA and are widely used in orthopaedics. CPCs may exhibit a similar composition to that of endogenous bone mineral and it has been demonstrated by Cox., *et al.* [358] that these systems may be formulated into efficacious antimicrobial carriers for use with metallic implants. However, as evidenced by Zhu., *et al.* [359], CSC provides a

much higher osseointegration potential than CPC, although faster degradation kinetics of CSC should be considered. In some cases, a combination of both cements is formulated in order to address the need of the application specific properties of a defect or implant [360,361]. The formulation of a SHRO calcium salt cement, specifically CSC is of great interest due to its wider usage and lower cost than calcium phosphate based cements [351]. It is hoped however, that any investigation would provide a contribution to knowledge that could be transferred between CSC and CPC systems.

Calcium sulphate cement (CSC)

Since its first use in 1892 CSC has been used in orthopaedics as a well-tolerated bone regenerative material, with clinical use surpassing the majority of the currently available biomaterials [362,363]. This success is due to low cost, ease of storage and deliverability [364]. CSC is formed as an injectable paste that may be easily and directly delivered to the defect site, whereby it undergoes almost complete resorption without stimulating an *in vivo* inflammatory response [351].

To create CSC raw calcium sulphate dihydrate otherwise known as "gypsum" is mined, purified and heated to remove water, in a process known as calcination [365]. The product of this process is calcium sulphate hemihydrate (CSH), otherwise known as plaster of Paris [366]. CSH can reside in one of two forms, alpha (α) or beta (β), and although chemically identical and infrequently differentiated in literature, differ in lattice structure and crystal size [351,367]. α-CSH is characterised by well-structured crystals that are larger in size than that of β-CSH, which is considered, relative to α-CSH, to be softer and more soluble [368,369].

When CSH is combined with water CSC is formed by means of a exothermic reaction which can increase the surrounding temperature to 42°C [367,370]. Often more water is added than that suggested by the molar equation equivalent to form a workable paste [351]. Excess water can however lead to a greater degree of porosity and therefore produce an exponentially mechanically weaker cement [371]. The setting of CSC progresses through a dissolution-precipitation reaction that is compatible within the physiological environment (Eq.2.7) [351]. As CSH dissolves a saturated solution of CSC is formed, which then proceeds to precipitate out by means of crystal nucleation. Both nucleation and growth continue reducing the concentration of CSC in solution allowing for further dissolution of CSH. Cycles of dissolution and precipitation further increase nucleation and growth of crystals ending in a solid CSC product [363,372].

$$CaSO_4 \cdot 0.5H_2O + 1.5H_2O \rightarrow CaSO_4 \cdot 2H_2O \qquad \text{(Eq.2.7)[351]}$$

Biocompatibility

The biocompatibility of implantable materials is essential and dependent upon the complex interactions that occur at the implant-host interface [373]. The absence of a significant host reaction to implantation is important, many studies have reported low degrees of inflammation and fast, complete resorption of CSC, when compared to other regenerative materials [363].

As an initial assessment of biocompatibility, the interactions between mammalian cells and the material substrate may be investigated. To this end Payne., *et al.* [374] cultured human fibroblast cells onto Polytetrafluoroethylene (ePTFE), polylactic acid (PLLA) and CSC, utilising polystyrene as a control. It was discovered that cells were able to migrate furthest on CSC and

in contrast to that of the other substrates maintain cellular morphology. CSC has also been shown to increase microvascular density, suggestive of an enhanced angiogenic effect [375]. Improved vascularity could also help to explain some of the biological effects elicited by CSC implants. Immunohistochemistry conducted by Walsh., *et al.* [375] identified increased localized concentrations of bone morphogenetic protein (BMP-2 and BMP-7) as well as platelet derived growth factor (PDGF) and transforming growth factor-β (TGF-β), essential biological molecules in the process of connective tissues regeneration.

In addition to considering the direct interaction of cells on biomaterials it is also important to consider the influence of any degradation products. During CSC dissolution calcium ions are released from the scaffold which may, as suggested by Park., *et al.* [376], stimulate osteoblast differentiation. In addition, Yamauchi., *et al.* [377] indicates that calcium ions may also incite proliferation and modulate osteoid synthesis. Furthermore, as osteoclasts contain calcium sensing receptors, it is theorised that activity could be regulated due to the localized concentration of calcium ions. As CSC dissolution increases local calcium concentration osteoclast activity may therefore be inhibited and thus promote bone formation [378]. pH at the implant site is also lowered as a result of the dissolution of CSC [363]. This can lead to localized demineralisation and the release of growth factors previously locked into the bone matrix. Release of biomolecules such as BMP would boost mesenchymal stem cell differentiation and thus increase bone formation [375]. The properties of CSC are summarised in Table 2.7.

Table 2.7. Properties of calcium sulphate. Derived from Thomas., *et al.* [363].

Properties
Fast resorption with a low degree of inflammation
Superior fibroblast substrate
Localised increase in calcium ion concentration potentially stimulating bone growth
Angiogenic potential
Locally altered pH stimulates bone growth
Setting kinetics can be influenced by additives

Antibiotics, vital to modern medicine are also often added to CSC with gentamicin, a broad spectrum aminoglycoside antibiotic, the most popular prophylactic since the early 1970's [379–381]. Resistance to gentamicin, like all mainstream antibiotics, is ever increasing and despite a 2002 report by Thornes *et al.* stating that it is unsuitable for use in bone cements for revision surgery due to the development of resistance, widespread clinical use has continued [382,383]. As such, the incorporation of novel antimicrobials into CSCs that provide a viable alternative to commonly used prophylactics, such as SHRO is deemed a worthwhile pursuit [382,384].

Characterisation of Bone Cements

The evaluation of a bone cements, its properties and its characteristics can be determined by various methods (Table 2.8). These include but are not limited to methodologies that identify setting time, crystal structure, chemical composition and mechanical properties.

Table 2.8. Key Bone Cement Characterisation Techniques

Characteristic Assessed	Test/Methods
Setting Time	Gillmore Needle
Crystal Structure	Microscopy (SEM)
Chemical Composition	Raman Spectroscopy
	X-ray Diffraction
Mechanical Properties	Compression Testing

The setting time of CSC is relatively fast; however, kinetics can be affected when other compounds are included. Additives, known as accelerators can increase the rate of setting or compounds termed retardants may be used to slow the reaction [351,385]. Common accelerators of the CSC setting kinetics include inorganic salts and chitosan, which can increase seed crystal density [363,386]. In contrast, biological macromolecules such as proteins have been found to retard the setting of CSC by inhibiting crystal formation and preventing the complete hydration of CSH [363,364]. This can in some cases delay the setting time drastically, and as a result pre-set CSC formulations may be preferable [351].

Setting time can be assessed using a technique known as the Gillmore needle [387–389]. Specifically, the ASTM standard C266-15 methodology measures the elapsed time between setting initiation to that at which no indentation, by a needle of specific weight, can be detected upon the cement allowing for the determination of the initial and final setting times [390]. Furthermore, cement fragments may be analysed by SEM (section 2.5.2) to evaluate the interconnected crystal structure with individual units assessed for size and arrangement [391,392].

Raman spectroscopy and X-ray diffraction (XRD) are two techniques commonly used to determine the chemical composition of a material [393]. Exemplified in work by Hughes., *et al.* [391] and Prieto-Taboada., *et al.* [394] both Raman spectroscopy and XRD can be used to

identify and quantify the phases present in CSC. Raman spectroscopy works by scattering and detecting light [395]. By focusing a high intensity laser on a material, it is possible to cause light scattering. While the majority of the light detected will be of the same wavelength used as the source (Rayleigh scatter) some will have been scattered, inelastically, at a different wavelength, characteristic to that of the material (Raman scatter) [396,397]. The different wavelengths detected are compiled to form a Raman spectrum whereby peaks are specific to that of molecular bond vibration, groups of bonds and structure [398]. In comparison XRD exploits the elastic scattering of X-ray photons by atoms in a lattice to measure the constructive interference of a monochromatic beam and produce a diffraction pattern [399,400]. Each diffraction pattern is determined by atomic positions within the planes of the lattice and hence XRD provides a fingerprint of a material, allowing for the identification of phases to occur [401,402].

Given the mechanical role of skeletal tissue it is important to characterise the behaviour of bone cements under loading. In order to characterise the mechanical properties of a cement, compression testing is typically employed to determine elastic and plastic deformation, compressive strength, and Young's modulus [403,404]. This methodology determines a materials behaviour under increasing compressive force until failure occurs [405,406]. Material deformation during loading is recorded and the compressive stress and strain plotted (Figure 2.8) [407]. This information can be used to identify the maximum stress a material can sustain before fracture (compressive strength) [406]. The strength of a bone depends on the region in which it is located for example human trabecular bone harvested from the mandible (0.2 - 11 MPa) and femoral head (3 - 8 MPa), are substantially lower than that of compact load bearing cortical bone (110 MPa) [408–410]. Young's modulus (E) can also be calculated from the stress-strain curve by dividing the uniaxial stress (σ) by the strain (ϵ) (Eq.2.8) [411]. This describes the

elastic component of the compound by measuring a materials ability to withstand changes in length under compression.

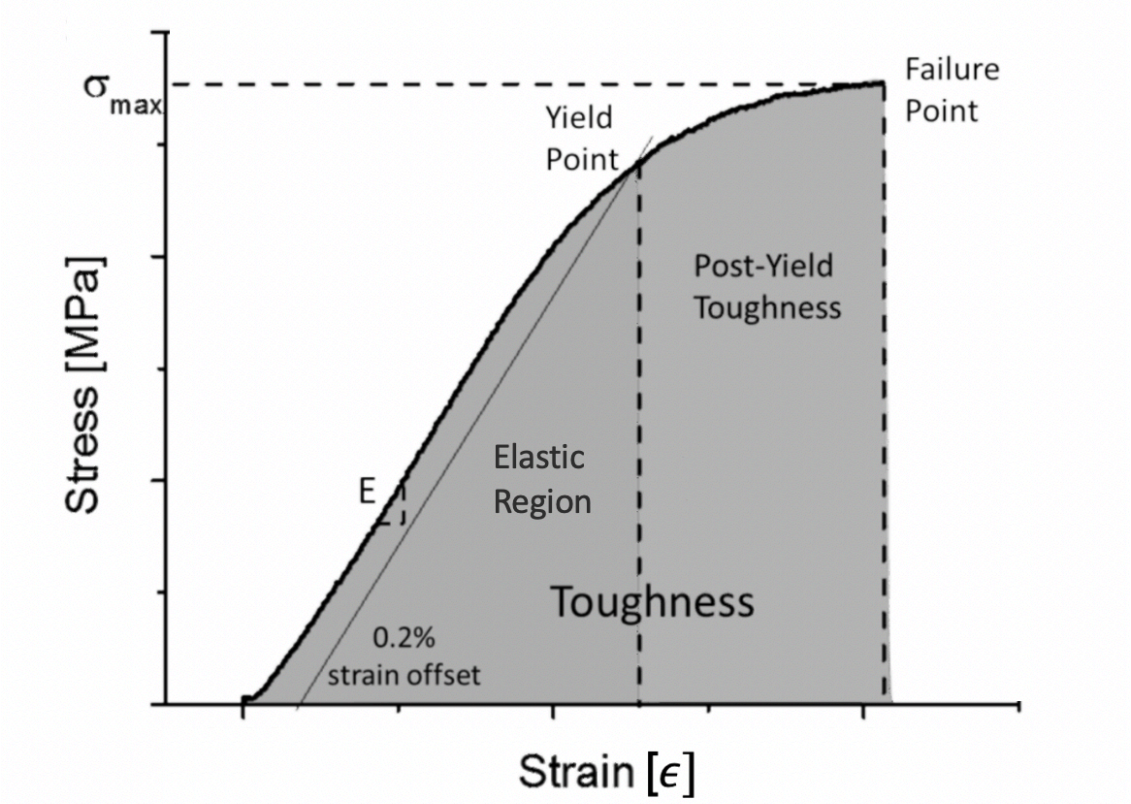

Figure 2.8. An Example Stress-Strain Curve of Bone Undergoing Compression Testing *Adapted from Unal. *et al.*, [412]

$$E = \frac{\sigma}{\epsilon} \quad \text{(Eq.2.8)[411]}$$

CHAPTER THREE

3. FUNDAMENTAL ANALYSIS OF SURGIHONEYRO™ COMPOSITION AND ENZYME KINETICS

3.1 Introduction

With annual death tolls from AMR predicted to be greater than cancer by 2050, research into new antimicrobials and methods to more effectively deliver existing compounds are crucial to maintaining current quality of life [33,92,384]. The increasing difficulty and costs associated with the discovery of novel antimicrobials, however, means that there are few new compounds being developed [413,414]. In an effort to fill this gap researchers are looking for inspiration in natural materials. The diverse roles of ROS in the body, including in response to infection and wound healing, has attracted much attention [154]. However, the fast reactivity of ROS, such as hydrogen peroxide means high doses must be used to stay above the microbicidal level for a therapeutically relevant period of time [163]. To more effectively utilise ROS a mechanism by which to stabilise and controllably release lower doses is required.

Production of ROS is a mechanism by which certain honeys are prevented from spoiling [39]. ROS in honey is produced by the water sensitive enzymatic oxidation of glucose (Equation 3.1). The levels of H_2O_2 produced via this reaction is wholly dependent upon honey composition, which varies according to floral source, weather conditions, temperature, geological location and storage time [415–417]. An average honey is composed of three main components, fructose (≈38%), glucose (≈31%) and water (≈17%). The remaining constituents

are other sugars, acids, proteins, vitamins and minerals [142]. Inherently, endogenous water within the honey structure is bound to sugar molecules and is low in concentration, providing many of the systems physicochemical characteristics (e.g. viscosity).

$$C_6H_{12}O_6 + H_2O + O_2 \xrightarrow{GOx} C_6H_{12}O_7 + H_2O_2 \quad \text{Eq. 3.1[42]}$$

In order to realise the potential use of honey as a viable antimicrobial treatment, a product capable of delivering specific and controlled amounts of ROS over a clinically relevant time period is needed. As an engineered medical grade honey, SHRO meets this realisation and promising *in vitro* and *in vivo* evidence has been collected which demonstrates the production of ROS and its effects, at concentrations of 250 µM over a 24 hour period [43,44,167–170]. This degree of potency, within the range of that produced by endogenous macrophages is capable of stimulating a systemic response while also inducing bacteriostatic and bactericidal effects [77,155,162].

However, despite the engineered ability of SHRO to produce ROS *in situ*, which circumvents the issues related with batch to batch variation of naturally derived honeys, it is still inherently viscous and adherent. Thereby to realise the potential of SHRO as an alternative to conventional antibiotics there is a need to formulate it into different physical structures that are optimised to release clinically relevant ROS concentrations [418]. Before this formulation challenge may be tackled, it is critical to develop a fundamental understanding of SHRO and the mechanism by which it is able to produce an antimicrobial effect.

Hydrogen peroxide, such as that produced enzymatically from SHRO (Eq. 3.1), can be used as an oxidising agent [419]. By exploiting the chemistry of o-dianisidine it is possible to

catalytically reduce hydrogen peroxide to water using a peroxidase enzyme. This produces an oxidised form of o-dianisidine (Eq. 3.2), which has a strong absorbance at 500nm [174,420]. By monitoring the change in absorbance at this wavelength as the reaction progresses the kinetics of SHRO specific glucose oxidase can be studied. Specifically the kinetics of this reaction can be mathematically described using the Michaelis-Menten equation (Eq. 3.3) that states the reaction rate (V) is equal to the maximum rate achieved (V_{max}) multiplied by the concentration of the substrate [S] divided by that of the Michaelis constant (K_M) plus the concentration of the substrate [173].

$$H_2O_2 + o\text{-}dianisidine \xrightarrow{POD} oxidised\ o\text{-}dianisidine + H_2O \qquad \text{Eq.3.2 [174]}$$

$$V = \frac{V_{max}[S]}{K_M + [S]} \qquad \text{Eq. 3.3 [173]}$$

As aforementioned honey is a highly saturated sugar solution that contains a large variety of additional compounds [142]. Arguably, for the purpose of developing an antimicrobial effect through the production of hydrogen peroxide, the most important compounds are glucose, glucose oxidase and water [42]. Hydrogen peroxide can be assessed fluorospectrometrically by using a peroxidase substrate, which reacts with hydrogen peroxide in a 1:1 stoichiometry to generate resorufin, a highly fluorescent molecule [421]. In contrast, to assess glucose concentration, adenosine triphosphate (ATP) is used to phosphorylate glucose in a reaction catalysed by hexokinase (HK) [422]. In the presence of nicotinamide adenine dinucleotide (NAD) the reaction product, glucose-6-phosphate is then oxidised to form 6-phospho-gluconate in a further reaction catalysed by glucose-6-phosphate dehydrogenase (G6PDH). This oxidation process reduces NAD to an equimolar amount of nicotinamide

adenine dinucleotide + hydrogen (NADH), this proportionality therefore directly relates to the concentration of glucose present and is measured by means of absorbance (Eq.3.4) [423,424].

$$Glucose + ATP \xrightarrow{HK} Glucose\text{–}6\text{–}Phosphate + ADP$$

$$Glucose\text{–}6\text{–}Phosphate + NAD \xrightarrow{G6PDH} 6\text{–}Phosphogluconate + NADH \qquad \text{Eq. 3.4[424]}$$

Further to the enzymatic investigations proposed thus far, refractometry can be used to investigate the composition of SHRO. Refractometry measures the refractive index of the material and this in turn can inform on the concentration of dissolved substances within a material [425]. With specific reference to that of honey, refractometry may be used to assess total water and sugar content [426,427].

This chapter aims to elucidate the enzyme kinetics of SHRO, characterise its chemical composition and assess efficacy *in vitro* as well as any cytotoxicity against human dermal fibroblasts. By better understanding the performance of SHRO this will help to guide the work conducted in Chapter 4-6, which focus on formulating new, efficacious, easy to deliver systems.

3.2 Materials and Methods

3.2.1 Enzyme kinetics

Peroxidase (POD – Sigma Aldrich, UK) and glucose oxidase (GOx – Sigma Aldrich, UK) enzyme stock solutions at concentrations of 125 and 500 units/mL were prepared in line with the definition that 1 unit is defined as the amount of the enzyme that catalyses the conversion of 1 micro-mole of substrate per minute. In addition, 50 mM sodium acetate buffer was prepared (Fisher Scientific, UK)

100 mL of buffer solution was then oxygenated, and pH adjusted to 6, unless specified, using 1 M hydrochloric acid (Sigma Aldrich, UK) or 1 M Sodium hydroxide (Sigma Aldrich, UK). Making sure to protect from light, 10 mg of o-dianisidine dihydrochloride (o-DDH - Sigma Aldrich, UK) was dissolved in 4 mL deionised (DI) water of which 2.68 mL of o-DDH solution was added to 97.32 mL of sodium acetate buffer solution to form a 0.21 mM o-DDH solution.

Separately 20 mL of β-D-(+) glucose solution in DI water (0.02-0.14 M - Fisher Scientific, UK) was prepared. 50 μL GOx stock was then added to 950 μL of DI water to create a 25 unit/mL solution. Immediately before use 96 mL of o-DDH solution was combined with 20 mL of glucose solution to form the "*reaction cocktail*" and pH adjusted where necessary. In addition, 480 μL of POD stock solution was added to 520 μL DI water to prepare a 60 purpurogallin units/mL solution. Furthermore, 20 μL of 25 unit/mL GOx solution was combined with 980 μL DI water to create a 0.5 units/mL GOx solution. Upon completion of these steps, each component was pipetted into a 96 well plate as indicated in Table 3.1 and mixed well. Wells containing SHRO (Matoke Holdings Ltd., UK) were treated with the same components as the blank controls owing to the fact that GOx was already present in the

formulation. Each variable was run in triplicate. Absorbance (A_{500}) was recorded every 30 seconds for 6 minutes and the maximum linear rate was obtained over a minimum of a 1 minute period and a minimum of 4 points as detailed in Figure 3.1.

Table 3.1 Well plate component quantities for the kinetic determination of glucose oxidase behaviour.

	Test Components (μL)	Blank Components (μL)
First add:		
Reaction Cocktail	93.6	93.6
POD Solution	3.2	3.2
DI Water	0.0	3.2
Then add:		
Glucose Oxidase	3.2	0.0

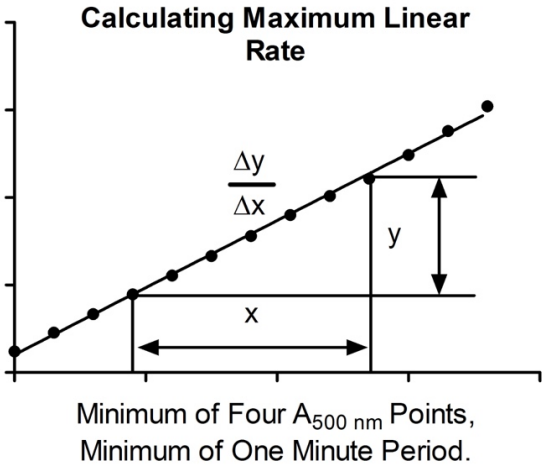

Figure 3.1. Calculating the maximum linear rate of an enzymatic reaction using a minimum of four points over a one minute period.

3.2.2 Glucose assay

A glucose (HK) assay kit (Sigma Aldrich, UK) was used to determine glucose concentration in SHRO samples. The manufacturer's instructions were followed, briefly; the glucose assay reagent was prepared with 1.5 mM NAD, 1.0 mM ATP, 1.0 unit/mL hexokinase, 1.0 unit/mL glucose-6-phosphate dehydrogenase reconstituted in 20 mL of water. 10 µL of sample was added to 1.0 mL of glucose assay reagent and incubated for 15 minutes at room temperature (20 ± 1°C). Sample and reagents blanks were also prepared in the same manner, replacing the glucose assay reagent and samples volume respectively with identical volumes of deionised water. This allowed for the calculation of the total blank absorbance value by the addition of the absorbance values pertaining to the sample blank and reagent blank. Each variable was run in triplicate with absorbance measured at 340 nm against deionised water and glucose concentration calculated using Eq. 3.5, whereby the change in absorbance (A_{Test}-$A_{Total\ Blank} = \Delta A$), total assay volume (TV), molecular weight of glucose (180.2) and dilution factor (F) used in sample preparation are multiplied together. This value is then divided by the multiplication of the millimolar extinction coefficient of NADH at 340 nm (ε - 6.22), light path (d – 1cm), samples volume and the conversion factor from µg to mg (1000).

$$mg\ glucose\ mL^{-1} = \frac{(\Delta A)(TV)(Molecular\ Weight\ of\ glucose)(F)}{(\varepsilon)(d)(SV)(\mu g\ to\ mg\ conversion\ factor)} \quad \text{Eq.3.5}$$

3.2.3 Refractometry

0.5 mL of sample was added to the prism surface of an ORA-3H refractometer (Kern & Sohn GmbH, Germany). Using the prism cover the sample was spread evenly over the entire surface and excess wiped away. The device was held horizontally for 30 seconds to allow for optimal temperature equalisation between the samples and the refractometer, focus adjusted, and measurements read. All samples were run in triplicate.

3.2.4 Zone of inhibition assay

Luria-Bertani (LB) broth (Sigma Aldrich, UK) and LB broth with agar (Sigma Aldrich, UK) were prepared in distilled water to concentrations of 20 g/L and 35 g/L, respectively. Both were then sterilised in an autoclave for 20 minutes at 121°C under 100 kPa of pressure. Overnight cultures of *Staphylococcus aureus* (*S. aureus* - ATCC 29213), *Escherichia coli* (*E. coli* - MG1655) and *Pseudomonas aeruginosa* (*P. aeruginosa* - NCTC 13437) were prepared in 5 mL of LB broth inoculated with one bacterial colony. Using an Evolution 300 UV-VIS spectrophotometer (Thermo Scientific, UK) at 600 nm the optical density of each overnight culture was measured and diluted to 0.04. LB broth with agar was used to form plates, which were then inoculated with bacteria. Using a 10 mm sterile borer, wells were created in the center of the inoculated agar. 250 µL of either SHRO tube (100, 50, 5, 0.5% v/v) or H_2O_2 (3, 0.3, 0.03, 0.003% v/v) was added to each well and then incubated at 37°C for 24 hours. The zones formed from inhibited bacterial growth were then measured using a ruler, and the bore hole diameter deducted. Each SHRO tube concentration and bacterial strain were run in triplicate.

3.2.5 Human dermal fibroblast culture and cell viability

It was important to assess the effects of SHRO tubes and control H_2O_2 concentrations on mammalian cell behaviour. Human dermal fibroblasts (HDF - ATCC Cat. PCS-201-012; Passage number 8) were cultured in Dulbecco's modified eagle medium (DMEM - Sigma Aldrich, UK) supplemented with 10% fetal bovine serum (Sigma Aldrich, UK), 1% w/v penicillin/streptomycin (Sigma Aldrich, UK), and L-glutamine (Sigma Aldrich, UK). All cultures were allowed to attach to the well plate for 24 hours, incubated at 37°C with 5% CO_2. Well plates were initially inoculated with 5 x 10^4 cells/mL per well for 96-well plates. After 24 hours DMEM media was replaced with DMEM containing either SHRO from tubes at

concentrations of 50, 5, 0.5, 0.05, 0.005 and 0.0005% or H_2O_2 at concentrations of 3, 0.3, 0.03, 0.003, 0.0003 and 0.00003%. Well plates were then incubated at 37°C with 5% CO_2 and media changed on days 3 and 7.

Cell viability was assessed on days 1, 3 and 7 using a live/dead assay (Thermo Fisher, UK) following the manufacturers protocol. Briefly, cells were seeded in a 96-well plate and treated with SHRO or H_2O_2 containg media in triplicate. At each time point, media was removed from the cells and then washed with phosphate buffered saline (PBS). Dyes were then added, and the well plate was incubated in darkness for 15 minutes at room temperature. The dye solution was removed, and PBS used to wash the cells that were then fixed with 4% paraformaldehyde solution (PFA – Sigma Aldrich, UK). Fluorescent images were then acquired using an Invitrogen EVOS M5000 microscope (Thermo Fisher, UK). Each sample was run in triplicate.

3.2.6 Hydrogen peroxide assay

A fluorescent assay kit (Sigma Aldrich, UK) was used to determine hydrogen peroxide release from the different SHRO samples and concentrations. Prior to testing a calibration curve was created using hydrogen peroxide standards 10, 3, 1, 0.3, 0.1, 0.03, 0.01 and 0 µM (Figure 3.2). The manufacturer's instructions were followed, briefly the following standard solutions were made: a master mix containing 50 µL red peroxidase substrate, 200 µL of 20 units/mL peroxidase, 4.75 mL assay buffer, and hydrogen peroxide standards between 10 µM and 0 µM.

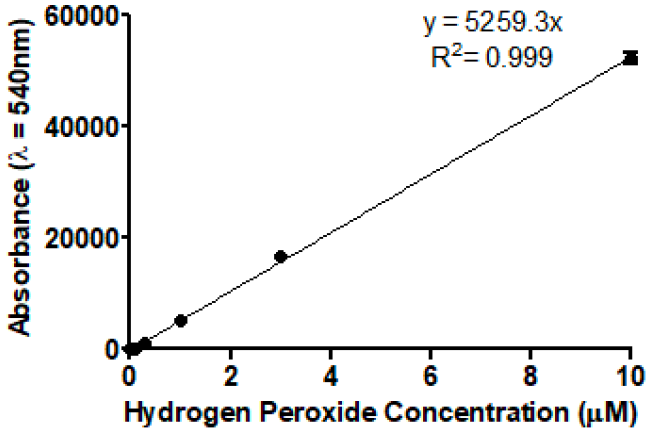

Figure 3.2. Calibration curve of absorbance measured at λ_{ex} = 540nm/λ_{em}= 590nm to determine hydrogen peroxide concentration.

50 µL of sample or standard was then added from each time point to separate wells and 50 µL of master mix was added (Figure 3.3). Wells were mixed, protected from light and incubated at room temperature for 30 minutes. The fluorescence intensity was then measured (λ_{ex} = 540nm/λ_{em}= 590nm) using a Tecan Spark plate reader (Tecan Trading AG, Switzerland). Each SHRO concentration was tested in triplicate.

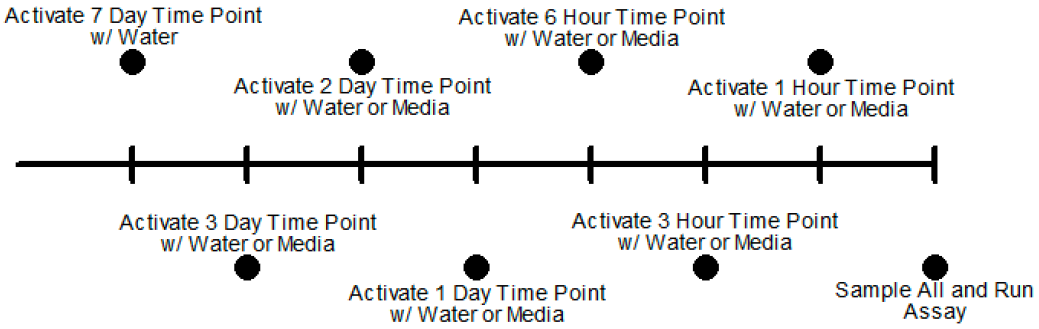

Figure 3.3 Experimental timeline showing activation of samples for different time point converging on t = 0 when the assay was run.

3.2.7 Statistical analysis

GraphPad Prism® 5.0 software was used to perform statistical analysis. T-tests were used to determine significance whereby values of $p < 0.05$ were considered significant and p values indicated as follows $p < 0.05$ (*), $p < 0.01$ (**), $p < 0.001$ (***). Data is presented throughout as mean ± standard deviation.

3.3 Results

The production of hydrogen peroxide with changing glucose molarities was investigated using enzyme kinetics (Figure 3.4a). Glucose at concentrations of 0.02, 0.06, 0.1 and 0.14 M utilising 0.5 units/mL GOx under the standard conditions of pH 6 and 26°C displayed an increasing Vmax with rising glucose concentration. However, at a glucose concentration of 0.1 M and above, the enzyme becomes fully saturated with substrate and the rate of hydrogen peroxide production plateaus, with absorbance measured at a constant rate of 0.00094 s^{-1} (Figure 3.4b). The effect of changing glucose oxidase concentration on kinetics was also explored. Glucose oxidase at concentrations of 0.25, 0.5 and 1 unit/mL were assessed at a glucose concentration 0.1 M under standard conditions (Figure 3.4c). As expected, it was found that Vmax increases proportionally (R^2 = 0.994) with increasing concentrations of glucose oxidase (GOx) (Figure 3.4d).

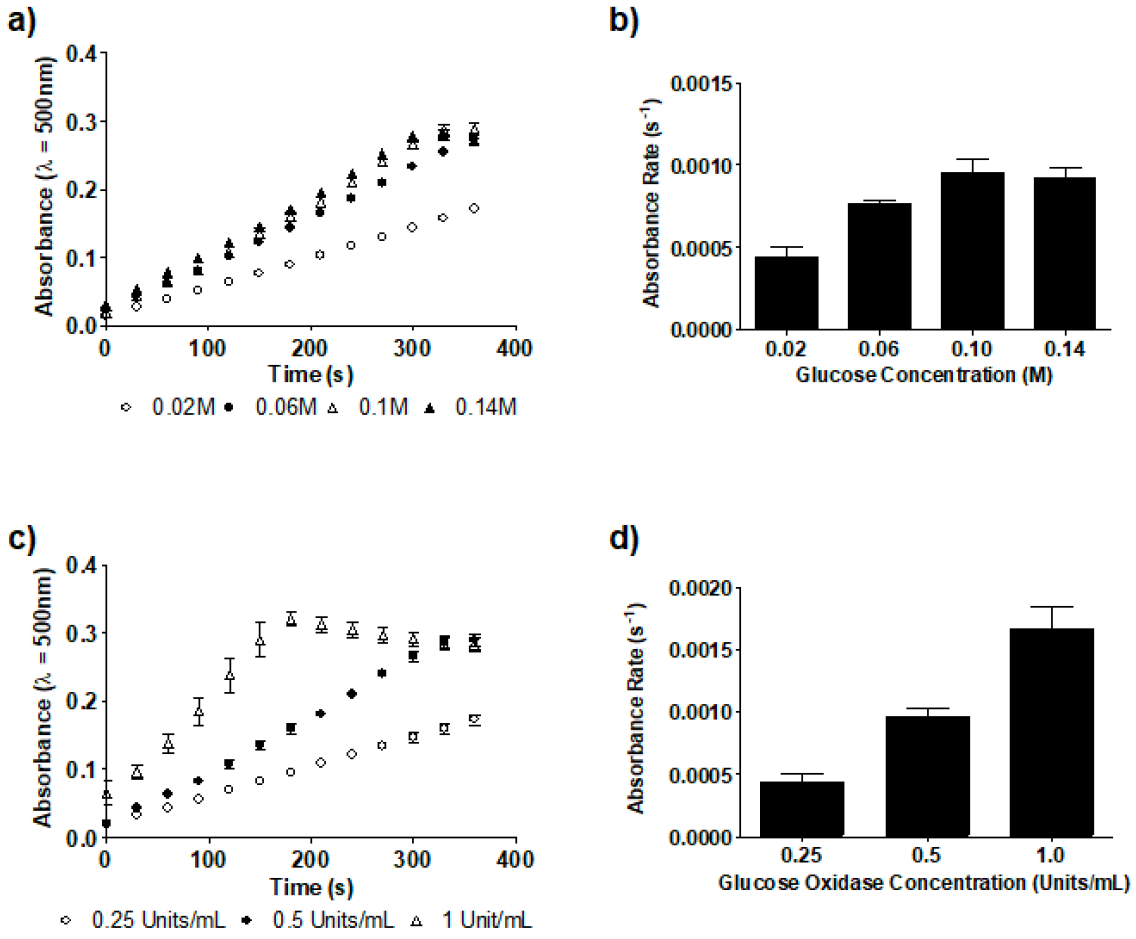

Figure 3.4. Effect of glucose concentration on hydrogen peroxide production (a) and rate of production (b) with 0.5 units/mL GOx in solution. Effect of glucose oxidase concentration on hydrogen peroxide production (c) and rate of production (d) utilising 0.1 M glucose. All solutions were adjusted to pH 6 and a temperature of 26°C. n=3, error bars represent standard deviation.

The effect of changing pH values between 4 and 8 on the enzyme kinetics of the reaction was also explored (Figure 3.5a). It was observed that as pH values rise above 4, Vmax increases and peaks at a pH of 6 with an absorbance rate of 0.00094 s^{-1}. A further increase in pH reduced the rate of reaction with a pH of 8 displaying a 62% slower absorbance rate of 0.00036 s^{-1}. An optimal working range therefore is identified between pH values 5 and 7, producing absorbance rates of 0.00092 and 0.0009 s^{-1}, respectively (Figure 3.5b). As peak performance was obtained

by reactions carried out at pH 6, further experiments were carried out using buffer solutions adjusted to this pH. The effect of temperatures between the range of 26 and 40˚C were also tested (Figure 3.5c). It was found that reactions carried out at these temperatures had no significant impact on the rate of reaction (Figure 3.5d). Therefore, further experiments were carried out at 26˚C in line with the working temperature of the plate reader used to record absorbance.

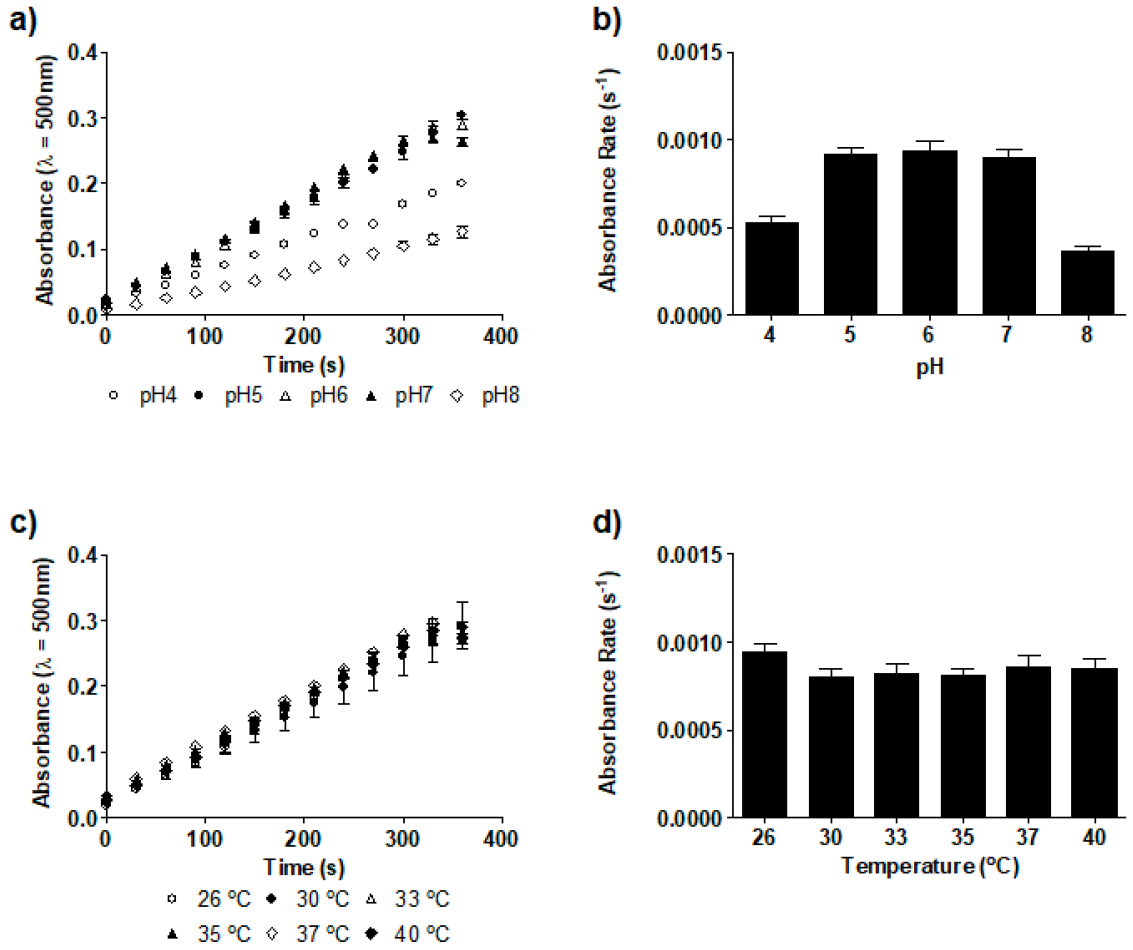

Figure 3.5. Effect of pH on hydrogen peroxide production (a) and rate of production (b) at 26°C. Effect of temperature on hydrogen peroxide production (c) and rate of production (d) at pH 6. All solutions contained 0.1 M glucose and 0.5 units/mL GOx. n=3, error bars represent standard deviation.

Building upon the fundamental knowledge gained from the kinetics of glucose oxidase, the composition of SHRO was investigated, specifically the glucose, total sugar and water content. There was very little inter sample variation between samples taken from the tube (Figure 3.6a) or sachet variants (Figure 3.6b), however tube formulations of SHRO were found to contain an average of 231.9 ± 7.8 mg/g of glucose compared to a sachet of SHRO that contained an average of 359.5 ± 6.5 mg/g of glucose (Figure 3.6c). Similar trends were also discovered in the total sugar content with the tube and sachet containing 78.9 ± 0.07% and 82.0 ± 0.03%, respectively (Figure 3.6d). Water content did however differ with the tube found to contain an average of 19.4 ± 0.08% water and the sachet found to contain 16.3 ± 0.05% water (Figure 3.64e).

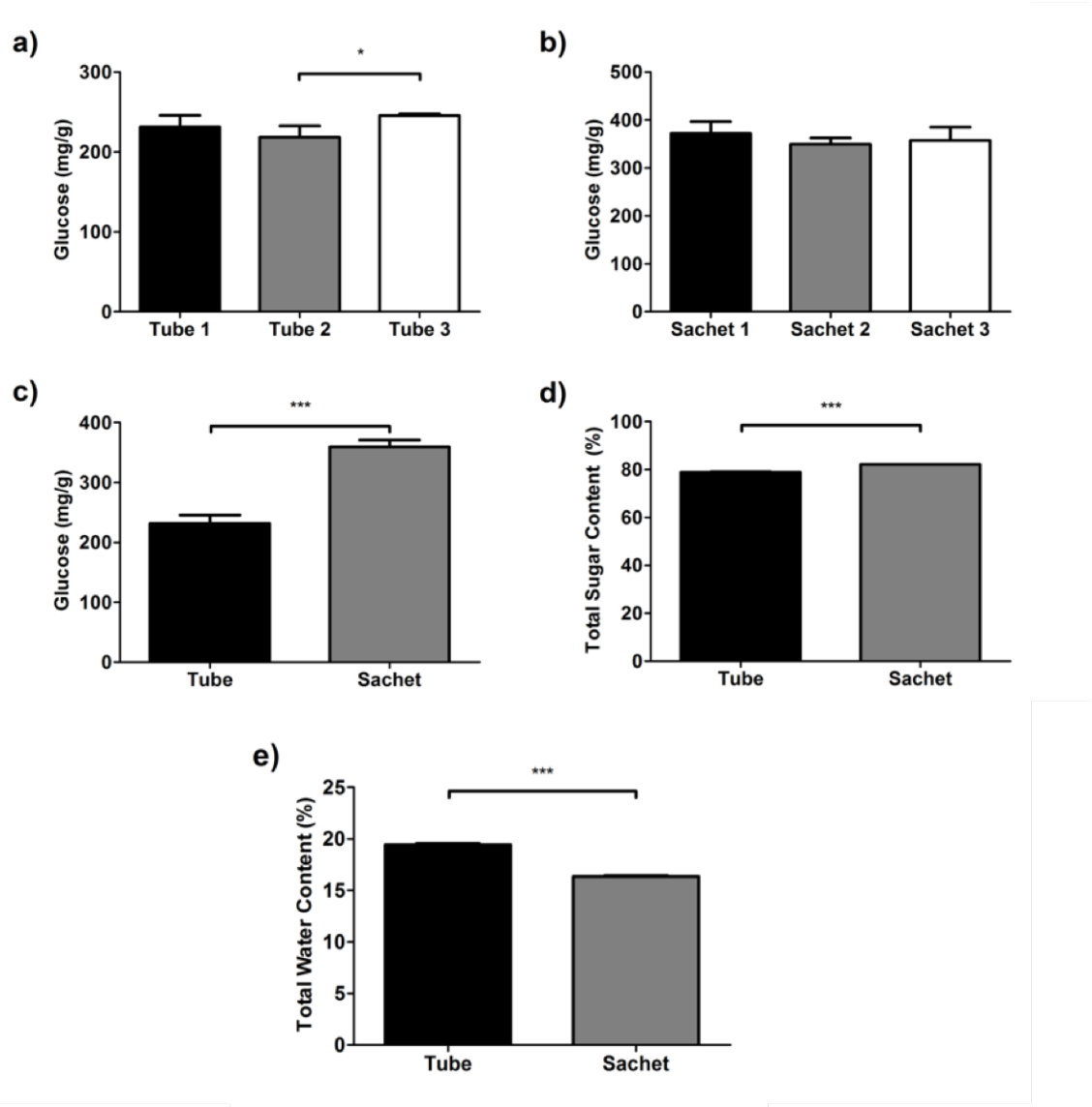

Figure 3.6. Glucose concentration of SurgihoneyRO™ tubes (a), sachets (b) and a comparison of glucose concentration (c), total sugar content (d) and water content (e) in both the tubes and the sachets. n=3 in addition to three technical repeats per tube and sachet, error bars represent standard deviation.

The amount of GOx in both the sachet and tube was unknown. However, the concentration of glucose in both samples and the way in which GOx behaves under set conditions has been elucidated, this enables the concentration of GOx to be calculated from the maximum linear rate of reaction (Vmax) (Figure 3.7a). It was found that the tube had a

higher rate of reaction that that of the sachet with a Vmax value of 0.0011 s^{-1} in comparison to 0.00090 s^{-1} for the sachet (Figure 3.7b). From this, the concentration of glucose oxidase units per mL can be calculated (Figure 3.7c). Subsequently, by incorporating the dilution factor, the concentration of glucose oxidase units per gram could also be calculated. It was found that the SHRO tube contained 11.8 units of glucose oxidase per gram in comparison to 6.19 units of glucose oxidase per gram from the sachet (Figure 3.7d).

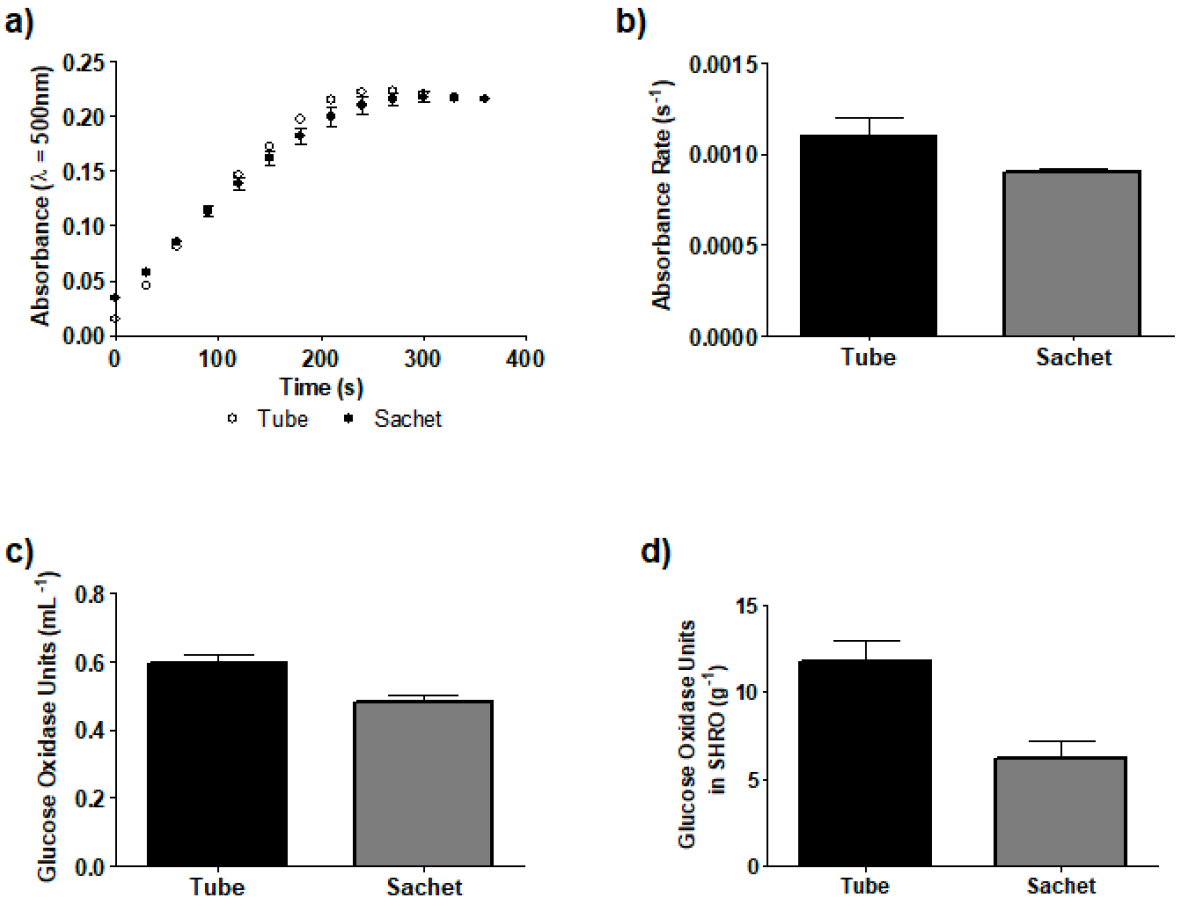

Figure 3.7. Hydrogen peroxide production (a) and rate of production (b) between SurgihoneyRO™ tubes and sachets, calculated value of glucose oxidase units present in solution (c) and calculated glucose oxidase units in SurgihoneyRO™ (d). All solutions were adjusted to pH 6 and 26°C. n=3, error bars represent standard deviation.

A hydrogen peroxide assay was conducted to assess the production of H_2O_2 from SHRO tube and sachet samples over a 1 hour period. The results obtained showed that the SHRO tube produced higher concentrations of H_2O_2 than the sachet with concentrations of 1.0 g/L producing 6.2 ± 0.1 and 4.9 ± 0.3 µM respectively. Both samples produced linear relationships between H_2O_2 production and SHRO concentrations producing near identical R^2 values of 0.998 (Figure 3.8a). The SHRO sachet was later discontinued as the higher water content in the SHRO tube enabled easier delivery without compromising the efficacy of the formulation.

Further assessment of H_2O_2 production at different SHRO concentrations was conducted over 7 days. It was notable that production of H_2O_2 in 50% SHRO tube solutions reduced by 40% over the first 6 hours from 1372 ± 87.4 to 821 ± 67.2 µM post activation of the enzymatic reaction with media. H_2O_2 concentration decreased further to 376 ± 2.8 µM (73%) over the course of 24 hours and 106 ± 46.6 µM after 72 hours. In contrast, 5 and 0.5% SHRO tube solutions increased post activation reaching values of 821 ± 33.8 µM and 289 ± 15.6 µM, respectively over 24 hours and 853 ± 14.6 µM and 610 ± 34.3 µM, respectively over 72 hours, both eclipsing that of the 50% solution. The remaining SHRO tube solutions produced H_2O_2 concentrations of less than 79 ± 4.3 µM over the 7 day period (Figure 3.8b).

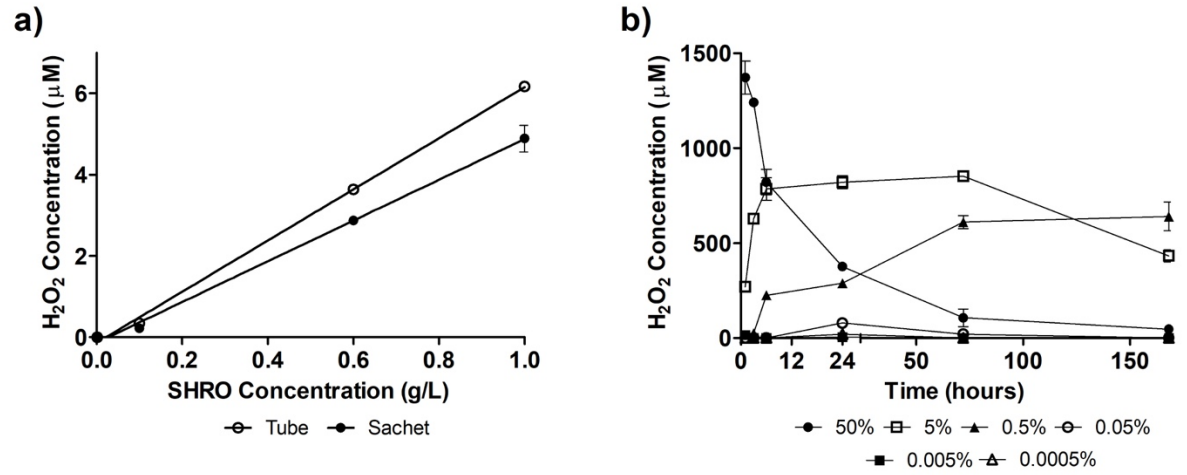

Figure 3.8. Release of hydrogen peroxide from both SurgihoneyRO™ tube and sachet samples (a) and at different percentage concentrations of SurgihoneyRO™ tube samples (b). n=3, error bars represent standard deviation.

Zone of inhibition experiments were conducted to determine how varying concentrations of SHRO from tubes samples and H_2O_2 impacted the degree of microbial efficacy. Neat SHRO in addition to 50 and 5% concentrations were capable of inhibiting the growth of clinically relevant *S. aureus* (Figure 3.9a), *P. aeruginosa* (Figure 3.9b) and *E.coli* (Figure 3.8c) producing larger zones with higher concentrations of SHRO. All tested H_2O_2 concentrations (3, 0.3, 0.03, 0.003%) were also capable of inhibiting *S. aureus* (Figure 3.9d), however, 0.003% H_2O_2 was unable to inhibit the growth of *P. aeruginosa* (Figure 3.9e) and *E.coli* (Figure 3.9f). As expected, similar to SHRO higher doses of H_2O_2 displayed a bigger zone of inhibited growth.

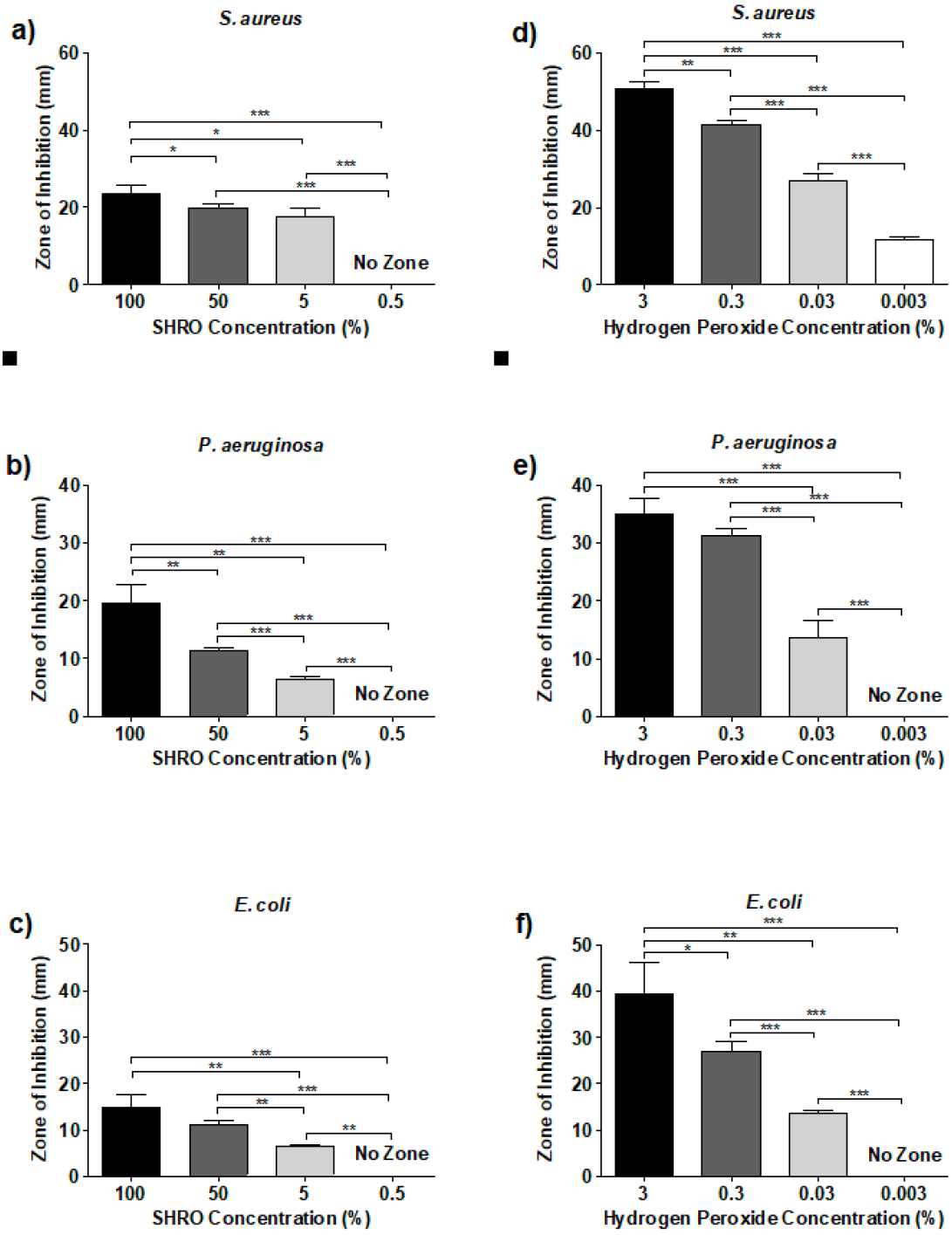

Figure 3.9. Zone of inhibition sizes following SHRO treatment for S. aureus (a), P. aeruginosa (b) and E. coli (c). Zone of inhibition sizes following hydrogen peroxide treatment for S. aureus (d), P. aeruginosa (e) and E. coli (f). n=3, error bars represent standard deviation.

Having determined the efficacious range of SHRO tubes and H_2O_2 it was important to test the cytotoxicity of these samples against mammalian cells. Interestingly, media with 50% SHRO produced a high level of HDF cell viability after 7 days (Figure 3.10a). In contrast, the wells containing concentrations of 5 and 0.5% SHRO exhibited total cell death (Figure 3.10b-c). At SHRO concentrations lower than 0.5%, cell viability was comparable to the cell only control (Figure 3.10d-f). Alternatively, when the media contained H_2O_2 total cell death occurred at concentrations between 3 and 0.003% (Figure 3.10g-j). Only at concentrations below 0.003% do cells exhibit comparable cellular viability with that of the control (Figure 3.10k-l). In all cases where cells remained viable after 7 days cells displayed a normal morphology and were indistinguishable from that of the control (Figure 3.10m-n).

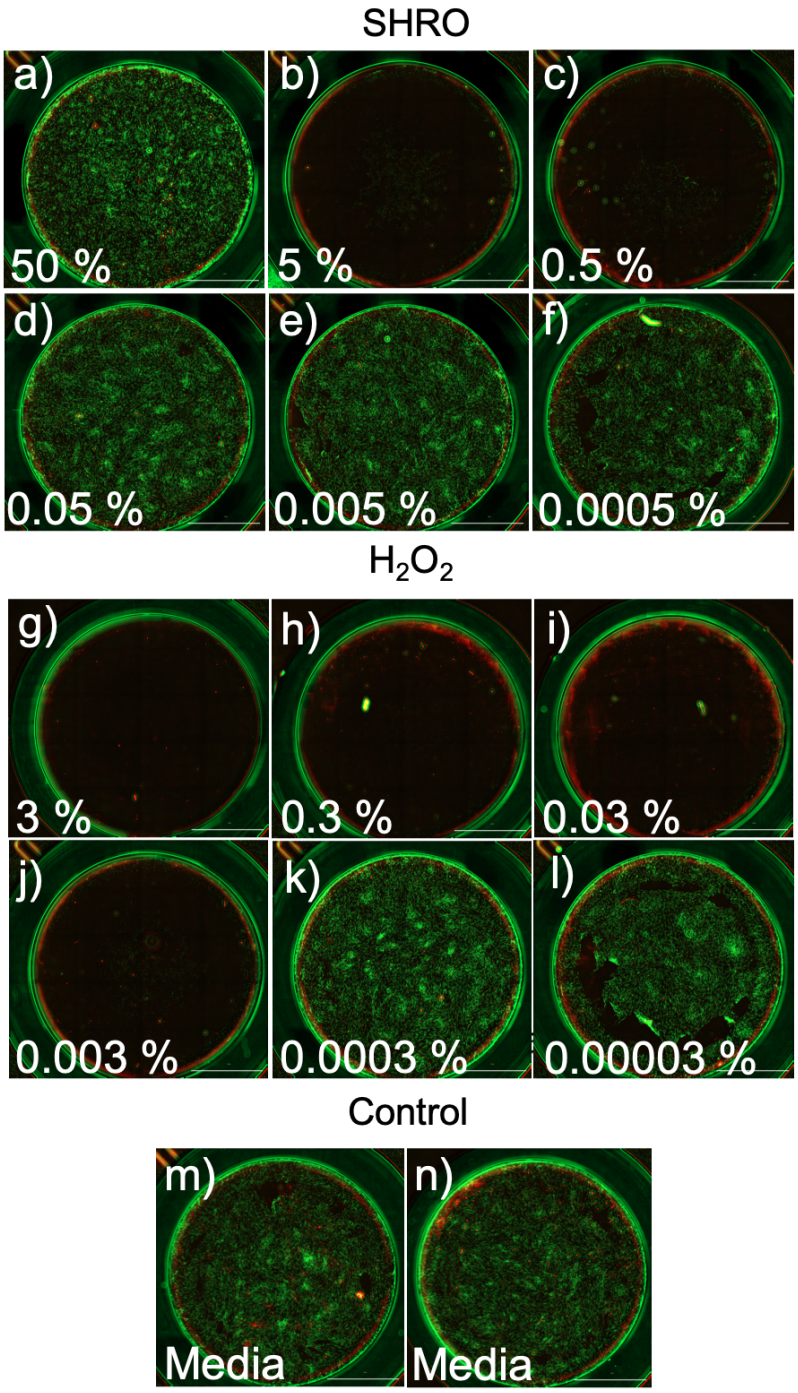

Figure 3.10. Fluorescent micrographs demonstrating viability of human dermal fibroblast (HDF) cells cultured with 50 (a), 5 (b), 0.5 (c), 0.05 (d), 0.005 (e) and 0.0005% (f) SHRO and 3 (g), 0.3 (h), 0.03 (i), 0.003 (j), 0.0003 (k) and 0.00003% (l) hydrogen peroxide. Control cells were cultured in DMEM (m-n) and stained with Syto 10 (green – live cells) and ethidium homodimer (red – dead cells) after 7 days.

3.4 Discussion

To realise the potential of honey as an antimicrobial treatment, SHRO, an engineered medical grade honey has the capacity to produce a specific amount of ROS independent of the honeys floral source. Previous studies demonstrated the complete eradication of *Staphylococcus aureus* (*S.aureus*) and *Pseudomonas aeruginosa* (*P.aeruginosa*), in addition to drug and multidrug resistant strains, MRSA and vancomycin-resistant *Enterococcus faecium* [43,44,167–170]. SHRO, however, similarly to natural honey presents highly viscous and adherent characteristics making delivery difficult and hindering widespread clinical use [170,418]. Before delivery systems may be developed to increase SHRO versatility and expand application areas, a fundamental understanding of the enzyme kinetics and chemical composition must be elucidated. In addition, the determination of cellular viability will help inform the development of new formulations.

The enzymatic oxidation of glucose was assessed whereby it was observed that the reaction velocities (Vmax) increased with increasing glucose concentrations. However, at concentrations above 0.1 M the reaction exhibited a zero order profile, in line with that expected of enzyme saturation kinetics (Figure 3.4a-b) [428]. The resultant effect is therefore that Vmax was no longer dependent upon glucose concentration, a phenomenon comparable to results obtained by Odebunmi., *et al.* [174]. In order to assess and understand both the kinetic activity and composition of SHRO it was necessary to investigate the impact of different concentrations of glucose oxidase on the reaction as well as differing reaction conditions. As predicted by the Michalis-Menton equation (Eq. 3.3) at constant glucose concentration (0.1 M) it was found that the Vmax increased proportionally to increasing enzyme concentration (R^2 = 0.994) (Figure 3.4 c-d) [173]. However, limitations of the study are due to only three concentrations being tested, conclusions of the linear effect can only be drawn within an

enzyme concentration range of 0.25-1.0 units/mL. Furthermore, the determination of reaction velocities at different pH environments was assessed. The results, in line with studies by Gibson., *et al.* [429] and Weibel., *et al.* [430] indicate a reduction in the catalytic ability of GOx with enzyme activity at low and high pH values inhibited due to the reduction in electron transfer and charge to the oxygen molecule. A range of pH values were identified between pH 5 and 7 for which the enzyme was most efficient with a peak velocity achieved at pH 6 (Figure 3.5a-b). In comparison to the normal physiological pH (7.4) of the body, the range at which the enzyme is most efficient is more comparable to that associated with the skin (pH ~5.5). A review by Schmid-Wendtner., *et al.* [431] suggests that by using products with a pH between 5 and 6 it may help to prevent and treat skin conditions. Furthermore, ROS concentrations between 5 and 250 μM have been shown to induce a immune response such as that of inflammation, which plays a critical role in wound healing [155,432]. An attempt was also made to study the catalysed oxidation reaction of glucose at different temperatures, however there was no notable change in Vmax, conflicting with results published by Odebunmi., *et al.* [174] and Gibson., *et al.* [433] who noted an increase in reaction velocities with an increase in temperatures (Figure 3.5c-d). The likely reasoning behind this being that insufficient time was given for temperatures within the wells to equilibrate and thus was a limitation of the methodology.

With the kinetic effect of change in substrate and enzyme concentrations exposed to different pH values at 26°C elucidated, the composition of two currently available SHRO products can be assessed. In order to evaluate the enzyme concentration within the two samples the glucose levels of both must be calculated. It was determined that tube formulations which contained more water (19.4 ± 0.08%) and less total sugar content (78.9 ± 0.07%) than the SHRO sachet (16.3 ± 0.05% and 82.0 ± 0.03% respectively) also contained less glucose with 231.9 ± 7.8 mg/g in the tube compared to 359.5 ± 6.5 mg/g in the sachet (Figure 3.6a-e).

However, both fell within the range expected within a honey product [434]. The determination of the amount of glucose present in the SHRO samples allows for the calculation of GOx concentrations. As the kinetics of the reaction at 0.1 M are understood and with the effect of changing GOx concentration linear in effect, by diluting both formulations to 0.1 M the unknown concentration of GOx can be elucidated. The tube SHRO samples were found to have a greater rate of reaction indicative of higher levels of GOx than that of the sachet (Figure 3.7a-b). Accounting for dilution in the original mass of honey, it was found that the tubes contained 11.8 units/g compared to 6.19 units/g in the SHRO sachet samples, suggesting that the tubes had a greater propensity to generate H_2O_2 (Figure 3.7c-d).

The production of hydrogen peroxide as well as other ROS is vital to the antimicrobial effect elicited by SHRO [170,418]. Due to this it is important to conclusively analyse the H_2O_2 production of the SHRO tubes and sachets, this was achieved using a fluorometric technique. Notably the SHRO tube produced significantly ($p = 0.02$) more H_2O_2 than that of the sachet with concentrations of 1.0 g/L releasing 6.2 ± 0.1 and 4.9 ± 0.3 μM of H_2O_2 respectively (Figure 3.8a). This supported the evidence that the SHRO tube contained more GOx. With the greater ability to generate ROS despite its lower inherent glucose concentration and its higher endogenous water content, which allows for easier handling, SHRO sachet products were discontinued, with further investigations conducted using SHRO tube samples. Interestingly in contrast to other concentrations, the production of H_2O_2 in 50% SHRO solutions was found to reduce by 40% after 6 hours producing no significant difference to that of 5% SHRO solutions. The production of H_2O_2 in 50% SHRO solutions continued to fall below the μM concentrations produced by 5% SHRO with the 0.5% SHRO solution eclipsing the produced levels of H_2O_2 from the 50% SHRO solution after 3 days (Figure 3.8b). In order to establish efficacy, a zone of inhibition test was used to find at which concentration SHRO

maintained the ability to inhibit growth. It was found that 100, 50 and 5% solutions of SHRO inhibited growth of clinically relevant *S. aureus*, *P. aeruginosa* and *E. coli* with zones of inhibition proportional to the concentration of SHRO added. The higher the concentration the larger the zone of inhibition (Figure 3.9a-c). These results although comparable with the current literature were in contrast to the amount of ROS that was found to be produced by the formulations in this study. However, zones of inhibition were carried out on agar plates which contain 98.5% water and therefore as the solution diffuses through the plate it also diluted the solution. It is theorised that this phenomenon is the resultant effect of insufficient free water being available in a 50% solution to maintain the reaction over time and therefore this was indicated by a decrease in ROS production in the hydrogen peroxide assay. This is further supported by Olaitan., *et al.* [435] who states that honey is highly osmotic and thus draws water into its structure leaving less water available to react with the substrate and causing a decrease in the production of ROS over time. In addition, due to the high total sugar contents of SHRO, complete dissolution of the glucose and enzyme may not have been achieved at 50% dilution, hindering the reaction. This work suggests that further dilution would be necessary in order to permit the reaction to occur over longer periods of time. Limitations of this study found that concentrations greater than 50% could not be fully dissolved in solution. Furthermore, assay method limitations dictate a maximum final concentration of 10 µM, requiring significant dilutions of the formula and increasing the availability of water to activate production of ROS. Due to this achieving baseline ROS activity within SHRO using this methodology is not possible.

As a control H_2O_2 at different concentrations (3.0 - 0.003%) were tested. Results showed zones of inhibited growth for all concentrations when treating Gram positive *S. aureus*, however, the lowest concentration 0.003% was unable to inhibit Gram negative *P. aeruginosa*

and *E.coli* (Figure 3.9d-f). It is well known that Gram negative bacteria can be more difficult to treat and it is reported by *Fischbach., et al.* [436] that the additional protection offered by the outer membrane of the cell may require higher doses of ROS in order to treat an infection.

Previous studies have indicated that the presence of ROS can damage DNA and as such further assessment of cell viability was undertaken utilising and treating *in vitro* cultures of HDF cells [36,437]. Interestingly, it was found that cells treated with 50% SHRO DMEM media proliferated well, displaying high levels of viability and a normal morphology, comparable to that of the controls over 7 days (Figure 3.10a). This was in contrast to DMEM media with 5 and 0.5% SHRO, which exhibited total cell death (Figure 3.10b-c). These results support the hypothesis posed by the hydrogen peroxide assay for which it implied that in 50% solutions of SHRO there is not enough free water to sustain the production of H_2O_2 over time. Furthermore, the level of ROS produced by the 50% SHRO solution after 72 hours was 106 ± 46.6 μM, which although has been shown to induce some stress responses is not high enough to induce apoptosis, unlike the concentrations of ROS produced by 5% (853 ± 14.6 μM) and 0.5% (610 ± 34.3 μM) formulations [155]. However, it is worth noting however that these experiments were conducted using DMEM instead of assay buffer. Assay buffer carefully regulates pH at pH 6. In contrast, DMEM modulates a physiological pH of 7.4 and is supplemented with FBS, L-glutamine and a combination of penicillin and streptomycin. These components may therefore affect the stability of ROS production and therefore limitations are produced in the ability to directly compare results. In addition, the postulated reason for the efficacious inhibition of bacterial growth for both neat SHRO and 50% solutions is that the experimental set up is ran on agar plates through which the SHRO solution diffuses out of the well and into the surrounding gel. As agar gel is 98.5% water, as the SHRO diffuses through the media it also becomes more dilute and thus activates and maintains the production of

SHRO. As SHRO concentrations were lowered below that of 0.5% cell viability was indistinguishable from that of the control (Figure 3.10d-f). Furthermore, DMEM media with H_2O_2 found that total cell death occurred at concentrations between 3 and 0.003% (Figure 3.10g-j), only concentrations below 0.003% are comparable with that of the control (Figure 3.10k-l).

3.5 Conclusion

The research in this study elucidated the enzyme kinetics of SHRO as well as the chemical composition and cellular viability in order to help inform developmental pathways for which to formulate new, efficacious, easy to deliver systems. The kinetics of the enzymatic oxidation of glucose reaction catalysed by glucose oxidase was studied over a number of experimental conditions. It was found that the reaction velocities (Vmax) increased with glucose and GOx concentration, until complete enzyme saturation was achieved, at which point Vmax values plateaued. A range of pH values were identified between pH 5 and 7 for which the enzyme was most efficient with a peak reaction velocity achieved at pH 6.

Kinetics were elucidated at a temperature of 26°C in line with the limitations of the methodology and the equipment, providing greater understanding of the reaction process as well as allows for the investigation of SHRO composition. It was determined that the less viscous, easier to handle, SHRO tube formulations contained more water and less total sugar content than that of the sachet. Furthermore, the SHRO tube formulation also contained less glucose but more GOx (231.9 ± 7.8 mg/g and 11.8 units/g respectively) when compared to the sachet (359.5 ± 6.5 mg/g and 6.19 units/g respectively) leading to the SHRO tube formulation exhibiting a higher level of H_2O_2 production and the discontinuation of the sachet product. The influence of the SHRO tube formulation on the viability of both bacteria and HDF cells was also tested, with concentrations above 5% were needed in order to inhibit bacterial growth. It was, however highlighted through fluorometric analysis that at concentrations of 50%,SHRO solutions did not have the required water availability to maintain production of H_2O_2 overtime and as such was able to provide conditions for which HDF cells could proliferate, express a high degree of viability and exhibit a normal morphology. This was in contrast to 5% and 0.5% SHRO solutions that caused total cell death over the same time

period. A direct comparison cannot be made between the methodology used to determine HDF viability and bacterial inhibition as within the DMEM media used to culture the HDF cells the SHRO concentration is fixed whereas in the case of the inhibition assay the SHRO solutions dilutes as it diffuses through the aqueous agar gel, providing the necessary water for activation but also reducing the concentration.

Overall this work highlights the fundamental mechanism by which future delivery systems will be based upon. It also expands the knowledge of both limitations and characteristics associated with SHRO, helping to guide the development of new formulations.

CHAPTER FOUR

4. REACTIVE OXYGEN EMULSION DELIVERY SYSTEMS

Data in this chapter is also presented in the following published article found in Appendix 1: T.J. Hall, J.M.A. Blair, R.J.A. Moakes, E.G. Pelan, L.M. Grover, S.C. Cox, Antimicrobial emulsions: Formulation of a triggered release reactive oxygen delivery system, Mater. Sci. Eng. C. 103 (2019) 1–10. doi:10.1016/j.msec.2019.05.020.

4.1 Introduction

SHRO elicits an antimicrobial response due to the production of ROS, which is produced by means of a water initiated, enzyme mediated, oxidation of glucose reaction (Figure 4.1a). SHRO contains 16-20% water but this is bound to sugars and is not free to react [183]. As a consequence, to avoid premature production of ROS before clinical application a non-aqueous vehicle is required. The scope of this work is to formulate a product which can be stored and activated *in situ*. Furthermore, it should improve the ease of handling SHRO, and facilitate controlled release of ROS. One such approach may be to create an emulsion that incorporates SHRO into its non-aqueous phase (Figure 4.1b).

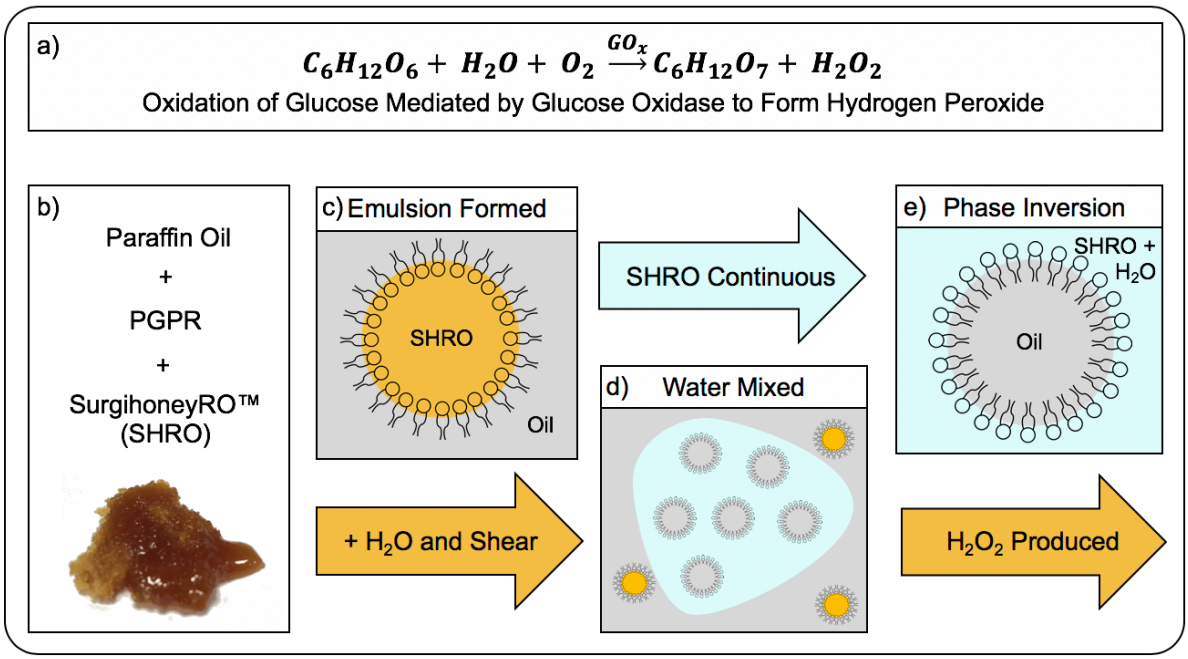

Figure 4.1 Schematic highlighting the production of hydrogen peroxide and reactive oxygen species through the aerobic glucose oxidase mediated oxidation reaction of glucose and water (a). The key components of a SurgihoneyRO™ in oil emulsion (b), in which SHRO is the dispersed phase (c). After addition of water and shear (d) phase inversion of the emulsion occurs (e) allowing for the production of hydrogen peroxide and other reactive oxygen species.

An emulsion can be defined as a dispersion of droplets of one liquid in another, in which it is not soluble or miscible [197]. There are two basic forms of emulsions: (1) oil in water, denoted O/W and (2) water in oil (W/O) [185]. Emulsions are inherently thermodynamically unstable and systems quickly phase separate after manufacture to reduce the unfavourably high energy states associated with interfacial tension (IFT) [438]. To improve stability over time, typically emulsifiers or surfactants are used, these lower the tension between the two species allowing the persistence of droplets, which may contain actives, over longer time scales [439].

Mechanical energy, such as shear is commonly applied by a homogeniser device and often used to create and disperse droplets of one phase within another [187]. According to

Silva., et al. [440] the more energy that the system is subject to the smaller the droplets are formed. Stokes law (Eq. 4.1) states that a smaller particle diameter (r) induces a lower creaming/settling velocity (v), implying that the generation of small droplets is important for product stability [441]. Velocity is calculated taking into account density differences ($\Delta\rho$) under the effect of gravity (g) and the viscosity of the continuous phase (η) [202,212].

$$v = \frac{2r^2(\rho_2-\rho_1)g}{9\eta} \quad \text{(Eq. 4.1)[202]}$$

When an emulsion is formulated with approximately equal proportions of water and oil, it is often referred to as a cream [184]. Commonly, a thickening agent is added to the emulsion in order to achieve specific rheological properties that relate to a positive sensory perception [442]. To achieve such characteristics, creams are typically non-Newtonian, viscoelastic materials with an inherent microstructure responsible for the production of an elastic response to shear [443]. This produces yield stress values that allow for easy spreading.

The elastic shear-response of a material is characterised by its storage modulus (G'), which corresponds to the emulsions storage of elastic energy [444]. The viscous shear-response is however, governed by the loss modulus (G'') that quantifies energy dissipation from unrecoverable viscous loss [445]. The energy stored and lost during a deformation cycle can be measured by calculating the loss tangent $(\tan\delta)$, which is the ratio of G'' to G' (Eq. 4.2)[446]. At low shear rates a low phase angle (δ) is typically associated with a topical cream. Creams generally exhibit pseudoplastic behaviour (shear thinning), whereby viscosity monotonically decreases as a function of shear rate. As the application of shear stops, the structure regenerates in a transient manner, known as thixotropy [240]. Low shear viscosity

allows the product to maintain a high viscosity, whilst at higher shear rates viscosity is reduced, facilitating tubular extraction and subsequent spreading action.

$$\tan \delta = \frac{G'}{G''} \quad \text{(Eq. 4.2)[446]}$$

Active containing emulsions must be formulated to enable a therapeutic response to a target area. As such emulsions with therapeutics residing in the dispersed phase must have an inherent mechanism for release and activation of the compound such as phase inversion (Section 2.5.1) which may be triggered by the introduction of particular flows (shear induced), changing temperature, alterations in phase volumes (known as catastrophic phase inversion (CPI)), change in pH or the addition of salts [212].

The focus of this study is to formulate an emulsion system that enables easy delivery of ROS at concentrations capable of inducing a therapeutic antimicrobial response (>25 μM) (Figure 4.1). It is hypothesised that by incorporating the SHRO in oil, this will help to protect the agent from premature ROS activation and provide a treatment option for minor topical infections such as that from a cut, scape or burn. By optimising the dispersion of SHRO, shear thinning behaviour could be achieved easing application (Figure 4.1). Further development will look to maintain the shear thinning behaviour whilst increasing the viscosity of the emulsion to form a cream, with the aim of improving stability. This work will use an inversion trigger whereby water and shear are added to the system until the emulsion inversion point is exceeded and CPI occurs. This work is the first report of an engineered emulsion system to controllably deliver ROS and demonstrates it is capable of eradicating clinically relevant bacteria *in vitro* [170].

4.2 Materials and Methods

4.2.1 Materials

LB broth, LB broth with agar, analytical grade paraffin oil, XG and magnesium sulphate heptahydrate were supplied by Sigma Aldrich, UK. Other oils used in this study (vegetable, olive and corn) were commercially sourced. PGPR was provided by Palsgaard, Denmark and SHRO was supplied by Matoke Holdings, UK. Aerosil fumed silica (AR816) was provided by Aerosil, UK. All materials were used as delivered and no further purification or modifications were made.

4.2.2 Emulsion formulation

Formulation optimisation

Emulsions were created in a two-step process using a T18 Ultra Turrax® disperser (IKA, UK). The oil phase (paraffin, vegetable, olive or corn oil) was combined with PGPR for 1 min at 10,000 rpm. SHRO was then added dropwise, using a 5 mL syringe, to the oil and surfactant mixture. Unless specified post SHRO addition, shear was applied at 10,000 rpm until a total time of 10 minutes had elapsed. The final emulsions were stored in a temperature controlled laboratory set at 21°C until needed. Percentages are denoted as (v/v) and indicate the amount of SHRO present in the formulation. The oil used can be assumed to be paraffin oil with the surfactant (PGPR) volume set at 2% unless otherwise stated. All emulsions were formulated in triplicate.

Process optimisation

60% SHRO emulsions were formulated and processing temperature was assessed under room temperature and ice bath conditions using a digital thermometer. The applied shear rate and time was also investigated after SHRO addition. In addition to the standard

10,000 rpm, shear rates of 6000rpm and 8000rpm were investigated and these were applied over 6, 8 or 10 minutes. All emulsions were formulated in triplicate.

4.2.3 Cream Formulation

Creams were based upon 60% SHRO emulsions formed using the protocol stated in section 4.2.2. Creams containing fumed silica were manufactured by first dispersing AR816 Aerosil fumed silica in paraffin oil under high shear (10000 rpm) prior to formulation at total concentrations of 1 (SHRO_AR1) and 2% (SHRO_AR2). Standard emulsion formation protocol was then followed. Alternatively, creams were formulated with XG. In order to incorporate XG into the dispersed phase, 0.5% (w/v) was completely dissolved in glycerol using a high shear mixer at 10000 rpm and allowed to cool. SHRO was then added to the glycerol in a 50:50 ratio, with the resultant solution used to form the dispersed phase, following standard protocol (SHRO_XG1). The protocol used to form SHRO_XG1 was then used as the base for the formation of a fourth cream containing 0.5% (w/v) magnesium sulphate heptahydrate. This was added and dissolved simultaneously with the glycerol (SHRO_XG2). All creams were formulated in triplicate.

4.2.4 Visual characterisation of emulsion stability

Emulsions were formulated according to the method in section 4.2.2 and monitored over a 7-day period at 21°C. At each time point (1, 2, 3 and 7 days) an image was taken using an iPhone X camera at 1.0 x zoom, from a distance of 15 cm and level with the meniscus of the sample. To enable measurement calibration a fixed scale was placed next to the sample during capture. Images were visually assessed to determine if droplet sedimentation or separation of phases occurred. *Image J* software (1.47v National Institutes of Health, USA) was

used to calibrate images and obtain a quantitative measurement of separation. Three samples of each emulsion variant were measured in order to obtain a mean and standard deviation.

4.2.5 Interfacial tension measurements

As a quantitative indicator of stability, interfacial tension measurements were conducted using a K100 force Tensiometer (Krüss. GmbH, Germany). The plate was immersed at a depth of 3 mm at the interface of the paraffin oil and the SHRO. Experiments were run until the interfacial tension measurements had reached equilibrium. PGPR was premixed into the oil phase at 0, 0.5, 1.0, 2.0 and 4% before testing and each concentration was run in triplicate.

4.2.6 Rheological characterisation of SHRO in paraffin oil emulsions

An AR-G2 rheometer (TA Instruments, UK) with sandblasted parallel plates (size = 40 mm, gap height = 1 mm) was used to determine the viscoelastic properties of emulsions immediately after manufacture (day 0) and after 7 days of storage at 21°C. Prior to testing on day 7 the emulsions were shaken for 1 minute by hand in order to resuspend the droplets. Viscosity was determined by means of a shear rate sweep from 1.0 to 100.0 s^{-1} conducted over a period of 5 minutes at 21°C. From this sweep, a shear rate of 4.1 s^{-1} was used to characterise behaviour prior to storage. This shear rate is representative of a low shear post-mixing state, such as that achieved following a shake before use directive [447]. A shear rate of 99.7 s^{-1} was isolated to describe the behaviour under higher shear application, representative of the typical forces involved in extrusion from a tube [448].

The linear viscoelastic region (LVR) was identified for all tested emulsions using a strain sweep with frequency set at 1 Hz. This data was used to select a percentage strain value that

fell within the LVR. Frequency sweeps were then carried out from 0.1 to 100 Hz at 21°C and 0.5% strain to obtain storage (G') and loss (G'') moduli.

It was important to determine the rate of viscosity recovery after simulated application to ensure that the emulsion structure was not altered. Formulations were subjected to 100 s^{-1} for 30 seconds at 21°C to mimic extrusion. Shear rate was then reduced to 1.0 s^{-1} and viscosity monitored for 30 seconds. This process was repeated thrice, and the hysteresis results plotted.

4.2.7 Size analysis of dispersed SHRO droplets

Laser diffraction measurements were recorded by a Malvern 3000 Mastersizer (Malvern Instruments, UK). Refractive indexes (RI) of 1.487 and 1.473 were used for SHRO and paraffin oil, respectively. RI was determined using an ORA-3HA refractometer (Kern-Sohn, Germany) and manufacturer provided values. The software used to calculate size distribution assumed spherical droplets in a uniform media. Size distribution was measured on days 0 and 7 to investigate the occurrence of coalescence. Each emulsion ratio was measured in triplicate and with three readings per experimental run.

4.2.8 Conductivity measurements

Conductivity was measured using a HI99300 conductivity test meter (Hanna Instruments, UK) to assess whether CPI had occurred. Measurements were taken before and after shear of the samples and the controls (oil and deionised water). Emulsions were diluted with deionised water in a 1:2 ratio and vortexed for 1 minute to trigger inversion.

4.2.9 Hydrogen peroxide release from SHRO emulsions and creams

As an indicator of formulation efficacy, a fluorescent assay kit (Sigma Aldrich, UK) was used to determine hydrogen peroxide release. Prior to testing a calibration curve was created using hydrogen peroxide standards 10, 3, 1, 0.3, 0.1, 0.03, 0.01 and 0µM. A further calibration curve was created using SHRO 2.0, 1.5, 1.0 and 0.5 g/L. This was used to determine dilution factors given the assay concentration limits. For the assay, 1 mL of each sample was diluted with 2 mL of deionised water and vortexed for 10 seconds to allow phase inversion to occur. This was then further diluted by adding 0.1 mL to 30 mL of deionised water (1:300) to conduct the assay for each time point (1, 3, 6, 12 and 24 hours) (Figure 4.2). The manufacturer's instructions were followed, briefly the following standard solutions were made: a master mix containing 50 µL red peroxidase substrate, 200 µL of 20 units/mL peroxidase, 4.75 mL assay buffer, and hydrogen peroxide standards between 0 µM and 10 µM. 50 µL of sample or standard was added to 50 µL of master mix, which were then mixed by pipetting, protected from light and incubated at room temperature for 30 minutes. The fluorescence intensity was then measured (λ_{ex} = 540nm/λ_{em}= 590nm) using a Tecan Spark plate reader (Tecan Trading AG, Switzerland). Each emulsion was tested in triplicate.

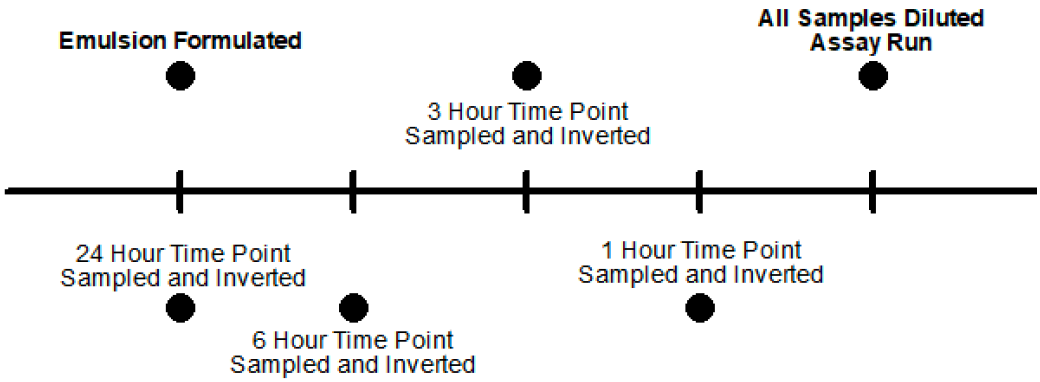

Figure 4.2. Timeline describing experimental design and sampling timepoints for fluorometric determination of hydrogen peroxide

4.2.10 In vitro efficacy of SHRO emulsions and creams

LB broth and LB broth with agar was reconstituted with distilled water to concentrations of 20 g/L and 35 g/L respectively, both were sterilised by autoclaving for 20 minutes at 121°C and 100 kPa.

Overnight cultures of Staphylococcus aureus (S. aureus - ATCC 29213), Escherichia coli (E. coli - MG1655) and Pseudomonas aeruginosa (P. aeruginosa - NCTC 13437) were prepared by inoculating one colony of each strain into 5 mL of LB broth. The optical density of each overnight culture was then measured at 600 nm using a Spectronic Helios Gamma UV-Vis Spectrophotometer (Thermo Fisher Scientific, UK) and diluted to 0.04.

Agar plates were created from LB broth with agar and inoculated with bacteria. A 10 mm sterile hole borer was then used to create a well in the center of the inoculated agar. 1 mL of each emulsion was diluted with 2 mL of deionised water and vortexed for 1 minute in order to trigger the release of ROS. 250 μL of diluted emulsion was then added to the well and incubated at 37°C for 24 hours. Zones of inhibited bacterial growth were then measured, and the bore hole diameter was deducted from the total zone size. Each emulsion formulation and bacterial strain were run in triplicate.

4.2.11 Statistical analysis

GraphPad Prism® 5.0 software was used to perform statistical analysis. T-tests were used to determine significance whereby values of $p < 0.05$ were considered significant and p values indicated as follows $p < 0.05$ (*), $p < 0.01$ (**), $p < 0.001$ (***). Data is presented throughout as mean ± standard deviation.

4.3 Results

4.3.1 Optimisation of SHRO emulsion formulations

Paraffin oil emulsions containing 30% SHRO and 2% PGPR were found to have a slower sedimentation rate (29.6 ± 8.6%) over 7 days than emulsions formulated with olive (73.9 ± 1.1%), corn (86.0 ± 4.7%) or vegetable oil (78.5 ± 1.1%) (Figure 4.3a). With the exception of paraffin oil, the resultant emulsion instabilities were not reversible by inversion or shaking as phase separation had occurred. Emulsions comprised of paraffin oil maintained the integrity of the SHRO droplets and after initial sedimentation could be re-dispersed by inversion (see images in Figure 4.3a). Coalescence and phase separation did not occur in paraffin oil emulsion systems over the 7 days of storage. 1,2,3 and 7 days were selected in order to represent time points throughout a period of treatment.

An increase in SHRO concentration for paraffin oil samples resulted in a lower rate of sedimentation (Figure 4.3b). Notably, emulsions containing >50% SHRO showed no indication of sedimentation over a 7 day period. Emulsions containing 40 and 30% SHRO displayed sedimentation rates of 9.0 ± 1.8 and 29.6 ± 8.6%, respectively over 7 days.

Further testing determined that emulsions containing < 2% PGPR sedimented after 7 days (Figure 4.3c). After 24 hours, sedimentation was observed for both the 60 and 50% SHRO emulsions, which contained 0.5% PGPR with sedimentation rates of 15.3 ± 1.0 and 22.8 ± 5.0%, respectively. Over time, sedimentation progressed and at day 7 was recorded for 60% SHRO emulsions as 40.6 ± 2.0 and 50.4 ± 5.0% for 50% SHRO emulsions. With an increase in surfactant to 1%, sedimentation was reduced. After 3 days emulsions containing 60% SHRO still displayed no sedimentation, emulsions that contained 50% SHRO, however sedimented by 3.2 ± 1.1%. After 7 days, 60 and 50% SHRO emulsions containing 1% PGPR showed no

significant difference in sedimentation with rates of 13.1 ± 0.3 and 13.5 ± 1.1% respectively (Figure 4.3c). The stability improvements observed for samples with 2% PGPR, justifies selecting this concentration of surfactant for the remainder of the study.

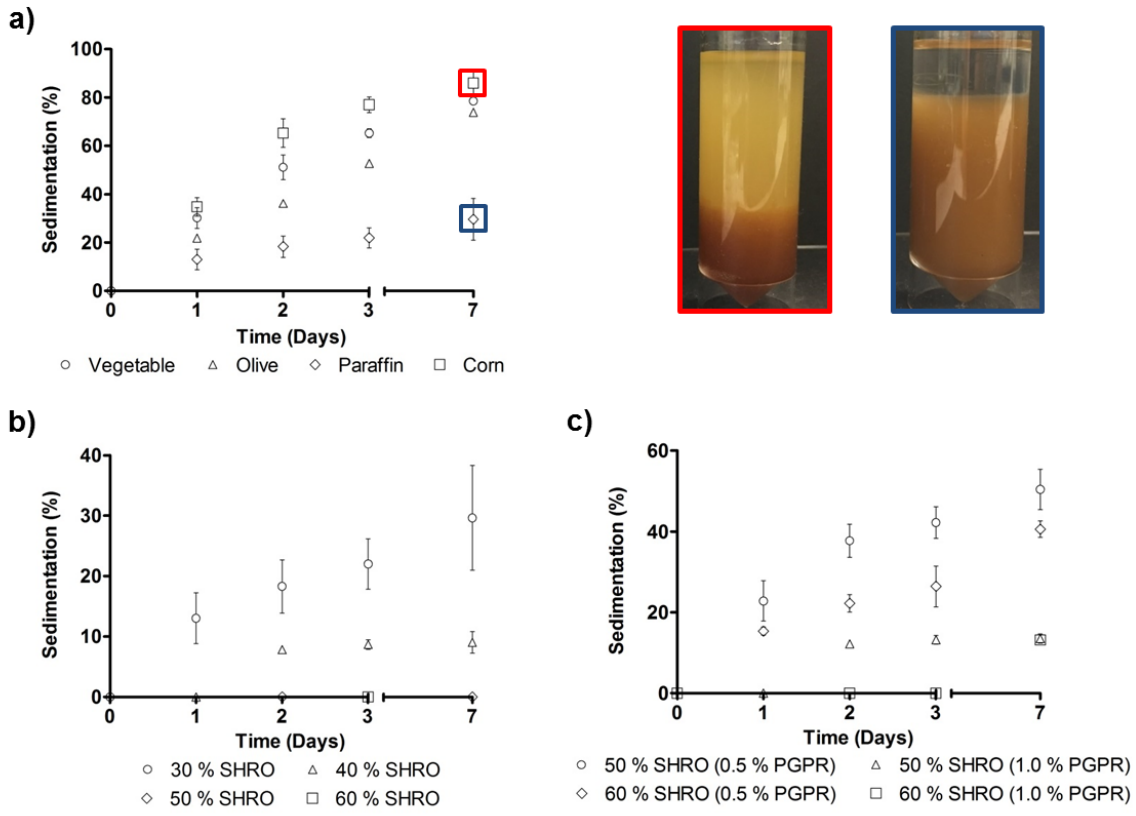

Figure 4.3. Influence of emulsion formulation factors on the rate of droplet sedimentation formulated and stored at room temperature (21°C): oil type (a), dispersed phase (SHRO) concentration (b) and emulsifier (PGPR) concentration (c). Each emulsion was formulated and tested in triplicate with error bars displaying standard deviation.

The concentration of PGPR in the emulsion was further investigated in order to determine the IFT between the paraffin oil and SHRO. With no PGPR dispersed within the system, a high IFT was measured (35.9 ± 0.8mN/m). As PGPR was increased to 0.5% the IFT significantly reduced by 82.8% to 6.2 ± 0.2 mN/m. IFT continued to reduce until 2% PGPR was incorporated into the system whereby the IFT appears to plateau as there was no further

significant decrease in IFT between 2% (5.18 ± 0.3 mN/m) and 4% (5.19 ± 0.1 mN/m) PGPR concentrations (p = 0.98) (Figure 4.4).

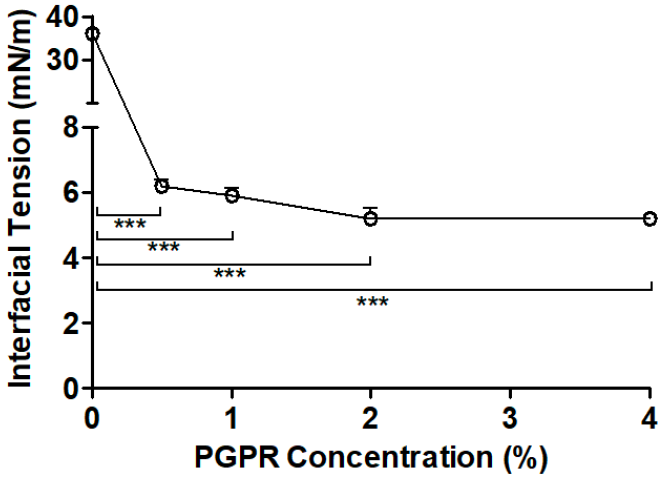

Figure 4.4. Interfacial tension measurements between paraffin oil and SurgihoneyRO™ with varying concentrations of polyglycerol polyricinoleate surfactant.

The ratio of SHRO to paraffin oil within the emulsion significantly alters the overall viscosity (Figure 4.5a). An increase in the concentration of SHRO increased viscosity across all shear rates tested (1.0 – 100 s^{-1}). Apparent viscosities on day 0 and day 7 respectively measured at 19.3 ± 0.2 Pa · s and 13.42 ± 0.2 Pa · s (60%), 9.7 ± 0.3 Pa · s and 6.9 ± 0.5 Pa · s (50%) and 1.4 ± 0.2 Pa · s and 1.8 ± 0.7 Pa · s (30%) at a shear rate of 4.1 s^{-1}. After storage for 7 days at 21°C there was a 20 – 35% reduction in viscosity at all tested shear rates between 60 and 50% SHRO emulsions. In contrast, the 30% SHRO emulsion formulation showed no significant difference in viscosity after the 7-day storage period (Figure 4.5b).

The apparent viscosity profile of the emulsions differed to that of the control, unprocessed SHRO. At lower shear (4.1 s^{-1}), 60 and 50% SHRO emulsions had a higher viscosity than SHRO alone. In contrast, at a higher shear rate (99.7 s^{-1}), it was found that all of

the emulsions except 60% SHRO, displayed lower apparent viscosities on day 0 compared to SHRO alone (Figure 4.5c).

When SHRO emulsions are rapidly switched from a low (1.0 s^{-1}) to a higher shear (100 s^{-1}) the viscosity reduces but quickly recovers exhibiting shear thinning behaviour (Figure 4.5d). The SHRO emulsions did display hysteresis upon application and removal of shear as the recovery viscosity of the formulation is lower than that of the initial measurement (Figure 4.5d).

Analysis of the viscoelastic properties of the emulsions determined that higher concentrations of SHRO exhibited higher G' and G'' values. At 5 Hz, for 60 and 50% SHRO emulsions, the G' was higher than that of the G". However, 30% SHRO emulsions exhibited similar G' and G" values at 5 Hz. At higher frequencies (30 Hz) G" exceeded G' for all formulations (Figure 4.5e). The frequency at which crossover occurred was found to increase with increasing SHRO concentration. At day 0 this phenomenon occurred at 63.1 Hz, 50.1 Hz and 1.6 Hz for 60, 50 and 30% SHRO emulsions, respectively and 50.1 Hz, 39.8 Hz and 0.8 Hz on day 7 (Figure 4.5f).

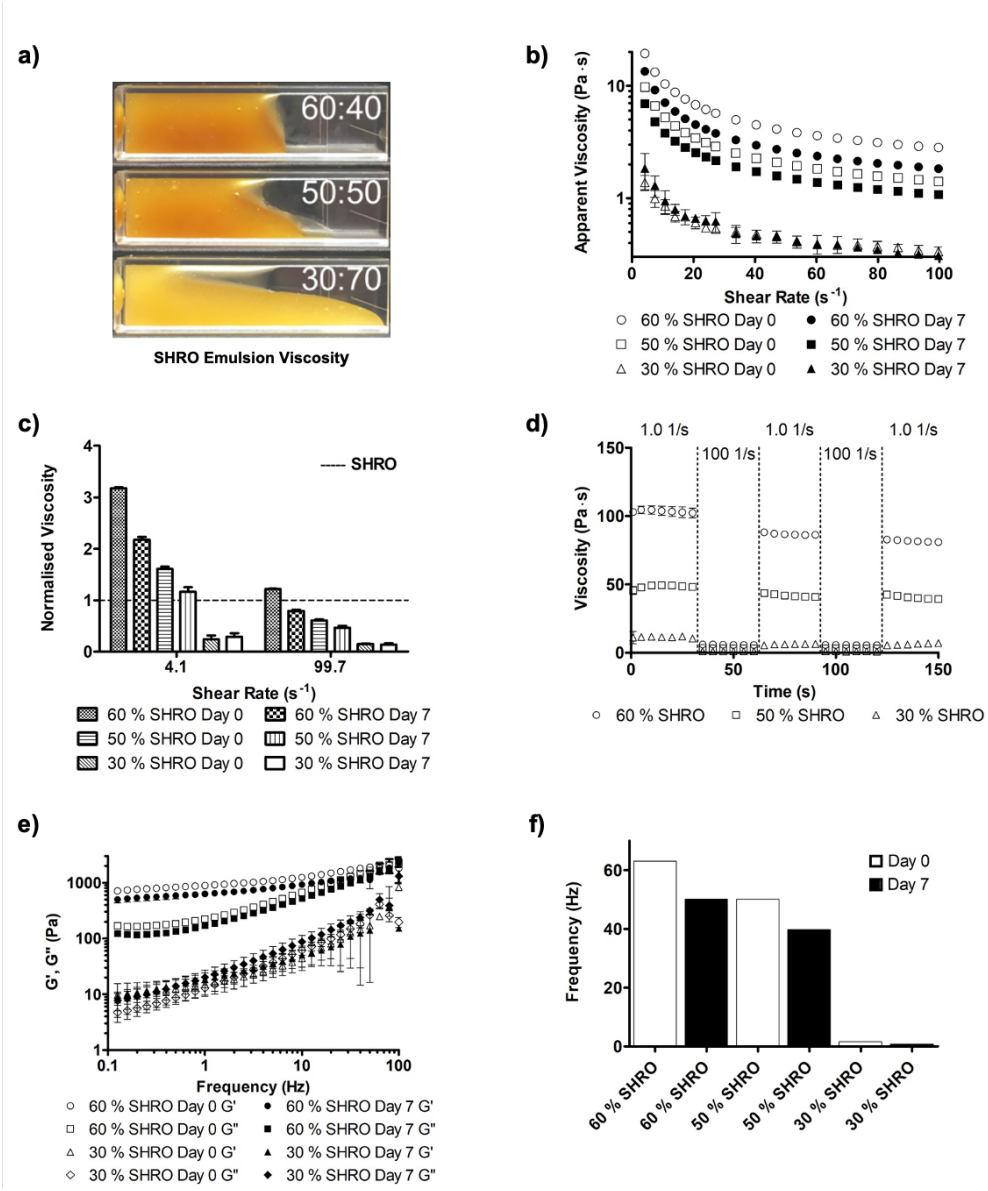

Figure 4.5. Visualisation of 60, 50 and 30% SHRO emulsion formulations (a), rheological characterisation of 60, 50 and 30% SHRO emulsions immediately after formulation (day 0) and after 7 days of storage at room temperature highlighting apparent viscosity (b), the viscosity of 60, 50 and 30% SHRO emulsions normalised against SHRO at low (4.1 s^{-1}) and high (99.7 s^{-1}) shear (c), shear thinning behaviour of 60, 50 and 30% SHRO emulsions at shear rates of 1.0 s^{-1} and 100 s^{-1} conducted at 21°C (d), frequency sweep of 60 and 30% SHRO emulsions conducted at 0.5% strain at 21°C (e) and the frequency at which G" begins to exceed G' for 60, 50 and 30% SHRO emulsions, conducted at 0.5% strain at 21°C (f). n = 3 and error bars represent standard deviation.

The size of the dispersed SHRO droplets were investigated after manufacture (day 0) and following 7 days of storage. The median diameter (D_{50}) of the droplets at day 0 for 30, 50 and 60% SHRO emulsions were found to be 4.92 ± 0.44 μm, 2.09 ± 0.07 μm and 2.07 ± 0.02 μm, respectively. For all samples there was no significant difference found in D_{50} droplet size between days 0 and day 7 (Table 4.1).

Table 4.1. Droplet sizes in 60, 50 and 30% SHRO emulsions at days 0 and 7. A two tailed t-test was conducted between D_{50} measurements for days 0 and day 7 in order to assess significance ($P<0.05$). n=3, ±standard deviation. *N=No and Y=Yes

Emulsion	Size (μm)			Sig. Diff. P < 0.05 (Y/N)*
	D_{10}	D_{50}	D_{90}	
30% SHRO				
Day 0	1.70 ±0.39	4.92 ±0.44	11.77 ±1.48	N
Day 7	1.48 ±0.21	4.11 ±0.31	9.88 ±0.64	
50% SHRO				
Day 0	1.22 ±0.08	2.09 ±0.07	3.61 ±0.09	N
Day 7	1.23 ±0.03	2.09 ±0.02	3.48 ±0.01	
60% SHRO				
Day 0	1.18 ±0.12	2.07 ±0.02	41.89 ±54.4	N
Day 7	1.12 ±0.09	2.42 ±0.26	72.13 ±5.93	

In order to assess the inversion of the emulsion under application of water and shear, conductivity measurements were taken. Neat paraffin oil has no measurable conductivity (0 µS) as such when it is the continuous phase the emulsions, regardless of SHRO concentration, exhibit no conductivity. Following addition of deionised water and applied shear, conductivity measurements showed readings of 219.7 ± 6.7 µS, 204.7 ± 6.7 µS and 181.3 ± 8.4 µS for 60, 50 and 30% SHRO emulsions respectively, indicating CPI (Figure 4.6a).

The ability to maintain antimicrobial efficacy of SHRO once formulated into an emulsion is paramount. Therefore, it was important to assess the levels of hydrogen peroxide production following phase inversion of the SHRO emulsions. It was found that the emulsion with the highest ratio of SHRO produced the most hydrogen peroxide; 60% SHRO emulsions produced 4.2 ± 0.2 µmol g^{-1} after 24 hours and the 50 and 30% formulations released significantly less at 1.9 ± 0.03 µmol g^{-1} and 0.7 ± 0.03 µmol g^{-1}, respectively (Figure 4.6b).

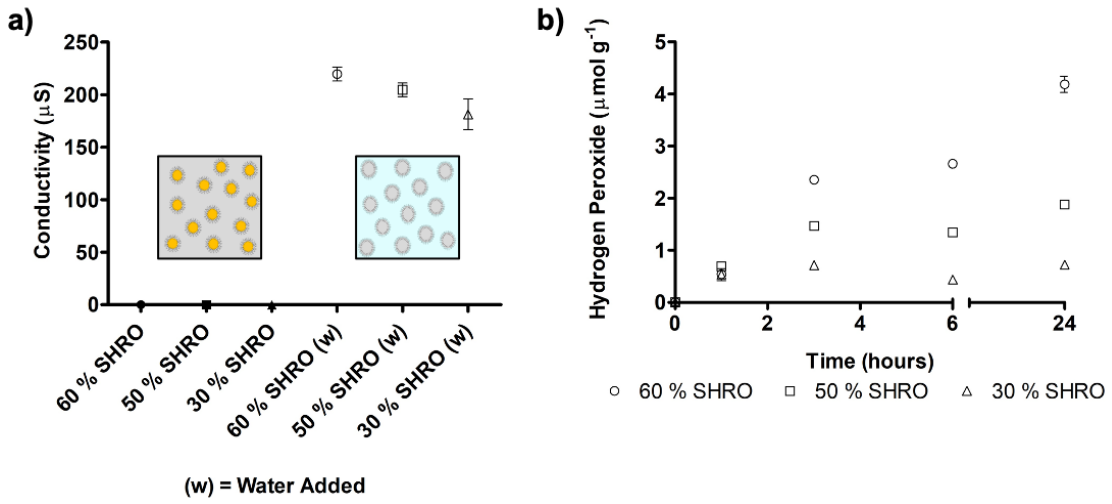

Figure 4.6 Conductivity of SHRO emulsions before and after phase inversion (a) and the normalised production of hydrogen peroxide over time (b). n = 3 and error bars represent standard deviation.

Unprocessed SHRO controls showed that the bioengineered honey had the potential to be efficacious against *S. aureus, P. aeruginosa and E. coli* (Figure 4.7a). Emulsions with 60, 50 and 30% SHRO were then tested against the same bacterial strains with efficacy compared to neat SHRO diluted in water to the same concentration as would be found within each emulsion. All formulations were shown to inhibit the growth of the Gram positive bacteria, *S. aureus* (Figure 4.7b). However, only 60 and 50% SHRO emulsions produced enough ROS to inhibit the growth of Gram negative bacteria *P. aeruginosa* and *E. coli* (Figure 4.7c-d). No significant difference was identified between the efficacy of the emulsions and their equivalent SHRO dilutions when tested against *S. aureus.* These results were replicated in both Gram negative bacteria with the exception of the 30% SHRO emulsions, which did not inhibit bacterial growth and may indicate that processing conditions are reducing the productivity of the enzyme (Figure 4.7)

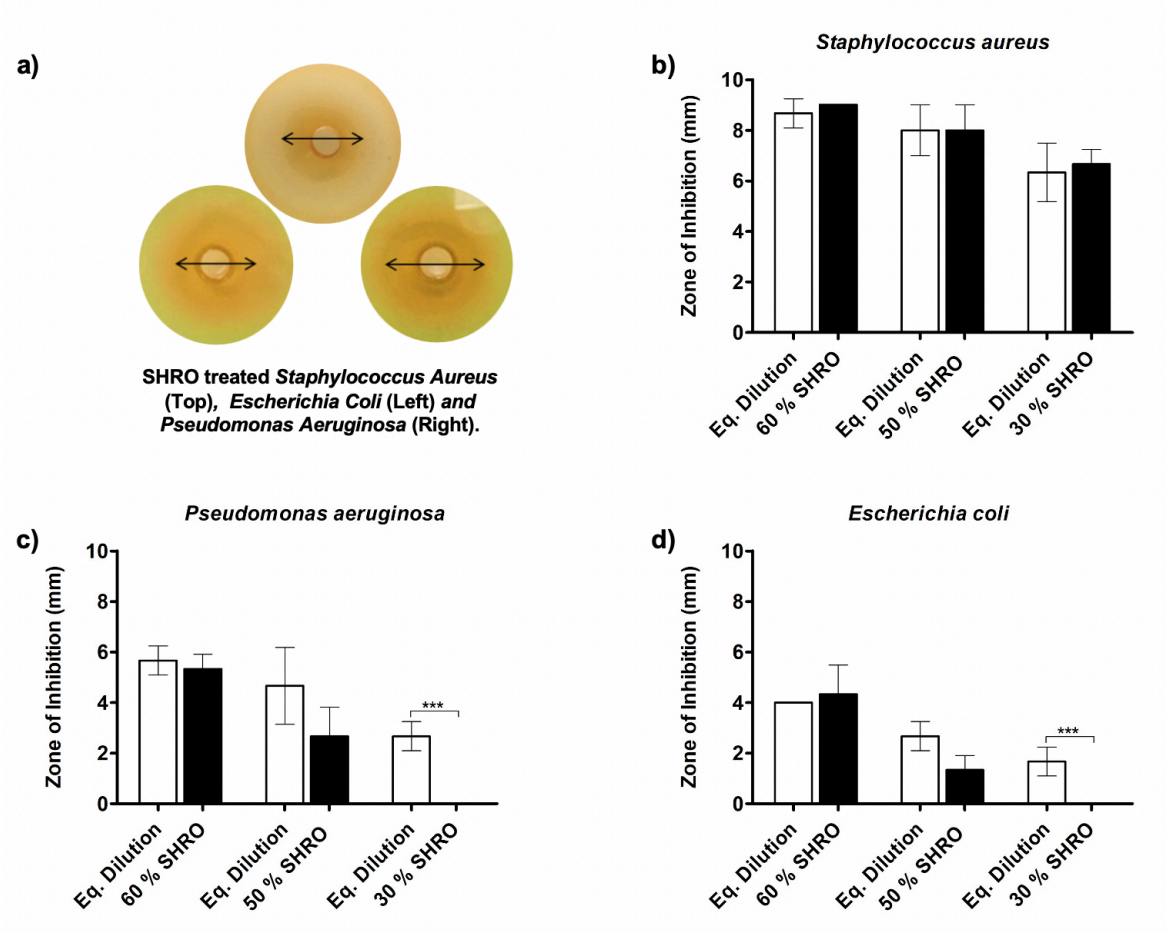

Figure 4.7. SHRO treated Staphylococcus aureus, Escherichia coli and Pseudomonas aeruginosa (a), Inverted SHRO emulsions and the zones of inhibition by treating Staphylococcus aureus (b), Escherichia coli (c) and Pseudomonas aeruginosa (d). Agar plates were inoculated with bacterial culture (OD_{600} 0.04) at 37°C for 24 hours before treatment. Bore hole size = 10 mm.

4.3.2 Investigation of the SHRO emulsion processes

In addition to optimising the formulation of the emulsion it was also important to assess if and how a change in processing conditions effects the stability of the emulsion. Investigations were carried out on 60% SHRO emulsions due to the presence of a higher concentration of active and the demonstration of greater stability than those previously tested. When formulated under standard conditions (10000 rpm for 10 min) at room temperature it was found that the

temperature during processing rose to 78.8 ± 2.1°C, which is above the denaturation temperature of the enzyme glucose oxidase (GOx - 55°C). In comparison when the same emulsion was formulated within an ice bath the final temperature upon the cessation of shear reduced by 22% and was determined to be significantly lower ($p < 0.0001$) at 61.5 ± 3.7°C (Figure 4.8a).

When stored and formulated at room temperature (21°C) no visual sedimentation over a 7 day period occurred, however when formed in an ice bath the same emulsion exhibited reduced stability, with 4.88 ± 1.8% sedimentation occurring after 7 days of storage at room temperature. In comparison when stored at a higher temperature (37°C) to replicate that of the body temperature, the sedimentation rate over the 7 day period increased for both the emulsion formulated at room temperature (1.87 ± 3.2%) and that formulated on ice (6.43 ± 3.7%) (Figure 4.8b).

Taking into consideration the denaturation temperature of GOx and due to the fact, that forming the emulsions at room temperature produces significantly more heat than emulsions formed in an ice bath, further investigation was conducted with emulsions formed on ice. The effect of different shear times and rates were explored where it was found that once the shear was reduced from 10000 rpm to 8000 rpm the final temperature of the emulsion fell below that of the denaturation temperature of GOx (42.3 ± 2.1°C). It was also identified that when the total time was reduced from 10 minutes to 8 minutes while still applying a shear rate of 10000 rpm, temperature also reduced to below that of the denaturation temperature of GOx (50.3 ± 2.2°C). Overall, a decrease in total shear time reduced the maximum processing temperature for all tested shear rates. (Figure 4.8c). However, the decrease in shear rate and

shear time appears to come at the cost of stability with greater separation occurring under these conditions (Figure 4.8d).

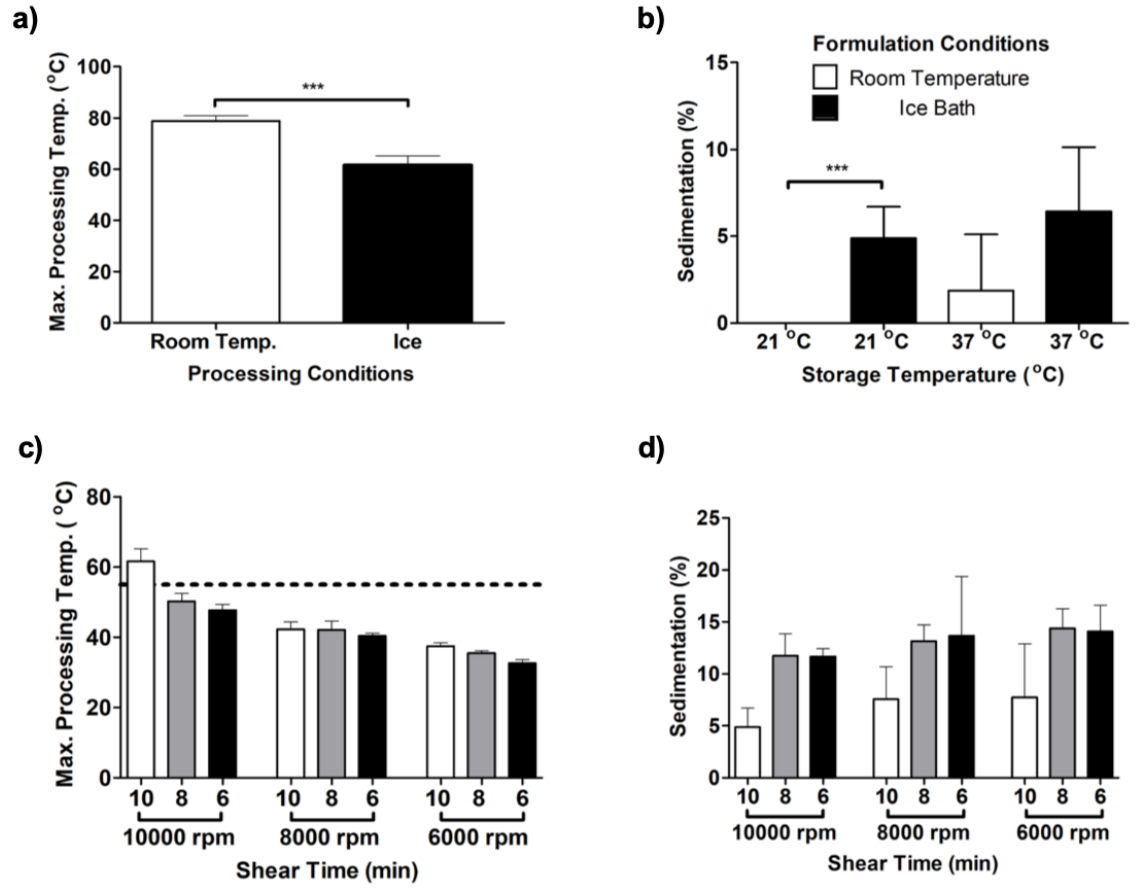

Figure 4.8. Investigating the effect of formulating a 60% SHRO emulsion at room temperature and using an ice bath (a), effect of emulsion stability after 7 days due to emulsion storage at 21°C and 37°C (b), effect of shear time and rate on maximum processing temperature when formulating emulsions in an ice bath (c), and effect of shear time and rate on emulsion stability after 7 days when emulsions are formulated in an ice bath (d).

4.3.3 SHRO cream formulation

All cream formulations exhibited pseudoplastic flow, with apparent viscosities for fume silica containing creams (SHRO_AR1 and SHRO_AR2) measured at 12.1 ± 1.1 Pa · s and 20.4 ± 1.4 Pa · s, respectively at a shear rate of 10 1/s (Figure 4.9a). These values were

significantly lower than that produced by creams containing xanthan gum with SHRO_XG1 and SHRO_XG2, which exhibited viscosities of 33.2 ± 6.7 Pa · s and 28.0 ± 1.1 Pa · s, respectively (Figure 4.9b). However, under higher shear (100 1/s) SHRO_XG1 (5.0 ± 0.6 Pa · s) produced comparable viscosities to that of SHRO_AR2 (6.2 ± 0.6 Pa · s). Interestingly, despite SHRO_XG2 displaying a similar shear thinning response to that of SHRO_XG1 until approximately 50 1/s, this behaviour appears to plateau between 50 1/s and 200 1/s only varying between 11.3 ± 0.9 Pa · s and 9.0 ± 0.1 Pa · s. In comparison SHRO_XG1 values decrease from 7.9 ± 1.9 Pa · s to 2.2 ± 1.0 Pa · s between the same shear rates.

Furthermore, when creams were rapidly switched from a low (1.0 1/s) to a higher shear (100 1/s) the viscosity reduces but typically recovers within a few seconds exhibiting shear thinning behaviour. With the exception of SHRO_AR1, all formulated creams were observed to exhibit hysteresis upon the application and removal of shear as indicated by the recovery viscosity being lower than the initial pre-shear measurement (Figure 4.9c-d). SHRO_XG2 was found to display the greatest difference in recovery viscosity with reductions of 44% (Figure 4.9d).

Analysis of the viscoelastic properties of the creams determined that SHRO_AR1 and both xanthan gum creams (SHRO_XG1 and SHRO_XG2) displayed higher storage (G') than loss (G'') moduli values across all tested frequencies (0 – 100 Hz). However, although SHRO_AR2 creams demonstrated comparable G' values to that of SHRO_AR1 creams at a frequency of 25 Hz (1060.3 ± 1.2 Pa and 1046.9 ± 2.6 Pa respectively), at 40 Hz G" in the SHRO_AR2 sample exceeded that of G' (Figure 4.9e-f).

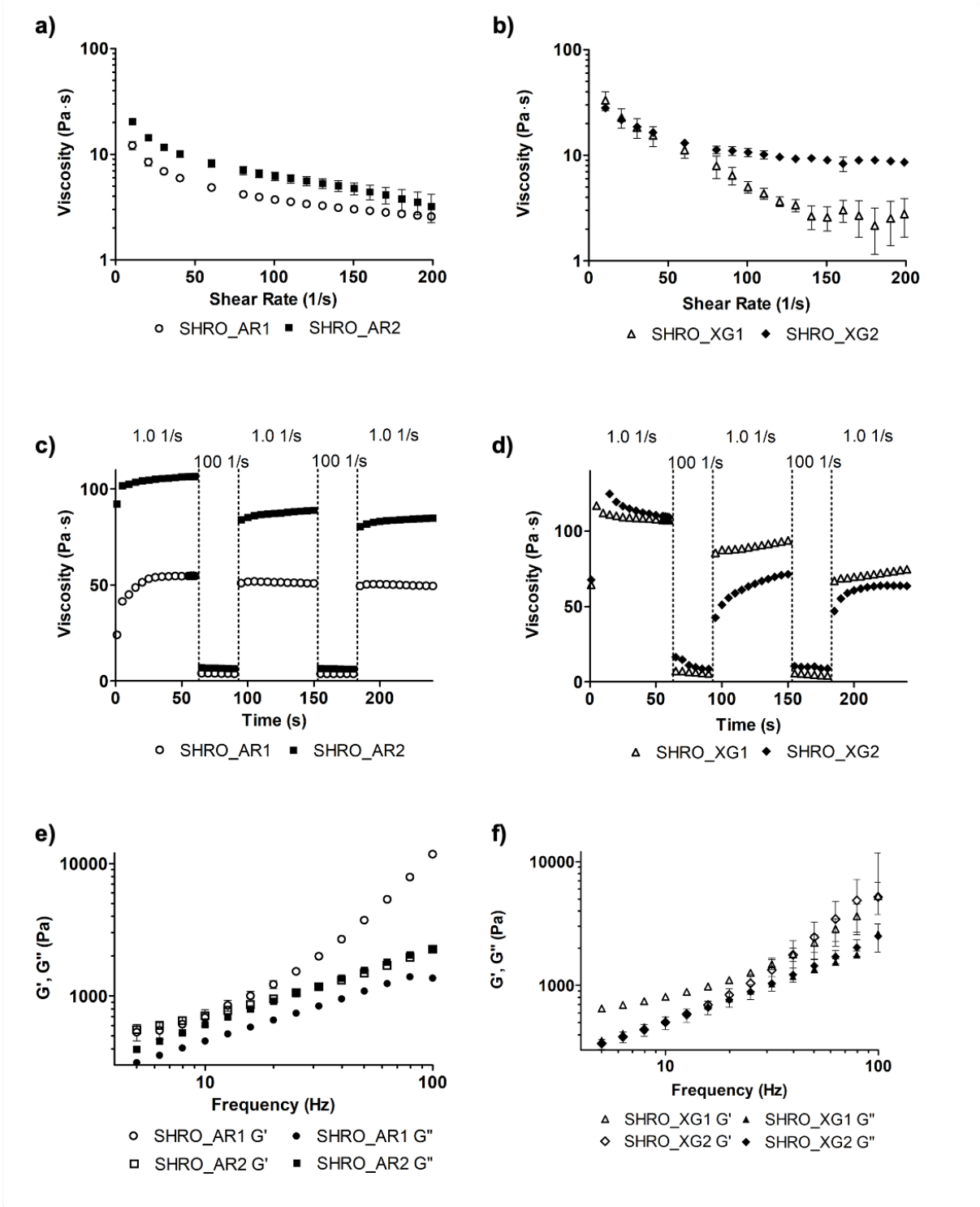

Figure 4.9 The viscosity of SHRO_AR1, SHRO_AR2 (a), SHRO_XG1 and SHRO_XG2 creams (b), alternating loops of high (100.0 1/s) and low (1.0 1/s) shear for SHRO_AR1, SHRO_AR2 (c), SHRO_XG1 and SHRO_XG2 (d), frequency sweeps of SHRO_AR1 and SHRO_AR2 (e), SHRO_XG1 and SHRO_XG2 (f) creams conducted at 0.5% strain and 21°C.

It was found that immediately after manufacturing, fumed silica creams exhibited smaller dispersed droplets and a narrower size distribution compared to formulations thickened with XG. SHRO_AR1 and SHRO_AR2 creams were found to have average median diameters (D_{50}) of 2.7 μm and 2.2 μm respectively (Table 4.2.). In contrast xanthan gum based creams produced wide particle size distributions with median diameters of 79.4 μm (SHRO_XG1) and 47.4 μm (SHRO_XG2) (Table 4.2.).

Table 4.2. Particle size distribution of Aerosil fumed silica creams (SHRO_AR1 and SHRO_AR2), and xanthan gum creams (SHRO_XG1 and SHRO_XG2).

Cream Formulation	Size (μm)		
	D_{10}	D_{50}	D_{90}
SHRO_AR1	1.4	2.7	5.0
SHRO_AR2	0.7	2.2	7.1
SHRO_XG1	35.5	79.4	141.3
SHRO_XG2	25.1	47.4	112.2

The ability to maintain antimicrobial efficacy of the creams once formulated was essential. Therefore, it was important to assess the levels of hydrogen peroxide production following phase inversion. It was found that both SHRO_AR1 (1.4 ± 0.5 μmol g^{-1}) and SHRO_AR2 (1.2 ± 0.3 μmol g^{-1}) produced similar hydrogen peroxide concentrations over a 24 hour period as those formulated using xanthan gum (SHRO_XG1 – 1.5 ± 0.4 μmol g^{-1} and SHRO_XG2 – 1.4 ± 0.07 μmol g^{-1}). However, SHRO_AR1 and SHRO_AR2 were found to produce 12.1 ± 0.5 and 11.5 ± 0.4 μmol g^{-1} of hydrogen peroxide respectively over a 7 day period. The was in clear contrast to the amount of hydrogen peroxide produced by SHRO_XG1 (3.1 ± 0.2 μmol g^{-1}) and SHRO_XG2 (2.4 ± 0.4 μmol g^{-1}) over the same time

period (Figure 4.10a). Despite these differences in released H_2O_2 concentrations, all creams were found to inhibit the growth of *S.aureus*. That said both fumed silica creams (SHRO_AR1 and SHRO_AR2) demonstrated the ability to produce zone of inhibition 42% larger than creams containing xanthan gum (SHRO_XG1 and SHRO_XG2) (Figure 4.10b).

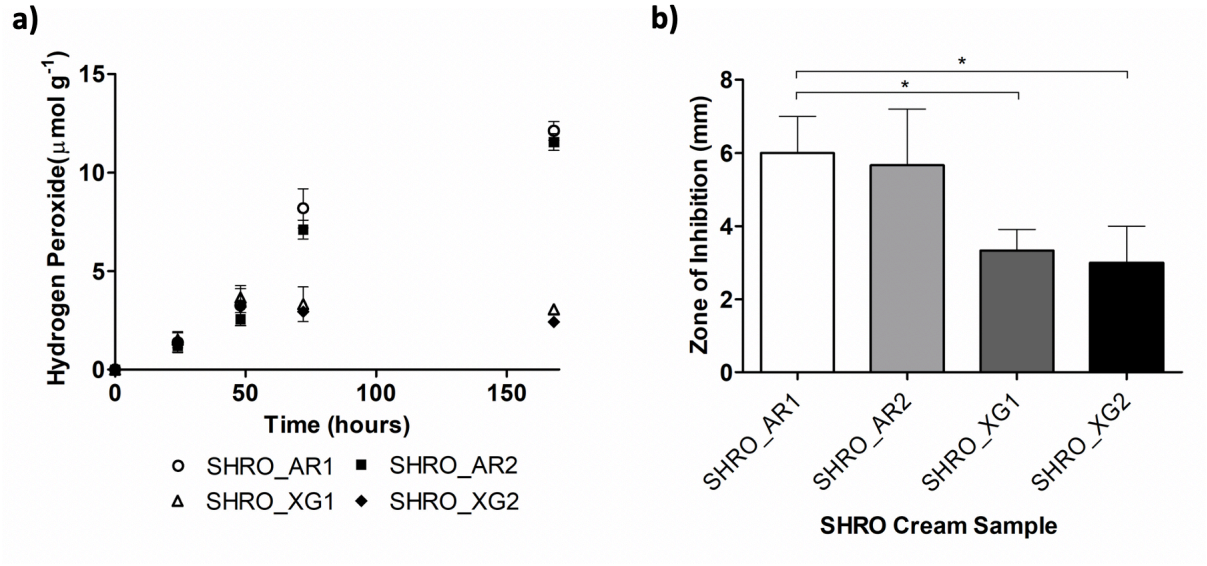

Figure 4.10 Normalised hydrogen peroxide production (a) and zones of inhibition from *Staphylococcus aureus*, treated by inverted Aerosil fumed silica (SHRO_AR1, SHRO_AR2) and xanthan gum creams (SHRO_XG1 and SHRO_XG2) (b).

4.4 Discussion

4.4.1 Optimisation of SHRO emulsion formulation

SHRO is engineered to deliver tailored doses of ROS and does not rely on specific flora or environmental conditions for its antibiotic activity like natural honeys, such as Manuka. Since it is engineered, this means that the level of potency can be controlled. Previous studies looking at the efficacy of SHRO have reported promising results, but despite this, there are limitations associated with delivering it to wound sites [43,44,167–169,418]. Currently much like commercial honey, it is a concentrated polymer blend that is sticky, viscous and hard to handle. These characteristics make it difficult to apply. This study has demonstrated a method by which to deliver SHRO that enables stable storage whilst maintaining the ability to inhibit bacterial growth when ROS production is trigged. This is achieved by the formulation of emulsions, which undergo CPI when exposed to water and shear.

By creating a SHRO-in-oil emulsion it allows modification of the viscosity, a critical characteristic that may determine ease of product delivery. In addition, by creating an emulsion devoid of free water the risk of premature production of ROS is reduced. This is essential for efficacy and shelf life. One of the main challenges when developing an emulsion is addressing the inherent thermodynamic instability of the system. Investigation of SHRO stability within different oil phases showed that paraffin oil produced an emulsion that did not coalesce or show signs of flocculation or creaming. Furthermore, the dispersed SHRO was found to sediment at a slower rate than emulsions formulated with olive, corn or vegetable oil (Figure 4.3a). In the cases of the emulsions containing vegetable, olive or corn oil the resultant instability was not reversible by means of inversion and shaking, indicating that phase separation had occurred. Although sedimentation is not ideal for this application, since it did not occur immediately and the dispersed droplets could be redistributed easily in paraffin oil, further investigation was

deemed necessary. Notably, the need for redistribution of dispersed phases before application is common practise among formulations that contain unstable components. Shaking can produce an even droplet distribution and therefore administration of a uniform dose, a factor highlighted for its importance by Stringer and Bryant in the formation of corticosteroid emulsions [449]. However, maintaining a formulation temperature lower than that of the denaturation temperature of GOx is crucial in order to protect efficacy and control dosing. Promisingly, a comparison of droplet size between days 0 and 7 demonstrated that no coalescence occurred for any of the formulated SHRO paraffin oil emulsions (Table 4.1).

Optimising dispersed phase ratios (30-60%) with a set concentration of PGPR (2%), found that formulations with a higher concentration of SHRO sedimented the least (Figure 4.3b). Further, no significant difference in droplet size for the 60% SHRO emulsion was observed over 7 days of storage. This effect is likely due to two factors. Firstly, the droplets formed in the 50 and 60% emulsions are small (around 2 μm) and suffer less from sedimentation compared to the 5 μm droplets of the 30% emulsion, thus reducing sedimentation at higher phase volumes [450]. The second factor is that as more SHRO is added the volume occupied by droplets in the system also increases. This higher packing fraction physically prevents sedimentation and results in an increase in viscosity (Figure 4.5), which is known to reduce sedimentation speed [253,451]. Notably, both 50 and 60% SHRO emulsions showed no sedimentation over 7 days. The low HLB value (1.5) associated with PGPR clearly aids the stabilisation of the SHRO in oil system. It was determined that 2% was the minimum concentration of PGPR required to stabilise these systems (Figure 4.3c). This was further explained by conducting IFT measurements where it was confirmed that at 2% PGPR concentration the IFT was significantly reduced in comparison to lower concentrations with a reduction in IFT of 85.52% compared to systems without PGPR. It was also found that higher

concentrations of PGPR did not further decrease the IFT between the phases and as such was the optimal concentration tested (Figure 4.4).

Promisingly, all of the paraffin oil emulsions displayed shear thinning behaviour (Figure 4.5b). This will help to ease delivery, as common methods of administration, such as sprays and creams, often involve the application of shear. Sprays however, by definition, produce a mist of fine droplets which although provides a more convenient application for the end user, it can be difficult to apply enough such that a therapeutic dose is delivered. Therefore, in order to realise this as a viable strategy higher efficacy formulation may be required. This is in contrast to that of a cream delivery whereby the user can apply the product more liberally to the wound area. Although all of the paraffin oil emulsions displayed shear thinning behaviour, after storage for 7 days there was a significant ($p < 0.05$) reduction in viscosity at all tested shear rates for 60 and 50% SHRO, interestingly a phenomenon not apparent in the 30% formulations. The difference between the apparent viscosity of 60 and 50% SHRO emulsions on days 0 and 7 is likely due to an interaction between dispersed droplets, which requires greater shear than that exerted from shaking to mix the emulsion back to its original form [450,451]. This was not the case with the 30% SHRO emulsion; with greater range of movement, due to the lower packing fraction and lower interactions between droplets, viscosities comparable with that of day 0 could be achieved. As demonstrated by the results here and as described by Stokes law, an increase in viscosity slows the rate of sedimentation [451–453]. Future applications could use modifiers to increase the viscosity, thus avoiding the need to shake before use. This may however prevent the use of delivery systems only suitable for lower viscosity fluids, for example pump spray bottles. This data highlights a trade-off between stability and ease of application; while the 30% emulsion exhibits 29.6 ± 8.6% sedimentation after 7 days it has the lowest viscosity widening the possible administration devices that could be used. That said, it is notable

that under high shear all SHRO emulsions exhibited significantly reduced viscosities (Figure 4.5c), which will aid delivery and application. Further, it is advantageous that when all formulations were rapidly switched from high to low shear, in the absence of water, viscosity is quickly recovered (Figure 4.5d). This means that the viscosity can be reduced in order to deliver the emulsion but then as the shear rate reduces the emulsion quickly becomes more viscous meaning it is more likely to be retained at the site of delivery [454,455]. All SHRO emulsions displayed hysteresis, with 60% emulsions demonstrating the highest decrease in viscosity after 3 cycles (21%.) However, it was not deemed to affect the final application but warrants further investigation.

Frequency sweeps were also conducted to elucidate the viscoelastic properties and stability of the emulsions. Oscillatory rheology was used to determine the value of the storage (G') and loss modulus (G") at between 0 – 100 Hz, with care that testing was conducted at a strain value (0.5%) within the LVR of all samples. This was concluded to be an important assessment of emulsion stability by Tadros, 2004 [253]. The viscosity profile of the emulsions revealed that both G' and G" rapidly increase with frequency (Figure 4.5e), with the dependence on frequency considered to be due to the effect of energy dissipation within droplets [254]. The relative values of G' and G'' are known to be indicative of a change in fluid structure [255]. At 5 Hz, 60 and 50% SHRO emulsions exhibited a higher G' than G'', which demonstrates they exhibit a gel like structure. In contrast, 30% SHRO formulations were observed to have similar G' and G'' values (28.9 ± 8.7 – 54.0 ± 17.1 Pa) at this frequency. This correlates with observations that the stability is increased in emulsion formulations with higher concentrations of SHRO as droplets begin to structure and cause an increase in viscosity [251]. At higher frequencies the emulsions undergo a viscoelastic transition, this is where G" exceeds that of G' [456]. This occurred for all samples tested indicating that the droplets within the

emulsion interact at a small length scale and as such do not relax quickly. This decreases the elastic behaviour and thus becomes more viscous, or liquid-like [457]. The frequency at which G' and G'' crossover increased with rising SHRO concentration. This means that the ease of delivery decreases with increasing SHRO as more energy is required to extrude the emulsion from the delivery device.

In addition to easing the delivery of SHRO, this work aimed to create an emulsion that could be triggered to release ROS *in situ*. Through the addition of water under shear it was possible to cause the developed emulsions to catastrophically phase invert (CPI) leading to activation of SHRO (Figure 4.6a). It is proposed that water may either be co-delivered with the emulsion or media at the wound site could be used in order to trigger release. However, since available moisture will significantly vary at different wound sites it is suggested that co-delivery may be a more reproducible approach [308,458]. In order to confirm that CPI had occurred, conductivity measurements were taken (Figure 4.6a). Neat paraffin oil has no measurable conductivity. When SHRO is dissolved in deionised water a current is allowed to flow due to the greater mobility of free ions [456]. Water was added to the emulsion and shear was applied causing an increase in conductivity to 181.3 ± 14.6 – 219.7 ± 6.7 μS with formulations containing higher concentrations of SHRO allowing a greater current to flow. These measurements confirmed that CPI had occurred and that the continuous phase is a combination of SHRO and water. However, limitations within this study only addressed CPI at one time point after formulation and did not measure conductivity over time. This would therefore provide a more conclusive assessment to ensuring availability of the active to react with water throughout therapeutic window (24 hours).

It is known that the release of ROS, such as hydrogen peroxide is the dominant factor to the antimicrobial efficacy of SHRO [418]. As such, it was critical that SHRO droplets within the emulsion could still be activated to produce ROS after being exposed to water through phase inversion. As expected, it was found that the emulsion with the highest ratio of SHRO (60%) produced the most hydrogen peroxide; 4.2 ± 0.2 μmol g^{-1} after 24 hours. A controlled and predictable release is critical to ensuring an effective and safe dose is delivered throughout the period of application [459]. Promisingly, release of ROS was observed for the entire time period tested (Figure 4.6b). For a topical application, stable release over 24 hours would mean that the treatment would only have to be applied at most once daily and therefore makes it more convenient for the patient or healthcare professional applying the product, however more *in vitro* testing would be required in order to further inform on dosing regimens. In addition, as elucidated in Figure 4.8a the maximum temperature reached during formulation of the emulsion was higher than that of the denaturation temperature of GOx, and although there is little evidence to support that efficacy was significantly altered it cannot be ruled out. Therefore, alternative formulation methodology should be explored to minimise the implications exposing GOx to high temperature may have on the efficacy of the formulation.

Having assessed the viability of ROS production from the formulated SHRO emulsions, clinically relevant bacterial species found in topical wounds [41] were inoculated onto agar plates and the SHRO emulsions ability to inhibit growth was measured. Unprocessed SHRO controls showed that the bioengineered honey had the potential to be efficacious against *S. aureus, P. aeruginosa* and *E. coli* (Figure 4.7a). This is consistent with previous *in vitro* evaluations of SHRO [43,44,165,167,168,418,460]. Despite releasing different levels of ROS over 24 hours, inhibition of Gram positive bacteria *S. aureus* was achieved for all tested inverted emulsions (Figure 4.7b). In contrast, inhibition of *P. aeruginosa* and *E. coli* was only observed for

emulsions containing 50 or 60% SHRO. It is known that Gram negative bacteria are inherently harder to kill compared with Gram positive species since they contain an extra layer of protection in the form of an outer membrane. Previous studies have demonstrated that higher doses of ROS are necessary to inhibit Gram negative bacterial growth [436]. The ability to increase the baseline efficacy of SHRO, as reported by Dryden et al., [43] may provide a solution. Working with a batch of SHRO with higher ROS production would enable the lower viscosity characteristics of 30% SHRO emulsions to be exploited to ease application while delivering a dose also capable of killing Gram negative bacteria.

4.4.2 Investigation of SHRO emulsion processing

To further develop and improve the emulsion system the emulsification process was investigated, specifically shear rate and length of shear application. 60% SHRO emulsions were chosen for this study since they exhibit greater stability compared to other formulations and contains the most active. As aforementioned, upon assessing the temperature of the emulsion following formulation it was discovered that this was far in excess of that of the denaturation temperature of the enzyme glucose oxidase (55°C), which in theory could hinder efficacy and affect the ability to administer a uniform dose [151]. This enzyme is responsible for the oxidation of glucose and the subsequent production of hydrogen peroxide, which is necessary for the product to elicit an antimicrobial effect [152]. Therefore in order to protect further formulations from loss of efficacy emulsions were formulated using an ice bath, inspired by the work of Peng., *et al.* [461]. This significantly reduced the maximum processing temperature by 22% to 61.54 ± 3.7°C (Figure 4.8a). By forming the emulsion in an ice bath, however it did comprise the emulsion stability, as it was found that when stored bench top at 21°C, sedimentation occurred over 7 days, which did not occur when processing was conducted at room temperature. As storage temperature was increased to 37°C to replicate that of body

temperature, emulsions produced both using an ice bath and at room temperature demonstrated instability. Those formed on ice however were found to sediment the most (Figure 4.8b). This is likely due to the fact that higher temperatures have a greater ability to reduce the viscosity of emulsion components during the formulation process, particularly in this case that of the dispersed phase [187]. This reduction in temperature caused by the use of an ice bath means there is less energy in a system with a higher viscosity, leading to larger droplets which sediment faster. In storage higher temperature however increase the Brownian motion of the particles, accelerating instability mechanisms such as sedimentation and coalescence [462].

During the optimisation of the formulation the efficacy of the emulsions were tested against an equivalent dilution of SHRO where it was demonstrated that in most cases there was no apparent reduction in inhibitory ability. This technique however is low in resolution and at lower concentrations (30% SHRO) against Gram negative bacteria, where zone sizes were considerably smaller, the equivalent dilution was found to inhibit growth, but the emulsion did not. This may, at least in part, be due to the processing conditions. As formulating on ice significantly reduced the final emulsion temperature post processing further investigations were carried out to assess how a change in shear time and rate affects the temperature and the stability of the emulsion. Both a reduction in shear time and shear rate were found to have a negative impact on the rate of sedimentation with an increase of 55.2% when shear was reduced from 10000 rpm (4.88 ± 1.8%) to 8000 rpm (7.57 ± 3.1%) and an increase of 140.9% when the total shear time was reduced from 10 minutes (4.88 ± 1.8%) to 8 minutes (11.75 ± 2.1%) (Figure 4.8d). However, a reduction in both shear time and shear rate were found to positively impact the final emulsion temperature; emulsions formulated at speeds of 8000 rpm over 10 minutes resulted in a maximum processing temperature below that of the

denaturation temperature of glucose oxidase (42.30 ± 2.1°C). Equally a total shear time of 8 minutes while keeping the shear rate at 10000 rpm was also found to reduce the temperature to below the denaturation threshold (50.30 ± 2.2°C) (Figure 4.8c). As aforementioned the occurrence of sedimentation although not ideal, providing it can easily be re-disbursed and does not lead to coalescence, can be mitigated by imposing a shake before use directive.

4.4.3 SHRO cream formulation

Creams were formulated with 1% (SHRO_AR1) and 2% (SHRO_AR2) Aerosil fumed silica (AR816) to thicken the continuous phase of the emulsion or xanthan gum (SHRO_XG1) to thicken the dispersed phase of the emulsion. Magnesium sulphate heptahydrate was added to one formulation of xanthan gum cream (SHRO_XG2) with the aim of reducing polymer entanglements between the glycerol and thickening agent, in line with methodology proposed by Ciullo., *et al.* [463].

By utilising thickening agents such as; fumed silica and xanthan gum, it allows for the rheological properties to be tailored. In addition to building upon the SHRO emulsion formulations it was essential that efficacy was maintained, and instability issues addressed. While the size of the droplet does not directly influence the production of ROS as the emulsions are activated by phase inversion, they do impact stability. One of the issues highlighted in the development of the SHRO emulsion was that of sedimentation, by incorporating fumed silica or xanthan gum into the formulation this was found to significantly increase stability as there was no indication of sedimentation after 1 month of storage at 37°C. Furthermore, droplet sizes indicate that while dispersed droplets in the fumed silica creams were similar in size to that of the SHRO emulsions at approximately 2.5 μm, xanthan gum based creams produced wider particle size distributions with median diameters of 79.4 μm (SHRO_XG1) and 47.4 μm

(SHRO_XG2) (Table 4.2). In SHRO formulations it was noted that the bigger the droplet size the greater the instability (Stokes law) this still remains the case, however as the creams demonstrate a greater bulk viscosity than that of the SHRO emulsions, they exhibit a slower rate of sedimentation [202,212].

Rheological measurements indicated that both xanthan gum creams have significantly higher viscosities than that produced using fumed silica, however similar to the SHRO emulsions all creams exhibited pseudoplastic flow, demonstrating a reduction in viscosity with an increase in shear, a characteristic ideal for cream application (Figure 4.9a). At low shear (10.0 1/s), as expected creams with a higher concentration of fumed silica displayed higher viscosities with SHRO_AR2 producing a viscosity of 20.4 ± 1.4 Pa · s compared to 12.1 ± 1.1 Pa · s for SHRO_AR1. More viscous creams, however, were produced with xanthan gum with viscosities of 33.2 ± 6.7 Pa · s (SHRO_XG1) and 28.0 ± 1.1 Pa · s (SHRO_XG2) at the same shear rate. Low shear rates are known to deconstruct random polymer entanglements and explains the primary decreases in viscosity observed. At higher shear rates however, the reduction in viscosity is more likely attributable to the cleavage of hydrogen bonds and the breakage of Van der Waal interactions, leading to thixotropic effects [464]. Although SHRO_XG2 did not respond in the same manner as the other cream samples as it appears to plateau in viscosity at a much lower shear rate (80.0 1/s) and maintains a higher viscosity in comparison to the other samples. This effect is likely attributable to the interaction of XG with the magnesium salt [463].

Furthermore, when creams were rapidly switched from a low (1.0 1/s) to a higher shear (100 1/s) the viscosity reduces but quickly recovered, this is a characteristic that would enable ease of delivery to the application site where viscosity recovery would facilitate product

retention locally. However, the SHRO cream formulations, with the exception of SHRO_AR1, did display hysteresis upon the application and removal of shear to a greater extent than the SHRO emulsion. SHRO_XG2 was found to display the greatest difference in recovery viscosity with reductions of 44% (Figure 4.9d). This could imply a permanent breakdown of microstructure, reducing its ability to be retained on the skin with time [465].

Frequency sweeps further elucidated the viscoelastic properties of the cream. In line with the results measured for SHRO emulsions both G' and G" were found to increase with frequency an effect attributed to the dissipation of energy within the droplets (Figure 4.9e-f) [253,254]. SHRO_AR1 and both xanthan gum creams (SHRO_XG1 and SHRO_XG2) displayed higher G' than G" values across all tested frequencies. This indicated that under all tested conditions the formulation retains a gel like structure. However, although SHRO_AR2 creams demonstrated comparable G' values as SHRO_AR1 creams at low frequencies (25 Hz) both G' (1060.3 ± 1.2 Pa) and G" (1046.9 ± 2.6 Pa) displayed similar values at 40 Hz, which indicates a breakdown of the microstructure (Figure 4.9e-f) [255]. This is not ideal since it may increase variability of performance if this formulation is applied at different rates.

As with the SHRO emulsion, the development of an SHRO cream was with the intention to trigger the activation of ROS *in situ* through catastrophic phase inversion. In order to assess that this phenomenon still occurred when the creams were subjected to water and shear, a hydrogen peroxide assay was conducted. It was found that all creams; SHRO_AR1 (1.4 ± 0.5 μmol g^{-1}), SHRO_AR2 (1.2 ± 0.3 μmol g^{-1}), SHRO_XG1 (1.5 ± 0.4 μmol g^{-1}) and SHRO_XG2 (1.4 ± 0.01 μmol g^{-1}) produced similar amounts of hydrogen peroxide over a 24 hour period. However, concentrations of hydrogen peroxide produced by creams require 48 hours (2.2-4.2 μmol g^{-1}) to reach comparable levels as that produced by the equivalent SHRO

emulsion after 24 hours (4.2 ± 0.2 μmol g^{-1}). This implies that the addition of a thickening agent reduces the rate at which hydrogen peroxide is produced. It was also demonstrated that whilst both fumed silica creams, SHRO_AR1 (12.1 ± 0.5 μmol g^{-1}) and SHRO_AR2 (11.5 ± 0.4 μmol g^{-1}), produced similar amounts of hydrogen peroxide over a 7 day period. Those formulated using xanthan gum, SHRO_XG1 (3.1 ± 0.2 μmol g^{-1}) and SHRO_XG2 (2.4 ± 0.4 μmol g^{-1}), produced significantly less H_2O_2. This is likely due to the addition of glycerol, which is required in these formulations to dissolve the xanthan gum, hence there is lower concentration of SHRO within the cream (Figure 4.10a). However, despite producing differing amounts of hydrogen peroxide, all creams were found to inhibit the growth of *S.aureus.* Fumed silica creams, however, exhibited significantly large inhibition zones of inhibition (42%) than XG formulations (Figure 4.10b).

4.5 Conclusion

The overall aim of this thesis is to address the need for alternative topical infection treatments to current antibiotics. In this chapter this has been achieved by successfully formulating an emulsion containing SHRO, which has been engineered to enable triggered release of antimicrobial reactive oxygen species via phase inversion. The hypothesis that an oil-based emulsion would protect, store, and release SHRO under shear and dilution with water at the time of application has been demonstrated *in vitro*. This mechanism could be initiated by added or topical moisture, such as wound exudate and shear produced by hand or a delivery device.

Emulsion composition was optimised to achieve the desired shear thinning behaviour, easing delivery and promoting retention of the active at the site of infection. Stability observations revealed that a small degree of sedimentation did occur, over 7 days, for emulsions containing a dispersed phase of <50% SHRO, this was shown to be reversible by shaking. Conveniently this redistributed droplets evenly, which is known to improve dose reproducibility. Hydrogen peroxide measurements indicated that formulations with higher concentrations of SHRO produced greater levels of reactive oxygen species with 60% SHRO emulsions producing 4.2 ± 0.2 μmol g^{-1} after 24 hours. Emulsions with 30, 50, and 60% SHRO were tested against clinically relevant bacterial species; *Staphylococcus aureus*, *Pseudomonas aeruginosa* and *Escherichia coli.* It was found that 60 and 50% SHRO emulsions were efficacious against all species.

In addition, it was found that post formulation the temperature of the emulsion was higher than that of the enzyme's denaturation temperature. As a result, the formation of emulsions in an ice bath was investigated, which significantly reduced the temperature of the

emulsion post processing. Furthermore, processing temperature was also reduced below the critical denaturation temperature by reducing shear rate and shearing time, however these process alterations did enhance the rate of droplet sedimentation.

Following optimisation of a based SHRO emulsion, Aerosil fumed silica and xanthan gum were explored as thickening agents to create cream formulations. It was discovered that 1% fumed silica displayed better rheological characteristics than xanthan gum samples, whilst also producing a product with enhanced stability and maintaining a shear thinning effect for ease of delivery. Importantly, efficacy was also maintained, demonstrating that emulsion technologies can be used to effectively store and deliver water sensitive antimicrobials, with the possibility to engineer triggered release mechanisms that facilitate *in situ* activation.

CHAPTER FIVE

5. REACTIVE OXYGEN POWDER DELIVERY SYSTEMS

5.1 Introduction

Given the significant use of lyophilisation to increase the shelf-life and stabilise sensitive medical products, including antibiotics and enzymes [304], this may be a promising formulation approach to transform SHRO into a non-adherent material while enabling controlled release of ROS. There are a number of drying methods that may be employed to create lyophilised powders. Of particular relevance to temperature sensitive therapeutics, like SHRO, freeze drying is a low temperature (-55°C) lyophilisation technique that utilises a vacuum (4 x 10^{-4} mbar) to extract water from a sample by means of sublimation [283]. This process transforms a material from its solid phase into its gaseous phase without going through the liquid intermediary step [466]. As such high processing temperatures are avoided, which is advantageous given GOx within SHRO denatures at temperatures greater than 55°C (Eq. 5.1).

$$C_6H_{12}O_6 + H_2O + O_2 \xrightarrow{GOx} C_6H_{12}O_7 + H_2O_2 \quad \text{(Eq. 5.1)}$$

Producing honey powder via freeze drying would facilitate easy delivery by reducing issues related to the viscosity and adhesiveness associated with the raw product. This method of delivery would also enhance usability by being more tailorable to the end use allowing for system that can be packaged in multiple ways such as that of a sachet, powder shaker or powder

spray device. However, formulating a dry powder from SHRO is inherently challenging due to the high concentration of sugars and organic acids [293,294]. This composition produces a product characterised by low glass transition temperatures (T_g), often reported below -50°C [291,292]. At the T_g honey changes from a glassy state to a soft viscoelastic material with a very high viscosity [295]. In order to produce a powder, the material must remain in its glassy form at operational temperatures, i.e. room temperature [296]. During the freeze drying process if the temperature of the honey in the drying chamber is higher than that of the T_g the result is a viscoelastic material that will adhere to the chamber surface. This prevents the drying process from occurring and the formation of a free-flowing powder is not possible [296,297]. To dry a material of this type, either the temperature of the drying chamber has to be kept below that of the T_g, however this can be difficult due to the T_g of honey often being lower than that of the drying chamber (-55°C), or the composition of the material needs to be modified to achieve a higher T_g. In order to increase the T_g drying agents such as starch, maltodextrin or gum Arabic are typically added [298]. These substances increase the T_g by reducing particle to particle cohesion, and in turn less agglomeration reduces water-holding capacity [299,300]. This means that the product remains in a glassy state throughout the drying process, enabling the water content of the honey to be removed and a powder to be formed [301].

Once lyophilised, products are notoriously hydroscopic which can cause storage issues and airtight containers must be used in order to prevent rehydration [467]. In addition to, in order to reduce the relative humidity within the sample container desiccants are often used [468]. Given that the antimicrobial mechanism of SHRO is initiated by water it is essential that SHRO powders are stored to minimise rehydration post freeze-drying.

As an alternative to formulating powder from SHRO, a ROS producing powder could theoretically be formed totally synthetically by combining only the compounds needed for the enzymatic oxidation of glucose to take place (Eq. 5.1). This mixture of glucose and GOx would therefore utilise the same mechanism of action as that of SHRO but without the additional components found within honey. Such a system still possesses limitations on storage similar to that of SHRO powder, in addition to potential issues with enzyme stability.

Beyond powder formulation, given the known benefits of using hydrogels in wound care, the incorporation of a superabsorbent to the product in order to facilitate *in situ* gelation may enhance treatment. Specifically it has been shown that the moist environment provided by a hydrogel dressing simplifies healing phases such as granulation, the repair of the epidermis, and the removal of dead tissue [314–317]. Furthermore, by gelling *in situ* it will also form a barrier preventing the any further infection or wound contamination from the environment. The advantages of formulating a product in such away over existing commercially available products (Table 2.5) is that it provides greater functionality. The superabsorbent component would be able to remove exudate from the wound similar to the action of that of foam, alginate and hydrofiber dressing, yet once exudate has been removed it can keep moisture localised ensuring that the wound does not dry out, as is the action of a hydrogel dressing. Existing hydrogel product are currently applied already hydrated and thus their capacity to absorb is very limited, therefore their applicational purpose is to provide hydration to the wound site. However, much like the absorbent dressing currently on the market there is limitations on how much exudate is able to be absorb and this will dictate how often the dressing is changed.

For the first time, this study demonstrates the potential to formulate a powder system that enables the delivery of ROS as an alternative to current antimicrobials or antibiotics. Both

the transformation of SHRO into a powder, with the aid of a drying agent, and the formulation of synthetic reactive oxygen powder, circumvents current issues with water sensitivity, viscosity, and adherence therefore easing delivery and broadening clinical application. It is further proposed that the addition of a superabsorbent to form a hydrogel upon contact with wound exudate, enables *in situ* ROS activation (Figure 5.1). Overall, this chapter reports the formulation of a novel antimicrobial technology that provides a physical barrier to protect the wound from further infection, creates a moist environment to facilitate healing, and has the potential to be used in combination with a range of therapeutic molecules.

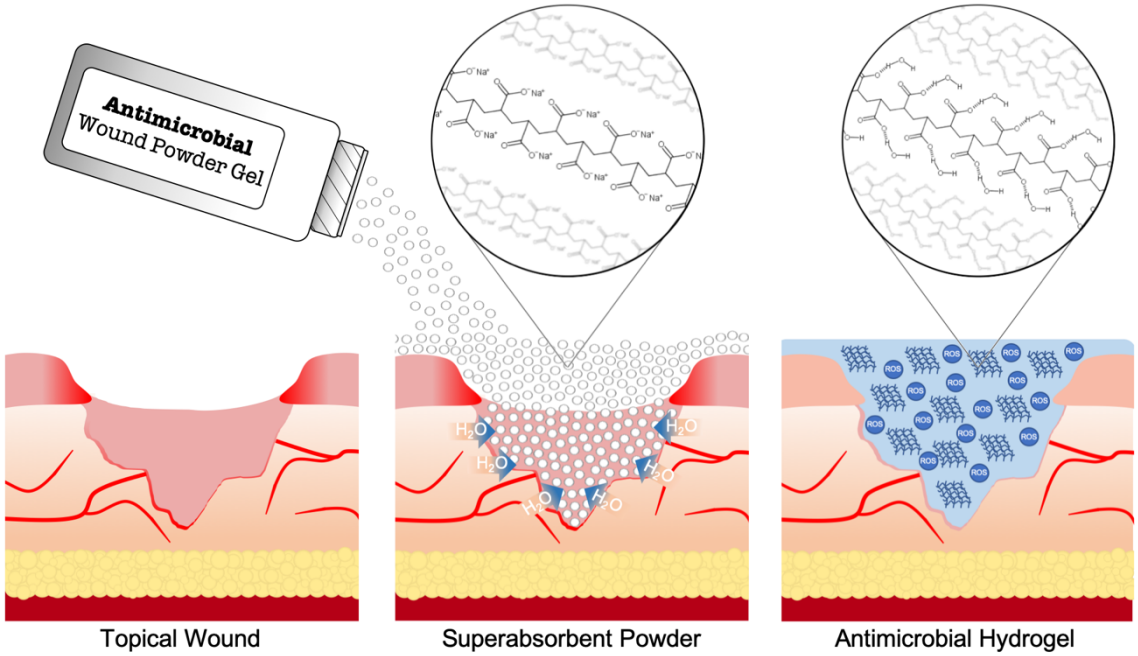

Figure 5.1. A schematic diagram depicting the topical application of powder to a wound site, which is activated *in situ* to produce reactive oxygen species and elicit an antimicrobial response, whilst also rapidly forming a hydrogel to provide an ideal, protective, wound healing environment.

5.2 Materials and Methods

5.2.1 SHRO powder formulation

Neat SHRO (Matoke Holdings, UK) was added in varying concentrations (50 – 70%) to either methylated-β-cyclodextrin (MCD – CycloLab R&D Ltd., Hungary) or (2-hydroxypropyl)-β-cyclodextrin (HCD - CycloLab R&D Ltd., Hungary). Concentrations of SHRO present within a formulation are denoted as % (w/w) and are indicated by the numerical value adjacent to the drying agent acronym e.g. MCD 50 utilises methylated-β-cyclodextrin as the drying agent and contains 50% SHRO. Further, the addition of sodium polyacrylate (SPA – Sigma Aldrich, UK) was explored with specific MCD or HCD formulations. Incorporation of SPA is indicated by the percentage value adjacent to the sodium polyacrylate acronym.

5.2.2 Freeze drying

Before lyophilisation, SHRO, drying agent and those formulations that contain SPA were then mixed at room temperature 21°C using a spatula until a homogenous paste was formed. Formulations were then frozen at -80°C for 24 hours and freeze dried for 72 hours using a Lablyo mini freeze dryer (Frozen in Time, UK). Freeze drying was performed under high (4×10^{-4} mbar) vacuum conditions with the condenser temperature set at -55°C. Upon removal from the freeze dryer, samples were milled using a pestle and mortar to form a powder.

5.2.3 Synthetic reactive oxygen powder formulations

Mixtures of analytical reagent grade D-glucose anhydrous (Fischer Scientific, UK) and GOx (Matoke Holdings, UK) at concentrations of 0.2, 0.1 and 0.05% w/w were formed. Powders were weighed using a Quintix® Analytical Balance 60 (Sartorius, UK) and mixed in a 50 mL centrifuge tub, at room temperature (21°C), by continuous oscillation on top of a

benchtop votexer for 5 minutes. Formulations where glucose was replaced with fructose to assess stability were created using analytical reagent grade D-Fructose (Fischer Scientific, UK) and mixed using the same methodology as above.

5.2.4 Powder characterisation and storage

Mass Loss

Mass loss due to the removal of water from the formulation was determined using a Pioneer balance (Ohaus, Switzerland) with mass measurements taken both before and after freeze drying. Each SHRO powder formulation was run in triplicate.

Fourier-transform infrared spectroscopy (FTIR)

To confirm processing did not change the chemical structure of SHRO, FTIR spectra were obtained using a Nicolet 380 spectrometer (Thermo electron corporation, UK). For each sample, 64 scans were taken at a resolution of 4 cm^{-1} and averaged spectra are presented.

Scanning electron microscopy (SEM)

Scanning electron microscopy (SEM) was used to assess the morphology and size of freeze dried powder particles. Images were captured at an electron acceleration voltage of 15 kV using a TM3030Plus tabletop microscope (Hitachi Group, UK) in back scattered mode. All samples were mounted onto aluminium stubs using carbon tape and gold sputter coated to ensure conductivity.

Particle size

A QICPIC (Sympatec, UK) high speed dynamic image analyser was used to size SHRO powder particles. The camera frame rate was set at 100 fps with a particle fall height of 40 cm.

Particle size was determined using the EQPC mode, which calculated the diameter of a circle that had the same area as the projected area of the particle. Each powder formulation was analysed in triplicate.

Powder flowability

The angle of repose and Hausner ratio were determined in order to assess powder flow, which would influence ease of delivery and packing within the wound. Angle of repose was calculated by using a short-stemmed powder funnel, which was clamped 10 cm above a level surface. While blocking the opening, 5 g of powder sample was added to the funnel and the obstruction was subsequently removed to allow the powder to flow onto the surface below. The height and diameter of the powder pile was then measured, and the angle of repose calculated using trigonometry.

Hausner ratio was calculated by first recording the initial powder volumes (v_i), then interparticulate voids, reduced by a mechanical tap (tapped density), were minimised by use of a vibrating plate. Vibrations were applied for 5 minutes after which there was no difference in recorded volume. Final powder volumes (v_f) were recorded and the Hausner ratio was calculated using Eq. 5.2. Each SHRO powder formulation was run in triplicate.

$$H = \frac{v_i}{v_f} \qquad \text{(Eq. 5.2)}$$

Powder storage

Lyophilised powders were immediately transferred from the freeze dryer into an airtight universal container, which included the addition of 2g of silica beads to acts as a desiccant to reduce the relative humidity within the container.

5.2.5 SHRO powder gel characterisation

Absorbency

0.1 g of SHRO powder was added to a 20 mL test tube and 0.1 mL of distilled water was then added to the test tube and allowed to rehydrate for 5 minutes. The test tubes were then inverted for 10 seconds onto a water sensitive surface to assess absorbency. Distilled water was continually added in 0.1 mL volumes leaving 5 minutes between each addition until water was no longer absorbed by the SHRO powder.

Rheology

Each SHRO powder containing SPA was first measured out to 1 g and added to either 5 or 20 mL of distilled water at room temperature (21°C). A Kinexus Ultra+ rheometer (Malvern Instruments, UK) equipped with 40 mm serrated parallel plates to minimise wall slip during the determination of the SHRO gel's viscoelastic properties. All tests were conducted at 33°C to simulate skin temperature, with samples given 2 minutes of temperature equilibration time. Gap height was set at 1 mm. First, a strain sweep with the frequency fixed at 1 Hz was conducted to identify the % strain values that fall within the linear viscoelastic region. Frequency sweeps were then carried out using 0.1% strain and frequencies from 0.1 to 100 Hz to obtain storage (G') and loss (G'') moduli.

5.2.6 In vitro antibacterial properties of SHRO powder

Hydrogen peroxide assay

Hydrogen peroxide concentrations released from SHRO powders were determined by an Amplex red peroxide fluorescent assay kit (Thermo Fisher Scientific, UK). A calibration curve was first created using H_2O_2 standards at the following concentrations 10, 3, 1, 0.3, 0.1 and 0 μM. For the assay, 0.1 g of each powder was firstly dissolved in 40 mL of phosphate

buffered saline (PBS) to form a stock solution. At each time point, 50 µL was taken from each of the stock solutions and further diluted in 10 mL of PBS. A reagent master mix was then formed containing 50 µL red peroxidase substrate, 100 µL of 10 units/mL peroxidase, and 4.85 mL assay buffer. 50 µL of SHRO powder or H_2O_2 standard was added to each well to which 50 µL of master mix was then added. Wells were then mixed by pipetting and incubated for 30 minutes protected from light. Fluorescence intensity was then measured (λ_{ex} = 540nm/λ_{em}= 590nm) using a Tecan Spark plate reader (Tecan Trading AG, Switzerland). Each SHRO powder was tested in triplicate.

Zones of inhibition

LB broth (Sigma Aldrich, UK) and LB broth with agar (Sigma Aldrich, UK) were prepared in distilled water to concentrations of 20 g/L and 35 g/L, respectively. Both were then sterilised in an autoclave for 20 minutes at 121°C under 100 kPa of pressure. Overnight cultures of *Staphylococcus aureus* (*S. aureus* - ATCC 29213), *Escherichia coli* (*E. coli* - MG1655) and *Pseudomonas aeruginosa* (*P. aeruginosa* - NCTC 13437) were prepared in 5 mL of LB broth inoculated with one bacterial colony. Using an Evolution 300 UV-VIS spectrophotometer (Thermo Scientific, UK) at 600 nm the optical density of each overnight culture was measured and diluted to 0.04. LB broth with agar was used to from plates, which were then inoculated with bacteria. Using a 10 mm sterile borer, wells were created in the center of the inoculated agar. 0.2 g of neat SHRO powder was added to each well and then incubated at 37°C for 24 hours. The zones formed from inhibited bacterial growth were then measured, and the bore hole diameter deducted. Testing of SHRO powder efficacy in solution was achieved by creating different concentrations of SHRO powders (0.2 - 0.005 g/mL). 250 µL of each concentration was pipetted into each well, incubated at 37°C for 24 hour, zones of inhibition measured and well size deducted. Each SHRO powder formulation and bacterial strain were run in triplicate.

5.2.7 In vitro biocompatibility

Human dermal fibroblast cell culture

It was important to confirm the SHRO powders had no detrimental effects on mammalian cell behaviour. HDF (ATCC Cat. PCS-201-012; Passage number 8) were cultured in DMEM (Sigma Aldrich, UK) and supplemented with 10% v/v fetal bovine serum (Sigma Aldrich, UK), 1% v/v penicillin/streptomycin (Sigma Aldrich, UK), and L-glutamine (Sigma Aldrich, UK). All cultures were allowed to attach to the well plate for 24 hours incubated at 37°C with 5% CO_2. Well plates were initially seeded with 5 x 10^4 cells/mL per well for 96-well plates. After 24 hours DMEM media was replaced with DMEM containing different concentrations of SHRO powder variants and incubated at 37°C and 5% CO_2 with media changed on days 3 and 7.

HDF cell viability - live/dead assay

Cell viability was assessed on days 1, 3 and 7 using a live/dead assay (Thermo Fisher, UK) following the manufacturers protocol. Briefly, cells were seeded in a 96-well plate and treated with SHRO powder containing media. At each time point, media was removed from the cells and then washed with PBS. Dyes were then added, and the well plate was then incubated in darkness for 15 minutes at room temperature. The dye solution was removed, and PBS used to wash the cells that were then fixed with 4% PFA (Sigma Aldrich, UK). Fluorescent images were then acquired using an Invitrogen EVOS M5000 microscope (Thermo Fisher, UK). Each sample was run in triplicate.

HDF cell proliferation - XTT assay

Cell proliferation was assessed on days 1, 3 and 7 by means of an XTT assay (Biological Industries, Israel) and the manufacturers protocol was followed. Briefly, cells were seeded in a 96-well plate and treated with SHRO powder containing media. 0.1 mL of activation solution was added to 5 mL XTT assay reagent to form the reaction solution. 50 mL of reaction solution was then added per well and incubated for 2 hours at 37°C and 5% CO_2. Absorbance was then measured using a Tecan Spark plate reader (Tecan Trading AG, Switzerland) set at 450 nm with media only readings subtracted from wells containing SHRO powders. Blank subtracted values were then normalised against control wells containing HDF cells and DMEM media. Each sample was run in triplicate.

5.2.8 Ex-vivo porcine wound model

Commercially available porcine skin (Skin for sale, UK) was cut using a scalpel in order to create a lesion. The site was dampened with 2mL of water to mimic wound exudate and approximately 1g of SHRO powder containing +40% SPA was applied using a shaker applicator. Images were taken before, during and after addition of the SHRO powder. Post gelation, a cross section of the wound was created using a scalpel and imaged using an iPhone x camera.

5.2.9 Statistical analysis

GraphPad Prism® 5.0 software was used to perform statistical analysis. T-tests were used to determine significance whereby values of $p < 0.05$ were considered significant and p values indicated as follows $p < 0.05$ (*), $p < 0.01$ (**), $p < 0.001$ (***). Data is presented throughout as mean ± standard deviation.

5.3 Results

5.3.1 SHRO powder formulation

β-cyclodextrin derivatives (CD), MCD and HCD were utilised for their superior drying ability of SHRO when compared to other drying agents, such as maltodextrin and gum arabic (Figure 5.2a). The ability of β-cyclodextrin to promote the removal of water from the sample and hence provide the ability to form a flowable powder post freeze drying was tested. SHRO water loss post freeze drying was measured at 0.20 ± 0.02, 0.25 ± 0.03 and 0.23 ± 0.02 g per gram of MCD 70, MCD 50 and HCD 50 powder, respectively (Figure 5.2b). This revealed no significant difference between equivalent MCD and HCD samples ($p = 0.45$), or for powders with 20% more SHRO ($p = 0.08$, MCD 70 versus MCD 50).

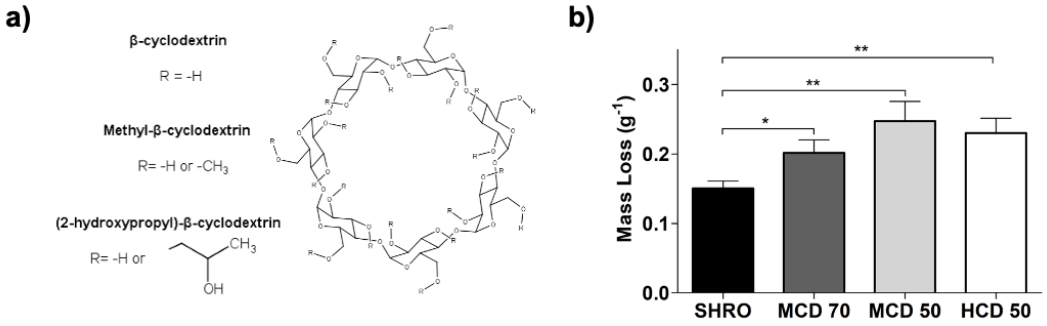

Figure 5.2. Chemical structure of β-cyclodextrin, methylated-β-cyclodextrin (MCD), and (2-hydroxypropyl)-β-cyclodextrin (HCD) (a) and a comparison of the mass loss from pure SHRO and SHRO powders as a result of freeze drying (b). n=3, error bars represent standard deviation.

Importantly FTIR spectra confirmed that the incorporation of these compounds and the removal of water did not influence the chemical composition of the SHRO, specifically relating to bonds characteristic of carbohydrate structures. The two water bands observed at 3284 cm^{-1} (OH – stretch) and 1641 cm^{-1} (OH – deformation) in samples MCD 50 and HCD

50, were reduced in intensity compared to the SHRO control, indicating a lower water content (Figure 5.3a). Characteristic carbohydrate regions between 1800 cm^{-1} and 500 cm^{-1} were also analysed. These wavelengths correspond to the most sensitive absorption region for SHRO, MCD and HCD (Figure 5.3b). SHRO sugar peaks include the stretching of the C-O band in the C-O-C linkage (1110 cm^{-1}), C-OH group/C-C stretch in the carbohydrate structure (1043 cm^{-1}) and C-H bending of the carbohydrate (918 cm^{-1}). MCD and HCD show a prominent absorption band at 1083 cm^{-1} corresponding to the C-H and C-O stretching vibrations. This band is absent in the SHRO spectrum but can be observed in the MCD 50 and HCD 50 samples. Similarly, SHRO characteristic peaks at 815 cm^{-1} and 773 cm^{-1} can be observed in MCD 50 and HCD 50 but not in the drying agent controls. With no significant change or shifts in peaks this indicates that compositional integrity of the active, SHRO has been maintained, which will be vital for producing an antimicrobial effect.

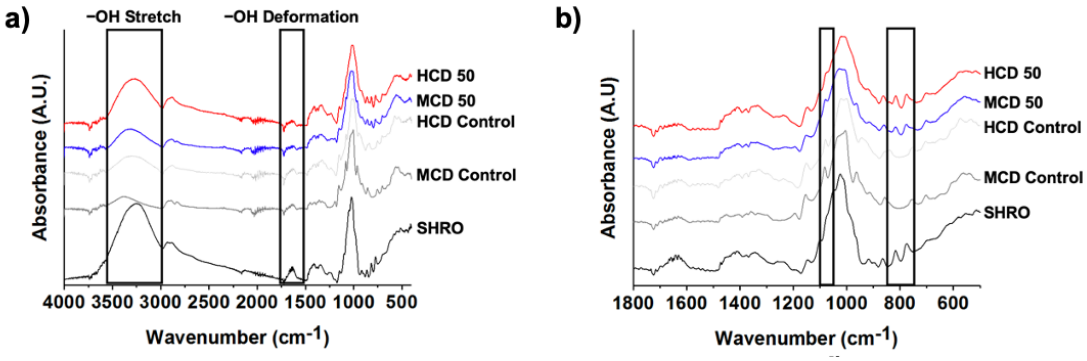

Figure 5.3. Average FTIR spectra (64 scans) of SHRO powders made with MCD and HCD along with controls that contained no honey at wavelengths between 500 - 1800 cm^{-1} (a) and 500 - 4000cm^{-1}(b). Scans were taken at a resolution of 4 cm^{-1}.

In all cases the addition of MCD or HCD resulted in significantly more water removal compared with SHRO alone, demonstrating the effectiveness of the selected drying agents (Figures 5.4a-d). Notably, the resultant freeze-dried powders made from different β-cyclodextrin derivatives, were homogeneous and indistinguishable under SEM (Figures 5.4e-g).

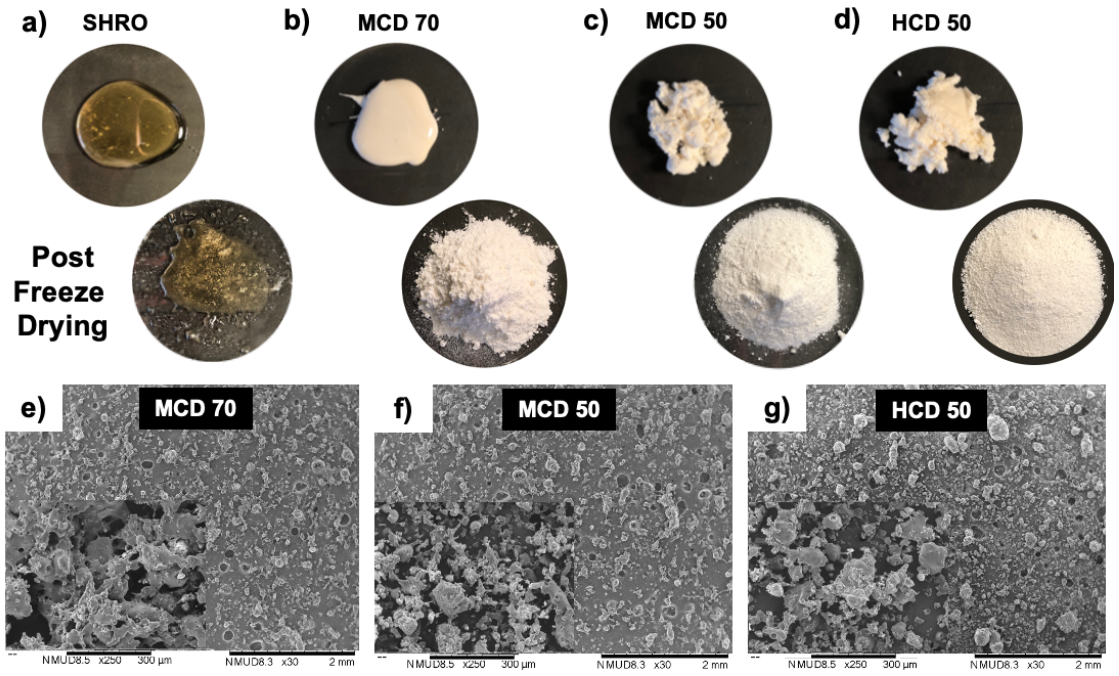

Figure 5.4. Images were taken of SHRO (a), MCD 70 (b), MCD 50 (c) and HCD 50 (d) formulations before and after freeze drying with higher magnification SEM images of MCD 70 (e), MCD 50 (f) and HCD 50 (j) also acquired.

SHRO powder was further characterised by particle size and its ability to flow, which both play a role in effective delivery of the product and ensure sufficient packing within the wound (Figure 5.1). The particle size for all SHRO powders MCD 50 – 70 and HCD 50 fell within identical distributions with an average diameter of approximately 205 μm (Figure 5.5a). A funnel technique was used to obtain the angle of repose of all samples, which defines the transition between phases of a granular material and allows for the quantitative measure of

powder flowability (Figure 5.5b). Increasing SHRO concentration in MCD samples from 50 to 70% was found to significantly ($p = 0.04$) reduce powder flowability as indicated by a 12.5% increase in angle of repose between MCD 50 (26.3±0.86°) and MCD 70 (29.6±1.6°). The average angle of repose for samples containing 50% SHRO powder and utilising HCD was 22.9±0.55° (Figure 5.5c). Notably this was significantly lower than equivalent MCD samples ($p = 0.005$). The reduction in flowability may also be due to the absorption of water from the environment. As the experiment was benchtop and not under condition of low relative humidity water content may have rapidly increased and resulted in the agglomeration of particles.

In order to determine the relative effect of interparticle interactions and how this may impact flowability, the Hausner ratio was calculated using Eq. 5.2 and methodology depicted in Figure 5.5d. Despite formulations exhibiting variations in flowability, there was no statistically significant differences in Hausner ratios indicating that the propensity of samples to be compressed was comparable between MCD 70 (1.38±0.08), MCD 60 (1.47±0.02), MCD 50 (1.43±0.08), and HCD 50 (1.43±0.17) (Figure 5.5e).

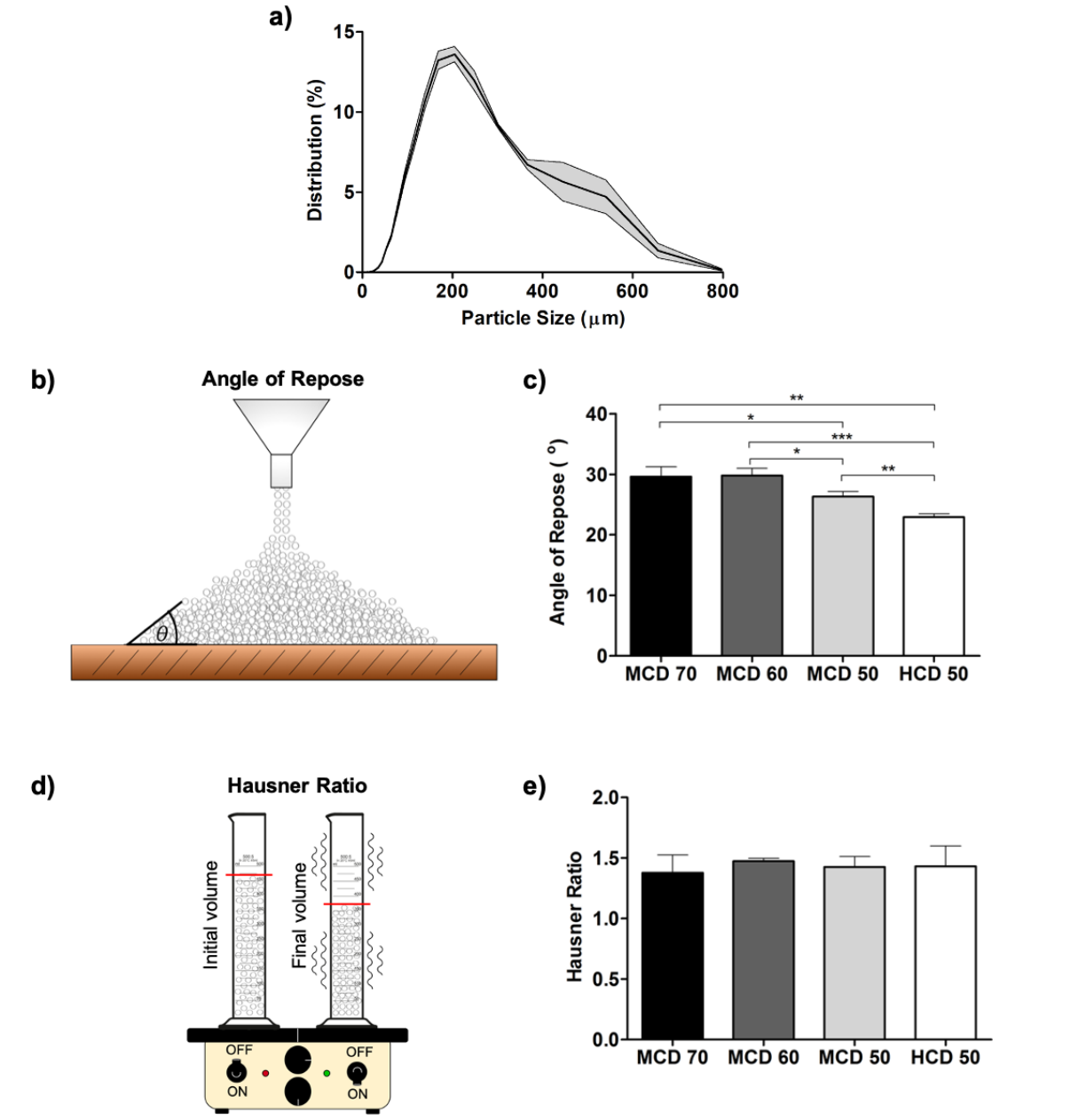

Figure 5.5. Typical particle size distribution of SHRO powders with an average size of approximately 205 μm (a), schematic representing angle of repose measure that is an indicator of flowability (b), differences in the angle of repose for samples with varying SHRO content and drying agent (c), diagram depicting density determination methodology used to calculate Hausner ratio, a determinant of packing efficiency (d), and the calculated Hausner ratio of SHRO powders (e). n=3, error bars represent standard deviation.

In an effort to localise the powder at the defect site and to protect the wound from further infection, the addition of a superabsorbent (SPA) was explored. Specifically, the aim of incorporating SPA was to enable the powder to transform into a hydrogel through absorption of wound exudate. Concentrations of 10 – 40% were selected in order to provide a broad range of values with higher concentrations expected to provide greater absorption properties. To begin this optimisation process, the ability of each formulation (MCD 70 – 50 and HCD 50) to absorb water was measured. As may be expected, a positive linear correlation was observed between SPA addition and water absorption capacity. Remarkably, despite honey being known for osmotic behaviour, generally formulations with SHRO absorbed less water than equivalent controls (no SHRO and same SPA content). Specifically, MCD 70, MCD 50 and HCD 50 with +10% w/w SPA absorbed 39.67±6.4, 29.67±2.5, 37.33±1.5 mL g^{-1} respectively while the equivalent amount of SPA had the capacity to absorb 41.16±2.1 mL g^{-1}. It is also remarkable that when comparing between samples containing SHRO, for 20 and 40% w/w SPA samples MCD 70 exhibited lower absorbency compared to MCD 50 and HCD 50, despite this formulation containing 20% more honey (Figure 5.6a-b).

The viscoelastic properties of gels developed from the SHRO powder formulations were assessed to determine whether they exhibited sufficient flexibility to conform and protect the wound bed. Notably, all of the formed protective layers were found to exhibit dominant G' values across all tested frequencies, which is characteristic behaviour of a gel system. The drying agent (MCD vs HCD) and concentration of SHRO (MCD 50 vs MCD 70) had no significant impact on G' values ($p > 0.05$). An increase in SPA from 10 to 40% w/w, however did increase the G' value indicative of a stiffer gel (Figure 5.6c-d). When additional water was added to the formulations this caused a reduction in G', a trend observed across all frequency values.

Limitations of this study found that if less than 5 mL per g was added, a brittle gel was little homogeneity was formed and therefore the rheological properties could not be fully elucidated.

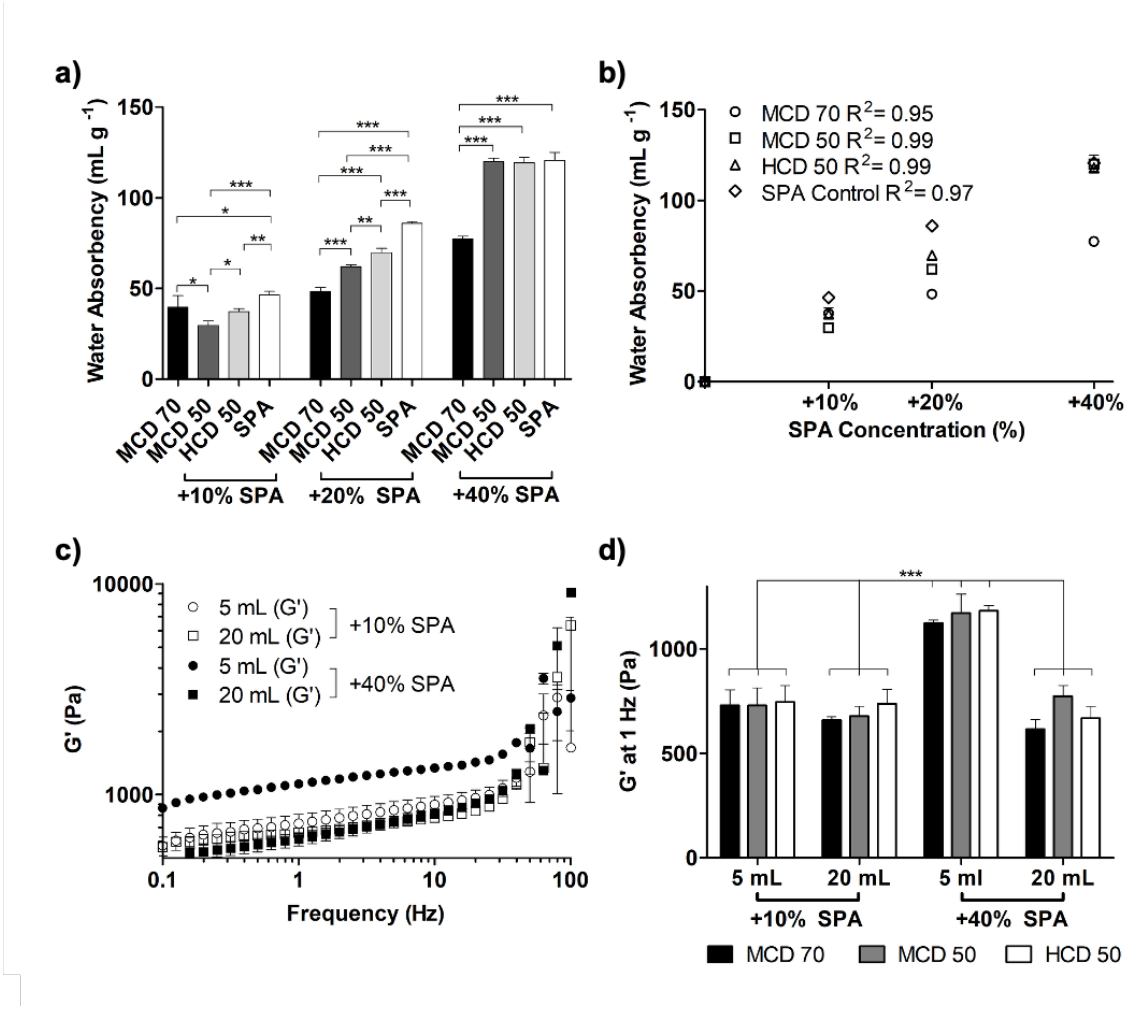

Figure 5.6. Absorption capacity of SHRO powders with +10, 20 and 40% SPA (a) and the relationship between SPA addition and water absorbency for different drying agents with SPA used as a control (b). Viscoelastic properties of SHRO powder gels with +10 and 40% SPA conducted at 0.1% strain and 33°C after addition of 5 or 20 mL distilled water (c) and the comparison of storage modulus at a frequency of 1 Hz (d). n=3, error bars represent standard deviation.

A hydrogen peroxide assay was conducted over 8 days to confirm that the processing conditions used for powder formation did not adversely affect the efficacy of incorporated

SHRO. Promisingly all formulations were found to produce H_2O_2 over this time period (Figure 5.7a). It is notable that release was fastest from MCD 70. After 4 days, MCD 70 (29.97 ±1.3 μmol g^{-1}) exhibited a significantly higher concentration of hydrogen peroxide compared to MCD 50 and HCD 50 (21.45 ±1.6, and 18.88 ±1.7 μmol g^{-1}, respectively). However, after 8 days no significant differences in H_2O_2 concentrations were observed (Figure 5.7a).

Zone of inhibition experiments were conducted to determine if varying levels of H_2O_2 produced from different powder formulations impacted the degree of microbial efficacy (Figure 5.7b). Promisingly, all of the powder variants were capable of inhibiting the growth of clinically relevance Gram negative (*P. aeruginosa and E.coli*) and Gram positive species (*S. aureus*). Despite variations in H_2O_2 release kinetics, there was no significant difference in the size of inhibition zones formed for MCD 70, MCD 50 and HCD 50 powders against all tested bacteria (Figure 5.7c-e). The amount of powder required to be efficacious was also determined by conducting a minimum inhibitory concentration assays using MCD 70. The results show efficacy against *S. aureus* down to a concentration of 0.005 g mL^{-1} (Figure 5.7f).

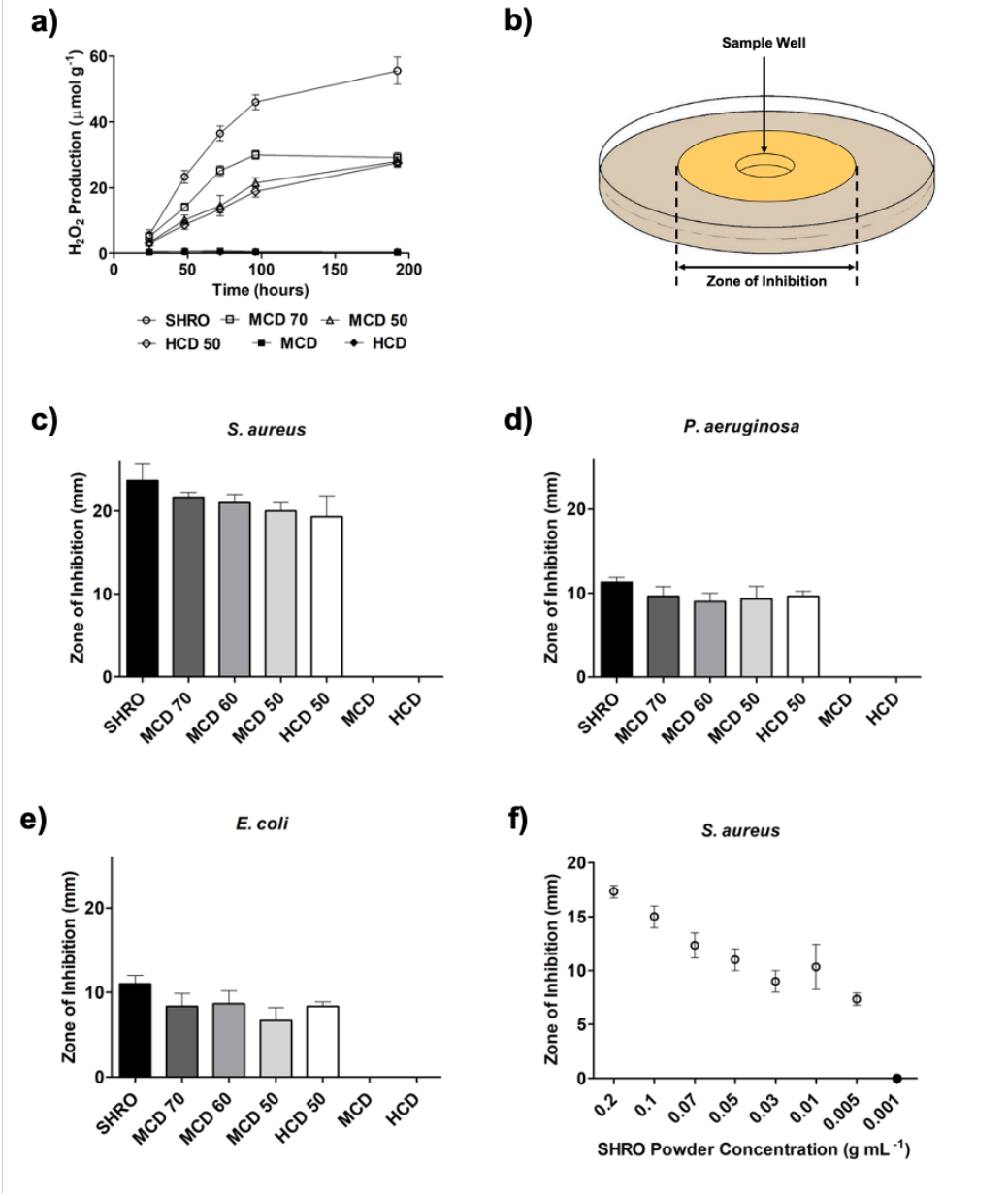

Figure 5.7. Normalised hydrogen peroxide production from SHRO powder formulations (a), schematic diagram depicting zone of inhibition methodology (b), size of inhibition zones after SHRO powder treatment for S. aureus (c), P. aeruginosa (d) and E. coli (e). Determination of minimum inhibitory concentration of MCD 70 against S. aureus (f). n=3, error bars represent standard deviation.

Having determined the efficacious range of MCD 70 it was important to confirm that the levels of H_2O_2 released were not cytotoxic to mammalian cells. Promisingly no adverse effect on HDF viability was observed at a powder concentration of 0.01 g mL^{-1} (Figure 5.8a-h). Over a period of one week, the majority of cells remained viable, exhibiting an elongated morphology at day 7 (Figure 5.8e-h). To further reinforce these findings, an XTT cell proliferation assay was conducted (Figure 5.8i-j). These results demonstrated HDFs exhibited levels of proliferation comparable to cell only controls at powder concentrations of 0.01 and 0.05 g mL^{-1} for all formulations. Furthermore, for HCD 50 proliferation was not impacted at a higher concentration of 0.15 g mL^{-1} (Figure 5.8g-h).

The ability of the gel formed from MCD 70 + 40% SPA to conform within a 3D defect was assessed using an ex-vivo porcine model in which a wound was created using a scalpel (Figure 5.8k) and moistened to stimulate exudate before powder addition (Figure 5.8l). Within <1 minute this powder sample was observed to transform into a gel (Figure 5.8m). Promisingly cross-section dissection of the model revealed that the gel had expanded to fill the wound creating a tight interface across the entire defect (Figure 5.8n). It is proposed that this ability to easily conform in 3D would prevent the wound environment from being invaded with further bacteria while keeping the delivery of ROS localised to the site of infection.

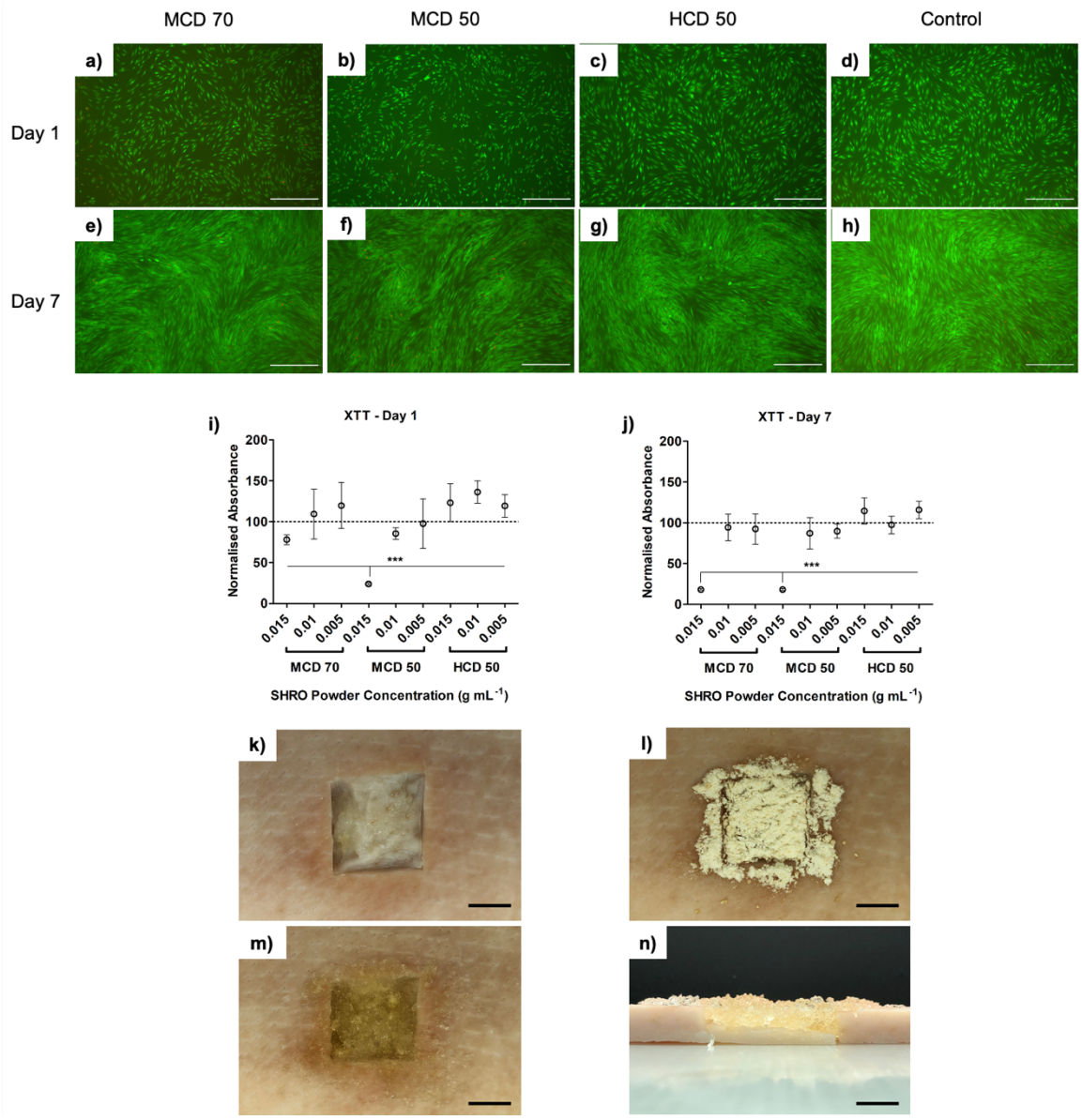

Figure 5.8. Fluorescent micrographs demonstrating viability of human dermal fibroblast (HDF) cells cultured with 0.01 g mL-1 of SHRO powders and stained with Syto 10 (green – live cells) and ethidium homodimer (red – dead cells) after 1 (a-d) and 7 days (e-h) (scale bars – 1000 µm). Quantification of HDF proliferation by XTT assay and normalised to cell only controls after 1 (i) and 7 (j) days of culture with powder formulations. A 1cm^2 3D wound formed with a scalpel in ex-vivo porcine skin (k), application of SHRO powder to the dampened defect using a shaker applicator (l), with gelation occurring in < 1 minute (m), which expanded to fill the entire defect creating a tight interface with the surrounding tissue (n) (scale bars – 10 mm). n=3, error bars represent standard deviation.

5.3.2 Synthetic reactive oxygen powder formulation

Following the successful formulation of SHRO powder variants, investigations were made to formulate a synthetic reactive oxygen powder. Three formulations were created with 0.2, 0.1 and 0.05% GOx incorporated into the powder systems. The ability of these systems to produce and release hydrogen peroxide immediately post-production was tested (Figure 5.9a). it was found that levels of H_2O_2 rose steadily over a 72 hours period where they peaked, producing concentrations of 2.44 ± 0.09, 2.10 ± 0.08 and 1.96 ± 0.05 $mmolg^{-1}$ respectively. After 72 hours, the concentration of hydrogen peroxide reduced slightly to 2.09 ± 0.02, 1.59 ± 0.05, 1.47 ± 0.06 $mmolg^{-1}$ respectively after 7 days. Powders were then stored at room temperature (21°C) for 10 and 18 days following production, before re-assessment of each powder's hydrogen peroxide producing capability. After 10 days of storage it was found that the level of hydrogen peroxide produced was significantly reduced. The release profile was similar to that measured initially post formulation, however after 72 hours hydrogen peroxide concentrations were reduced by 43.7 (1.38 ± 0.6 $mmolg^{-1}$), 69.2 (0.65 ± 0.3 $mmolg^{-1}$) and 77.6% (0.44 ± 0.49 $mmolg^{-1}$) respectively. This phenomenon continued and after 18 days of storage concentrations of hydrogen peroxide produced were only 0.86, 0.95 and 0.05% of the original value tested immediately postproduction (Figure 5.9b). Further confirmation of a decrease in efficacy was also prevalent in the results from bacterial zones of inhibition tests. The ability for the 0.2% GOx synthetic formulations to inhibit the growth of *S. aureus* was assessed immediately postproduction, and then again after 10 and 18 days, complimentary to that of the hydrogen peroxide assay. It was found that the zone produced initially were large in size (24.7 ± 1.5 mm) that decreased to (11.3 ± 1.5 mm) after 10 days and after 18 days no zone of inhibition was detected (Figure 5.9c). Controls of both glucose and water produced no capacity to inhibit bacteria inferring that activity is due to the presence of GOx and the enzymatic reaction that occurs.

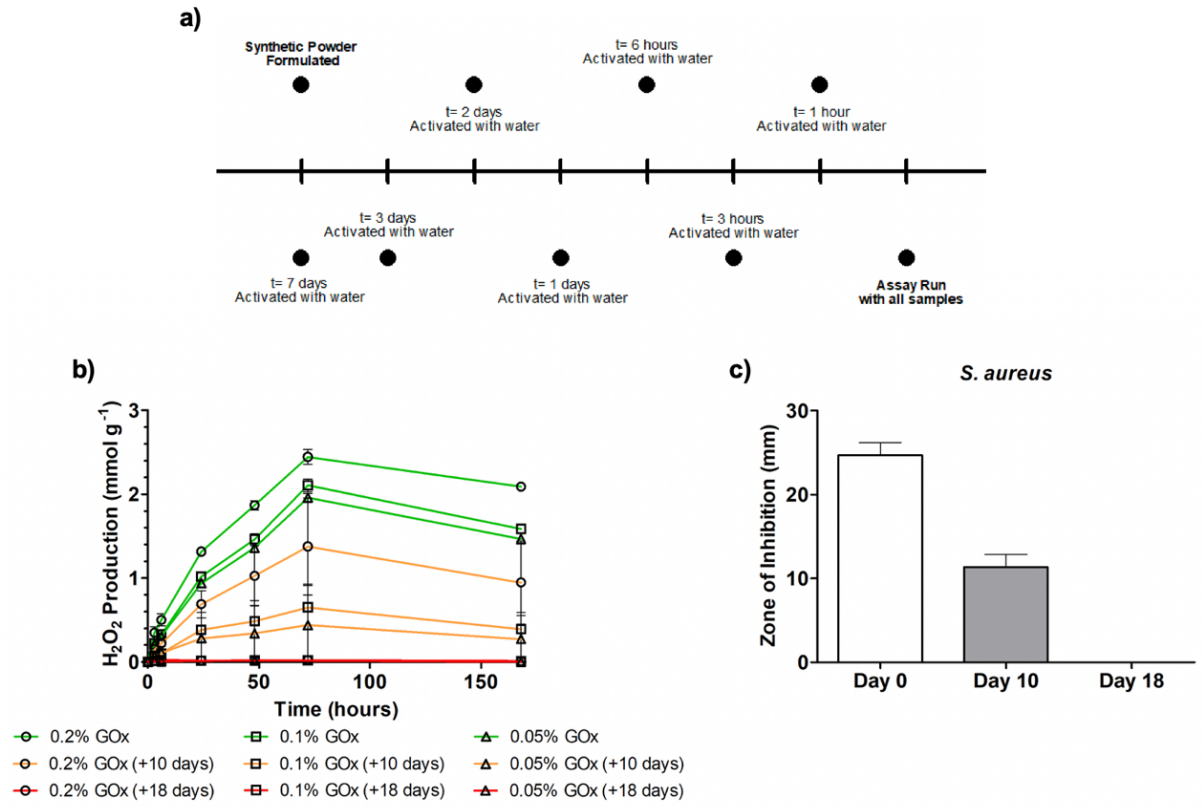

Figure 5.9. Experimental plan (a) for determining hydrogen peroxide production of synthetic reactive oxygen powder formulations containing 0.2, 0.1, and 0.05% glucose oxidase after 0, 10 and 18 days of storage at room temperature (21°C) (b). Zone of inhibition produced by treating Staphylococcus aureus with 0.2% GOx synthetic reactive oxygen powder formulations after 0, 10 and 18 days of storage at room temperature (21°C) (c). Controls of glucose and water were used both eliciting no reaction. n=3, error bars represent standard deviation.

Further testing was conducted in order to better understand the capacity reduction of synthetic powders to produce hydrogen peroxide. Glucose in 0.2% formulations was replaced with inert fructose, to prevent the enzymatic oxidation reaction from occurring (Eq. 5.1). These formulations were stored for a week at room temperature (21°C) and tested for hydrogen peroxide release at a 24 hour time point on days 0, 1, 3 and 7 (0.2% fructose control) (Figure 5.10a). To assess if the presence of glucose during storage caused the decrease in efficacy noted

in Figure 5.9, glucose was added to the 0.2% fructose formulations immediately before assessing the hydrogen peroxide production at a 24 hour time point on days 0, 1, 3 and 7 (0.2% fructose-glucose). As expected without the presence of glucose the 0.2% fructose control indicated negligible concentrations of hydrogen peroxide over the 7 days of storage. A decreasing trend however was noted when assessing the capacity of 0.2% fructose formulations to produce hydrogen peroxide when glucose is added prior to testing. A 24 hour time point taken after 7 days of storage, produced 0.35 ± 0.02 $mmolg^{-1}$ of hydrogen peroxide. This was significantly less than that measured post-formulation where hydrogen peroxide concentrations were 0.68 ± 0.05 $mmolg^{-1}$ indicating a trend of a reducing capacity to produce hydrogen peroxide over the storage period (Figure 5.10b).

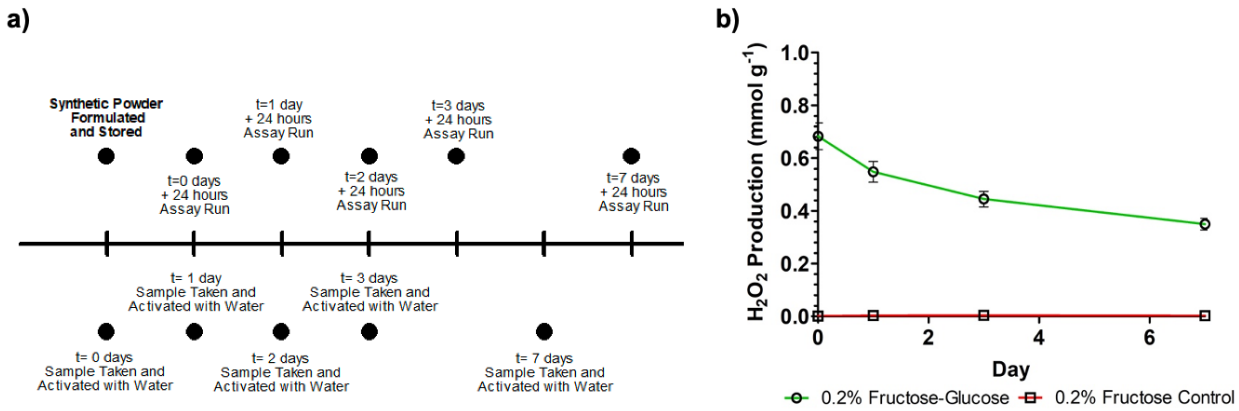

Figure 5.10. Experimental plan (a) for determining hydrogen peroxide release from 0.2% synthetic reactive oxygen powder formulated with fructose in place of glucose, stored for 0, 1, 3 and 7 days after which glucose was added to the formulation (b). Measurements were taken 24 hours after the addition of glucose.

5.4 Discussion

5.4.1 SHRO powder formulation

SHRO, an engineered medical grade honey, has the capacity to generate ROS through a reaction between glucose and water, which is mediated by the enzyme glucose oxidase (Eq. 5.1). Existing literature has demonstrated the efficacy of SHRO, both *in vitro* and *in vivo,* against a range of Gram negative and Gram positive bacteria, including antibiotic resistant species (e.g. MRSA) [43,44,167–170]. However, the highly viscous and adherent nature of SHRO makes it difficult to deliver and is preventing it from being used more widely in infection treatment [170,418]. Herein we demonstrate the possibility to use starch based drying agents to facilitate freeze drying of SHRO and form a free-flowing powder, which enables easy application. These formulations were further enhanced by the incorporation of a superabsorbent compound enabling ROS production to be initiated through absorption of wound exudate while transforming the powder into a gel, creating a protective barrier capable of promoting healing.

In selecting a drying technique, it was important to consider the thermal instability of SHRO since above 55°C enzymatic production of ROS is significantly reduced [151]. As such, low temperature methods were explored, namely freeze drying, a technique that has been employed to lyophilise other temperature sensitive therapeutics, such as vaccines [469]. However, it was not possible to dry SHRO on its own since the water present was bound too tightly to sugar molecules. Therefore the addition of drying agents were explored to increase the glass transition temperature [298]. Two compounds were tested for this purpose MCD and HCD. It was found that only the latter two had the capacity to dry mixtures containing ≥ 50% SHRO. Compared with the other tested agents, it is proposed that the additional methylation present in MCD and HCD helps to decrease particle to particle interaction and this reduces the ability of SHRO to retain water (Figure 5.2a). Interestingly when comparing MCD and

HCD, the former, with a higher degree of methylation, was capable of drying mixtures containing up to 70% SHRO, in comparison to only 50% with the latter [299,300].

Following successful drying, it was important to confirm that neither MCD nor HCD had a detrimental effect on antimicrobial efficacy of SHRO. FTIR was used to study the molecular interactions within the powder formulations and concluded that there were no structural or chemical changes. Peaks at wavelengths characteristic of both SHRO and the drying agent were present in the final products with no evidence of peak shifts or changes (Figure 5.3a-b). By observing the relative intensity of the bands at 3284 and 1641 cm^{-1} variation in water content could be determined, with SHRO exhibiting the greatest intensity in these regions [470]. This comparison revealed that MCD 50 formulations showed lower intensities in the water bands than HCD 50, indicating that MCD has an enhanced ability to remove water from SHRO during the drying process. Mass loss measurements corroborated this finding, with MCD displaying 65% more mass loss than SHRO alone and 7% more than equivalent HCD formulations (Figure 5.3b). The ability to produce a free flowing powder at 70% when using MCD also demonstrates the enhanced drying capacity for this compound compared to HCD, which was only able to dry formulations consisting of up to 50% SHRO (Figures 5.4a-d).

To assess the ease of delivering each powder to a wound, flowability was measured along with the packing ability of each formulation since this will influence dosage. The three formulations selected for further testing (MCD 70, MCD 50 and HCD 50) were found to exhibit comparable particle size distributions. Notably, all samples exhibited a broad range of particle sizes with average $D_{10,}$ D_{50} and D_{90} values of 88, 205 and 391 μm, respectively (Figure 5.5a). This is likely due to two reasons; firstly, compared with other grinding techniques (e.g.

ball milling), hand grinding of SHRO powders is likely a relatively inefficient methodology that typically does not produce a narrow particle size range [471]. Secondly, it is likely that particle-particle interactions led to aggregations during analysis, evidence for this can be observed in the SEM images (Figure 5.4f-g). Size alone is not enough to infer or predict the flow properties of a powder, Fu., *et al.* [472] states that the shape of the particle has a greater influence than the size. This indicates that improvements in grinding may be required in order to improve flow. Given the similar particle size distributions, it was interesting that a significant difference in the angle of repose was observed between these samples (Figure 5.5c). Angle of repose was measured at between 23-30° for all samples, indicative of good flow properties [473]. This methodology is most significantly affected by factors such as the sliding and rolling of particles, interparticle friction, and size [474–476]. Since the size distribution was similar, it is suggested that the HCD powders exhibit lower angles of repose due to reduced particle friction driven by a more spherical morphology, however this is not supported by the high resolution SEM images (Figure 5.4f-g). Remarkably, *Zhou., et al.* [477] concluded that angle of repose measurements were less sensitive to density and interparticle interaction, factors which are influential in the determination of a powders Hausner ratio. This explains the conflicting trends observed between the angle of repose measurement (Figure 5.5c) and Hausner ratio (Figure 5.5e), which suggests that all powders have an equal ($p > 0.05$) but poor ability to flow (1.37-1.47) [478]. However, it is also highlighted that all SHRO powder formulations had the same propensity to compress and therefore the mass dosage delivered to a defined wound area would likely be similar. Furthermore, it is notable that MCD 70 contains a greater proportion of active and therefore would be expected to release more H_2O_2, which was confirmed through *in vitro* experiments (Figure 5.7a). With conflicting measurements, likely due to a combination of a high degree of non-sphericity amongst the particle population and the probability that the powder is absorbing environmental moisture causing aggregation, a third methodology is

proposed. Carr's compressibility index is an alternative way of determining powder flow similar to that of Hausner ratio and could complement existing data to inform on the improvement of powder flow. Furthermore, this could be conducted in a controlled desiccated environment.

There is a wide body of existing literature that evidences the benefits of using hydrogels in wound dressings [310–313]. In particular, absorbent systems like alginate are cited for their promising absorption capabilities of up to 20 times their weight in fluid making them useful for treating infected wounds [479]. Alongside this, the introduction of topical negative pressure has improved management of complex wounds [479–481]. Here the incorporation of a superabsorbent (SPA) was explored to support management of wound exudate and through *in situ* gelation, localise the powder formulations while creating a protective barrier to prevent further contamination (Figure 5.1). When in contact with water there is a tendency for the sodium in the polyacrylate to be displaced by H_2O and replaced within the polymer network causing it to swell. Rheological analysis (Figure 5.6c) demonstrated characteristic gel behaviour for all samples, as indicated by G' exceeding G'' at all tested frequencies (0.1-100 Hz). The mechanical properties of skin produces young moduli values of between 4.6 – 20 MPa with storage (G') and loss moduli (G'') measuring at 400 Pa and 100 Pa respectively [482,483]. These results suggest that the gel formed provides a stiffer scaffold than that of skin which supports its use as a protective barrier. Comparisons cannot be made with regards to the Youngs modulus due to limitations regards to equipment availability.

Through the use of an *ex-vivo* porcine model, we demonstrate that the swelling of the polymer network creates a tight interface at the wound periphery (Figure 5.7n). It is postulated that this expansion may be exploited to locally apply negative pressure across the interface. The linear correlation between SPA and gel absorption capacity suggests that the degree of swelling,

and thus applied pressure, could be controlled through adding more superabsorbent. MCD 70, MCD 50 and HCD 50 powders maintained integrity up to 77.3 ± 1.5, 120.0 ± 2.0, 119.3 ± 3.1 mL g^{-1} of water, respectively when 40% SPA was added (Figure 5.6a). SPA concentration was found to be the predominant factor influencing storage and loss modulus (Figure 5.6c-d) with another factor being SHRO concentration. Specifically, it was observed that MCD 70, which contained more active had a reduced ability to hold water in the formed polymer network compared to MCD 50 (Figure 5.6b). This is likely due to the increased generation of free ions from formulations with higher SHRO content, which may disrupt the attraction of water to the polymer chain [484].

The production of hydrogen peroxide and other ROS is well documented to be the dominant factor in the antimicrobial effect elicited by SHRO [170,418]. On that premise it was vital that post formulation the engineered SHRO powders retained their ability to produce hydrogen peroxide (Figure 5.7a). It was found that powders with higher concentrations of SHRO had a faster rate of reaction, with MCD 70 producing 5.15 ±2.0 μmol g^{-1} of hydrogen peroxide after 24 hours. This was in comparison to MCD 50 (3.34 ±0.12 μmol g^{-1}) and HCD 50 (3.11 ±0.30 μmol g^{-1}), which produced comparable levels of H_2O_2 suggesting the predominant factor in determining dosage was SHRO concentration. Producing a formulation capable of controlled, predictable production of hydrogen peroxide ensures that effective and non-cytotoxic dosing can be delivered throughout the application period [459]. Promisingly, it was found that all the SHRO powders continued to produce and maintain levels of hydrogen peroxide throughout the entire testing period (8 days). However, it is notable for topical application, dressing changes would typically be done more frequently, most commonly every 24-48 hours, although some dressing can last for as long as a week [485]. Based on these release profiles, it will be important to provide application advice to align wound care regimes with the

dosage time scale for the SHRO powders, which is suggested to be a maximum of one week. For shorter application periods, the faster rate of hydrogen peroxide generation by MCD 70 formulations may be beneficial to treating infected wounds that also exhibit exudate.

Previous *in vitro* studies have shown that unprocessed SHRO was efficacious against a range of clinically relevant bacteria, including *S.aureus, P. aeruginosa*, and *E.coli* [43,44,165,167,168,170,418,460]. A inhibition zone test [41], depicted in Figure 5.7b was used to confirm whether the H_2O_2 concentrations released from powder formulations containing between 50 and 70% SHRO were able to inhibit the growth of Gram positive *S.aureus*, and two Gram negative species *P.aeruginosa* and *E.coli* (Figure 5.7c-e). After 24 hours MCD 70, MCD 50, and HCD 50 had inhibited the growth of all tested species. Notably, larger zones of inhibition were measured for *S.aureus* compared with *P.aeruginosa* and *E.coli*, which is consistent with results attained by *Hall., et al.* [170] whereby the Gram negative bacteria proved more difficult to inhibit. It has also been suggested by *Fischbach., et al.* [436] that higher doses of ROS may be required in order to inhibit the growth of Gram negative bacteria due to the additional protection of the outer membrane. Higher concentrations of ROS may be achieved by adjusting the baseline efficacy of SHRO, as is reported by *Dryden., et al.* [43]. This offers the possibility to form powders that are more effective against Gram negative organisms, however given the influence of SHRO on water absorption capacity it would be important to determine if these changes have any knock-on effects to the gel's physical behaviour. Since *S.aureus* was found to be the most sensitive bacteria to treatment with all SHRO powders and with no significant difference between powder formulations, further investigations were conducted to assess at which concentration an inhibition zone was no longer formed. This test differed to that of the previous studies as in place of neat powder, solutions were diluted in order to attain specific SHRO powder concentrations, this methodology also reflected that used to determine

cell viability. It was found that in all cases the lowest concentration that still produced a zone of inhibition was 0.005 g mL^{-1}, demonstrating the potential of using this formulation on extremely wet wounds (Figure 5.7f).

Both Fang [437] and Memar., *et al.* [36] have previously reported the possibility of DNA damage as a result of H_2O_2 dosing. As such, it was important to confirm whether the levels released from the formulated powders had an effect on cell viability or proliferation. Promisingly at powder concentrations of 0.01 g mL^{-1} or below a balance was struck between antimicrobial efficacy and an absence of detrimental effects on endogenous cells. This was confirmed through staining of live cells and imaging with confocal microscopy (Figure 5.8a-h), which revealed high degrees of viability and an elongated morphology during the 7 days of culture. XTT analysis confirmed that HDF proliferation was not significantly altered in the presence of 0.01 g mL^{-1} and below concentrations of SHRO powders compared with cell only controls over 7 days (Figures 5.8i-j). Although Fibroblast viability is not affected, it would be expected that as the SHRO powder has the ability to generate an inhibitory effect (H_2O_2 >25 μM) it would also illicit an immune response in the body, such as the recruitment of macrophages. Further studies may investigate if an inflammatory response is stimulated in Fibroblast cells due to the presence of SHRO powder using a human IL-8/CXCL8 ELISA [77].

5.4.2 Synthetic reactive oxygen powder formulation

Having successfully formulated an efficacious superabsorbent SHRO powder capable of inhibiting the growth of bacteria, whilst also providing a beneficial and protective wound healing environment. Further investigations were made into the development of a totally synthetic, reactive oxygen delivering, powder system. This system looked to utilise the

enzymatic oxidation of glucose reaction as means to generate reactive oxygen species *in situ*. Different concentrations of enzyme (0.2 – 0.05%) were tested in order to create products with different release profiles for study. All synthetic powder variants were found to successfully produce hydrogen peroxide, with concentrations peaking after 3 days at concentrations of 2.44 ± 0.09, 2.10 ± 0.08 and 1.96 ± 0.05 $mmolg^{-1}$ for 0.2, 0.1 and 0.05% GOx formulations, respectively. This level of hydrogen peroxide generation would be expected to elicit and antimicrobial effect, however, significant dilution (>2 L) would be required in order to reduce the concentration down to a comparable level to that of the respiratory burst of ROS produced by macrophages. Therefore, it is highly likely that at this concentration apoptosis of endogenous cells would occur. As this system is totally synthetic, the process is completely tailorable allowing a restriction in substrate concentration to control the maximum amount of ROS that is produced and for the enzyme quantity to be regulated to dictate the kinetics of the reaction. From this a number of ROS therapeutic concentrations could be targeted such as that associated with antimicrobial effects (25-500 μM), immune responses (5-250 μM) and wound healing (0.1-10 μM) [77,155,162].

The stability of the system, however, did appear to be an issue, as the ability for the synthetic powders to produce hydrogen peroxide reduced with storage time. 0.2, 0.1 and 0.05% formulations demonstrated a 43.7, 69.9 and 77.6% reduction after 10 days of storage and >99% reductions across all three synthetic powders after 18 days (Figure 5.9b). This significant reduction in efficacy was also evident when used to treat *S. aureus* with synthetic powders stored for different lengths of time (Figure 5.9c).

A study was then conducted in order to assess a hypothesis based upon research by Harris., *et al.* [486] that suggests the instability could be due to small amounts of water present

within the glucose powder, activating the production of hydrogen peroxide, and forming an environment conducive to the degradation of the enzyme. However, this was disproven as when glucose was replaced during storage with fructose, which is inert in specific terms to the reaction in question, hydrogen peroxide generation was still affected (Figure 5.10). This indicates an inherent instability with the enzyme itself, an issue not apparent in SHRO powder formulations. It is well known and described, such as in work by Bucekova., *et al.* [487] and Albaridi [488], that honey contains a multitude of different compounds, with chemicals such as thiols and polyphenols known for their ability to help protect the functionality of enzymes [489,490]. This may explain the noticeable differences in stability between that of the enzyme in the formulated SHRO powder systems and that of the synthetic reactive oxygen powder. Further research by Dubey., *et* al [491] indicates that free enzymes have a lower stability than that of immobilised enzymes with results specifically identifying improved storage stability when the enzyme was bound to a substrate. To increase storage stability it has also been noted that storing under fridge or freezer conditions can extend enzyme life [492–494].Moving forwards a number of works such as that by Trau., *et al.* [495] and Zhu., *et al.* [496] utilise encapsulation techniques as a mechanism to help prevent the inactivation of glucose oxidase and may offer a solution to the instability associated with storage over time.

5.5 Conclusion

The research in this chapter addresses a fundamental need for the development of new antimicrobials and effective systems by which to deliver them. This has been achieved by successfully formulating powders, which contain SHRO a novel engineered honey, for the prevention and treatment of topical wound infections. Through utilisation of freeze drying and addition of CD based drying agents, we demonstrate it is possible to formulate free-flowing powders without compromising antimicrobial efficacy of the temperature sensitive enzyme within SHRO. Specifically, MCD and HCD proved to be the most effective agents at removing water from SHRO. In comparison, the additional methylation of MCD allowed for the incorporation of up to 70% SHRO (20% > HCD and 30% > CD) whilst still producing a free-flowing powder.

Selected MCD and HCD formulations were further enhanced through addition of a superabsorbent, sodium polyacrylate. This increased the water absorption capacity of the powder, enabling formation of a hydrogel at the wound site while activating production of antimicrobial reactive oxygen species. Specifically, addition of 40% superabsorbent resulted in a capacity to absorb up to 120.7 ±4.5 mL g^{-1} of water. Application in an ex-vivo porcine model demonstrated that swelling of the polymer network resulted in the formation of a protective gel barrier, which may prevent further wound contamination and aid healing.

Importantly the incorporation of drying agents was not found to change the chemical composition of SHRO. The levels of hydrogen peroxide produced (3.1 – 5.2 µmol g^{-1} in 24 hours) proved to efficacious against clinically relevant Gram positive and Gram negative bacterial species; *Staphylococcus aureus, Pseudomonas aeruginosa* and *Escherichia coli*. Furthermore,

SHRO powder formulations were found not to elicit any detrimental effects on the viability or proliferation of human dermal fibroblast cells over 7 days.

In addition to SHRO powder delivery systems, synthetic reactive oxygen delivery systems were also formulated. The rationale behind this study was to expand the number of applicational areas by developing a completely tailorable product, devoid of the undesirable properties associated with that of freeze drying a honey product. However, although possessing the potential to deliver efficacious concentrations of reactive oxygen species at concentrations exceeding that which can be produced using SHRO powders there was an inherent enzyme stability issue, which reduced the capacity for the powder to generate ROS over time, requiring further research and development.

In this chapter, it was demonstrated that optimised SHRO powders exhibited broad spectrum efficacy against clinically relevant bacteria without causing harm to endogenous cells. Furthermore, the development of synthetic reactive oxygen powders offers flexibility and easily tailorable dosing. Overall this work highlights the potential of reactive oxygen powder delivery systems as a means by which to expand the clinical usability of alternative antimicrobials, offering the field a powerful new tool in the fight against development of resistant microbes. Further experimentation could see studies designed to improve the flow characteristics of SHRO powder. This could be achieved by using a ball mill for uniform powder grinding, with determination of flow assessed by means of the Carr compressibility index in a desiccated environment. In addition to this, work on stabilising the GOx in the synthetic powder formulation would allow for longer term storage and efficacy.

CHAPTER SIX

6. REACTIVE OXYGEN IMPLANTABLE CEMENT DELIVERY SYSTEMS

6.1 Introduction

Hard tissue defects can arise following disease or trauma, including the excision of infected tissue and benign or cancerous growths. While bone exhibits a capacity to "self-heal" small defects, those larger than a critical size require surgical intervention. In this case, bone graft or biomaterials may be used to repair the defect and provide a scaffold for new hard tissue deposition. It is essential that these materials are well tolerated by the body (i.e. biocompatible), resorbed at a rate that matches bone formation, cost-effective, easily stored and easy to apply within the clinical setting. To this end, there has been a vast emergence of calcium-salt based cement systems in recent decades [351].

In particular, CSC has been widely adopted clinically. This success is due to the formation of an injectable paste that may be easily and directly delivered to the defect site. Advantageously, the setting reaction of calcium sulphate, which progresses through a dissolution-precipitation reaction, is compatible with the physiological environment (Eq. 6.1). The cement can therefore harden *in situ* to provide a scaffold for new bone formation. This feature of CSC gives rise to beneficial properties that can enhance patient recovery and well-being, such as the loading of antibiotics.

$$CaSO_4 \cdot 0.5H_2O + 1.5H_2O \rightarrow CaSO_4 \cdot 2H_2O \quad \text{(Eq. 6.1)}$$

Antibiotics are vital to modern medicine, helping to protect patients from infection that may be the result of injury, a compromised immune system, or the undertaking of procedures such as surgery [497,498]. It is therefore alarming that bacteria are rapidly evolving resistance to many antibiotics, which may be attributed to global misuse [33,34]. Gentamicin, a broad spectrum aminoglycoside antibiotic has been loaded into bone cements to provide a prophylactic effect since the early 1970's [379–381]. Resistance to gentamicin, like all mainstream antibiotics, is ever increasing and despite a 2002 report by Thornes *et al.* stating that it is unsuitable for use in bone cements for revision surgery due to the development of resistance, widespread clinical use has continued [382,383]. As such, the development of novel antimicrobials that provide a viable alternative to commonly used prophylactics, as well as systems by which to enable efficacious delivery, are a healthcare priority [382,384].

The promising potency of SHRO by means of the production of reactive oxygen species, such as hydrogen peroxide (Eq. 6.2), makes it an interesting candidate for further investigation into its ability to replace more traditional antibiotics for use in infection prevention or treatment. To date, little work had been done to assess the capability of this water sensitive active with existing biomaterial delivery systems.

$$C_6H_{12}O_6 + H_2O + O_2 \xrightarrow{GOx} C_6H_{12}O_7 + H_2O_2 \quad \text{(Eq. 6.2)}$$

For the first time, this chapter highlights the potential to formulate a calcium sulphate and SHRO cement producing an antimicrobial regenerative scaffold. Herein, we address the challenging water-sensitive nature that accompanies the use of ROS producing honey products

by limiting its exposure to free water. This is achieved by locking excess water within the crystal structure of hydrated cement. Furthermore, key physicochemical properties of this novel cement are analysed to determine usability, including compressive strength, setting time and injectability. Alongside antibacterial testing, a scratch assay was conducted. In summary, SHRO enriched cements were shown to kill and inhibit bacteria without inducing an inflammatory response or affecting the rate of wound healing using osteoblast bone cells.

6.2 Materials and Methods

6.2.1 Preparation of cement

Cements were prepared with a liquid to powder (L:P) ratio of 0.2 mL/g. Anti-bacterial derivatives contained 0.1 g of SHRO per gram of cement powder. Briefly, calcium sulphate hemihydrate ($CaSO_4 \cdot 0.5H_2O$) powder (Sigma Aldrich, UK) was combined with distilled water and mixed for 30 seconds to form a workable paste before hardening (CS_Control). SHRO (Matoke Holdings, UK) was combined either as an initial constituent of the cement (CS_SHRO1) or combined with cement paste 4 minutes after the initial 30 second mixing time (CS_SHRO2).

Once mixed, pastes were cast into a split mold and placed upon a vibrating plate to reduce air bubbles within the final cement samples. The cement filled split mold was incubated at 37^{o}C for 12 hours to produce 6 by 13 mm (D:H) cylindrical test specimens. Initial and final setting times were determined using Gillmore needle apparatus and following ASTM standard C266-15. Briefly, cement pastes were prepared and manipulated into a flat-topped pat. The initial setting time was determined by vertically applying a 113.4±0.5 g weighted needle with a tip diameter of 2.12±0.05 mm to the top surface of the pat, and taken as the point at which no appreciable indent was observed post addition of the liquid component. The final setting time was determined by vertically applying a 453.6±0.5 g weighted needle with a tip diameter of 1.06±0.05 mm to the top surface of the pat and taken as the point at which no appreciable indent was observed post addition of the liquid component. Measurements were recorded at 10 minute intervals in triplicate.

6.2.2 Cement characterisation

Cement degradation was examined by static ageing. Individual cast cement cylinders were placed in a cylindrical container with a diameter of 22.1 mm and fully submerged in 2.5 mL of distilled water. Changes in mass were recorded at days 7, 14 and 21 in triplicate.

Mechanical testing was performed using a Zwick/Roell Z030 Universal testing rig equipped with a 50 kN load cell. Compression tests were undertaken at a loading rate of 2 mm/min. Following a specimen pre-load of 5 N, force versus deformation curves were recorded in triplicate.

Scanning electron microscopy (SEM) was used to image cement fracture surfaces. Imaging was performed using a Hitachi TM3030Plus tabletop instrument. Back scattered electron (BSE) and secondary electron (SE) were acquired with an acceleration voltage of 15 kV. All SEM samples were mounted onto aluminium stubs using double sided carbon discs, and gold coated to ensure conductivity.

To assess any change in phase composition over time, powder X-ray diffraction (XRD) was performed using a Bruker D8 Advance instrument equipped with a Cu X-ray source (1.5418 Å) and LYNXEYE (1D mode) detector. Diffraction patterns were acquired between $10 - 50^{o}$ 2θ with a step size of 0.02^{o} and step time of 0.3 seconds. Raman spectroscopy was also performed using a Renishaw inVia™ Raman microscope equipped with 633 nm laser and 1200 l/mm grating. Scans were an average of 3 accumulations acquired at 1 % power and 30 seconds exposure time, with the baseline subtracted and cosmic rays removed using WiRE™ software.

6.2.3 Anti-bacterial properties of cements

Initially the capacity of the cements to generate H_2O_2 was determined. Cast cement cylinders (section 6.2.1) were placed in a cylindrical container with a diameter of 22.1 mm and fully submerged in 2.5 mL of distilled water. Supernatant was recovered at 1, 3, 6 and 24 hours as well as at 4 and 7 days. H_2O_2 was detected using a fluorometric hydrogen peroxide assay kit (Sigma Aldrich, UK) in triplicate. Due to the instability of the H_2O_2 molecule, collection of samples was staggered, such that supernatant from each time point was collected and assayed simultaneously.

Anti-bacterial activity of cements was then determined by an agar diffusion method. Nutrient agar plates were prepared by pouring 25 mL of sterilized nutrient agar into Petri dishes. Once solidified, condensation was eliminated by placing the agar filled Petri dishes in a 60°C dry heat oven. Overnight cultures of *S. aureus.* (ATCC 29213) and *P. aeruginosa* (NCTC 13437) were prepared by inoculating one colony of each strain into 5 mL of Luria-Bertani (LB) broth (Sigma Aldrich, UK) and incubated at 37°C for 16 hours in a shaking incubator (150 rpm). Each overnight culture was then diluted to an optical density (OD_{600}) value of 0.02, using an Evolution 300 UV-VIS spectrophotometer (Thermo Scientific, UK). The plates were then inoculated with bacteria, using a hockey stick spreader to ensure maximum coverage. A sterile hole borer (Sigma Aldrich, UK) was then used to create a 10 mm diameter well in the center of the inoculated agar. For the pre-set samples cement supernatant was recovered after 24 hours, of which 250 µL was transferred to inoculated agar wells (CS_SHRO2 Dry). Alternatively, 250 µL of cement paste was directly injected into the well (CS_SHRO2 Wet). A gentamicin dose comparison was prepared at a concentration of 0.0024 g/mL. This equates to the same calculated mass of hydrogen peroxide released after 24 hours from CS_SHRO2 scaffolds. Plates were then incubated at 37°C for 24 hours. Zones of inhibition (ZOI)

measurements were taken conservatively (smallest diameter of zone) using a ruler. Experiments were performed in triplicate.

6.2.4 Osteoblast cell migration and inflammatory response

Osteoblast migration was assessed by means of an *in vitro* scratch assay. 500,000 osteoblast like cells (SAOS-2 – Passage number 28) were seeded into each well of a Corning™ 24 well plate (Sigma Aldrich, UK) and incubated in a HeraCell 150i CO_2 incubator (Thermo Scientific, UK) for 3 days at 37°C with 5% CO_2. A vertical scratch across the well was then made using a pipette tip. The cells were subsequently washed using PBS (Thermofisher, UK) to remove debris and McCoy's 5A modified media (Fisher Scientific, UK) was replaced. Cement samples were then suspended in the cell media using Falcon™ trans-well inserts with a pore size of 0.4 μm (Fisher Scientific, UK). Images were taken every 24 hours using an Eclipse TE300 Inverted Phase Contrast Microscope (Nikon Instruments Incorporated, UK) and cell migration distance was calculated using Image J (1.47v National Institutes of Health, USA).

The inflammatory response to the calcium sulphate control cement (CS_Control) and SHRO loaded samples (CS_SHRO1 and CS_SHRO2) was determined using a human IL-8/CXCL8 enzyme-linked immunosorbent assay (ELISA) (R&D Systems, USA). The manufacturer's protocol was followed to conduct the ELISA. The optical density was measured at a wavelength of 450 nm using an Infinite F200 Pro (Tecan, UK).

6.2.5 Statistical analysis

Statistical analysis was performed in GraphPad Prism® 5.0 software. Two-way ANOVA was used to determine statistical differences between groups. A students t-test was used for post-

hoc testing. An alpha value of 0.05 was used for all tests. Values of $p < 0.05$ were considered significant.

6.3 Results

6.3.1 Cement preparation

An overview of the preparation of each cement, as well as associated setting time, is provided in Table 6.1. Production of CS_Control, CS_SHRO1 and CS_SHRO2 cements with a L:P ratio of 0.2 mL/g resulted in workable pastes that could be transferred to a split mould and produce cylindrical test specimens. Initial and final setting times were determined using Gillmore needles. Calcium sulphate hemihydrate ($CaSO_4 \cdot 0.5H_2O$) combined with water alone (CS_Control) resulted in the most rapidly setting paste, possessing an initial and final setting time of 10 and 20 minutes, respectively. Addition of SHRO as an initial component of the paste formulation (CS_SHRO1), extended the initial and final setting times to 30 and 40 minutes, respectively. In comparison, if the calcium sulphate hemihydrate ($CaSO_4 \cdot 0.5H_2O$) cement was left to harden for 4 minutes prior to the addition of SHRO (CS_SHRO2), initial (20 mins) and final (30 mins) setting times were extended to a lesser extent than for CS_SHRO1.

Table 6.1. Overview of cement preparation and setting parameters. Setting times were acquired from n=3 pastes and are recorded to the nearest 10 minutes.

Cement	Preparation overview	Preparation time	Initial setting time	Final setting time
CS_Control	Calcium sulphate hemihydrate and water, 30 seconds mixing	30 seconds	10 minutes	20 minutes
CS_SHRO1	Calcium sulphate hemihydrate, SHRO and water, 30 seconds mixing	30 seconds	30 minutes	40 minutes
CS_SHRO2	Calcium sulphate hemihydrate and water, 30 seconds mixing, wait 4 minutes, add SHRO, 30 seconds mixing	5 minutes	20 minutes	30 minutes

6.3.2 Cement characterisation

Cement degradation was examined by statically ageing specimens in distilled water over a period of 3 weeks. All specimens remained intact with negligible evidence of either fragmentation or degradation (Figure 6.1a). Weekly measurements showed minimal variation in mass over a three week period, with a maximum 3% increase at week 2. In contrast, CS_SHRO1 and CS_SHRO2 cements were both shown to lose 2-4% mass by week 3 and exhibited comparable degradation kinetics to each other (Figure 6.1b).

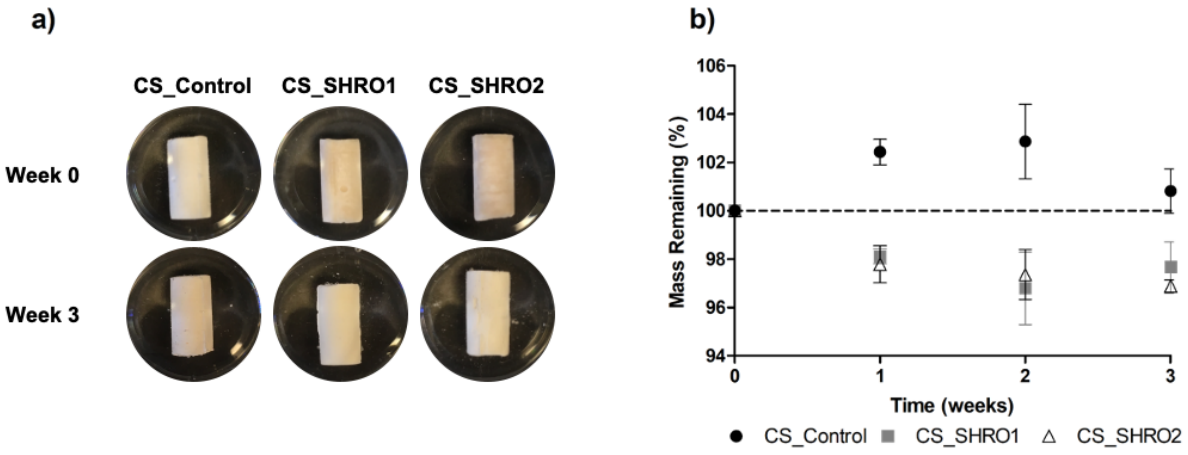

Figure 6.1. Appearance (a) and measured changes in mass (b) for CS_Control, CS_SHRO1 and CS_SHRO2 cements as prepared (Week 0) and following 3 weeks of static ageing in distilled water (Week 3).

Raman spectroscopy confirmed the predominant phase of CS_Control, CS_SHRO1 and CS_SHRO2 cements as calcium sulphate dihydrate ($CaSO_4 \cdot 2H_2O$) (Figure 6.2a). Vibrational modes indicative of SO_4 tetrahedra were identified in all samples. Consistent with calcium sulphate dihydrate ($CaSO_4 \cdot 2H_2O$) peaks were identified at 1009 cm^{-1} (symmetric stretching, υ^1), 415 cm^{-1} and 493 cm^{-1} (symmetric bending, υ^2), 1137 cm^{-1} (antisymmetric stretching, υ^3), and 620 cm^{-1} and 670 cm^{-1} (antisymmetric bending, υ^4).

Prior to ageing, XRD analysis demonstrated that all samples consisted of two crystalline phases (Figure 6.2b). Diffraction peaks at 15, 29, 30 and 32° 2θ (*) were matched to the star rated ICDD pattern for $CaSO_4 \cdot 0.5H_2O$ (01-083-0438). The remaining peaks at 12, 21, 29, 31 and 33° 2θ (•) were matched to the star rated ICDD pattern for $CaSO_4 \cdot 2H_2O$ (01-070-0983). Quantification of phases revealed that $CaSO_4 \cdot 0.5H_2O$ and $CaSO_4.2H_2O$ constitute all pre-aged cement samples at an approximate ratio of 1:2. Following ageing, only minor quantities

(< 5%) of $CaSO_4 \cdot 0.5H_2O$ remained in any of the cement scaffolds due to further hydration within the aqueous environment (Table 6.2).

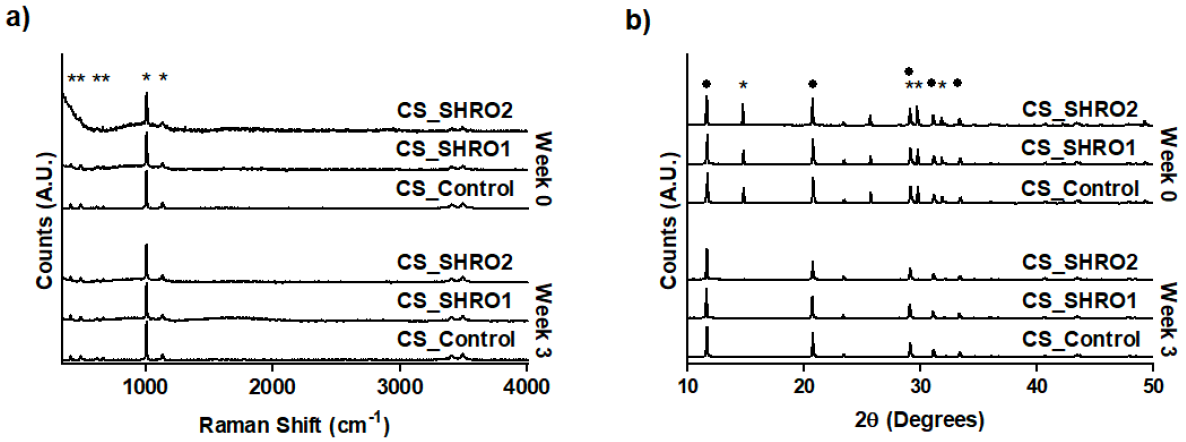

Figure 6.2. Raman spectra (a) and XRD powder diffraction patterns (b) for CS_Control, CS_SHRO1 and CS_SHRO2 cements as prepared (Week 0) and following 3 weeks of static ageing in distilled water (Week 3).

Table 6.2. Overview of cement composition as prepared (Week 0) and following 3 weeks of static ageing in distilled water (Week 3).

Cement	Week 0		Week 3	
	$CaSO_4 \cdot 0.5H_2O$	$CaSO_4 \cdot 2H_2O$	$CaSO_4 \cdot 0.5H_2O$	$CaSO_4 \cdot 2H_2O$
CS_Control	36.6%	63.4%	4.3%	95.7%
CS_SHRO1	34.7%	65.3%	2.2%	97.8%
CS_SHRO2	39.8%	60.2%	3.5%	96.5%

The mechanical properties of the cement specimens were assessed using compression testing. Stress-strain curves revealed distinct regions of elastic and plastic deformation, reflective of the specimens catastrophically failing and then progressively fracturing in multiple locations (Figure 6.3a-b). Average compressive strength and Young's modulus were determined (Figure

6.3c-d). Compressive strength values of 37.9 ± 5.2, 22.6 ± 5.0 and 23.5 ± 6.4 MPa were achieved by unaged CS_Control, CS_SHRO1 and CS_SHRO2 samples respectively with the unaged CS_Control demonstrating a significant ($p < 0.05$) increase in compressive strength in comparison to both CS_SHRO1 and CS_SHRO2 cements. Following 3 weeks of ageing, there was no significant difference in compressive strength between CS_Control, CS_SHRO1 and CS_SHRO2 samples (35.0 ± 8.9 MPa, 31.3 ± 7.0 MPa and 32.2 ± 5.8 MPa respectively). In terms of Young's modulus, no significant differences were observed between CS_Control (1.9 ± 0.7 GPa), CS_SHRO1 (1.1 ± 0.9 GPa) and CS_SHRO2 (0.8 ± 0.5 GPa) specimens prior to ageing. Similarly, no significant differences were found after degradation experiments. Moreover, the compressive strength and Young's modulus values of samples before and after ageing (3 weeks) were analysed using a t-test and all exhibited p-values of > 0.05.

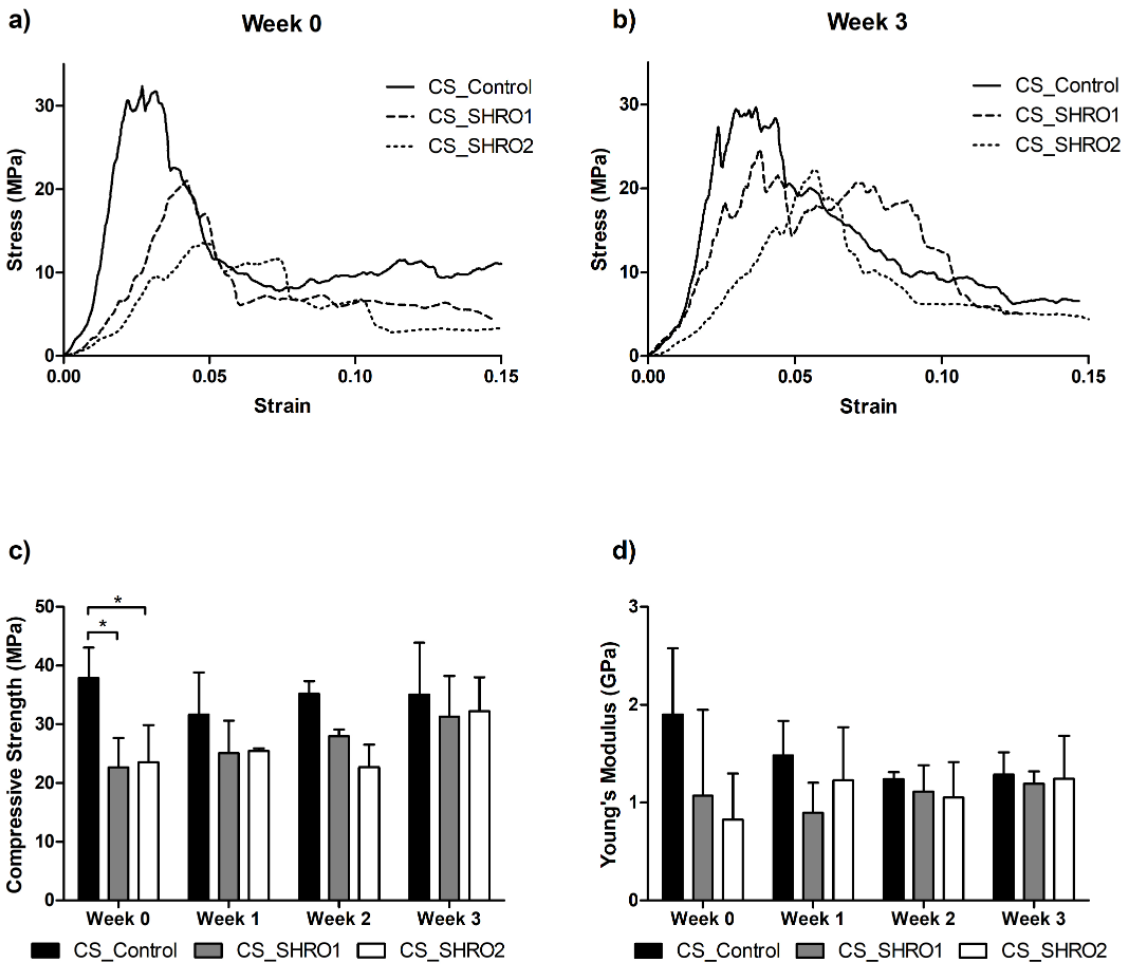

Figure 6.3 Average compressive stress vs. strain curves for CS_Control, CS_SHRO1 and CS_SHRO2 cements (a) as prepared (Week 0) and following (b) 3 weeks of static ageing in distilled water (n=3). (c) Compressive strength and (d) Young's modulus properties for CS_Control, CS_SHRO1 and CS_SHRO2 cements as prepared (Week 0), and following 1 week, 2 weeks and 3 weeks of static ageing in distilled water (Week 1, Week 2 and Week 3 respectively) (mean± SD, n=3).

Cement fracture surfaces were analysed using SEM prior to and following ageing. As prepared CS_Control, CS_SHRO1 and CS_SHRO2 cements appeared to consist of a dense, irregular, network of interconnected high-aspect ratio crystals typical of both $CaSO_4 \cdot 0.5H_2O$ and $CaSO_4 \cdot 2H_2O$ (Figure 6.4a-c). Individual crystal units exhibited approximate dimensions

of 3 x 3 x 15 μm in all samples. Cements subjected to ageing showed no notable deviation in microstructure compared to as prepared cements and further between specimen groups (Figure 6.4d-f).

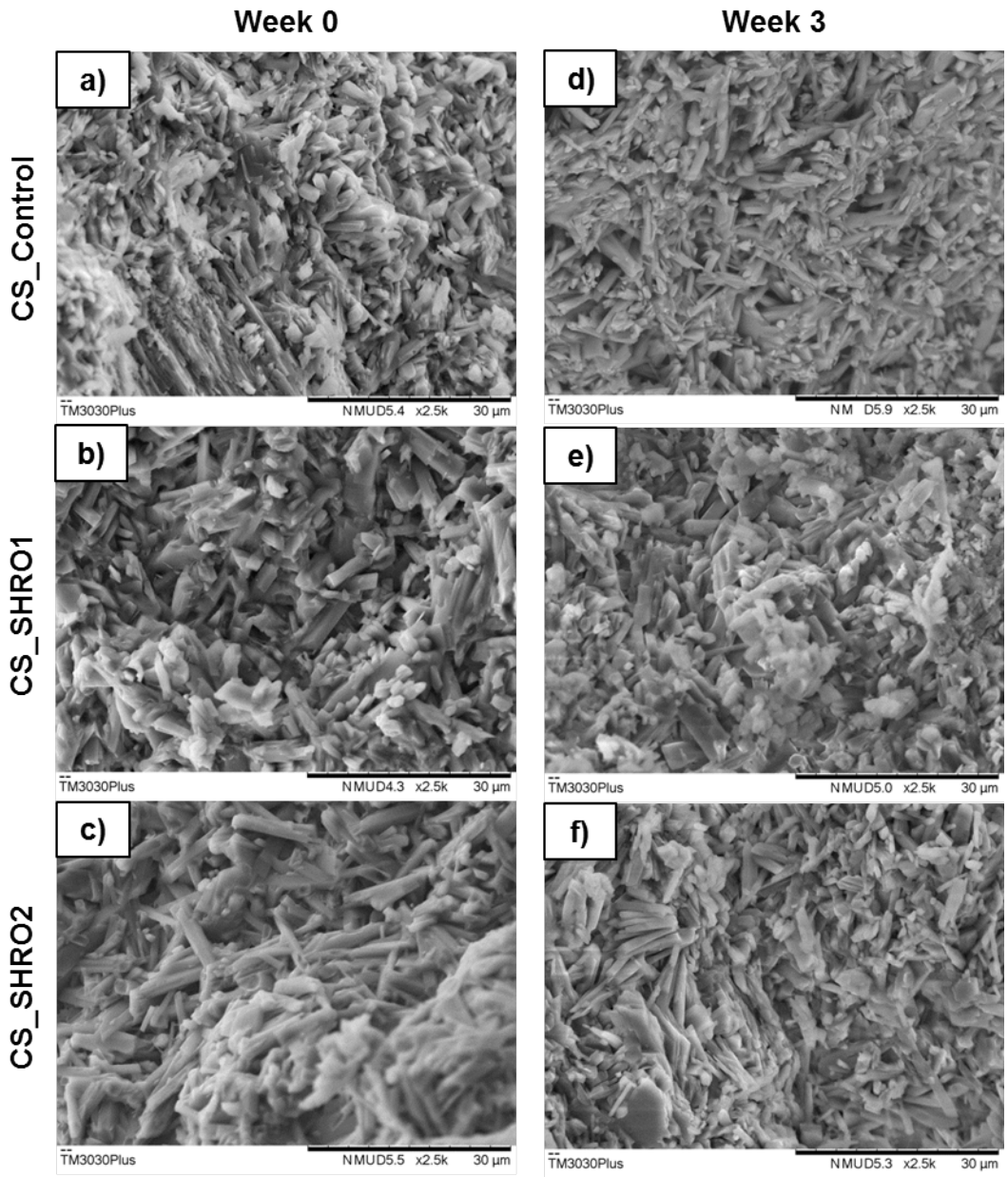

Figure 6.4. SEM images of CS_Control (a), CS_SHRO1 (b) and CS_SHRO2 (c) cement fracture surfaces as prepared (Week 0), and CS_Control (d), CS_SHRO1 (e) and CS_SHRO2 (f) cement fracture surfaces following 3 weeks of static ageing in distilled water (Week 3).

6.3.3 Antibiotic efficacy and cellular response

The generation of H_2O_2 from CS_Control, CS_SHRO1 and CS_SHRO2 cements in distilled water was measured over a period of 72 hours (Figure 6.5a). CS_Control cements consistently produced baseline levels of up to 0.006 ± 0.001 µmol g^{-1} H_2O_2 while peak levels of

production were detected at 24 hours for CS_SHRO1 (0.28 ± 0.03 μmol g^{-1}) and CS_SHRO2 (0.72 ± 0.1 μmol g^{-1}) formulations. After 48 hours, H_2O_2 levels returned to baseline concentrations.

Having demonstrated higher H_2O_2 peak values, CS_SHRO2 cements were tested for their antimicrobial potency in pre-set (dry) and wet states (Figure 6.5b). Levels of H_2O_2 generated from all CS_SHRO2 samples were sufficient for inhibiting the growth of both *S. aureus* and *P. aeruginosa.* H_2O_2 enriched supernatant collected after 24 hours from pre-set CS_SHRO2 cylinders gave zones of inhibition measuring 7.7 ± 0.6 mm for the Gram positive *S. aureus*, whilst zones of inhibition for the Gram negative *P. aeruginosa* measured at 5.7 ± 0.6 mm. This was significantly smaller ($P < 0.05$) than those measured for samples set *in situ*, which produced zones of inhibition measuring 14.7 ± 1.2 and 11.7 ± 1.0 mm for *S. aureus.* and *P. aeruginosa,* respectively. Promisingly, CS_SHRO2 set *in situ* showed no significant difference in inhibition to that of a comparable dose of gentamicin producing zones of 15.3 ± 0.6 (*S. aureus*) and 12.7 ± 1.5 mm (*P. aeruginosa)*.

A scratch assay was performed in the presence of CS_Control and CS_SHRO2 cements in order to determine the effect on osteoblast migration as a simple model for bone regeneration (Figure 6.5c). The scratch (distance between cells) initially measured at 404.50 ± 38.9, 339.50 ± 36.1 and 380.00 ± 1.4 μm for CS_Control, CS_SHRO2 and media only samples, respectively. After 48 hours it was shown that in all cases that cells migrated across the gap, reducing the initial size of the scratch by 82.2% (CS_Control), 76.29% (CS_SHRO2) and 87.76% (Media control).There was found to be no significant difference ($P > 0.05$) in cell migration distance across the "wound gap" between samples and controls. Alongside the scratch assay, expression of inflammatory chemokines were assessed and no significant

differences in CXCL8 level were observed between the CS_Control (31.40 ± 6.3 pg/μL), SHRO containing cements (31.83 ± 5.8 pg/μL) and media alone (31.78 ± 6.3 pg/μL) (Figure 6.5d).

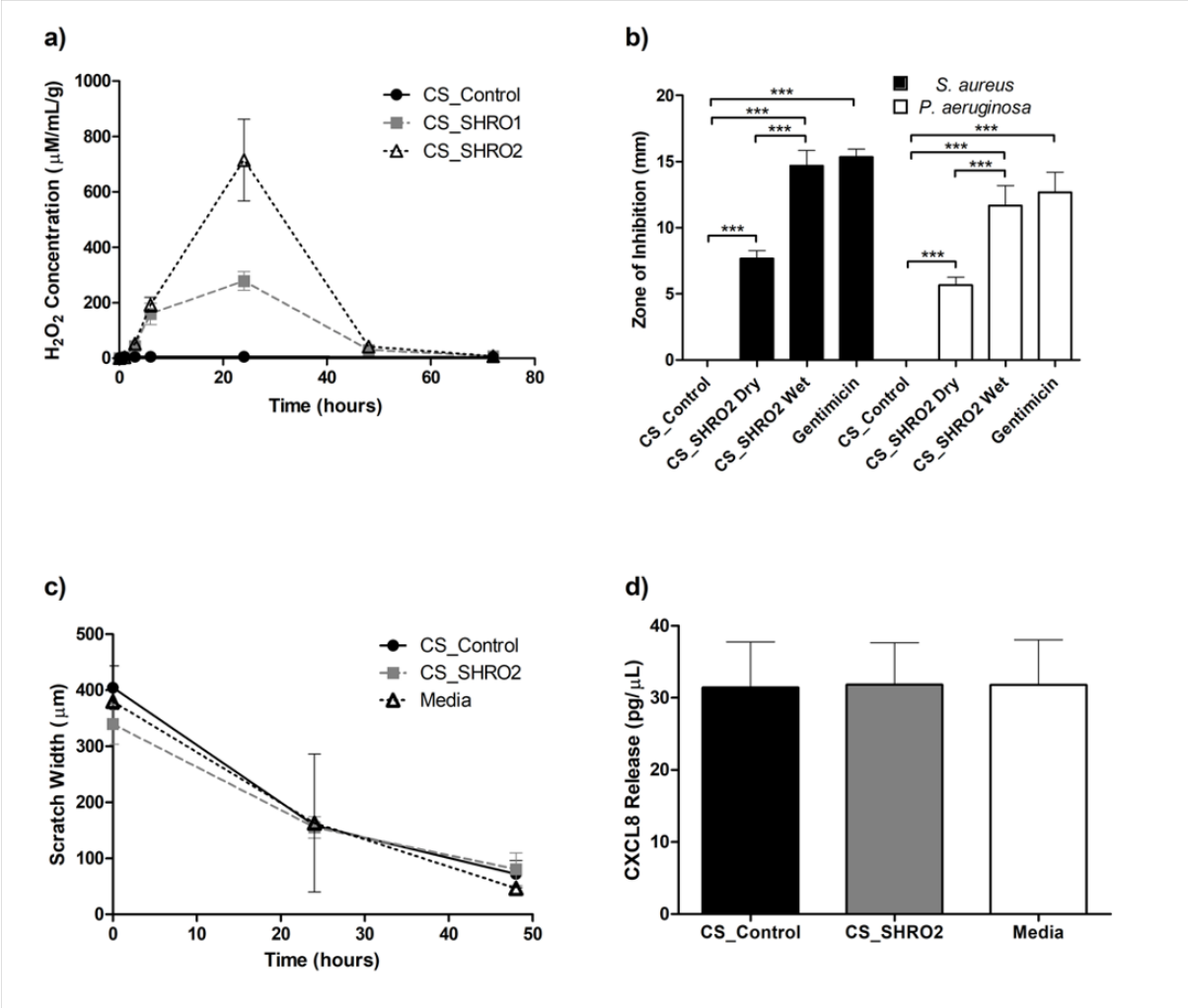

Figure 6.5. (a) Normalised hydrogen peroxide production for CS_Control, CS_SHRO1 and CS_SHRO2 cements in distilled water (mean± SD, n=3). (b) Zones of Inhibition for *Staphylococcus aureus* (*S. aureus*) and *Pseudomonas aeruginosa* (*P. aeruginosa*) in the presence of CS_Control, CS_SHRO1 and CS_SHRO2 cement supernatants (mean± SD, n=3). (c) Scratch assay and (d) human IL-8/CXCL8 enzyme-linked immunosorbent assay to determine the cellular effect of CS_Control and CS_SHRO2 scaffolds in comparison to media alone on wound healing using osteoblast cells (mean± SD, n=2).

6.4 Discussion

In recent decades the emergence of calcium-based scaffolds, such as calcium sulphate cement, to augment bone defects and provide a scaffold for cellular integration has proved highly successful. However, in order to enhance patient recovery these systems are often prophylactically loaded with antibiotics - commonly gentamicin. Antibiotics are a cornerstone of modern medicine and as such the current rapid evolution of resistant species is an alarming threat. This work has demonstrated a methodology to incorporate an alternative antimicrobial substance, specifically a reactive oxygen producing honey (SHRO), into a calcium sulphate cement. Importantly it is demonstrated that structural integrity of the SHRO containing cement is maintained while exhibiting comparable potency to an antibiotic control against Gram negative and Gram positive species.

An initial study into the degradation of SHRO cements showed minimal variation in mass over a three week period, with a maximum 3% increase at week 2 for the control CS cement. This increase is likely due to the precipitation of calcium dihydrate from unreacted calcium hemihydrate as the water infiltrates the scaffold. In contrast, CS_SHRO1 and CS_SHRO2 cements were both shown to lose 2-4% mass by week 3 and exhibited comparable degradation kinetics to each other (Figure 6.1b). This is likely due to the SHRO locked within the cement scaffold dissolving in the water and diffusing out into solution.

While degradation kinetics showed little variability in mass loss over a three week period once the cement was set. It was observed that adding SHRO to calcium sulphate hemihydrate ($CaSO_4 \cdot 0.5H_2O$) and water increased the time taken to form a completely hardened scaffold, which suggests that either the honey is altering the reaction products or the setting kinetics. The extent to which setting is delayed is dependent upon the timing of SHRO incorporation into

the ceramic matrix. It is postulated that the osmotic nature of the SHRO actively removes the free water required for the dissolution of calcium sulphate hemihydrate ($CaSO_4 \cdot 0.5H_2O$) and subsequently delays the precipitation of calcium sulphate dihydrate ($CaSO_4 \cdot 2H_2O$) (Eq. 6.1). A theory supported by Raman spectroscopy and XRD, which indicate that no additional reaction products have been formed. Hall, *et al.,* [170] demonstrated that the presence of additional water prior to application leads to premature ROS production and a reduction in antimicrobial efficacy at point of use. The osmotic nature of SHRO also allows for the honey to be incorporated into the developing ceramic matrix during preparation. SHRO draws water from the hardening matrix, acting as a liquefier, this allows for homogeneous mixing. In theory, less free water would be available for osmotic extraction by SHRO given the partial transformation into the stable hydrated calcium sulphate ($CaSO_4 \cdot 2H_2O$) phase during the 4 minute initial setting period.

It was hypothesised that locking water into the crystal structure of the hydrated calcium sulphate ($CaSO_4 \cdot 2H_2O$) would benefit the antimicrobial efficacy of CS_SHRO2 scaffolds, as this reduces the free water available to generate ROS species on contact with SHRO. Therefore, CS_SHRO2 cement will possess a greater potential to generate ROS following setting over CS_SHRO1 cement. Notably it was found that CS_SHRO2 produced > 2.5 times more hydrogen peroxide (0.72 ± 0.1 μmol g^{-1}) over 24 hours than CS_SHRO1 (0.28 ± 0.03 μmol g^{-1}) despite both formulations containing the same amount of active supporting the hypothesis that ROS production is affected by free water availability. Currently, antibiotics are prescribed prophylactically in order to decrease postoperative infections, however antimicrobial prophylaxis is to be discontinued 24 hours after surgery as stated by the guidelines [499]. The timeframe of antimicrobial activity for these cements therefore falls within the

recommended guidelines. Interestingly however as the ROS falls rapidly after 24 hours the concentrations of ROS could be beneficial for bone regeneration [155].

Following preparation, there were notable differences in scaffold appearance between groups. Compared to CS_Control cements, which were pure white, SHRO infused CS_SHRO1 and CS_SHRO2 cements were distinguishable by a slight golden colouration. During ageing experiments, the supernatant surrounding CS_Control specimens remained clear. Within 24 hours, the ageing supernatant of CS_SHRO1 and CS_SHRO2 specimens took on a golden hue. This is suggested to be an indicator of water infiltration within the internal structure of cements and the leeching of SHRO from these scaffolds. This may account for the mass reduction (2-4%) observed in the honey containing samples (Figure 6.1b). As indicated by the Raman spectra and XRD patterns, calcium sulphate hemihydrate is detected in all of the prepared samples. Its presence is likely due to the cements being prepared with the least possible volume of water to form a workable paste, making water a limiting reagent of the setting reaction in order to restrict its interaction with SHRO and prevent premature production of ROS (Eq. 6.2). Unreacted calcium sulphate hemihydrate in the cement scaffolds was then found to convert to calcium sulphate dihydrate during the ageing experiment (Table 6.2), explaining why CS_Control cements gain 3% mass during the first 2 weeks of ageing. Following 3 weeks of ageing, the mass of CS_Control specimens was comparable to the week 0 cylinders, suggesting some degradation of the cement scaffold. Interestingly, the changes in mass are not monotonic, suggesting a dynamic relationship between mass increase due to the further precipitation of calcium sulphate dihydrate and the loss of scaffold due to the release of the therapeutic additive and cement degradation.

At week 0, SHRO addition was found to reduce the mechanical integrity of the materials as Control scaffolds (CS_Control) possessed higher compressive strength and Young's modulus values compared to CS_SHRO1 and CS_SHRO2 (Figure 6.3e-f). As the honey is not a particulate antimicrobial, it was not expected to act as a filler within the bulk matrix [500]. Interestingly, it has previously been showed that the strength of calcium-based cement can be influenced by the addition of antibiotic compounds, possibly through mechanisms of chemical interaction during the setting period that can alter the scaffold microstructure [501]. Mechanical properties of cement scaffolds are highly dependent on microstructural features, such as pore size and pore distribution, which present weak points in the scaffold that may initiate crack formation [502,503]. Given that SHRO is osmotic and has a naturally low pH (3.8), it may influence the setting reaction and microstructural characteristics of calcium sulphate cement by drawing water away from the progressing reaction (Eq. 6.1) [504]. This could restrict precipitation and possibly promote pore formation. Further testing to evidence this theory should be undertaken with the determination of sample porosity. This would provide conclusive evidence as to the effect SHRO has on the structure of CS cement. Although SHRO has the potential to influence the microstructure of cement, at the loading levels employed minimal deviations in microstructure were observed. Although the resulting compressive strengths of the scaffolds exceed those of human trabecular bone harvested from various sites of the human body, including the mandible (0.2 - 11 MPa) and femoral head (3 - 8 MPa), the values are substantially lower than that of compact load bearing cortical bone (110 MPa) [408–410]. These scaffolds may therefore provide sufficient mechanical stability in augmentation sites within non-load bearing anatomical regions. Given that the scaffolds retain mechanical properties and undergo minimal degradation over the course of in vitro ageing, SHRO incorporated cements may be suitable as regenerative scaffolds over an extended period of time if required [505].

It has been demonstrated that the release of ROS, such as hydrogen peroxide, from SHRO is pertinent to its antimicrobial efficacy [418]. CS_SHRO2 demonstrated greater capacity for the generation of hydrogen peroxide as per the hypothesis and as thus justifies the selection of CS_SHRO2 for further testing. CS_SHRO2 was tested for its antimicrobial efficacy against clinically relevant bacterial species [41], by means of agar diffusion tests, examining the zones of inhibited growth on inoculated agar plates. The preparation of CS_SHRO2 cements for this *in vitro* assay was conducted in two ways, the first by forming pre-set cylinders that were then immersed in distilled water and incubated at 37˚C for 24 hours. Hydrogen peroxide enriched supernatant was then removed and added to the wells in the agar. This methodology allows the antimicrobial efficacy of the cement post setting to be examined while also assessing whether this material could be used as a pre-set granule formulation to provide a prophylactic regenerative template. It was found that CS_SHRO2 pre-set cement does have the ability to inhibit the growth of both Gram positive *S. aureus* and Gram negative *P. aeruginosa*, however the zones of inhibition were significantly smaller ($P<0.05$) than those of cements directly injected into the well and allowed to set (Figure 6.5b). The reduced antibacterial potency of the pre-set formulation suggests that a degree of ROS activation occurs during hardening. To enable this novel antimicrobial cement to be used in its pre-set form it may be possible to increase the baseline efficacy of the incorporated SHRO, as reported by Dryden *et al.,* [43]. Promisingly, when the CS_SHRO2 paste is administrated directly into the agar plate the resultant zones of inhibition were comparable to an equivalent dose of gentamicin. The ability to kill both Gram positive and Gram negative organisms is consistent with that of previous *in vitro* studies involving SHRO and thus further demonstrates it is a viable alternative to traditional antibiotics [170,418].

Having assessed the potent antimicrobial viability of the CS_SHRO2 cement formulation it was necessary to investigate the effect these formulations would have upon endogenous osteoblast cells that would be present in the surrounding defect tissue. This was achieved by conducting a scratch assay and an ELISA detecting inflammatory chemokines. The scratch assay, a methodology described by Liang, *et al.*, [506], is based upon observing and measuring the migration of the leading edge of a confluent cell monolayer, across an artificially formed gap "scratch", until new cell to cell contact is achieved. No impairment of osteoblast migration was observed in the presence of CS_SHRO2 scaffolds, which is promising since maintenance of wound healing would be critical to patient recovery. This cellular compatibility was further supported by investigating the degree of inflammatory chemokines produced by the osteoblast cells. Interleukin 8 (CXCL8) is produced by cells, such as osteoblasts as an environmental immune response in order to stimulate macrophage recruitment to a particular site [507,508]. It was found that there was no significant difference in CXCL8 concentration in the media containing CS_Control cements supporting claims in the literature that calcium sulphate does not elicit an inflammatory response [363]. CS_SHRO2 scaffolds also exhibited this absence of an inflammatory response suggestive of a compatible relationship between the scaffold, released SHRO, and the endogenous cells.

6.5 Conclusion

In conclusion this chapter addresses the need for the production of a regenerative bone tissue scaffolds that engender efficacious alternative antimicrobial solutions to use instead of traditional antibiotics. This has been achieved by formulating calcium sulphate cements that incorporate a reactive oxygen producing honey (SHRO). Promisingly, the compressive strength of SHRO loaded calcium sulphate cements was shown to be comparable to trabecular bone and not significantly different to a control calcium sulphate formulation (CS_Control) after a period of 3 weeks. As such, SHRO loaded calcium sulphate cement may be deemed mechanically suitable for use in trabecular bone augmentation, in particular craniomaxillofacial sites.

The antimicrobial efficacy of SHRO is largely due to a water initiated and enzyme mediated oxidation of glucose, which produces ROS, which lead to microbial killing. By incorporating SHRO into the developing scaffold matrix, it was hypothesised that the water would already be bound in the crystal structure of the hydrated calcium sulphate phase. This methodology of incorporation was shown to limit premature activation of ROS. In addition, in order for an antimicrobial effect to occur the concentration of ROS must be >25 μM, this efficacy was demonstrated after 24 hours *in vitro* against clinically relevant Gram positive (*S. aureus*) and Gram negative (*P. aeruginosa*) bacteria. Furthermore, after 48 hours this novel SHRO loaded calcium sulphate cement was not found to inhibit would healing or elicit an inflammatory response in osteoblast bone cells, supporting the theory that as ROS concentrations declines from that which proves an antimicrobial affect, concentration beneficial for wound healing (0.1-10μM) may be generated.

In summary, this study presents promising evidence that other antimicrobials, such as SHRO, may be used as alternatives to traditional antibiotics in bone cements, which is a timely development in the wake of the bacterial resistance crisis.

CHAPTER SEVEN

7. CONCLUSIONS AND FUTURE WORK

7.1 General Overview

AMR is growing at an unprecedented rate, with 10 million people per year predicted to die annually from resistant infections by 2050. Antimicrobials are vital to modern medicine and therefore, research into novel antimicrobials and systems by which to effectively deliver them is a healthcare priority.

Honey used topically for millennia in wound care applications can deliver a potent antimicrobial effect, however, its potency may differ greatly from batch to batch. To circumvent this issue, a bioengineered antimicrobial honey (SHRO) with promising activity was used. The antimicrobial properties elicited from SHRO are predominantly owed to the production of ROS by means of a water-sensitive enzymatic reaction. Currently, much like honey SHRO is an adherent, highly viscous product, packaged in both a tube and a sachet, but with limited clinical use and application. The aim of this thesis was to overcome these issues to produce delivery systems which ease application and deliver an efficacious dose of ROS. Previous use of ROS in wound care has been at high, often cytotoxic doses in order to sustain activity. However, as SHRO generates ROS lower local concentrations of ROS can be generated to replicate doses familiar to the body such as that produced by macrophages (10-1000 μM) or in wound healing (0.1-10 μM) [77,155].

In chapter 3, the enzyme kinetics responsible for the production of ROS were elucidated and the chemical composition of SHRO unravelled. It was found that the reaction

velocities (Vmax) increased with glucose and GOx concentrations, until values plateaued upon complete enzyme saturation. A pH range between pH 5 and 7 was also identified as producing the fastest rates of reaction, with a peak reaction velocity achieved at pH 6. Compositionally, it was determined that the SHRO tube formulations contained 3.1% more water and less total sugar content than the sachet sample. Furthermore, the SHRO tube formulation also contained less glucose but more GOx when compared to the sachet, leading to the SHRO tube formulation exhibiting a higher level of H_2O_2 production (6.2 ± 0.1 μM compared to 4.9 ± 0.3 μM after 1 hour). The influence of SHRO on viability of both bacteria and human dermal fibroblasts (HDF) was also tested, highlighting that concentrations above 5% were needed in order to inhibit bacterial growth and that at concentrations of 50% SHRO solutions did not have the required water availability to maintain production of H_2O_2 over 7 day period. As such, 50% SHRO solutions were able to provide conditions for which HDF cells could proliferate, express a high degree of viability and exhibit a normal morphology. This was in contrast to 5% and 0.5% SHRO solutions that caused total cell death over the same time period.

Beyond developing a better understanding of SHRO efficacy, novel delivery systems were engineered capable of easing application and offering *in situ* activation of ROS. Chapter 4, demonstrates and discusses the successful formulation of a W/O emulsion containing SHRO, which was engineered to trigger the release of antimicrobial H_2O_2 concentrations as a result of water addition and shear. This system protected, stored and released ROS at the time of application, producing 4.2, 1.9 and 0.7 μmol g^{-1} after 24 hours for 60, 50 and 30% emulsions respectively. Efficacy was also demonstrated *in vitro* against clinically relevant bacteria. However, although the system did appear stable after 7 days, this study would need to be extended as the shelf lives of a medical product would require much greater stability. Emulsion

composition was optimised to achieve the desired shear thinning behaviour, easing delivery and promoting retention of the active at the site of infection. Stability observations revealed that in some cases a small degree of sedimentation did occur, but for paraffin oil emulsions this was shown to be reversible by shaking. Conveniently this redistributed droplets evenly, which is known to improve dose reproducibility. Hydrogen peroxide measurements concluded that formulations with higher concentrations of SHRO produced greater levels of reactive oxygen species. Paraffin oil emulsions with 50 and 60% SHRO successfully inhibited clinically relevant *Staphylococcus aureus, Pseudomonas aeruginosa* and *Escherichia coli*. Post formulation, however, it was discovered that the temperature of the emulsion (78.8 ± 2.1°C) was higher than that of the enzyme's denaturation temperature (55°C), potentially impacting ROS production. The utilisation of an ice bath combined with a reduction in shear rate and time was found to reduce the formulation temperature to 61.54 ± 3.7°C, however this did result in an increase in sedimentation of 4.88 ± 1.8% over 7 days. Addition of Aerosil fumed silica to a 60% SHRO base emulsion enabled successfully formulation of a SHRO cream, which exhibited favourable rheological characteristics with enhanced stability to sedimentation. SHRO creams also maintaining antimicrobial efficacy by producing up to 1.4 ± 0.5 μmol g^{-1} after 24 hours. This was significantly less than the production of the base 60% emulsion, however after 7 days SHRO cream was found to produce up to 12.1±0.5 μmol g^{-1} which may indicate a slower production of ROS compared to that of the base formulation and provide a longer lasting treatment option.

The advantages of delivering SHRO in the form of an emulsion or cream is that it is easier to administer, as the formulated microstructure is shear-thinning and aids extrusion from the tube. In addition, there is a lack of adhesion and therefore dressings will not stick to the wound site. However, these emulsions are oil based and therefore when applied topically can

feel greasy. In addition, high temperatures reached during homogenisation adds complexity to the formulation.

Focus in chapter 5 was the development of another SHRO delivery system, specifically a ROS producing superabsorbent powder. The challenge here was to successfully formulate free flowing powders containing SHRO that were suitable for application to a topical wound for prevention or treatment of an infection. Through utilisation of freeze drying and addition of CD based drying agents, it was possible to engineer free-flowing powders without compromising the antimicrobial efficacy of the temperature sensitive enzyme within SHRO. Specifically, MCD and HCD proved to be the most effective drying agents at removing water from SHRO. MCD and HCD formulations containing between 50-70% SHRO were further enhanced through addition of a superabsorbent, sodium polyacrylate. This significantly increased the water absorption capacity of the powder and enabled the formation of a protective hydrogel at the wound site while activating production of antimicrobial ROS. SHRO powders were found to produce 5.1, 3.3 and 3.1 $\mu mol\ g^{-1}$ after 24 hours for MCD 70, MCD 50 and HCD 50 formulations respectively. Importantly the incorporation of drying agents was not found to change the chemical composition of SHRO, maintaining efficacy against clinically relevant bacterial species without eliciting any detrimental effects on HDF cells.

In an effort to form a less complex system, synthetic reactive oxygen delivery systems were also formulated from glucose and glucose oxidase. However, although possessing the potential to deliver tailorable, efficacious concentrations of ROS there was an inherent enzyme stability issue, which reduced the capacity for the powder to generate H_2O_2 by up to 78% over 10 days and over 99% after 18 days, requiring further research and development.

The advantages of delivering ROS in the form of a powder is its inherent flexibility. It is easy to deliver to any wound site and can be developed to have broad functionality such as the formation of a hydrogel *in situ*. However, the product is extremely hydroscopic and as such must be stored in an airtight container with relatively low humidity in order to prevent both powder cohesion and activation of ROS production.

The final ROS delivery system was outlined in chapter 6, where the formulation of an implantable SHRO loaded calcium sulphate bone cement was exhibited. Promisingly, the compressive strength of SHRO loaded calcium sulphate cements was shown to be comparable to trabecular bone and not significantly different to a control formulation without honey. As such, SHRO loaded calcium sulphate cement may be deemed mechanically suitable for use in trabecular bone augmentation, in particular craniomaxillofacial sites. By incorporating SHRO into the developing scaffold matrix, it was hypothesised that the water would already be bound in the crystal structure of the hydrated calcium sulphate phase. This methodology of delayed SHRO incorporation was shown to limit premature activation of ROS with formulations producing 0.28-0.72 ± 0.1 μmol g^{-1} after 24 hours. Efficacy was further demonstrated *in vitro* against clinically relevant bacteria and was not found to inhibit wound healing or elicit an inflammatory response in osteoblast bone cells. The advantage of delivering SHRO in a bone cement is that it offers an alternative to currently used antibiotics such as gentamicin and it can also deliver low concentrations of ROS which could aid in wound healing. However, the addition of SHRO to calcium hemihydrate during formulation does increases setting time.

In summary, the novel delivery systems presented in this thesis offer promising evidence that other antimicrobials, such as SHRO, may be used as alternatives to traditional antibiotics.

These developments are particularly timely given the growing impact of AMR and highlight that formulation engineering may enable society to more effectively use antimicrobials, offering hope to tackling this global challenge.

7.2 Limitations and Future Work

7.2.1 Fundamental understanding

Enzyme kinetics

In order to produce a clinically relevant product it is important that the mechanisms of action are well known and understood. Therefore, to add to knowledge and aid formulation of reactive oxygen delivery systems, it was necessary to elucidate the kinetics associated with glucose oxidase. In chapter 3 the effects of glucose, enzyme concentration and pH on reaction rate were determined. An attempt was made to study the catalysed oxidation reaction of glucose at different temperatures, using a temperature controlled plate reader, however there was no notable change in Vmax. This conflicted with results published by Odebunmi., *et al.* [174] and Gibson., *et al.* [433] who noted an increase in reaction velocities with an increase in temperatures. The likely reasoning behind this being that insufficient time was given for temperatures within the wells to equilibrate. As per the methodology, reagents were added and combined within the wells of a multi-well plate with the reaction initiated immediately prior to placing the plate into the plate reader with its temperature pre-set. However, the experimental protocol dictated a maximum run time of 6 minutes, seemingly insufficient time for well reagents to equilibrate at the selected temperature. Future work may look to acquire the use of a temperature controlled plate reader with injection ports. This would allow the well plate and reagents to equilibrate to the set temperature, with the reaction initiated *in situ* by feeding the enzyme solution through the ports. This work would help to provide information with regards to the kinetic activity of glucose oxidase at more physiologically relevant temperatures, for example those more closely related to the skin or internal body temperatures.

7.2.2 Reactive oxygen emulsion formulation

The hypothesis that an oil-based emulsion would protect, store, and release SHRO under shear and dilution with water at the time of application has been demonstrated in chapter 4. However, future work may look to investigate stability further and over longer periods of time. Optimisations may be made in the size of the SHRO droplets which are formed within an emulsion in order to increase stability, as well as further investigations into the impact of temperature on enzyme kinetics. Alternative emulsion formation methodologies may also be explored in order to aid this optimisation, such as that of a high pressure homogeniser. Emulsion composition has so far been optimised to achieve the desired shear thinning behaviour, easing delivery and promoting retention of the active at the site of infection. This technology has broad potential however, further development could see wider application and an increased uptake if presented in a sprayable format. To achieve this, investigations must be made into the reduction of the emulsion viscosity whilst also maintaining efficacy. As sketched in Figure 7.1 a reduced viscosity emulsion could in theory occupy 1 part of a split spray bottle, with the other section of the bottle filled with water. As the components from both portions of the spray bottle are drawn up the tube, they are allowed to mix in the nozzle head, providing the water and shear needed for the activation of ROS production. Alternatively, this concept could also be used in the creation of a synthetic reactive oxygen spray delivery system.

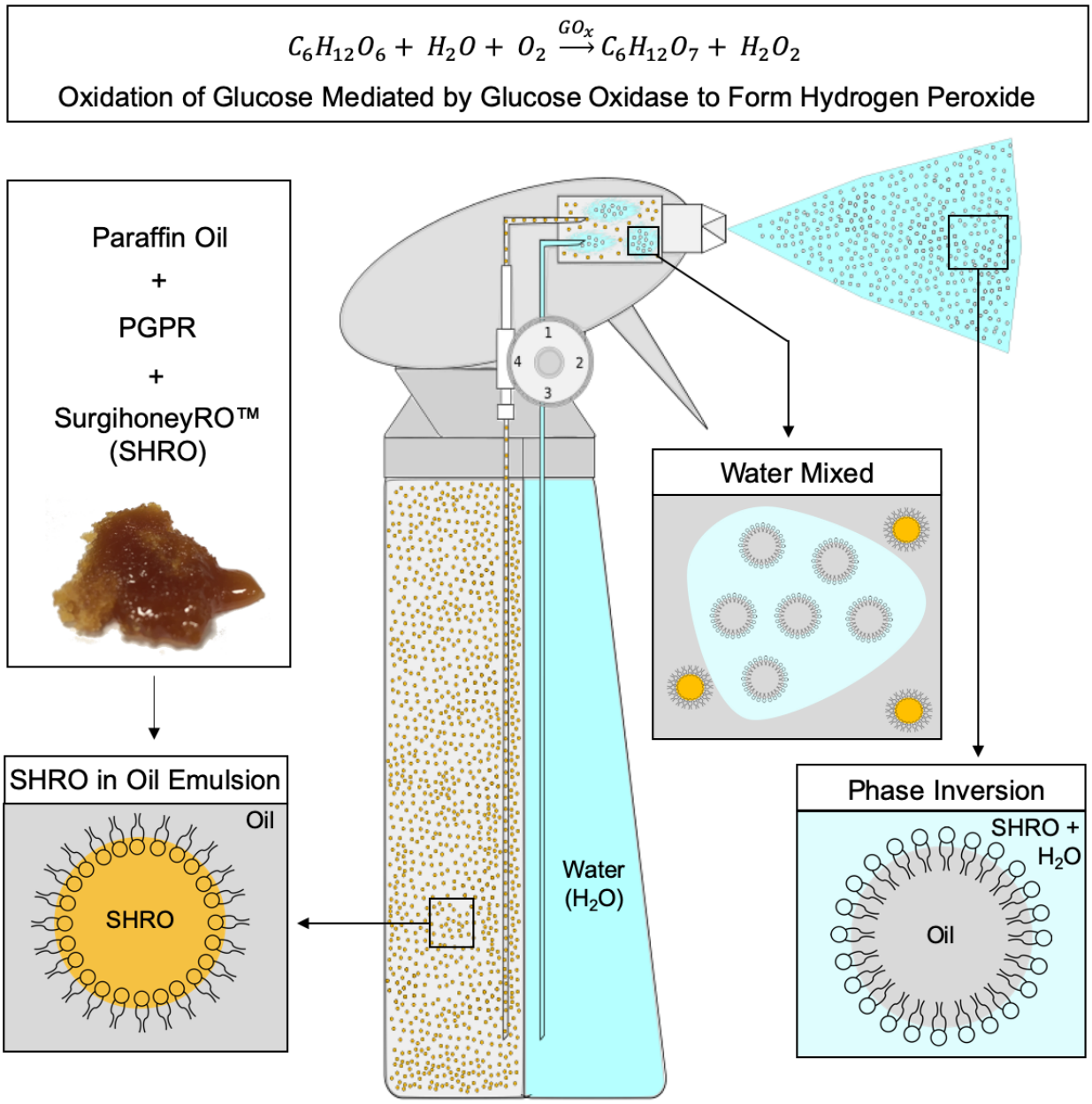

Figure 7.1 Example of a SHRO emulsion spray system envisaging the formation and occupation of a SHRO emulsion inside a compartment of the spray bottle. This is then drawn up and mixed with water where ROS production is activated by the shear forces exerted by the spray nozzle.

7.2.3 Reactive oxygen powder development

Enzyme stability

Chapter 5 demonstrated the successful formulation of SHRO containing powders, produced using freeze drying and the addition of β-cyclodextrin based drying agents. It was demonstrated that this was achieved without compromising antimicrobial efficacy of the temperature sensitive enzyme within SHRO. Furthermore, there was no indication of enzyme instability when stored over the periods of time tested, a characteristic present in all SHRO based formulations. In addition to SHRO powder delivery systems, synthetic reactive oxygen delivery systems were also formulated. However, although possessing the potential to deliver efficacious concentrations of reactive oxygen species there was an inherent enzyme stability issue, which reduced the capacity for the powder to generate ROS over time. It is indicated by a number of researchers that honey contains many different compounds, some of which are known to protect enzymatic activity [489,490]. Future work may look to investigate the mechanism behind the storage instability combined and explore the possibility to add stabilising compounds to the synthetic powder delivery system. It was also noted that storage temperature can play a role in the stability of the enzyme with lower temperatures often preferred [492–494]. A future study into synthetic powder stability at different temperatures could also be conducted. Furthermore, the literature suggests that stability can be increased by immobilising the enzyme onto substrate, or encapsulating glucose oxidase to prevent inactivation [495,496]. Both of these approaches could be investigated as means of improving the stability of the final product, which would be vital for clinical use.

Process development

In the process of developing SHRO powders as described in chapter 5, particle size was dictated by that associated with grinding by hand using a pestle and mortar. This limited the

particle size that could be achieved. It was also an ineffective method for producing a narrow size distribution, which would aid delivery. By utilising a more effective grinding instrument, such as a ball mill, it is theorised that smaller particles could be generated, which in turn would enhance flowability of the powder and the speed of ROS activation. It may also be beneficial to produce particles of such a size pertinent to that required for a dry powder spray, typically 5-50 μm producing a convenient, easy to use delivery system with broad applications [509,510].

Formulation development

Further developing the reactive oxygen powder delivery system in order to provide greater functionality such as formulating a powder that gels more cohesively. In addition to this the powder systems could also incorporate a haemostatic agent. These added functionalities could produce a product more suited to that of complex wounds. The added cohesiveness would enable a gel to form and mould to the wound and once formed have the ability to be removed as a single piece to make treatment more efficient overall. Combining this with a haemostatic agent, such as kaolin could be used to stop bleeding and prevent the blood from diluting and washing away the gel.

7.2.4 Reactive oxygen implantable systems development

Calcium sulphate cements that incorporate SHRO were formulated in chapter 6. The compressive strength of SHRO loaded calcium sulphate cements was shown to be comparable to trabecular bone and as such, SHRO loaded calcium sulphate cement may be deemed mechanically suitable for use in trabecular bone augmentation, in particular craniomaxillofacial sites. In this formulation SHRO was incorporated into the developing scaffold matrix as it was hypothesised that the water would already be bound in the crystal structure of the hydrated calcium sulphate phase. This methodology of incorporation was

shown to limit premature activation of ROS and shown to be efficacious *in vitro*. Future studies may look to incorporate SHRO into other bone cements, such as calcium phosphate. Specifically, it has been shown by Grover., *et al.* [511] that pre-mixed cements can be formulated with glycerol in place of the liquid phase. This was found not to affect compressive strength and would provide a solution to the premature activation of reactive oxygen species.

7.3 Overall Summary

The four experimental chapters of this thesis each contribute to knowledge by answering novel questions and providing promising solutions to the challenges surrounding the delivery of enzymatically produced and water-sensitive ROS. Central to achieving this was the adoption of a schematic formulation engineering approach to innovate controlled release delivery systems. This application driven work was underpinned by developing new understanding of honey's antimicrobial properties and composition. Each of the formulated delivery systems has potential to be used to apply SHRO instead of traditional antibiotics and deliver ROS to a wound site (Table 7.1).making them timely innovations that offer some hope to tackle the AMR crisis. It was found that within a 24 hour window, powder formulations are capable of producing the most ROS, while emulsions systems were found to have a slower production with cream formulations not peaking until after 7 days. Bone cement systems produced the least hydrogen peroxide over the course of 24 hours, however one of the major limitations with this system is the amount of SHRO that can be added. All formulations were found to be able to illicit an antimicrobial effect by producing zone of inhibition on plates of clinically relevant bacteria. However, concentration and dose is subject to the amount that the system is diluted. For topical application this may mean that for dry wounds more water will need to be added and for wet wounds either more regular dosing or a larger dosing. In addition, as these formulations reduce in ROS production levels may be more suited to wound healing offering further benefits to using *in situ* ROS producing systems. It is also notable that these controlled release approaches may also be adapted to deliver other water-sensitive molecules, which enhances the overall impact of this work.

Table 7.1 Comparison of hydrogen peroxide production of all SHRO formulations over a 24 hour period.

Formulation	Hydrogen Peroxide Production after 24h (μmol g^{-1})
SHRO	5.6
Emulsions	
60% SHRO	4.2
50% SHRO	1.9
30% SHRO	0.7
Creams	
SHRO_AR1	1.4
SHRO_AR2	1.2
SHRO_XG1	1.5
SHRO_XG2	1.4
Powders	
MCD 70	5.2
MCD 50	3.3
HCD 50	3.1
Bone Cement	
CS_SHRO1	0.28
CS_SHRO2	0.72

REFERENCES

[1] C.L. Ventola, The antibiotic resistance crisis: part 1: causes and threats, P T. 40 (2015) 277–283. https://www.ncbi.nlm.nih.gov/pubmed/25859123.

[2] G.M. Cragg, D.J. Newman, Medicinals for the Millennia, Ann. N. Y. Acad. Sci. 953a (2001) 3–25. doi:10.1111/j.1749-6632.2001.tb11356.x.

[3] K. Gould, Antibiotics: from prehistory to the present day, J. Antimicrob. Chemother. 71 (2016) 572–575. doi:10.1093/jac/dkv484.

[4] Microbiology Society, The History of Antibiotics, Antibiot. Antibiot. Resist. (2019). https://microbiologysociety.org/members-outreach-resources/outreach-resources/antibiotics-unearthed/antibiotics-and-antibiotic-resistance/the-history-of-antibiotics.html.

[5] L. Zaffiri, J. Gardner, L.H. Toledo-Pereyra, History of Antibiotics. From Salvarsan to Cephalosporins, J. Investig. Surg. 25 (2012) 67–77. doi:10.3109/08941939.2012.664099.

[6] W.W. Stead, The Origin and Erratic Global Spread of Tuberculosis: How the Past Explains the Present and Is the Key to the Future, Clin. Chest Med. 18 (1997) 65–77. doi:https://doi.org/10.1016/S0272-5231(05)70356-7.

[7] M.S. Dodd, D. Papineau, T. Grenne, J.F. Slack, M. Rittner, F. Pirajno, J. O'Neil, C.T.S. Little, Evidence for early life in Earth's oldest hydrothermal vent precipitates, Nature. 543 (2017) 60. https://doi.org/10.1038/nature21377.

[8] F. Frischknecht, O. Renaud, S.L. Shorte, Imaging today's infectious animalcules, Curr. Opin. Microbiol. 9 (2006) 297–306. doi:https://doi.org/10.1016/j.mib.2006.04.007.

[9] K.A. Smith, Louis Pasteur, the father of immunology?, Front. Immunol. 3 (2012) 1–10. doi:10.3389/fimmu.2012.00068.

[10] J.L. Turk, Paul Ehrlich--the dawn of immunology, J. R. Soc. Med. 87 (1994) 314–315.

https://www.ncbi.nlm.nih.gov/pubmed/8046698.

[11] G.F. Gensini, A.A. Conti, D. Lippi, The contributions of Paul Ehrlich to infectious disease, J. Infect. 54 (2007) 221–224. doi:https://doi.org/10.1016/j.jinf.2004.05.022.

[12] R. Aminov, History of antimicrobial drug discovery: Major classes and health impact, Biochem. Pharmacol. 133 (2017) 4–19. doi:https://doi.org/10.1016/j.bcp.2016.10.001.

[13] F. Bosch, L. Rosich, The Contributions of Paul Ehrlich to Pharmacology: A Tribute on the Occasion of the Centenary of His Nobel Prize, Pharmacology. 82 (2008) 171–179. doi:10.1159/000149583.

[14] L. V Stamm, Global Challenge of Antibiotic-Resistant Treponema pallidum, Antimicrob. Agents Chemother. 54 (2010) 583 LP – 589. doi:10.1128/AAC.01095-09.

[15] F. Stern, Paul Ehrlich: The Founder of Chemotherapy, Angew. Chemie Int. Ed. 43 (2004) 4254–4261. doi:10.1002/anie.200460632.

[16] A. Fleming, Penicillin, Br. Med. J. 2 (1941) 386. https://www.ncbi.nlm.nih.gov/pmc/articles/PMC2162878/.

[17] J.W. Bennett, K.-T.B.T.-A. in A.M. Chung, Alexander Fleming and the discovery of penicillin, in: Academic Press, 2001: pp. 163–184. doi:https://doi.org/10.1016/S0065-2164(01)49013-7.

[18] B.L. Ligon, Penicillin: its discovery and early development, Semin. Pediatr. Infect. Dis. 15 (2004) 52–57. doi:https://doi.org/10.1053/j.spid.2004.02.001.

[19] A. Fleming, On the Antibacterial Action of Cultures of a Penicillium, with Special Reference to Their Use in the Isolation of B. influenzae, Rev. Infect. Dis. 2 (1980) 129–139. http://www.jstor.org/stable/4452419.

[20] B.L. Ligon, Sir Alexander Fleming: Scottish researcher who discovered penicillin, Semin. Pediatr. Infect. Dis. 15 (2004) 58–64.

doi:https://doi.org/10.1053/j.spid.2004.02.002.

[21] R.G. Benedict, W.H. Schmidt, R.D. Coghill, A.P. Oleson, Penicillin. III. The Stability of Penicillin in Aqueous Solution, J. Bacteriol. 49 (1945) 85–95. https://www.ncbi.nlm.nih.gov/pubmed/16560901.

[22] H. Clarke, J. Johnson, R. Robinson, Brief History of the Chemical Study of Penicillin, in: H. Clarke (Ed.), Chem. Penicillin, Maple Press, York, 1949: pp. 3–9.

[23] R. Bud, Antibiotics: the epitome of a wonder drug, BMJ. 334 (2007) s6 LP-s6. doi:10.1136/bmj.39021.640255.94.

[24] E.L. Miller, The Penicillins: A Review and Update, J. Midwifery Womens. Health. 47 (2002) 426–434. doi:10.1016/S1526-9523(02)00330-6.

[25] B. Spellberg, D.N. Gilbert, The Future of Antibiotics and Resistance: A Tribute to a Career of Leadership by John Bartlett, Clin. Infect. Dis. 59 (2014) S71–S75. doi:10.1093/cid/ciu392.

[26] S. Sengupta, M. Chattopadhyay, H.-P. Grossart, The multifaceted roles of antibiotics and antibiotic resistance in nature , Front. Microbiol. . 4 (2013) 47. https://www.frontiersin.org/article/10.3389/fmicb.2013.00047.

[27] T. Baba, F. Takeuchi, M. Kuroda, H. Yuzawa, K. Aoki, A. Oguchi, Y. Nagai, N. Iwama, K. Asano, T. Naimi, H. Kuroda, L. Cui, K. Yamamoto, K. Hiramatsu, Genome and virulence determinants of high virulence community-acquired MRSA, Lancet. 359 (2002) 1819–1827. doi:https://doi.org/10.1016/S0140-6736(02)08713-5.

[28] L.L. Silver, Challenges of antibacterial discovery, Clin. Microbiol. Rev. 24 (2011) 71–109. doi:10.1128/CMR.00030-10.

[29] G.D. Wright, The antibiotic resistome: the nexus of chemical and genetic diversity, Nat. Rev. Microbiol. 5 (2007) 175–186. doi:10.1038/nrmicro1614.

[30] K. Lewis, Recover the lost art of drug discovery, Nature. 485 (2012) 439–440.

doi:10.1038/485439a.

[31] R. V Miller, K. Gammon, M.J. Day, Antibiotic resistance among bacteria isolated from seawater and penguin fecal samples collected near Palmer Station, Antarctica, Can. J. Microbiol. 55 (2009) 37–45. doi:10.1139/W08-119.

[32] K. Schiwon, K. Arends, K.M. Rogowski, S. Fürch, K. Prescha, T. Sakinc, R. Van Houdt, G. Werner, E. Grohmann, Comparison of Antibiotic Resistance, Biofilm Formation and Conjugative Transfer of Staphylococcus and Enterococcus Isolates from International Space Station and Antarctic Research Station Concordia, Microb. Ecol. 65 (2013) 638–651. doi:10.1007/s00248-013-0193-4.

[33] J. O'Neil, 'Review on Antimicrobial Resistance. Antimicrobial Resistance: Tackling a Crisis for the Health and Wealth of Nations, (2014) 1–20.

[34] J. O'Neill, Tackling Drug-Resistant Infections Globally: Final Report and Recommendations the Review on Antimicrobial Resistance, (2016). doi:10.1016/j.jpha.2015.11.005.

[35] U. Theuretzbacher, Global antibacterial resistance: The never-ending story, J. Glob. Antimicrob. Resist. 1 (2013) 63–69. doi:https://doi.org/10.1016/j.jgar.2013.03.010.

[36] M.Y. Memar, R. Ghotaslou, M. Samiei, K. Adibkia, Antimicrobial Use of Reactive Oxygen Therapy: Current Insights, Infect. Drug Resist. 11 (2018) 567–576. doi:10.2147/IDR.S142397.

[37] M. Dryden, Reactive Oxygen Species: A Novel Antimicrobial, Int. J. Antimicrob. Agents. 51 (2018) 299–303. doi:https://doi.org/10.1016/j.ijantimicag.2017.08.029.

[38] F. Vatansever, W.C.M.A. de Melo, P. Avci, D. Vecchio, M. Sadasivam, A. Gupta, R. Chandran, M. Karimi, N.A. Parizotto, R. Yin, G.P. Tegos, M.R. Hamblin, Antimicrobial Strategies Centered Around Reactive Oxygen Species-Bactericidal Antibiotics, Photodynamic Therapy, and Beyond, FEMS Microbiol. Rev. 37 (2013)

955–989. doi:10.1111/1574-6976.12026.

[39] C. Dunnill, T. Patton, J. Brennan, J. Barrett, M. Dryden, J. Cooke, D. Leaper, N.T. Georgopoulos, Reactive Oxygen Species (ROS) and Wound Healing: The Functional Role of ROS and Emerging ROS-Modulating Technologies for Augmentation of the Healing Process, Int. Wound J. 14 (2017) 89–96. doi:10.1111/iwj.12557.

[40] M.D. Mandal, S. Mandal, Honey: Its medicinal property and antibacterial activity, Asian Pac. J. Trop. Biomed. 1 (2011) 154–160. doi:10.1016/S2221-1691(11)60016-6.

[41] B.A. Lipsky, C. Hoey, Topical Antimicrobial Therapy for Treating Chronic Wounds, Clin. Infect. Dis. 49 (2009) 1541–1549. doi:10.1086/644732.

[42] P.H.S. Kwakman, S.A.J. Zaat, Antibacterial components of honey, IUBMB Life. 64 (2012) 48–55. doi:10.1002/iub.578.

[43] M. Dryden, G. Lockyer, K. Saeed, J. Cooke, Engineered honey: In vitro antimicrobial activity of a novel topical wound care treatment, J. Glob. Antimicrob. Resist. 2 (2014) 168–172. doi:10.1016/j.jgar.2014.03.006.

[44] M. Dryden, Reactive oxygen therapy: a novel antimicrobial, Int. J. Antimicrob. Agents. (2017). doi:10.1016/j.ijantimicag.2017.08.029.

[45] D. Ribet, P. Cossart, How bacterial pathogens colonize their hosts and invade deeper tissues, Microbes Infect. 17 (2015) 173–183. doi:https://doi.org/10.1016/j.micinf.2015.01.004.

[46] J. Peterson, Bacterial Pathogenesis, in: S. Baron (Ed.), Med. Microbiol., 4th ed., University of Texas Medical Branch, Galveston, 1996. https://www.ncbi.nlm.nih.gov/books/NBK8526/.

[47] E. Thursby, N. Juge, Introduction to the human gut microbiota, Biochem. J. 474 (2017) 1823–1836. doi:10.1042/BCJ20160510.

[48] H. Wang, C.-X. Wei, L. Min, L.-Y. Zhu, Good or bad: gut bacteria in human health

and diseases, Biotechnol. Biotechnol. Equip. 32 (2018) 1075–1080. doi:10.1080/13102818.2018.1481350.

[49] National Institutes for Health, Understanding Emerging and Re-emerging Infectious Diseases, in: Biol. Sci. Curric. Study, National Institutes of Health, Bethesda, 2007. https://www.ncbi.nlm.nih.gov/books/NBK20370/.

[50] B. Alberts, A. Johnson, J. Lewis, M. Raff, K. Roberts, P. Walter, Introduction to Pathogens, in: Mol. Biol. Cell, 4th ed., Garland Science, New York, 2002.

[51] M.E.J. Woolhouse, S. Gowtage-Sequeria, Host range and emerging and reemerging pathogens, Emerg. Infect. Dis. 11 (2005) 1842–1847. doi:10.3201/eid1112.050997.

[52] S. Mead, Prion disease genetics, Eur. J. Hum. Genet. 14 (2006) 273–281. doi:10.1038/sj.ejhg.5201544.

[53] J.A. Mastrianni, The genetics of prion diseases, Genet. Med. 12 (2010) 187–195. doi:10.1097/GIM.0b013e3181cd7374.

[54] K.D. Young, Bacterial morphology: why have different shapes?, Curr. Opin. Microbiol. 10 (2007) 596–600. doi:10.1016/j.mib.2007.09.009.

[55] M.C.F. van Teeseling, M.A. de Pedro, F. Cava, Determinants of bacterial morphology: From fundamentals to possibilities for antimicrobial targeting, Front. Microbiol. 8 (2017) 1–18. doi:10.3389/fmicb.2017.01264.

[56] R. Coico, Gram Staining, Curr. Protoc. Microbiol. 00 (2006) A.3C.1-A.3C.2. doi:10.1002/9780471729259.mca03cs00.

[57] M. Salton, K. Kim, Structure, in: S. Baron (Ed.), Med. Microbiol., 4th ed., University of Texas Medical Branch, Galveston, 1996. https://www.ncbi.nlm.nih.gov/books/NBK8477/.

[58] T.J. Silhavy, D. Kahne, S. Walker, The bacterial cell envelope, Cold Spring Harb. Perspect. Biol. 2 (2010) a000414–a000414. doi:10.1101/cshperspect.a000414.

[59] R. Yaeger, Protozoa: Structure, Classification, Growth and Development, in: S. Baron (Ed.), Med. Microbiol., 4th ed., University of Texas Medical Branch, Galveston, 1996. https://www.ncbi.nlm.nih.gov/books/NBK8325/.

[60] G.M. Walker, N.A. White, Introduction to Fungal Physiology, Fungi. (2017) 1–35. doi:doi:10.1002/9781119374312.ch1.

[61] I.L. King, Y. Li, Host-parasite interactions promote disease tolerance to intestinal helminth infection, Front. Immunol. 9 (2018) 1–10. doi:10.3389/fimmu.2018.02128.

[62] G.. Castro, Helminth: Structure, Classification, growth and Development, in: S. Baron (Ed.), Med. Microbiol., 4th ed., University of Texas Medical Branch, Galveston, 1996.

[63] G. Ridgway, P. Taylor, Microbiology and virology, in: P. Bennett, C.B.T.-B.S. in O. and G. (Fourth E. Williamson (Eds.), Basic Sci. Obstet. Gynaecol., 4th ed., Churchill Livingstone, 2010: pp. 107–130. doi:https://doi.org/10.1016/B978-0-443-10281-3.00011-7.

[64] H. Gelderblom, Structure and Classification of Viruses, in: S. Baron (Ed.), Med. Microbiol., 4th ed., University of Texas Medical Branch, Galveston, 1996.

[65] W.-S. Ryu, Virus Structure, in: W.-S.B.T.-M.V. of H.P.V. Ryu (Ed.), Mol. Virol. Hum. Pathog. Viruses, Academic Press, Boston, 2017: pp. 21–29. doi:https://doi.org/10.1016/B978-0-12-800838-6.00002-3.

[66] C. Weissmann, M. Enari, P.-C. Klöhn, D. Rossi, E. Flechsig, Transmission of prions, Proc. Natl. Acad. Sci. U. S. A. 99 Suppl 4 (2002) 16378–16383. doi:10.1073/pnas.172403799.

[67] D.D. Chaplin, Overview of the immune response, J. Allergy Clin. Immunol. 125 (2010) S3–S23. doi:10.1016/j.jaci.2009.12.980.

[68] A. Quinn, C. Raja-Gabaglia, S.C. Schneider, T. Braciak, E.E. Sercarz, Immune Response, in: P.J.B.T.-E. of I. (Second E. Delves (Ed.), Encycl. Immunol., 2nd ed.,

Elsevier, Oxford, 1998: pp. 1226–1229. doi:https://doi.org/10.1006/rwei.1999.0318.

[69] C. Janeway, P. Travers, M. Walport, M. Schlomchik, Principles of Innate and Adaptive Immunity, in: Immunobiol. Immune Syst. Heal. Dis., 5th ed., Garland Science, New York, 2001.

[70] R. Cano, H. Lopera, Introduction to T and B Lymphocytes, in: J. Anaya, Y. Shoenfeld, A. Rojas-Villarraga, R. Levy, R. Cervera (Eds.), Autoimmun. From Bench to Bedside, El Rosario University Press, Bogota, 2013. https://www.ncbi.nlm.nih.gov/books/NBK459471/.

[71] B. Alberts, A. Johnson, J. Lewis, M. Raff, K. Roberts, P. Walter, The Adaptive Immune System, in: Mol. Biol. Cell, 4th ed., Garland Science, New York, 2002. https://www.ncbi.nlm.nih.gov/books/NBK21070/.

[72] J.A. Champion, S. Mitragotri, Role of Target Geometry in Phagocytosis, Proc. Natl. Acad. Sci. U. S. A. 103 (2006) 4930–4934. doi:10.1073/pnas.0600997103.

[73] R.S. Flannagan, V. Jaumouillé, S. Grinstein, The Cell Biology of Phagocytosis, Annu. Rev. Pathol. Mech. Dis. 7 (2012) 61–98. doi:10.1146/annurev-pathol-011811-132445.

[74] P. Patel, S. Chatterjee, Innate and Adaptive Immunity: Barriers and Receptor-Based Recognition, in: S. Chatterjee, W. Jungraithmayr, D.B.T.-I. and I. in H. and D. Bagchi (Eds.), Immun. Inflamm. Heal. Dis., Academic Press, 2018: pp. 3–13. doi:https://doi.org/10.1016/B978-0-12-805417-8.00001-9.

[75] S. Dupré-Crochet, M. Erard, O. Nüβe, ROS production in phagocytes: why, when, and where?, J. Leukoc. Biol. 94 (2013) 657–670. doi:10.1189/jlb.1012544.

[76] H. Sies, Hydrogen peroxide as a central redox signaling molecule in physiological oxidative stress: Oxidative eustress, Redox Biol. 11 (2017) 613–619. doi:10.1016/j.redox.2016.12.035.

[77] P.A. Hyslop, D.B. Hinshaw, I.U. Scraufstatter, C.G. Cochrane, S. Kunz, K. Vosbeck,

Hydrogen peroxide as a potent bacteriostatic antibiotic: Implications for host defense, Free Radic. Biol. Med. 19 (1995) 31–37. doi:https://doi.org/10.1016/0891-5849(95)00005-I.

[78] C. Janeway, P. Travers, M. Walport, M. Schlomchik, Infectious Agents and How They Cause Disease, in: Immunobiol. Immune Syst. Heal. Dis., 5th ed., Garland Science, New York, 2001. https://www.ncbi.nlm.nih.gov/books/NBK27114/.

[79] S. Leekha, C.L. Terrell, R.S. Edson, General principles of antimicrobial therapy, Mayo Clin. Proc. 86 (2011) 156–167. doi:10.4065/mcp.2010.0639.

[80] N. Chandra, S. Kumar, Antibiotics Producing Soil Microorganisms, in: M.Z. Hashmi, V. Strezov, A. Varma (Eds.), Antibiot. Antibiot. Resist. Genes Soils, Springer International Publishing, 2017: pp. 1–18. doi:10.1007/978-3-319-66260-2_1.

[81] R.J. Fair, Y. Tor, Antibiotics and bacterial resistance in the 21st century, Perspect. Medicin. Chem. 6 (2014) 25–64. doi:10.4137/PMC.S14459.

[82] A.D. So, N. Gupta, O. Cars, Tackling antibiotic resistance, BMJ. 340 (2010) c2071. doi:10.1136/bmj.c2071.

[83] S.B. Levy, B. Marshall, Antibacterial Resistance Worldwide: Causes, Challenges and Responses, Nat. Med. 10 (2004) S122–S129. doi:10.1038/nm1145.

[84] R. Watson, Multidrug resistance responsible for half of deaths from healthcare associated infections in Europe, BMJ. 336 (2008) 1266 LP – 1267. doi:10.1136/bmj.39601.623808.4E.

[85] M.A. Kohanski, D.J. Dwyer, J.J. Collins, How antibiotics kill bacteria: from targets to networks, Nat. Rev. Microbiol. 8 (2010) 423–435. doi:10.1038/nrmicro2333.

[86] K. Gold, B. Slay, M. Knackstedt, A.K. Gaharwar, Antimicrobial Activity of Metal and Metal-Oxide Based Nanoparticles, Adv. Ther. 1 (2018) 1700033. doi:10.1002/adtp.201700033.

[87] A.J. Alanis, Resistance to Antibiotics: Are We in the Post-Antibiotic Era?, Arch. Med. Res. 36 (2005) 697–705. doi:https://doi.org/10.1016/j.arcmed.2005.06.009.

[88] P. Gardner, D. Smith, H. Beer, R. Moellering, Recovery of Resistance (R) Factors from a Drug-Free Community, Lancet. 294 (1969) 774–776. doi:https://doi.org/10.1016/S0140-6736(69)90482-6.

[89] J.L. Martínez, Natural Antibiotic Resistance and Contamination by Antibiotic Resistance Determinants: The Two Ages in the Evolution of Resistance to Antimicrobials, Front. Microbiol. 3 (2012) 1. doi:10.3389/fmicb.2012.00001.

[90] B. Spellberg, J.G. Bartlett, D.N. Gilbert, The Future of Antibiotics and Resistance, N. Engl. J. Med. 368 (2013) 299–302. doi:10.1056/NEJMp1215093.

[91] B. Spellberg, The Future of Antibiotics, Crit. Care. 18 (2014) 228. doi:10.1186/cc13948.

[92] J.M.A. Blair, M.A. Webber, A.J. Baylay, D.O. Ogbolu, L.J. V. Piddock, Molecular Mechanisms of Antibiotic Resistance, Nat. Rev. Microbiol. 13 (2014) 42–51. doi:10.1038/nrmicro3380.

[93] L. Zhu, J. Lin, J. Ma, J.E. Cronan, H. Wang, Triclosan resistance of Pseudomonas aeruginosa PAO1 is due to FabV, a triclosan-resistant enoyl-acyl carrier protein reductase, Antimicrob. Agents Chemother. 54 (2010) 689–698. doi:10.1128/AAC.01152-09.

[94] C.P. Randall, K.R. Mariner, I. Chopra, A.J. O'Neill, The Target of Daptomycin is Absent from Escherichia Coli and Other Gram-negative Pathogens, Antimicrob. Agents Chemother. 57 (2013) 637–639. doi:10.1128/AAC.02005-12.

[95] T. Tsuchido, M. Takano, Sensitization by Heat Treatment of Escherichia coli K-12 Cells to Hydrophobic Antibacterial Compounds, Antimicrob. Agents Chemother. 32 (1988) 1680–1683. doi:10.1128/aac.32.11.1680.

[96] G. Cheng, M. Dai, S. Ahmed, H. Hao, X. Wang, Z. Yuan, Antimicrobial Drugs in

Fighting against Antimicrobial Resistance, Front. Microbiol. 7 (2016) 470. doi:10.3389/fmicb.2016.00470.

[97] F. De la Cruz, J. Davies, Horizontal Gene Transfer and the Origin of Species: Lessons from Bacteria, Trends Microbiol. 8 (2000) 128–133. doi:https://doi.org/10.1016/S0966-842X(00)01703-0.

[98] J.W. Lee, Protocol Measuring Horizontal Gene Transfer from Algae to Non-Photosynthetic Organisms, MethodsX. 6 (2019) 1564–1574. doi:10.1016/j.mex.2019.05.022.

[99] A.R. Burmeister, Horizontal Gene Transfer, Evol. Med. Public Heal. 2015 (2015) 193–194. doi:10.1093/emph/eov018.

[100] D. Lebeaux, J.-M. Ghigo, C. Beloin, Biofilm-Related Infections: Bridging the Gap Between Clinical Management and Fundamental Aspects of Recalcitrance Toward Antibiotics, Microbiol. Mol. Biol. Rev. 78 (2014) 510–543. doi:10.1128/MMBR.00013-14.

[101] A. Penesyan, M. Gillings, I.T. Paulsen, Antibiotic Discovery: Combatting Bacterial Resistance in Cells and in Biofilm Communities, Molecules. 20 (2015) 5286–5298. doi:10.3390/molecules20045286.

[102] ReAct, Antibiotic Resistance Mechanisms, How Bact. Resist Antibiot. (2017). https://www.reactgroup.org/toolbox/understand/antibiotic-resistance/resistance-mechanisms-in-bacteria (accessed October 17, 2019).

[103] K.J. Shaw, P.N. Rather, R.S. Hare, G.H. Miller, Molecular Genetics of Aminoglycoside Resistance Genes and Familial Relationships of the Aminoglycoside-modifying Enzymes, Microbiol. Rev. 57 (1993) 138–163. http://mmbr.asm.org/content/57/1/138.abstract.

[104] K. Bush, J.F. Fisher, Epidemiological Expansion, Structural Studies, and Clinical

Challenges of New β-Lactamases from Gram-Negative Bacteria, Annu. Rev. Microbiol. 65 (2011) 455–478. doi:10.1146/annurev-micro-090110-102911.

[105] D.C. Hooper, G.A. Jacoby, Mechanisms of Drug Resistance: Quinolone Resistance, Ann. N. Y. Acad. Sci. 1354 (2015) 12–31. doi:10.1111/nyas.12830.

[106] H. Nikaido, Molecular Basis of Bacterial Outer Membrane Permeability Revisited, Microbiol. Mol. Biol. Rev. 67 (2003) 593–656. doi:10.1128/MMBR.67.4.593-656.2003.

[107] X.-Z. Li, P. Plésiat, H. Nikaido, The Challenge of Efflux-Mediated Antibiotic Resistance in Gram-Negative Bacteria, Clin. Microbiol. Rev. 28 (2015) 337 LP – 418. doi:10.1128/CMR.00117-14.

[108] V.M. D'Costa, K.M. McGrann, D.W. Hughes, G.D. Wright, Sampling the Antibiotic Resistome, Science (80-.). 311 (2006) 374–377. doi:10.1126/science.1120800.

[109] H. Mulcahy, L. Charron-Mazenod, S. Lewenza, Extracellular DNA Chelates Cations and Induces Antibiotic Resistance in Pseudomonas aeruginosa Biofilms, PLOS Pathog. 4 (2008) e1000213. https://doi.org/10.1371/journal.ppat.1000213.

[110] W. Khan, S.P. Bernier, S.L. Kuchma, J.H. Hammond, F. Hasan, G.A. O'Toole, Aminoglycoside Resistance of Pseudomonas Aeruginosa Biofilms Modulated by Extracellular Polysaccharide, Int. Microbiol. 13 (2010) 207–212. doi:10.2436/20.1501.01.127.

[111] W.-C. Chiang, M. Nilsson, P.Ø. Jensen, N. Høiby, T.E. Nielsen, M. Givskov, T. Tolker-Nielsen, Extracellular DNA Shields against Aminoglycosides in Pseudomonas aeruginosa Biofilms, Antimicrob. Agents Chemother. 57 (2013) 2352–2361. doi:10.1128/AAC.00001-13.

[112] K. Lewis, Persister Cells, Annu. Rev. Microbiol. 64 (2010) 357–372.

doi:10.1146/annurev.micro.112408.134306.

[113] D. Nguyen, A. Joshi-Datar, F. Lepine, E. Bauerle, O. Olakanmi, K. Beer, G. McKay, R. Siehnel, J. Schafhauser, Y. Wang, B.E. Britigan, P.K. Singh, Active Starvation Responses Mediate Antibiotic Tolerance in Biofilms and Nutrient-Limited Bacteria, Science (80-.). 334 (2011) 982–986. doi:10.1126/science.1211037.

[114] S.P. Bernier, D. Lebeaux, A.S. DeFrancesco, A. Valomon, G. Soubigou, J.-Y. Coppée, J.-M. Ghigo, C. Beloin, Starvation, Together with the SOS Response, Mediates High Biofilm-Specific Tolerance to the Fluoroquinolone Ofloxacin, PLOS Genet. 9 (2013) e1003144. https://doi.org/10.1371/journal.pgen.1003144.

[115] T.C.R. Conibear, S.L. Collins, J.S. Webb, Role of Mutation in Pseudomonas aeruginosa Biofilm Development, PLoS One. 4 (2009) e6289. https://doi.org/10.1371/journal.pone.0006289.

[116] G.M. Eliopoulos, J. Blázquez, Hypermutation as a Factor Contributing to the Acquisition of Antimicrobial Resistance, Clin. Infect. Dis. 37 (2003) 1201–1209. doi:10.1086/378810.

[117] J.P. Townsend, K.M. Nielsen, D.S. Fisher, D.L. Hartl, Horizontal Acquisition of Divergent Chromosomal DNA in Bacteria: Effects of Mutator Phenotypes, Genetics. 164 (2003) 13–21. http://www.genetics.org/content/164/1/13.abstract.

[118] M.R. Gillings, M.P. Holley, H.W. Stokes, Evidence for Dynamic Exchange of qac Gene Cassettes Between Class 1 Integrons and Other Integrons in Freshwater Biofilms, FEMS Microbiol. Lett. 296 (2009) 282–288. doi:10.1111/j.1574-6968.2009.01646.x.

[119] S. Domingues, K. Harms, W.F. Fricke, P.J. Johnsen, G.J. da Silva, K.M. Nielsen, Natural Transformation Facilitates Transfer of Transposons, Integrons and Gene Cassettes between Bacterial Species, PLOS Pathog. 8 (2012) e1002837. https://doi.org/10.1371/journal.ppat.1002837.

[120] M.R. Gillings, H.W. Stokes, Are humans increasing bacterial evolvability?, Trends Ecol. Evol. 27 (2012) 346–352. doi:https://doi.org/10.1016/j.tree.2012.02.006.

[121] Y. Morita, J. Tomida, Y. Kawamura, Responses of Pseudomonas aeruginosa to Antimicrobials, Front. Microbiol. 4 (2014) 422. https://www.frontiersin.org/article/10.3389/fmicb.2013.00422.

[122] L. Zhang, T.-F. Mah, Involvement of a Novel Efflux System in Biofilm-Specific Resistance to Antibiotics, J. Bacteriol. 190 (2008) 4447 LP – 4452. doi:10.1128/JB.01655-07.

[123] M. Haque, M. Sartelli, J. McKimm, M. Abu Bakar, Health care-associated infections - an overview, Infect. Drug Resist. 11 (2018) 2321–2333. doi:10.2147/IDR.S177247.

[124] A. Cassini, D. Plachouras, T. Eckmanns, M. Abu Sin, H.-P. Blank, T. Ducomble, S. Haller, T. Harder, A. Klingeberg, M. Sixtensson, E. Velasco, B. Weiß, P. Kramarz, D.L. Monnet, M.E. Kretzschmar, C. Suetens, Burden of Six Healthcare-Associated Infections on European Population Health: Estimating Incidence-Based Disability-Adjusted Life Years through a Population Prevalence-Based Modelling Study, PLoS Med. 13 (2016) e1002150–e1002150. doi:10.1371/journal.pmed.1002150.

[125] R. Scott, The Direct Medical Costs of Healthcare-Associated Infections in US Hospitals and the Benefits of Prevention, CDC. (2009). https://www.cdc.gov/hai/pdfs/hai/scott_costpaper.pdf (accessed October 12, 2019).

[126] D.M. Sievert, P. Ricks, J.R. Edwards, A. Schneider, J. Patel, A. Srinivasan, A. Kallen, B. Limbago, S. Fridkin, Antimicrobial-Resistant Pathogens Associated with Healthcare-Associated Infections Summary of Data Reported to the National Healthcare Safety Network at the Centers for Disease Control and Prevention, 2009–2010, Infect. Control & Hosp. Epidemiol. 34 (2013) 1–14. doi:DOI: 10.1086/668770.

[127] A.I. Hidron, J.R. Edwards, J. Patel, T.C. Horan, D.M. Sievert, D.A. Pollock, S.K.

Fridkin, Antimicrobial-Resistant Pathogens Associated With Healthcare-Associated Infections: Annual Summary of Data Reported to the National Healthcare Safety Network at the Centers for Disease Control and Prevention, 2006–2007, Infect. Control Hosp. Epidemiol. 29 (2008) 996–1011. doi:DOI: 10.1086/591861.

[128] World Health Organization, WHO Priority Pathogens List for R&D of New Antibiotics, (2017). https://www.who.int/news-room/detail/27-02-2017-who-publishes-list-of-bacteria-for-which-new-antibiotics-are-urgently-needed (accessed October 12, 2019).

[129] C. Willyard, The Drug-Resistant Bacteria that Pose the Greatest Health Threats, Nature. 543 (2017) 15. doi:10.1038/nature.2017.21550.

[130] The Pew Trust, Antibiotics Currently in Global Development, (2019). https://www.pewtrusts.org/en/research-and-analysis/data-visualizations/2014/antibiotics-currently-in-clinical-development (accessed October 14, 2019).

[131] V.L. Simpkin, M.J. Renwick, R. Kelly, E. Mossialos, Incentivising Innovation in Antibiotic Drug Discovery and Development: Progress, Challenges and Next Steps, J. Antibiot. (Tokyo). 70 (2017) 1087–1096. doi:10.1038/ja.2017.124.

[132] M.J. Renwick, V. Simpkin, E. Mossialos, Targeting Innovation in Antibiotic Drug Discovery and Development: The Need for a One Health – One Europe – One World Framework, 45th ed., European Observatory on Health Systems and Policies, Copenhagen, 2016.

[133] D. Hughes, A. Karlén, Discovery and Preclinical Development of New Antibiotics, Ups. J. Med. Sci. 119 (2014) 162–169. doi:10.3109/03009734.2014.896437.

[134] C.M. Morel, E. Mossialos, Stoking the antibiotic pipeline, BMJ. 340 (2010) 2115. doi:10.1136/bmj.c2115.

[135] D.J. Payne, Microbiology: Desperately seeking new antibiotics, Science (80-.). 321

(2008) 1644–1645. doi:10.1126/science.1164586.

[136] T. Hesterkamp, Antibiotics Clinical Development and Pipeline, in: M. Stadler, P. Dersch (Eds.), How to Overcome Antibiot. Cris., Springer, 2015: pp. 447–474.

[137] D.M. Brogan, E. Mossialos, A critical analysis of the review on antimicrobial resistance report and the infectious disease financing facility, Global. Health. 12 (2016) 8. doi:10.1186/s12992-016-0147-y.

[138] P. Fernandes, E. Martens, Antibiotics in Late Clinical Development, Biochem. Pharmacol. 133 (2017) 152–163. doi:https://doi.org/10.1016/j.bcp.2016.09.025.

[139] Editorial, Wanted: A Reward for Antibiotic Development, Nat. Biotechnol. 36 (2018) 555. doi:10.1038/nbt.4193.

[140] R. Cooper, Honey In Wound Care: Antibacterial Properties, GMS Krankenhhyg. Interdiszip. 2 (2007) 1–3. https://www.ncbi.nlm.nih.gov/pubmed/20204083.

[141] A.A. Machado De-Melo, L.B. de Almeida-Muradian, M.T. Sancho, A. Pascual-Maté, Composition and properties of Apis mellifera honey: A review, J. Apic. Res. 57 (2018) 5–37. doi:10.1080/00218839.2017.1338444.

[142] L.W. Doner, The sugars of honey—A review, J. Sci. Food Agric. 28 (1977) 443–456. doi:10.1002/jsfa.2740280508.

[143] D. Ball, The Composition of Honey, J. Chem. Educ. 84 (2007) 1643–1646. doi:10.1080/0005772X.1957.11094976.

[144] D.J. Willix, P.C. Molan, C.G. Harfoot, A Comparison of the Sensitivity of Wound-Infecting Species of Bacteria to the Antibacterial Activity of Manuka Honey and Other Honey, J. Appl. Bacteriol. 73 (1992) 388–394. doi:10.1111/j.1365-2672.1992.tb04993.x.

[145] P. Molan, T. Rhodes, Honey: A Biologic Wound Dressing, Wounds. 27 (2015) 141–151.

[146] N.F. Brady, P.C. Molan, C.G. Harfoot, The Sensitivity of Dermatophytes to the

Antimicrobial Activity of Manuka Honey and Other Honey, Pharm. Pharmacol. Commun. 2 (1996) 471–473. doi:10.1111/j.2042-7158.1996.tb00540.x.

[147] L. Vandamme, A. Heyneman, H. Hoeksema, J. Verbelen, S. Monstrey, Honey in Modern Wound Care: A Systematic Review, Burns. 39 (2013) 1514–1525. doi:https://doi.org/10.1016/j.burns.2013.06.014.

[148] J. Alvarez-Suarez, M. Gasparrini, T. Forbes-Hernández, L. Mazzoni, F. Giampieri, The Composition and Biological Activity of Honey: A Focus on Manuka Honey, Foods. 3 (2014) 420–432. doi:10.3390/foods3030420.

[149] J.M. Packer, J. Irish, B.R. Herbert, C. Hill, M. Padula, S.E. Blair, D.A. Carter, E.J. Harry, Specific Non-Peroxide Antibacterial Effect of Manuka Honey on the Staphylococcus Aureus Proteome, Int. J. Antimicrob. Agents. 40 (2012) 43–50. doi:https://doi.org/10.1016/j.ijantimicag.2012.03.012.

[150] J. Majtan, J. Bohova, E. Prochazka, J. Klaudiny, Methylglyoxal may affect hydrogen peroxide accumulation in manuka honey through the inhibition of glucose oxidase, J. Med. Food. 17 (2014) 290–293. doi:10.1089/jmf.2012.0201.

[151] G. Zoldák, A. Zubrik, A. Musatov, M. Stupák, E. Sedlák, Irreversible Thermal Denaturation of Glucose Oxidase from Aspergillus Niger is the Transition to the Denatured State with Residual Structure, J. Biol. Chem. 279 (2004) 47601–47609. doi:10.1074/jbc.M406883200.

[152] F.C. Bizerra, P.I. Da Silva Jr, M.A.F. Hayashi, Exploring the Antibacterial Properties of Honey and its Potential, Front. Microbiol. 3 (2012) 398. doi:10.3389/fmicb.2012.00398.

[153] J.M. Robinson, Reactive oxygen species in phagocytic leukocytes, Histochem. Cell Biol. 130 (2008) 281–297. doi:10.1007/s00418-008-0461-4.

[154] A. V Belikov, B. Schraven, L. Simeoni, T cells and reactive oxygen species, J. Biomed.

Sci. 22 (2015) 85. doi:10.1186/s12929-015-0194-3.

[155] H. Sies, D.P. Jones, Reactive oxygen species (ROS) as pleiotropic physiological signalling agents, Nat. Rev. Mol. Cell Biol. (2020). doi:10.1038/s41580-020-0230-3.

[156] S. Samarghandian, T. Farkhondeh, F. Samini, Honey and Health: A Review of Recent Clinical Research, Pharmacognosy Res. 9 (2017) 121–127. doi:10.4103/0974-8490.204647.

[157] S.A. Meo, S.A. Al-Asiri, A.L. Mahesar, M.J. Ansari, Role of Honey in Modern Medicine, Saudi J. Biol. Sci. 24 (2017) 975–978. doi:https://doi.org/10.1016/j.sjbs.2016.12.010.

[158] A. Jull, N. Cullum, J. Dumville, M. Westby, S. Deshpande, N. Walker, Honey as a Topical Treatment of Wounds, 2015. doi:https://doi.org/10.1002/14651858.CD005083.pub4.

[159] M. Lu, E.N. Hansen, Hydrogen Peroxide Wound Irrigation in Orthopaedic Surgery, J. Bone Jt. Infect. 2 (2017) 3–9. doi:10.7150/jbji.16690.

[160] T.A. Wilgus, V.K. Bergdall, L.A. Dipietro, T.M. Oberyszyn, Hydrogen peroxide disrupts scarless fetal wound repair, Wound Repair Regen. 13 (2005) 513–519. doi:10.1111/j.1067-1927.2005.00072.x.

[161] E.A. O'Toole, M. Goel, D.T. Woodley, Hydrogen Peroxide Inhibits Human Keratinocyte Migration, Dermatologic Surg. 22 (1996) 525–529. https://journals.lww.com/dermatologicsurgery/Fulltext/1996/06000/Hydrogen_Peroxide_Inhibits_Human_Keratinocyte.4.aspx.

[162] Y. Yao, H. Zhang, Z. Wang, J. Ding, S. Wang, B. Huang, S. Ke, C. Gao, Reactive oxygen species (ROS)-responsive biomaterials mediate tissue microenvironments and tissue regeneration, J. Mater. Chem. B. 7 (2019) 5019–5037. doi:10.1039/c9tb00847k.

[163] G. Zhu, Q. Wang, S. Lu, Y. Niu, Hydrogen Peroxide: A Potential Wound Therapeutic

Target?, Med. Princ. Pract. 26 (2017) 301–308. doi:10.1159/000475501.

[164] M. Dryden, G. Milward, K. Saeed, Infection Prevention in Wounds with Surgihoney, J. Hosp. Infect. 88 (2014) 121–122. doi:10.1016/j.jhin.2014.07.008.

[165] M. Dryden, F. Halstead, J. Cooke, Engineered Honey to Manage Bacterial Bioburden and Biofilm in Chronic Wounds, EWMA Free Pap. Sess. Infect. Antimicrob. (2015).

[166] M. Dryden, C. Goddard, A. Madadi, M. Heard, K. Saeed, J. Cooke, Using antimicrobial Surgihoney to prevent caesarean wound infection, Br. J. Midwifery. 22 (2014) 23–27. doi:10.12968/bjom.2014.22.2.111.

[167] M. Dryden, J. Cooke, R.J. Salib, R. Holding, S. Pender, J. Brooks, Hot Topics in Reactive Oxygen Therapy, J. Glob. Antimicrob. Resist. 8 (2017) 194–198. doi:10.1016/j.jgar.2016.12.012.

[168] F.D. Halstead, M.A. Webber, M. Rauf, R. Burt, M. Dryden, B.A. Oppenheim, In vitro activity of an engineered honey, medical-grade honeys, and antimicrobial wound dressings against biofilm-producing clinical bacterial isolates, J. Wound Care. 25 (2016).

[169] M. Dryden, A. Dickinson, J. Brooks, L. Hudgell, K. Saeed, K.F. Cutting, A multi-centre clinical evaluation of reactive oxygen topical wound gel in 114 wounds, J. Wound Care. 25 (2016) 140–146. doi:10.12968/jowc.2016.25.3.140.

[170] T.J. Hall, J.M.A. Blair, R.J.A. Moakes, E.G. Pelan, L.M. Grover, S.C. Cox, Antimicrobial emulsions: Formulation of a triggered release reactive oxygen delivery system, Mater. Sci. Eng. C. 103 (2019) 1–10. doi:10.1016/j.msec.2019.05.020.

[171] WHO, Prioritization of pathogens to guide discovery, research and development of new antibiotics for drug-resistant bacterial infections, including tuberculosis, WHO Press. (2017) 1–87.

[172] M.C.T.J.A.A.H.K.S.J.C. Dryden;, The use of Surgihoney to prevent or eradicate bacterial colonisation in dressing oncology long vascular lines, J. Wound Care. 23 (2014)

338–342. doi:10.12968/jowc.2014.23.6.338.

[173] P.M. Doran, Homogeneous Reactions, in: P.M.B.T.-B.E.P. (Second E. Doran (Ed.), Bioprocess Eng. Princ., 2nd ed., Academic Press, London, 2013: pp. 599–703. doi:https://doi.org/10.1016/B978-0-12-220851-5.00012-5.

[174] E.O. Odebunmi, S.O. Owalude, Kinetic and thermodynamic studies of glucose oxidase catalysed oxidation reaction of glucose, J. Appl. Sci. Environ. Manag. December. 11 (2007) 95–100. www.bioline.org.br/ja.

[175] T.-Y. Wang, M.D.J. Libardo, A.M. Angeles-Boza, J.-P. Pellois, Membrane Oxidation in Cell Delivery and Cell Killing Applications, ACS Chem. Biol. 12 (2017) 1170–1182. doi:10.1021/acschembio.7b00237.

[176] J. Willi, P. Küpfer, D. Evéquoz, G. Fernandez, A. Katz, C. Leumann, N. Polacek, Oxidative stress damages rRNA inside the ribosome and differentially affects the catalytic center, Nucleic Acids Res. 46 (2018) 1945–1957. doi:10.1093/nar/gkx1308.

[177] S. Kalghatgi, C.S. Spina, J.C. Costello, M. Liesa, J.R. Morones-Ramirez, S. Slomovic, A. Molina, O.S. Shirihai, J.J. Collins, Bactericidal Antibiotics Induce Mitochondrial Dysfunction and Oxidative Damage in Mammalian Cells, Sci. Transl. Med. 5 (2013) 192ra85-192ra85. doi:10.1126/scitranslmed.3006055.

[178] B. Dridi, A. Lupien, M.G. Bergeron, P. Leprohon, M. Ouellette, Differences in Antibiotic-induced Oxidative Stress Responses Between Laboratory and Clinical Isolates of Streptococcus Pneumoniae, Antimicrob. Agents Chemother. 59 (2015) 5420–5426. doi:10.1128/AAC.00316-15.

[179] D. Williamson, G. Carter, B. Howden, Current and Emerging Topical Antibacterials and Antiseptics: Agents, Action, and Resistance Patterns, Clin. Microbiol. Rev. 30 (2017) 827–860. doi:10.1128/CMR.00112-16.

[180] National Health Service, Key Facts, Prescr. Cost Anal. Engl. - 2015. (2016).

[181] D. Anderson, K. Podgorny, S. Berrios-Torres, D. Bratzler, E. Dellinger, L. Greene, A. Nyquist, L. Saiman, D. Yokoe, L. Maragakis, K. Kaye, Strategies to Prevent Surgical Site Infections in Acute Care Hospitals: 2014 Update, Infect. Control Hosp. Epidemiol. 35 (2014) 605–627. doi:10.1086/676022.

[182] J.M. Schierholz, J. Beuth, Implant infections: a haven for opportunistic bacteria, J. Hosp. Infect. 49 (2001) 87–93. doi:10.1053/jhin.2001.1052.

[183] W. Guo, X. Zhu, Y. Liu, H. Zhuang, Sugar and water contents of honey with dielectric property sensing, J. Food Eng. 97 (2010) 275–281. doi:10.1016/j.jfoodeng.2009.10.024.

[184] G.W. Lu, P. Gao, Emulsions and Microemulsions for Topical and Transdermal Drug Delivery, in: V.S.B.T.-H. of N.-I.D.D.S. Kulkarni (Ed.), Pers. Care Cosmet. Technol., William Andrew Publishing, Boston, 2010: pp. 59–94. doi:https://doi.org/10.1016/B978-0-8155-2025-2.10003-4.

[185] J.G. Speight, Introduction Into the Environment, in: J.G.B.T.-E.O.C. for E. Speight (Ed.), Environ. Org. Chem. Eng., Butterworth-Heinemann, 2017: pp. 263–303. doi:https://doi.org/10.1016/B978-0-12-804492-6.00006-X.

[186] M. Chappat, Some Applications of Emulsions, Colloids Surfaces A Physicochem. Eng. Asp. 91 (1994) 57–77. doi:https://doi.org/10.1016/0927-7757(94)02976-8.

[187] F. Goodarzi, S. Zendehboudi, A Comprehensive Review on Emulsions and Emulsion Stability in Chemical and Energy Industries, Can. J. Chem. Eng. 97 (2019) 281–309. doi:10.1002/cjce.23336.

[188] P. Bajpai, Colloid and Surface Chemistry, in: P.B.T.-B.H. of P. and P. (Third E. Bajpai (Ed.), Biermann's Handb. Pulp Pap., 3rd ed., Elsevier, 2018: pp. 381–400. doi:https://doi.org/10.1016/B978-0-12-814238-7.00019-2.

[189] G. Muschiolik, Multiple Emulsions for Food Use, Curr. Opin. Colloid Interface Sci. 12 (2007) 213–220. doi:https://doi.org/10.1016/j.cocis.2007.07.006.

[190] R. Pal, Rheology of Simple and Multiple Emulsions, Curr. Opin. Colloid Interface Sci. 16 (2011) 41–60. doi:https://doi.org/10.1016/j.cocis.2010.10.001.

[191] J. Knowlton, Emulsion Theory, in: H. Butler (Ed.), Poucher's Perfum. Cosmet. Soaps, Springer, Dordrecht, 1993: pp. 534–555. doi:https://doi.org/10.1007/978-94-011-1482-0_19.

[192] B. Bergenståhl, P.M. Claesson, Surface forces in emulsions, in: K.& F. Larsson S. (Ed.), Food Emuls. Third Ed. Revis. Expand., 3rd ed., Marcel Dekker, YKI – Ytkemiska institutet, 1997: pp. 57–109. http://urn.kb.se/resolve?urn=urn:nbn:se:ri:diva-13579.

[193] S. Mokhatab, W.A. Poe, J.Y. Mak, Phase Separation, in: S. Mokhatab, W.A. Poe, J.Y.B.T.-H. of N.G.T. and P. (Fourth E. Mak (Eds.), Handb. Nat. Gas Transm. Process., 4th ed., Gulf Professional Publishing, 2019: pp. 191–217. doi:https://doi.org/10.1016/B978-0-12-815817-3.00005-8.

[194] D. McClements, Food Emulsions: Principles, Practices, and Techniques, 2nd ed., CRC Press, Boca Raton, 2004.

[195] Q. Chang, Emulsion, Foam, and Gel, in: Q.B.T.-C. and I.C. for W.Q.C. Chang (Ed.), Colloid Interface Chem. Water Qual. Control, Academic Press, 2016: pp. 227–245. doi:https://doi.org/10.1016/B978-0-12-809315-3.00011-6.

[196] Y.-T. Hu, Y. Ting, J.-Y. Hu, S.-C. Hsieh, Techniques and Methods to Study Functional Characteristics of Emulsion Systems, J. Food Drug Anal. 25 (2017) 16–26. doi:https://doi.org/10.1016/j.jfda.2016.10.021.

[197] D.J. McClements, Critical review of techniques and methodologies for characterization of emulsion stability, Crit. Rev. Food Sci. Nutr. 47 (2007) 611–649. doi:10.1080/10408390701289292.

[198] B. Ozturk, D.J. McClements, Progress in Natural Emulsifiers for Utilization in Food Emulsions, Curr. Opin. Food Sci. 7 (2016) 1–6.

doi:https://doi.org/10.1016/j.cofs.2015.07.008.

[199] B.A. Khan, N. Akhtar, H.M.S. Khan, K. Waseem, T. Mahmood, A. Rasul, M. Iqbal, H. Khan, Basics of Pharmaceutical Emulsions: A Review, African J. Pharm. Pharmacol. 5 (2011) 2715–2725. doi:10.5897/AJPP11.698.

[200] M. Pathak, Nanoemulsions and Their Stability for Enhancing Functional Properties of Food Ingredients, in: A.E. Oprea, A.M.B.T.-N.A. in F. Grumezescu (Eds.), Nanotechnol. Appl. Food, Academic Press, 2017: pp. 87–106. doi:https://doi.org/10.1016/B978-0-12-811942-6.00005-4.

[201] B.U. Riebesehl, Drug Delivery with Organic Solvents or Colloidal Dispersed Systems, in: C.G. Wermuth, D. Aldous, P. Raboisson, D.B.T.-T.P. of M.C. (Fourth E. Rognan (Eds.), Pract. Med. Chem., 4th ed., Academic Press, San Diego, 2015: pp. 699–722. doi:https://doi.org/10.1016/B978-0-12-417205-0.00029-8.

[202] A.M. Spasic, Introduction, in: A.M.B.T.-I.S. and T. Spasic (Ed.), Rheol. Emuls., Elsevier, 2018: pp. 1–25. doi:https://doi.org/10.1016/B978-0-12-813836-6.00001-5.

[203] Y. Yamashita, R. Miyahara, K. Sakamoto, Emulsion and Emulsification Technology, in: K. Sakamoto, R.Y. Lochhead, H.I. Maibach, Y.B.T.-C.S. and T. Yamashita (Eds.), Cosmet. Sci. Technol., Elsevier, Amsterdam, 2017: pp. 489–506. doi:https://doi.org/10.1016/B978-0-12-802005-0.00028-8.

[204] J. Toro-Mendoza, D. Petsev, Brownian Dynamics of Emulsion Film Formation and Droplet Coalescence, Phys. Rev. E. Stat. Nonlin. Soft Matter Phys. 81 (2010) 51404. doi:10.1103/PhysRevE.81.051404.

[205] R.P. Borwankar, L.A. Lobo, D.T. Wasan, Emulsion stability — kinetics of flocculation and coalescence, Colloids and Surfaces. 69 (1992) 135–146. doi:https://doi.org/10.1016/0166-6622(92)80224-P.

[206] I.B. Ivanov, K.D. Danov, P.A. Kralchevsky, Flocculation and Coalescence of Micron-

Size Emulsion Droplets, Colloids Surfaces A Physicochem. Eng. Asp. 152 (1999) 161–182. doi:10.1016/S0927-7757(98)00620-7.

[207] H.A. Barnes, Rheology of emulsions — a review, Colloids Surfaces A Physicochem. Eng. Asp. 91 (1994) 89–95. doi:https://doi.org/10.1016/0927-7757(93)02719-U.

[208] V. Schmitt, S. Arditty, F. Leal-Calderon, Stability of Concentrated Emulsions, in: D.N.B.T.-I.S. and T. Petsev (Ed.), Interface Sci. Technol., Elsevier, 2004: pp. 607–639. doi:https://doi.org/10.1016/S1573-4285(04)80017-6.

[209] P. Taylor, Ostwald Ripening in Emulsions, Adv. Colloid Interface Sci. 75 (1998) 107–163. doi:https://doi.org/10.1016/S0001-8686(98)00035-9.

[210] S. Sajjadi, F. Jahanzad, M. Yianneskis, Catastrophic phase inversion of abnormal emulsions in the vicinity of the locus of transitional inversion, Colloids Surfaces A Physicochem. Eng. Asp. 240 (2004) 149–155. doi:10.1016/j.colsurfa.2004.03.012.

[211] A. Perazzo, V. Preziosi, S. Guido, Phase inversion emulsification : Current understanding and applications, Adv. Colloid Interface Sci. 222 (2015) 581–599. doi:10.1016/j.cis.2015.01.001.

[212] V. Preziosi, A. Perazzo, S. Caserta, G. Tomaiuolo, S. Guido, Phase Inversion Emulsification, Chem. Eng. Trans. 32 (2013) 1585–1590.

[213] I. Chauhan, K. Bhatia, M. Yasir, Status of Surfactants as Penetration Enhancers in Transdermal Drug Delivery, J. Pharm. Bioallied Sci. 4 (2012) 2–9. doi:10.4103/0975-7406.92724.

[214] S. Akbari, A.H. Nour, Emulsion Types, Stability Mechanisms and Rheology : A Review, Int. J. Innov. Res. Sci. Stud. 1 (2018) 14–21.

[215] Y. Nakama, Surfactants, in: K. Sakamoto, R.Y. Lochhead, H.I. Maibach, Y.B.T.-C.S. and T. Yamashita (Eds.), Cosmet. Sci. Technol., Elsevier, Amsterdam, 2017: pp. 231–244. doi:https://doi.org/10.1016/B978-0-12-802005-0.00015-X.

[216] S. Vaidya, A.K. Ganguli, Microemulsion Methods for Synthesis of Nanostructured Materials☆, in: D.L. Andrews, R.H. Lipson, T.B.T.-C.N. and N. (Second E. Nann (Eds.), Compr. Nanosci. Nanotechnol., 2nd ed., Academic Press, Oxford, 2019: pp. 1–12. doi:https://doi.org/10.1016/B978-0-12-803581-8.11321-9.

[217] C. Pulce, J. Descotes, Household Products, in: J.B.T.-H.T. DESCOTES (Ed.), Hum. Toxicol., Elsevier Science B.V., Amsterdam, 1996: pp. 683–702. doi:https://doi.org/10.1016/B978-044481557-6/50030-7.

[218] I. Effendy, H.I. Maibach, Surfactants and Experimental Irritant Contact Dermatitis, Contact Dermatitis. 33 (1995) 217–225. doi:10.1111/j.1600-0536.1995.tb00470.x.

[219] V. Madaan, A. chanana, M.K. Kataria, A. Bilandi, Emulsion Technology and Recent Trends in Emulsion Applications, Int. Res. J. Pharm. 5 (2014) 533–542. doi:10.7897/2230-8407.0507108.

[220] C. Genot, T.-H. Kabri, A. Meynier, Stabilization of Omega-3 Oils and Enriched Foods Using Emulsifiers, in: C. Jacobsen, N.S. Nielsen, A.F. Horn, A.-D.M.B.T.-F.E. with O.-3 F.A. Sørensen (Eds.), Food Enrich. with Omega-3 Fat. Acids, Woodhead Publishing, 2013: pp. 150–193. doi:https://doi.org/10.1533/9780857098863.2.150.

[221] Y. Zheng, M. Zheng, Z. Ma, B. Xin, R. Guo, X. Xu, Sugar Fatty Acid Esters, in: M.U. Ahmad, X.B.T.-P.L. Xu (Eds.), Polar Lipids Biol. Chem. Technol., Elsevier, 2015: pp. 215–243. doi:https://doi.org/10.1016/B978-1-63067-044-3.50012-1.

[222] J.J. Williams, Formulation of Carpet Cleaners, in: I. Johansson, P.B.T.-H. for C. of S. Somasundaran (Eds.), Handb. Cleaning/Decontamination Surfaces, Elsevier Science B.V., Amsterdam, 2007: pp. 103–123. doi:https://doi.org/10.1016/B978-044451664-0/50004-8.

[223] S.E. Flores-Villaseñor, R.D. Peralta-Rodríguez, J.C. Ramirez-Contreras, G.Y. Cortes-Mazatán, A.N. Estrada-Ramírez, Biocompatible Microemulsions for the

Nanoencapsulation of Essential Oils and Nutraceuticals, in: A.M.B.T.-E. Grumezescu (Ed.), Encapsulations Nanotechnol. Agri-Food Ind., Academic Press, 2016: pp. 503–558. doi:https://doi.org/10.1016/B978-0-12-804307-3.00012-0.

[224] J.G. Speight, Pharmaceuticals, in: J.G.B.T.-H. of I.H.P. Speight (Ed.), Handb. Ind. Hydrocarb. Process., Gulf Professional Publishing, Boston, 2011: pp. 467–497. doi:https://doi.org/10.1016/B978-0-7506-8632-7.10013-1.

[225] F.O. Oyedeji, I.E. Okeke, Comparative Analysis of Moisturising Creams from Vegetable oils and Paraffin oil, Res. J. Appl. Sci. 5 (2010) 157–160. doi:10.3923/rjasci.2010.157.160.

[226] M.A. Ruiz, J.L. Arias, V. Gallardo, Skin Creams Made with Olive Oil, in: V.R. Preedy, R.R.B.T.-O. and O.O. in H. and D.P. Watson (Eds.), Olives Oilive Oil Heal. Dis. Prev., Academic Press, San Diego, 2010: pp. 1133–1141. doi:https://doi.org/10.1016/B978-0-12-374420-3.00124-8.

[227] B. Viswanathan, Petroleum, in: B.B.T.-E.S. Viswanathan (Ed.), Energy Sources Fundam. Chem. Convers. Process. Appl., Elsevier, Amsterdam, 2017: pp. 29–57. doi:https://doi.org/10.1016/B978-0-444-56353-8.00002-2.

[228] E.W. Hammond, Vegetable Oils: Types and Properties, in: B.B.T.-E. of F.S. and N. (Second E. Caballero (Ed.), Encycl. Food Sci. Nutr., Academic Press, Oxford, 2003: pp. 5899–5904. doi:https://doi.org/10.1016/B0-12-227055-X/01225-6.

[229] A.L. Márquez, A. Medrano, L.A. Panizzolo, J.R. Wagner, Effect of Calcium Salts and Surfactant Concentration on the Stability of Water-in-Oil (W/O) Emulsions Prepared with Polyglycerol Polyricinoleate, J. Colloid Interface Sci. 341 (2010) 101–108. doi:https://doi.org/10.1016/j.jcis.2009.09.020.

[230] A.L. Márquez, G.G. Palazolo, J.R. Wagner, Water in Oil (W/O) and Double (W/O/W) Emulsions Prepared with Spans: Microstructure, Stability, and Rheology, Colloid

Polym. Sci. 285 (2007) 1119–1128. doi:10.1007/s00396-007-1663-3.

[231] S.M. Jafari, P. Paximada, I. Mandala, E. Assadpour, M.A. Mehrnia, Encapsulation by Nanoemulsions, in: S.M.B.T.-N.T. for the F. and N.I. Jafari (Ed.), Nanoencapsulation Technol. Food Nutraceutical Ind., Academic Press, 2017: pp. 36–73. doi:https://doi.org/10.1016/B978-0-12-809436-5.00002-1.

[232] F.Y. Ushikubo, F.S. Birribilli, D.R.B. Oliveira, R.L. Cunha, Y- and T-Junction Microfluidic Devices: Effect of Fluids and Interface Properties and Operating Conditions, Microfluid. Nanofluidics. 17 (2014) 711–720. doi:10.1007/s10404-014-1348-4.

[233] G. Chen, D. Tao, An Experimental Study of Stability of Oil–Water Emulsion, Fuel Process. Technol. 86 (2005) 499–508. doi:https://doi.org/10.1016/j.fuproc.2004.03.010.

[234] H. Schubert, R. Engel, Product and Formulation Engineering of Emulsions, Chem. Eng. Res. Des. 82 (2004) 1137–1143. doi:10.1205/cerd.82.9.1137.44154.

[235] O. Juntarasakul, K. Maneeintr, Evaluation of stability and viscosity measurement of emulsion from oil from production in northern oilfield in Thailand, IOP Conf. Ser. Earth Environ. Sci. 140 (2018). doi:10.1088/1755-1315/140/1/012024.

[236] T. Joseph Lin, Increasing Productivity by Reducing Carbon Footprint in Cosmetics Processing, in: K. Sakamoto, R.Y. Lochhead, H.I. Maibach, Y.B.T.-C.S. and T. Yamashita (Eds.), Cosmet. Sci. Technol., Elsevier, Amsterdam, 2017: pp. 657–670. doi:https://doi.org/10.1016/B978-0-12-802005-0.00039-2.

[237] W.H. Weheliye, T. Dong, P. Angeli, On the Effect of Surfactants on Drop Coalescence at Liquid/Liquid Interfaces, Chem. Eng. Sci. 161 (2017) 215–227. doi:https://doi.org/10.1016/j.ces.2016.12.009.

[238] L.Y. Yeo, O.K. Matar, E.S. Perez de Ortiz, G.F. Hewitt, Film Drainage Between Two

Surfactant-Coated Drops Colliding at Constant Approach Velocity, J. Colloid Interface Sci. 257 (2003) 93–107. doi:https://doi.org/10.1016/S0021-9797(02)00033-4.

[239] A. Romm, L. Ganora, D. Hoffmann, E. Yarnell, K. Abascal, M. Coven, Fundamental Principles of Herbal Medicine, in: A. Romm, M.L. Hardy, S.B.T.-B.M. for W.H. Mills (Eds.), Bot. Med. Womens Heal., Churchill Livingstone, Saint Louis, 2010: pp. 24–74. doi:https://doi.org/10.1016/B978-0-443-07277-2.00003-9.

[240] M. Lukic, I. Pantelic, S. Savic, Emulsion Systems: From Stability Concerns to Sensory Properties, in: I.B.T.-A.P. Pantelic (Ed.), Alkyl Polyglucosides, Woodhead Publishing, Oxford, 2014: pp. 73–105. doi:https://doi.org/10.1533/9781908818775.73.

[241] S.N. Kale, S.L. Deore, Emulsion Micro Emulsion and Nano Emulsion: A Review, Syst. Rev. Pharm. 8 (2016) 39–47. doi:10.5530/srp.2017.1.8.

[242] J. Swarbrick, J. Rubino, O. Rubino, The Science and Practice of Pharmacy, 21st ed., Lippincott Williams & Wilkins, Philadelphia, 2006.

[243] D. Camuffo, Physics of Drop Formation and Micropore Condensation, in: D.B.T.-M. for C.H. (Second E. Camuffo (Ed.), Microclim. Cult. Herit., 2nd ed., Elsevier, Boston, 2014: pp. 165–201. doi:https://doi.org/10.1016/B978-0-444-63296-8.00006-8.

[244] J.D. Berry, M.J. Neeson, R.R. Dagastine, D.Y.C. Chan, R.F. Tabor, Measurement of Surface and Interfacial Tension Using Pendant Drop Tensiometry, J. Colloid Interface Sci. 454 (2015) 226–237. doi:https://doi.org/10.1016/j.jcis.2015.05.012.

[245] L.M. Coucoulas, R.A. Dawe, The Calculation of Interfacial Tension From Sessile Drops, J. Colloid Interface Sci. 103 (1985) 230–236. doi:https://doi.org/10.1016/0021-9797(85)90095-5.

[246] S. Ebnesajjad, Surface Tension and Its Measurement, in: S.B.T.-S.T. of M. for A.B. Ebnesajjad (Ed.), Surf. Treat. Mater. Adhes. Bond., William Andrew Publishing, Norwich, NY, 2006: pp. 9–28. doi:https://doi.org/10.1016/B978-081551523-4.50004-

3.

[247] B.E. Rapp, Measuring Surface Tension and Free Surface Energy, in: B.E.B.T.-M.M. Rapp Mechanics and Mathematics (Ed.), Microfluid. Model. Mech. Mathmatics, Elsevier, Oxford, 2017: pp. 453–465. doi:https://doi.org/10.1016/B978-1-4557-3141-1.50022-8.

[248] J. Berthier, Theory of Wetting, in: J.B.T.-M.-D. and D.M. (Second E. Berthier (Ed.), Micro-Drops Digit. Microfluid., William Andrew Publishing, 2013: pp. 7–73. doi:https://doi.org/10.1016/B978-1-4557-2550-2.00002-X.

[249] Zhang, Denler, Friberg, Aikens, Phase Diagram and Emulsion Stability of Surfactant–Fragrance Systems, Int. J. Cosmet. Sci. 22 (2000) 105–119. doi:10.1046/j.1467-2494.2000.00007.x.

[250] S. Bjerregaard, C. Vermehren, I. Söderberg, S. Frøkjaer, Accelerated Stability Testing of a Water-in-Oil Emulsion, J. Dispers. Sci. Technol. 22(1) (2007) 23–31. doi:10.1081/DIS-100102677.

[251] L.G. Torres, R. Iturbe, M.J. Snowden, B.Z. Chowdhry, S.A. Leharne, Preparation of o/w Emulsions Stabilized by Solid Particles and Their Characterization by Oscillatory Rheology, Colloids Surfaces A Physicochem. Eng. Asp. 302 (2007) 439–448. doi:https://doi.org/10.1016/j.colsurfa.2007.03.009.

[252] S.R. Derkach, Rheology of emulsions, Adv. Colloid Interface Sci. 151 (2009) 1–23. doi:https://doi.org/10.1016/j.cis.2009.07.001.

[253] T. Tadros, Application of rheology for assessment and prediction of the long-term physical stability of emulsions, Adv. Colloid Interface Sci. 109 (2004) 227–258. doi:10.1016/j.cis.2003.10.025.

[254] Y. Otsubo, R.K. Prud'homme, Rheology of oil-in-water emulsions, Rheol. Acta. 33 (1994) 29–37. doi:10.1007/BF00453461.

[255] G. Tabilo-Munizaga, G. V Barbosa-Cánovas, Rheology for the food industry, J. Food Eng. 67 (2005) 147–156. doi:https://doi.org/10.1016/j.jfoodeng.2004.05.062.

[256] H. Saad Ali, R. Saad Suliman, B.M. A Elhaj, R. Suliman, Pharmaceutical Powder Dosage Forms: A Review, Int. J. Pharm. Clin. Res. 11 (2019) 20–22. www.ijpcr.com.

[257] F. Emami, A. Vatanara, E.J. Park, D.H. Na, Drying Technologies for the Stability and Bioavailability of Biopharmaceuticals, Pharmaceutics. 10 (2018) 131. doi:10.3390/pharmaceutics10030131.

[258] P. Intipunya, B.R. Bhandari, Chemical Deterioration and Physical Instability of Food Powders, in: L.H. Skibsted, J. Risbo, M.L.B.T.-C.D. and P.I. of F. and B. Andersen (Eds.), Chem. Deterior. Phys. Instab. Food Beverages, Woodhead Publishing, 2010: pp. 663–700. doi:https://doi.org/10.1533/9781845699260.3.663.

[259] S. Shanmugam, Granulation Techniques and Technologies: Recent Progresses, Bioimpacts. 5 (2015) 55–63. doi:10.15171/bi.2015.04.

[260] B. Armstrong, K. Brockbank, J. Clayton, Understand the Effects of Moisture on Powder Behavior, Chem. Eng. Prog. 110 (2014) 25–30.

[261] U. Zafar, V. Vivacqua, G. Calvert, M. Ghadiri, J.A.S. Cleaver, A Review of Bulk Powder Caking, Powder Technol. 313 (2017) 389–401. doi:https://doi.org/10.1016/j.powtec.2017.02.024.

[262] Z. Berk, Extraction, in: Z.B.T.-F.P.E. and T. Berk (Ed.), Food Process Eng. Technol., Academic Press, San Diego, 2009: pp. 259–277. doi:https://doi.org/10.1016/B978-0-12-373660-4.00011-9.

[263] K.N. Dyvelkov, J. Sloth, New Advances in Spray-Drying Processes, in: A.G. Gaonkar, N. Vasisht, A.R. Khare, R.B.T.-M. in the F.I. Sobel (Eds.), Microencapsul. Food Ind., Academic Press, San Diego, 2014: pp. 57–63. doi:https://doi.org/10.1016/B978-0-12-404568-2.00006-6.

[264] G.R. Nireesha, L. Divya, C. Sowmya, N. Venkateshan, M.N. Babu, V. Lavakumar, Lyophilization / Freeze Drying - A Review, Int. J. Nov. Trends Pharm. Sci. 3 (2013) 87–98.

[265] Y. Su, S. Xia, R. Wang, L. Xiao, Phytohormonal Quantification Based on Biological Principles, in: J. Li, C. Li, S.M.B.T.-H.M. and S. in P. Smith (Eds.), Horm. Metab. Signal. Plants, Academic Press, 2017: pp. 431–470. doi:https://doi.org/10.1016/B978-0-12-811562-6.00013-X.

[266] M.M. Houck, J.A. Siegel, Separation Methods, in: M.M. Houck, J.A.B.T.-F. of F.S. (Third E. Siegel (Eds.), Fundam. Forensic Sci., 3rd ed., Academic Press, San Diego, 2015: pp. 121–151. doi:https://doi.org/10.1016/B978-0-12-800037-3.00006-6.

[267] B. Law, HPLC–MS(MS) for bioanalysis in drug discovery and development, in: I.D.B.T.-H. of A.S. Wilson (Ed.), Handb. Anal. Sep. Bioanal. Sep., Elsevier Science B.V., 2003: pp. 271–292. doi:https://doi.org/10.1016/S1567-7192(03)80010-4.

[268] I. Rezić, A.J.M. Horvat, S. Babić, M. Kaštelan-Macan, Determination of Pesticides in Honey by Ultrasonic Solvent Extraction and Thin-layer Chromatography, Ultrason. Sonochem. 12 (2005) 477–481. doi:https://doi.org/10.1016/j.ultsonch.2004.07.004.

[269] J.J. Jiménez, J.L. Bernal, M.J. del Nozal, M. Novo, M. Higes, J. Llorente, Determination of Rotenone Residues in Raw Honey by Solid-Phase Extraction and High-Performance Liquid Chromatography, J. Chromatogr. A. 871 (2000) 67–73. doi:https://doi.org/10.1016/S0021-9673(99)01063-8.

[270] H.H. Hatt, A.C.K. Triffett, The Separation of Glucose and Fructose by Liquid-Liquid Extraction, J. Appl. Chem. 15 (1965) 556–569. doi:10.1002/jctb.5010151203.

[271] H.J. Wiggers, J. Cheleski, A. Zottis, G. Oliva, A.D. Andricopulo, C.A. Montanari, Effects of Organic Solvents on the Enzyme Activity of Trypanosoma Cruzi Glyceraldehyde-3-phosphate Dehydrogenase in Calorimetric Assays, Anal. Biochem.

370 (2007) 107–114. doi:https://doi.org/10.1016/j.ab.2007.06.042.

[272] F.D. Dick, Solvent Neurotoxicity, Occup. Environ. Med. 63 (2006) 179–221. doi:10.1136/oem.2005.022400.

[273] E. Drioli, A. Cassano, Advances in Membrane-Based Concentration in the Food and Beverage Industries: Direct Osmosis and Membrane Contactors, in: S.S.H.B.T.-S. Rizvi Extraction and Concentration Processes in the Food, Beverage and Nutraceutical Industries (Ed.), Sep. Extr. Conc. Process. Food, Beverage Nutraceutical Ind., Woodhead Publishing, 2013: pp. 244–283. doi:https://doi.org/10.1533/9780857090751.1.244.

[274] C.G. Kumar, S. Sripada, Y. Poornachandra, Status and Future Prospects of Fructooligosaccharides as Nutraceuticals, in: A.M. Grumezescu, A.M.B.T.-R. of M.S. in F.B. Holban (Eds.), Handb. Food Bioeng. Role Mater. Sci. Food Bioeng., Academic Press, 2018: pp. 451–503. doi:https://doi.org/10.1016/B978-0-12-811448-3.00014-0.

[275] M.-I. Ré, Formulating Drug Delivery Systems by Spray Drying, Dry. Technol. 24 (2006) 433–446. doi:10.1080/07373930600611877.

[276] C.P. Champagne, P. Fustier, Microencapsulation for delivery of probiotics and other ingredients in functional dairy products, in: M.B.T.-F.D.P. Saarela (Ed.), Funct. Dairy Prod., Woodhead Publishing, 2007: pp. 404–426. doi:https://doi.org/10.1533/9781845693107.3.404.

[277] K. Samborska, E. Langa, A. Kamińska-Dwórznicka, D. Witrowa-Rajchert, The Influence of Dodium Caseinate on the Physical Properties of Spray-Dried Honey, Int. J. Food Sci. Technol. 50 (2015) 256–262. doi:10.1111/ijfs.12629.

[278] Q. Tong, X. Zhang, F. Wu, J. Tong, P. Zhang, J. Zhang, Effect of Honey Powder on Dough Rheology and Bread Quality, Food Res. Int. 43 (2010) 2284–2288. doi:https://doi.org/10.1016/j.foodres.2010.08.002.

[279] E. Yener, S. Ungan, M. Özilgen, Drying Behavior of Honey-Starch Mixtures, J. Food Sci. 52 (1987) 1054–1058. doi:10.1111/j.1365-2621.1987.tb14274.x.

[280] M.D. Gouda, S.A. Singh, A.G.A. Rao, M.S. Thakur, N.G. Karanth, Thermal Inactivation of Glucose Oxidase: Mechanism and Stabilization Using Additives, J. Biol. Chem. 278 (2003) 24324–24333. doi:10.1074/jbc.M208711200.

[281] U.M. Shapla, M. Solayman, N. Alam, M.I. Khalil, S.H. Gan, 5-Hydroxymethylfurfural (HMF) Levels in Honey and Other Food Products: Effects on Bees and Human Health, Chem. Cent. J. 12 (2018) 35. doi:10.1186/s13065-018-0408-3.

[282] A. Ciurzyńska, A. Lenart, Freeze-Drying - Application in Food Processing and Biotechnology - A Review, Polish J. Food Nutr. Sci. 61 (2011) 165–171. doi:10.2478/v10222-011-0017-5.

[283] C. Ratti, Hot Air and Freeze-Drying of High-Value Foods: A Review, J. Food Eng. 49 (2001) 311–319. doi:https://doi.org/10.1016/S0260-8774(00)00228-4.

[284] M.D.L. de Castro, J.L.L. García, Analytical Freeze-Drying, in: M.D.L. de Castro, J.L.L.B.T.-T. and I. in A.C. García (Eds.), Tech. Instrum. Anal. Chem., Elsevier, 2002: pp. 11–41. doi:https://doi.org/10.1016/S0167-9244(02)80004-X.

[285] S. Shukla, Freeze Drying Process: A Review, Int. J. Pharm. Sci. Res. 2 (2011) 3061–3068.

[286] J.D. Mellor, G.A. Bell, Freeze-Drying - The Basic Process, in: B.B.T.-E. of F.S. and N. (Second E. Caballero (Ed.), Encycl. Food Sci., Academic Press, Oxford, 2003: pp. 2697–2701. doi:https://doi.org/10.1016/B0-12-227055-X/00519-8.

[287] C. Ratti, Freeze and Vacuum Drying of Foods, in: X.D. Chen, A. Mujumdar (Eds.), Dry. Technol. Food Process., 1st ed., John Wiley & Sons, Ltd, Oxford, 2009: pp. 225–250.

[288] A. Yadegari, F. Fahimipour, M. Rasoulianboroujeni, E. Dashtimoghadarm, M. Omidi,

H. Golzar, M. Tahriri, L. Tayebi, Specific Considerations in Scaffold Design for Oral Tissue Engineering, in: L. Tayebi, K.B.T.-B. for O. and D.T.E. Moharamzadeh (Eds.), Biomater. Oral Dent. Tissue Eng., Woodhead Publishing, 2017: pp. 157–183. doi:https://doi.org/10.1016/B978-0-08-100961-1.00010-4.

[289] N. Luo, H. Shu, Analysis of Energy Saving during Food Freeze Drying, Procedia Eng. 205 (2017) 3763–3768. doi:10.1016/j.proeng.2017.10.330.

[290] X. Zhang, M. Cresswell, Materials Fundamentals of Drug Controlled Release, in: X. Zhang, M.B.T.-I.C.R.T. Cresswell (Eds.), Mater. Concepts Adv. Drug Formul. Inorg. Control. Release Technol., Butterworth-Heinemann, Boston, 2016: pp. 17–55. doi:https://doi.org/10.1016/B978-0-08-099991-3.00002-8.

[291] L. Juszczak, T. Fortuna, Rheology of selected Polish honeys, J. Food Eng. 75 (2006) 43–49. doi:https://doi.org/10.1016/j.jfoodeng.2005.03.049.

[292] J. Ahmed, S.T. Prabhu, G.S. V Raghavan, M. Ngadi, Physico-chemical, rheological, calorimetric and dielectric behavior of selected Indian honey, J. Food Eng. 79 (2007) 1207–1213. doi:10.1016/j.jfoodeng.2006.04.048.

[293] V. Truong, B.R. Bhandari, T. Howes, Optimization of co-current spray drying process of sugar-rich foods. Part I—Moisture and glass transition temperature profile during drying, J. Food Eng. 71 (2005) 55–65. doi:https://doi.org/10.1016/j.jfoodeng.2004.10.017.

[294] G.R. Rodríguez-Hernández, R. González-García, A. Grajales-Lagunes, M.A. Ruiz-Cabrera*, M. Abud-Archila, Spray-Drying of Cactus Pear Juice (Opuntia streptacantha): Effect on the Physicochemical Properties of Powder and Reconstituted Product, Dry. Technol. 23 (2005) 955–973. doi:10.1080/DRT-200054251.

[295] A. Lazaridou, C.G. Biliaderis, N. Bacandritsos, A.G. Sabatini, Composition, thermal and rheological behaviour of selected Greek honeys, J. Food Eng. 64 (2004) 9–21.

doi:https://doi.org/10.1016/j.jfoodeng.2003.09.007.

[296] B.R. Bhandari, T. Howes, Implication of glass transition for the drying and stability of dried foods, J. Food Eng. 40 (1999) 71–79. doi:https://doi.org/10.1016/S0260-8774(99)00039-4.

[297] H. Umesh Hebbar, N.K. Rastogi, R. Subramanian, Properties of Dried and Intermediate Moisture Honey Products: A Review, Int. J. Food Prop. 11 (2008) 804–819. doi:10.1080/10942910701624736.

[298] J.K. Sahu, Effect of Additives on Vacuum Dried Honey Powder Properties, Int. J. Food Eng. v. v. 4 (2008).

[299] A. Verma, S.V. Singh, Spray Drying of Fruit and Vegetable Juices—A Review, Crit. Rev. Food Sci. Nutr. 55 (2015) 701–719. doi:10.1080/10408398.2012.672939.

[300] J.A. Grabowski, V.-D. Truong, C.R. Daubert, Spray-Drying of Amylase Hydrolyzed Sweetpotato Puree and Physicochemical Properties of Powder, J. Food Sci. 71 (2006) E209–E217. doi:10.1111/j.1750-3841.2006.00036.x.

[301] B. Nurhadi, R. Andoyo, Mahani, R. Indiarto, Study the properties of honey powder produced from spray drying and vacuum drying method, Int. Food Res. J. 19 (2012) 907–912.

[302] K.A. Gaidhani, M. Harwalkar, D. Bhambere, P.S. Nirgude, Lyophylization/Freeze drying - A Review, World J. Pharm. Res. 4 (2015) 516–543.

[303] G. Adams, The Principles of Freeze Drying, in: J. Day, G. Stacey (Eds.), Cryopreserv. Free. Protoc., 2nd ed., Humana Press, Totowa, 2007: pp. 15–38.

[304] X. (Charlie) Tang, M.J. Pikal, Design of Freeze-Drying Processes for Pharmaceuticals: Practical Advice, Pharm. Res. 21 (2004) 191–200. doi:10.1023/B:PHAM.0000016234.73023.75.

[305] P.M. Doran, Unit Operations, in: P.M.B.T.-B.E.P. (Second E. Doran (Ed.), Bioprocess

Eng. Princ., 2nd ed., Academic Press, London, 2013: pp. 445–595. doi:https://doi.org/10.1016/B978-0-12-220851-5.00011-3.

[306] S.M. Patel, T. Doen, M.J. Pikal, Determination of End Point of Primary Drying in Freeze-Drying Process Control, AAPS PharmSciTech. 11 (2010) 73–84. doi:10.1208/s12249-009-9362-7.

[307] M.G. Severo, A.S. Zeferino, C.R. Soccol, Development of a Rabies Vaccine in Cell Culture for Veterinary Use in the Lyophilized Form, in: V. Thomaz-Soccol, A. Pandey, R.R.B.T.-C.D. in B. and B. Resende (Eds.), Hum. Anim. Heal. Appl. Curr. Dev. Biotechnol. Bioeng., Elsevier, 2017: pp. 523–560. doi:https://doi.org/10.1016/B978-0-444-63660-7.00021-8.

[308] V. Jones, J.E. Grey, K.G. Harding, Wound dressings, BMJ. 332 (2006) 777 LP – 780. doi:10.1136/bmj.332.7544.777.

[309] G. Han, R. Ceilley, Chronic Wound Healing: A Review of Current Management and Treatments, Adv. Ther. 34 (2017) 599–610. doi:10.1007/s12325-017-0478-y.

[310] E. Caló, V. V Khutoryanskiy, Biomedical Applications of Hydrogels: A Review of Patents and Commercial Products, Eur. Polym. J. 65 (2015) 252–267. doi:https://doi.org/10.1016/j.eurpolymj.2014.11.024.

[311] K.E. Swindle-Reilly, M.A. Reilly, N. Ravi, Current Concepts in the Design of Hydrogels as Vitreous Substitutes, in: T. V Chirila, D.G.B.T.-B. and R.M. in O. (Second E. Harkin (Eds.), Biomater. Regen. Med. Ophthalmol., 2nd ed., Woodhead Publishing, 2016: pp. 101–130. doi:https://doi.org/10.1016/B978-0-08-100147-9.00005-5.

[312] C.K. Sudhakar, N. Upadhyay, A. Jain, A. Verma, R. Narayana Charyulu, S. Jain, Hydrogels—Promising Candidates for Tissue Engineering, in: S. Thomas, Y. Grohens, N.B.T.-N.A. for T.E. Ninan (Eds.), Nanotechnol. Appl. Tissue Eng., William Andrew Publishing, Oxford, 2015: pp. 77–94. doi:https://doi.org/10.1016/B978-0-323-32889-

0.00005-4.

[313] L.P. da Silva, M.T. Cerqueira, V.M. Correlo, R.L. Reis, A.P. Marques, Engineered Hydrogel-Based Matrices for Skin Wound Healing, in: M.S.B.T.-W.H.B. Ågren (Ed.), Wound Heal. Biomater., Woodhead Publishing, 2016: pp. 227–250. doi:https://doi.org/10.1016/B978-1-78242-456-7.00011-8.

[314] J.S. Boateng, K.H. Matthews, H.N.E. Stevens, G.M. Eccleston, Wound healing dressings and drug delivery systems: A review, J. Pharm. Sci. 97 (2008) 2892–2923. doi:10.1002/jps.21210.

[315] G.D. Winter, Formation of the Scab and the Rate of Epithelization of Superficial Wounds in the Skin of the Young Domestic Pig, Nature. 193 (1962) 293–294. doi:10.1038/193293a0.

[316] G.D. Winter, Effect of Air Exposure and Occlusion on Experimental Human Skin Wounds, Nature. 200 (1963) 378–379. doi:10.1038/200378a0.

[317] L.G. Ovington, Advances in wound dressings, Clin. Dermatol. 25 (2007) 33–38. doi:https://doi.org/10.1016/j.clindermatol.2006.09.003.

[318] H. Yasin, Z. Yousaf, Synthesis of Hydrogels and Their Emerging Role in Pharmaceuticals, in: A. Grumezescu (Ed.), Biomed. Appl. Nanoparticles, Cambridge, 2019: pp. 164–183.

[319] E.M. Ahmed, Hydrogel: Preparation, Characterization, and Applications: A Review, J. Adv. Res. 6 (2015) 105–121. doi:https://doi.org/10.1016/j.jare.2013.07.006.

[320] G. Kowalski, K. Kijowska, M. Witczak, L. Kuterasiński, M. Lukasiewicz, Synthesis and Effect of Structure on Swelling Properties of Hydrogels Based on High Methylated Pectin and Acrylic Polymers, Polymers (Basel). 11 (2019) 1–16. doi:10.3390/polym11010114.

[321] T. Manzur, S. Iffat, M.A. Noor, Efficiency of Sodium Polyacrylate to Improve

Durability of Concrete Under Adverse Curing Condition, Adv. Mater. Sci. Eng. 2015 (2015). doi:10.1155/2015/685785.

[322] G.C. Ritthidej, Nasal Delivery of Peptides and Proteins with Chitosan and Related Mucoadhesive Polymers, in: C.B.T.-P. and P.D. Van Der Walle (Ed.), Pept. Protein Deliv., Academic Press, Boston, 2011: pp. 47–68. doi:https://doi.org/10.1016/B978-0-12-384935-9.10003-3.

[323] L. Bell-young, Sodium Polyacrylate, Chemistry (Easton). (2018).

[324] K.G. Ewsuk, Powder Granulation and Compaction, in: K.H.J. Buschow, R.W. Cahn, M.C. Flemings, B. Ilschner, E.J. Kramer, S. Mahajan, P.B.T.-E. of M.S. and T. Veyssière (Eds.), Encycl. Mater. Sci. Technol., 2nd ed., Elsevier, Oxford, 2001: pp. 7788–7800. doi:https://doi.org/10.1016/B0-08-043152-6/01401-7.

[325] A. Hickey, S. Giovagnoli, Particle Size Measurement, in: AAPS Introd. Pharm. Sci. Pharm. Powder Part., Springer, Cham, 2018: pp. 31–48.

[326] M. Houghton, G. Amidon, Microscopic Characterization of Particle Size and Shape: An Inexpensive and Versatile Method, Pharm. Res. 9 (1992) 856–859.

[327] M. Cyr, A. Tagnit-Hamou, Particle Size Distribution of Fine Powders by LASER Diffraction Spectrometry. Case of Cementitious Materials, Mater. Struct. Constr. 34 (2001) 342–350. doi:10.1007/bf02486485.

[328] W. Yu, B.C. Hancock, Evaluation of Dynamic Image Analysis for Characterizing Pharmaceutical Excipient Particles, Int. J. Pharm. 361 (2008) 150–157. doi:https://doi.org/10.1016/j.ijpharm.2008.05.025.

[329] M. Jonasz, G.R. Fournier, The Particle Size Distribution, in: M. Jonasz, G.R.B.T.-L.S. by P. in W. Fournier (Eds.), Theor. Exp. Found. Light Scatt. by Part. Water, Academic Press, Amsterdam, 2007: pp. 267–445. doi:https://doi.org/10.1016/B978-012388751-1/50005-3.

[330] A. Yoshida, Y. Kaburagi, Y. Hishiyama, Scanning Electron Microscopy, in: M. Inagaki, F.B.T.-M.S. and E. of C. Kang (Eds.), Mater. Sci. Eng. Carbon, Butterworth-Heinemann, 2016: pp. 71–93. doi:https://doi.org/10.1016/B978-0-12-805256-3.00005-2.

[331] D. Brabazon, A. Raffer, Advanced Characterization Techniques for Nanostructures, in: W. Ahmed, M.J.B.T.-E.N. for M. Jackson (Eds.), Micro Nano Technol. Emerg. Nanotechnologies Manuf., William Andrew Publishing, Boston, 2010: pp. 59–91. doi:https://doi.org/10.1016/B978-0-8155-1583-8.00003-X.

[332] D.F. Heaney, Powders for Metal Injection Molding (MIM), in: D.F.B.T.-H. of M.I.M. Heaney (Ed.), Handb. Met. Inject. Molding, Woodhead Publishing, 2012: pp. 50–63. doi:https://doi.org/10.1533/9780857096234.1.50.

[333] D.J. Farina, Regulatory Aspects of Nasal and Pulmonary Spray Drug Products, in: V.S.B.T.-H. of N.-I.D.D.S. Kulkarni (Ed.), Pers. Care Cosmet. Technol. Handb. Non-Invasive Drug Deliv. Syst., William Andrew Publishing, Boston, 2010: pp. 247–290. doi:https://doi.org/10.1016/B978-0-8155-2025-2.10010-1.

[334] Sympatec GmbH, Dynamic Image Analysis, Part. Meas. (2019). https://www.sympatec.com/en/particle-measurement/sensors/dynamic-image-analysis/ (accessed November 21, 2019).

[335] U. Ulusoy, Quantifying of Particle Shape Differences of Differently Milled Barite Using a Novel Technique: Dynamic Image Analysis, Materialia. 8 (2019) 100434. doi:https://doi.org/10.1016/j.mtla.2019.100434.

[336] V.R. Nalluri, P. Schirg, X. Gao, A. Virdis, G. Imanidis, M. Kuentz, Different Modes of Dynamic Image Analysis in Monitoring of Pharmaceutical Dry Milling Process, Int. J. Pharm. 391 (2010) 107–114. doi:https://doi.org/10.1016/j.ijpharm.2010.02.027.

[337] Z. Berk, Fluid Flow, in: Z.B.T.-F.P.E. and T. (Third E. Berk (Ed.), Food Sci. Technol.

Food Process Eng. Technol., 3rd ed., Academic Press, 2018: pp. 31–78. doi:https://doi.org/10.1016/B978-0-12-812018-7.00002-6.

[338] J. Klausner, D. Chen, R. Mei, Experimental Investigation of Cohesive Powder Rheology, Powder Technol. 112 (2000) 94–101. doi:10.1016/S0032-5910(99)00310-1.

[339] P.D. Jager, T. Bramante, P.E. Luner, Assessment of Pharmaceutical Powder Flowability using Shear Cell-Based Methods and Application of Jenike's Methodology, J. Pharm. Sci. 104 (2015) 3804–3813. doi:https://doi.org/10.1002/jps.24600.

[340] P. García-Triñanes, S. Luding, H. Shi, Tensile Strength of Cohesive Powders, Adv. Powder Technol. 30 (2019) 2868–2880. doi:https://doi.org/10.1016/j.apt.2019.08.017.

[341] H.M. Beakawi Al-Hashemi, O.S. Baghabra Al-Amoudi, A Review on the Angle of Repose of Granular Materials, Powder Technol. 330 (2018) 397–417. doi:https://doi.org/10.1016/j.powtec.2018.02.003.

[342] T.F. Teferra, Engineering Properties of Food Materials, in: M.B.T.-H. of F. Kutz Dairy and Food Machinery Engineering (Third Edition) (Ed.), Handb. Farm, Dairy Food Mach. Eng., 3rd ed., Academic Press, 2019: pp. 45–89. doi:https://doi.org/10.1016/B978-0-12-814803-7.00003-8.

[343] R.B. Shah, M.A. Tawakkul, M.A. Khan, Comparative Evaluation of Flow for Pharmaceutical Powders and Granules, AAPS PharmSciTech. 9 (2008) 250–258. doi:10.1208/s12249-008-9046-8.

[344] L.A. Sherrington, A. Sherrington, Guaifenesin, in: H.G.B.T.-A.P. of D.S. and E. Brittain (Ed.), Anal. Profiles Drug Subst. Excipients, Academic Press, 1998: pp. 121–164. doi:https://doi.org/10.1016/S0099-5428(08)60754-6.

[345] X. He, Integration of Physical, Chemical, Mechanical, and Biopharmaceutical Properties in Solid Oral Dosage Form Development, in: Y. Qiu, Y. Chen, G.G.Z.

Zhang, L. Liu, W.R.B.T.-D.S.O.D.F. Porter (Eds.), Pharm. Theroy Pract. Dev. Solid Oral Dos. Forms, Academic Press, San Diego, 2009: pp. 407–441. doi:https://doi.org/10.1016/B978-0-444-53242-8.00018-7.

[346] A. Crouter, L. Briens, The Effect of Moisture on the Flowability of Pharmaceutical Excipients, AAPS PharmSciTech. 15 (2014) 65–74. doi:10.1208/s12249-013-0036-0.

[347] M. Ribeiro, F.J. Monteiro, M.P. Ferraz, Infection of Orthopedic Implants with Emphasis on Bacterial Adhesion Process and Techniques Used in Studying Bacterial-Material Interactions, Biomatter. 2 (2012) 176–194. doi:10.4161/biom.22905.

[348] R.A. Brady, J.G. Leid, J.W. Costerton, M.E. Shirtliff, Osteomyelitis: Clinical Overview and Mechanisms of Infection Persistence, Clin. Microbiol. Newsl. 28 (2006) 65–72. doi:https://doi.org/10.1016/j.clinmicnews.2006.04.001.

[349] M.-P. Ginebra, E.B. Montufar, Cements as Bone Repair Materials, in: K.M. Pawelec, J.A.B.T.-B.R.B. (Second E. Planell (Eds.), Bone Repair Mater., 2nd ed., Woodhead Publishing, 2019: pp. 233–271. doi:https://doi.org/10.1016/B978-0-08-102451-5.00009-3.

[350] P. Kumar, B. Vinitha, G. Fathima, Bone Grafts in Dentistry, J. Pharm. Bioallied Sci. 5 (2013) S125–S127. doi:10.4103/0975-7406.113312.

[351] E. Hughes, T. Yanni, P. Jamshidi, L.M. Grover, Inorganic Cements for Biomedical Application: Calcium Phosphate, Calcium Sulphate and Calcium Silicate, Adv. Appl. Ceram. 114 (2015) 65–76. doi:10.1179/1743676114Y.0000000219.

[352] F. Baino, Ceramics for Bone Replacement: Commercial Products and Clinical Use, in: P. Palmero, F. Cambier, E.B.T.-A. in C.B. De Barra (Eds.), Adv. Ceram. Biomater., Woodhead Publishing, 2017: pp. 249–278. doi:https://doi.org/10.1016/B978-0-08-100881-2.00007-5.

[353] M. Dadkhah, L. Pontiroli, S. Fiorilli, A. Manca, F. Tallia, I. Tcacencu, C. Vitale-

Brovarone, Preparation and Characterisation of an Innovative Injectable Calcium Sulphate Based Bone Cement for Vertebroplasty Application, J. Mater. Chem. B. 5 (2017) 102–115. doi:10.1039/c6tb02139e.

[354] D. Neut, H. van de Belt, J.R. van Horn, H.C. van der Mei, H.J. Busscher, Residual Gentamicin-Release from Antibiotic-Loaded Polymethylmethacrylate Beads After 5 years of Implantation, Biomaterials. 24 (2003) 1829–1831. doi:https://doi.org/10.1016/S0142-9612(02)00614-2.

[355] H. van de Belt, D. Neut, W. Schenk, J.R. van Horn, H.C. van der Mei, H.J. Busscher, Infection of Orthopedic Implants and the Use of Antibiotic-Loaded Bone Cements: A Review, Acta Orthop. Scand. 72 (2001) 557–571. doi:10.1080/000164701317268978.

[356] N.D. Mullins, B.J. Deadman, H.A. Moynihan, F.O. McCarthy, S.E. Lawrence, J. Thompson, A.R. Maguire, The Impact of Storage Conditions upon Gentamicin Coated Antimicrobial Implants, J. Pharm. Anal. 6 (2016) 374–381. doi:https://doi.org/10.1016/j.jpha.2016.05.002.

[357] B.K.B. Tay, V. V Patel, D.S. Bradford, Calcium Sulphate and Calcium Phosphate Based Bone Substitutes: Mimicry of the Mineral Phase of Bone, Orthop. Clin. North Am. 30 (1999) 615–623. doi:https://doi.org/10.1016/S0030-5898(05)70114-0.

[358] S.C. Cox, P. Jamshidi, N.M. Eisenstein, M.A. Webber, H. Hassanin, M.M. Attallah, D.E.T. Shepherd, O. Addison, L.M. Grover, Adding Functionality with Additive Manufacturing: Fabrication of Titanium-Based Antibiotic Eluting Implants, Mater. Sci. Eng. C. 64 (2016) 407–415. doi:https://doi.org/10.1016/j.msec.2016.04.006.

[359] X. Zhu, X. Chen, C. Chen, G. Wang, Y. Gu, D. Geng, H. Mao, Z. Zhang, H. Yang, Evaluation of Calcium Phosphate and Calcium Sulfate as Injectable Bone Cements in Sheep Vertebrae, J. Spinal Disord. Tech. 25 (2012) 333–337. doi:10.1097/BSD.0b013e3182213f57.

[360] M. Nilsson, E. Fernández, S. Sarda, L. Lidgren, J.A. Planell, Characterization of a Novel Calcium Phosphate/Sulphate Bone Cement, J. Biomed. Mater. Res. 61 (2002) 600–607. doi:10.1002/jbm.10268.

[361] G. Hu, L. Xiao, H. Fu, D. Bi, H. Ma, P. Tong, Study on Injectable and Degradable Cement of Calcium Sulphate and Calcium Phosphate for Bone Repair, J. Mater. Sci. Mater. Med. 21 (2010) 627–634. doi:10.1007/s10856-009-3885-z.

[362] R. Kallala, W.E. Harris, M. Ibrahim, M. Dipane, E. McPherson, Use of Stimulan Absorbable Calcium Sulphate Beads in Revision Lower Limb Arthroplasty: Safety Profile and Complication Rates, Bone Joint Res. 7 (2018) 570–579. doi:10.1302/2046-3758.710.BJR-2017-0319.R1.

[363] M. V Thomas, D.A. Puleo, Calcium Sulfate: Properties and Clinical Applications, J. Biomed. Mater. Res. Part B Appl. Biomater. 88B (2009) 597–610. doi:10.1002/jbm.b.31269.

[364] B.W. Darvell, Gypsum Materials, in: B.W.B.T.-M.S. for D. (Tenth E. Darvell (Ed.), Mater. Sci. Dent., 10th ed., Woodhead Publishing, 2018: pp. 40–69. doi:https://doi.org/10.1016/B978-0-08-101035-8.50002-X.

[365] J. Ricci, H. Alexander, P. Nadkarni, M. Hawkins, J. Turner, S. Rosenblum, L. Brezenoff, D. DeLeonardis, G. Pecora, Biological Mechanisms of Calcium Sulfate Replacement by Bone, in: J. Davies (Ed.), Bone Eng., Em Squared Inc., Toronto, 2000: pp. 332–344.

[366] National Center for Biotechnology Information, Calcium Sulphate Hemihydrate, PubChem Database. (2019).

[367] K. Anusavice, Gypsum Products, in: K. Anusavice (Ed.), Phillips' Sci. Dent. Mater., Saunders, St. Louis, 2003: pp. 255–281.

[368] F. Wirsching, Calcium Sulfate, Ullmann's Encycl. Ind. Chem. (2000).

doi:doi:10.1002/14356007.a04_555.

[369] A.H. Dewi, I.D. Ana, J. Wolke, J. Jansen, Behavior of Plaster of Paris-Calcium carbonate Composite as Bone Substitute. A Study in Rats, J. Biomed. Mater. Res. Part A. 101A (2013) 2143–2150. doi:10.1002/jbm.a.34513.

[370] F. Baino, Ceramics for Bone Replacement: Commercial Products and Clinical Use, in: F. Palmero, P; De Barra, E; Cambier (Ed.), Adv. Ceram. Biomater. Mater. Devices Challenges, Elsevier Ltd., 2017: pp. 249–271. doi:http://dx.doi.org/10.1016/B978-0-08-100881-2.00007-5.

[371] J. Barralet, T. Gaunt, A. Wright, I. Gibson, J. Knowles, Effect of Porosity Reduction by Compaction on Compressive Strength and Microstructure of Calcium Phosphate Cement, J. Biomed. Mater. Res. 63 (2002) 1–9. doi:10.1002/jbm.1074.

[372] A.J. Lewry, J. Williamson, The Setting of Gypsum Plaster - Part III The Effect of Additives and Impurities, J. Mater. Sci. 29 (1994) 6085–6090. doi:10.1007/BF00354546.

[373] J. Wataha, Biocompatability of Dental Materials, in: K. Anusavice (Ed.), Phillips' Sci. Dent. Mater., Elsevier, St. Louis, 2003: pp. 171–202.

[374] J.M. Payne, C.M. Cobb, J.W. Rapley, W.J. Killoy, P. Spencer, Migration of Human Gingival Fibroblasts Over Guided Tissue Regeneration Barrier Materials, J. Periodontol. 67 (1996) 236–244. doi:10.1902/jop.1996.67.3.236.

[375] W. Walsh, P. Morberg, Y. Yu, J. Yang, W. Haggard, P. Sheath, M. Svehla, W. Bruce, Response of a Calcium Sulfate Bone Graft Substitute in a Confined Cancellous Defect, Clin. Orthop. Relat. Res. 406 (2003) 228–236. doi:10.1097/01.blo.0000030062.92399.6a.

[376] E.K. Park, Y.E. Lee, J.-Y. Choi, S.-H. Oh, H.-I. Shin, K.-H. Kim, S.-Y. Kim, S. Kim, Cellular Biocompatibility and Stimulatory Effects of Calcium Metaphosphate on

Osteoblastic Differentiation of Human Bone Marrow-Derived Stromal Cells, Biomaterials. 25 (2004) 3403–3411. doi:10.1016/j.biomaterials.2003.10.031.

[377] M. Yamauchi, T. Yamaguchi, H. Kaji, T. Sugimoto, K. Chihara, Involvement of Calcium-Sensing Receptor in Osteoblastic Differentiation of Mouse MC3T3-E1 Cells, Am. J. Physiol. Metab. 288 (2005) E608–E616. doi:10.1152/ajpendo.00229.2004.

[378] T. Kameda, H. Mano, Y. Yamada, H. Takai, N. Amizuka, M. Kobori, N. Izumi, H. Kawashima, H. Ozawa, K. Ikeda, A. Kameda, Y. Hakeda, M. Kumegawa, Calcium-Sensing Receptor in Mature Osteoclasts, Which Are Bone Resorbing Cells, Biochem. Biophys. Res. Commun. 245 (1998) 419–422. doi:https://doi.org/10.1006/bbrc.1998.8448.

[379] J.. Wang, N. Dunne, Bone cement fixation: acrylic cements, in: P.A.B.T.-J.R.T. Revell (Ed.), Woodhead Publ. Ser. Biomater., Woodhead Publishing, 2008: pp. 212–251. doi:https://doi.org/10.1533/9781845694807.2.212.

[380] N. Dunne, J. Clements, J.. Wang, Acrylic cements for bone fixation in joint replacement, in: P.A.B.T.-J.R.T. Revell (Ed.), Woodhead Publ. Ser. Biomater., Woodhead Publishing, 2014: pp. 212–256. doi:https://doi.org/10.1533/9780857098474.2.212.

[381] G. Massazza, M. Crova, F. Galetto, A. Bistolfi, E. Verné, D. Deledda, S. Ferraris, M. Miola, A. Massè, Antibiotic-Loaded Cement in Orthopedic Surgery: A Review, ISRN Orthop. 2011 (2011) 1–8. doi:10.5402/2011/290851.

[382] M. Sparo, G. Delpech, N. García Allende, Impact on Public Health of the Spread of High-Level Resistance to Gentamicin and Vancomycin in Enterococci, Front. Microbiol. 9 (2018) 3073. doi:10.3389/fmicb.2018.03073.

[383] B. Thornes, P. Murray, D. Bouchier-Hayes, Development of resistant strains of Staphylococcus epidermidis on gentamicin-loaded bone cement in vivo, J. Bone Joint Surg. Br. 84-B (2002) 758–760. doi:10.1302/0301-620X.84B5.0840758.

[384] World Health Organization, Global action plan on antimicrobial resistance., WHO Press. (2015) 1–28. doi:ISBN 978 92 4 150976 3.

[385] C. Gao, S. Huo, X. Li, X. You, Y. Zhang, J. Gao, Characteristics of Calcium Sulfate/Gelatin Composite Biomaterials for Bone Repair, J. Biomater. Sci. Polym. Ed. 18 (2007) 799–824. doi:10.1163/156856207781367710.

[386] F.C. Welch, Effects of Accelerators and Retarders on Calcined Gypsum, J. Am. Ceram. Soc. 6 (1923) 1197–1207. doi:10.1111/j.1151-2916.1923.tb17689.x.

[387] M.M. Winkler, P. Monaghan, J.L. Gilbert, E.P. Lautenschlager, Comparison of Four Techniques for Monitoring the Setting Kinetics of Gypsum, J. Prosthet. Dent. 79 (1998) 532–536. doi:10.1016/S0022-3913(98)70174-X.

[388] B.W. Darvell, Casting Investments, in: B.W.B.T.-M.S. for D. (Tenth E. Darvell (Ed.), Mater. Sci. Dent., 10th ed., Woodhead Publishing, 2018: pp. 465–483. doi:https://doi.org/10.1016/B978-0-08-101035-8.50017-1.

[389] M. V Cabañas, L.M. Rodríguez-Lorenzo, M. Vallet-Regí, Setting Behavior and in Vitro Bioactivity of Hydroxyapatite/Calcium Sulfate Cements, Chem. Mater. 14 (2002) 3550–3555. doi:10.1021/cm021121w.

[390] ASTM C266-15, American Standard Test Method for Time of Setting of Hydraulic-Cement Paste by Gillmore Needles, ASTM International, West Conshohocken, 2015.

[391] E.A.B. Hughes, L.M. Grover, Characterisation of a Novel Poly (ether ether ketone)/Calcium Sulphate Composite for Bone Augmentation, Biomater. Res. 21 (2017) 1–11. doi:10.1186/s40824-017-0093-7.

[392] I.S. Sirota, S. V Dorozhkin, M. V Kruchinina, I. V Melikhov, Phase Transformation and Dehydration of Calcium Sulphate Dihydrate in Solution Studied by SEM, Scanning. 14 (1992) 269–275. doi:10.1002/sca.4950140505.

[393] E.R. Ravenhill, P.M. Kirkman, P.R. Unwin, Microscopic Studies of Calcium Sulfate

Crystallization and Transformation at Aqueous–Organic Interfaces, Cryst. Growth Des. 16 (2016) 5887–5895. doi:10.1021/acs.cgd.6b00941.

[394] N. Prieto-Taboada, O. Gómez-Laserna, I. Martínez-Arkarazo, M.Á. Olazabal, J.M. Madariaga, Raman Spectra of the Different Phases in the CaSO4–H2O System, Anal. Chem. 86 (2014) 10131–10137. doi:10.1021/ac501932f.

[395] Y. Liu, Raman, Mid-IR, and NIR Spectroscopic Study of Calcium Sulfates and Mapping Gypsum Abundances in Columbus Crater, Mars, Planet. Space Sci. 163 (2018) 35–41. doi:https://doi.org/10.1016/j.pss.2018.04.010.

[396] R.W. Welker, Size Analysis and Identification of Particles, in: R. Kohli, K.L.B.T.-D. in S.C. and C. Mittal (Eds.), Dev. Surf. Contam. Clean., William Andrew Publishing, Oxford, 2012: pp. 179–213. doi:https://doi.org/10.1016/B978-1-4377-7883-0.00004-3.

[397] R.R. Jones, D.C. Hooper, L. Zhang, D. Wolverson, V.K. Valev, Raman Techniques: Fundamentals and Frontiers, Nanoscale Res. Lett. 14 (2019) 231. doi:10.1186/s11671-019-3039-2.

[398] D. Torréns-Martín, L. Fernández-Carrasco, S. Martínez-Ramírez, J. Ibáñez, L. Artús, T. Matschei, Raman Spectroscopy of Anhydrous and Hydrated Calcium Aluminates and Sulfoaluminates, J. Am. Ceram. Soc. 96 (2013) 3589–3595. doi:10.1111/jace.12535.

[399] A.K. Chatterjee, X-Ray Diffraction, in: V.S. Ramachandran, J.J.B.T.-H. of A.T. in C.S. and T. Beaudoin (Eds.), Handb. Anal. Tech. Concr. Sci. Technol., William Andrew Publishing, Norwich, NY, 2001: pp. 275–332. doi:https://doi.org/10.1016/B978-081551437-4.50011-4.

[400] J.P. Patel, P.H. Parsania, Characterization, Testing, and Reinforcing Materials of Biodegradable Composites, in: N.G.B.T.-B. and B.P.C. Shimpi (Ed.), Biodegrad.

Biocompatible Polym. Compos., Woodhead Publishing, 2018: pp. 55–79. doi:https://doi.org/10.1016/B978-0-08-100970-3.00003-1.

[401] A. Eremin, A. Pustovgar, S. Pashkevich, I. Ivanova, A. Golotina, Determination of Calcium Sulfate Hemihydrate Modification by X-ray Diffraction Analysis, Procedia Eng. 165 (2016) 1343–1347. doi:https://doi.org/10.1016/j.proeng.2016.11.862.

[402] J. Epp, X-ray Diffraction (XRD) Techniques for Materials Characterization, in: G. Hübschen, I. Altpeter, R. Tschuncky, H.-G.B.T.-M.C.U.N.E. (NDE) M. Herrmann (Eds.), Mater. Charact. Using Nondestruct. Eval. Methods, Woodhead Publishing, 2016: pp. 81–124. doi:https://doi.org/10.1016/B978-0-08-100040-3.00004-3.

[403] I. Koh, A. López, B. Helgason, S.J. Ferguson, The Compressive Modulus and Strength of Saturated Calcium Sulphate Dihydrate Cements: Implications for Testing Standards, J. Mech. Behav. Biomed. Mater. 34 (2014) 187–198. doi:https://doi.org/10.1016/j.jmbbm.2014.01.018.

[404] M. Asadi-Eydivand, M. Solati-Hashjin, S.S. Shafiei, S. Mohammadi, M. Hafezi, N.A. Abu Osman, Structure, Properties, and In Vitro Behavior of Heat-Treated Calcium Sulfate Scaffolds Fabricated by 3D Printing, PLoS One. 11 (2016) e0151216–e0151216. doi:10.1371/journal.pone.0151216.

[405] M. Hafizal Hamidon, M.T.H. Sultan, A. Hamdan Ariffin, Investigation of Mechanical Testing on Hybrid Composite Materials, in: M. Jawaid, M. Thariq, N.B.T.-F.A. in B. Saba Fibre-Reinforced Composites and Hybrid Composites (Eds.), Fail. Anal. Biocomposites, Fibre-Reinforced Compos. Hybrid Compos., Woodhead Publishing, 2019: pp. 133–156. doi:https://doi.org/10.1016/B978-0-08-102293-1.00007-3.

[406] K. Dyamenahalli, A. Famili, R. Shandas, Characterization of Shape-Memory Polymers for Biomedical Applications, in: L.B.T.-S.M.P. for B.A. Yahia (Ed.), Shape Mem. Polym. Biomed. Appl., Woodhead Publishing, 2015: pp. 35–63.

doi:https://doi.org/10.1016/B978-0-85709-698-2.00003-9.

[407] N. Saba, M. Jawaid, M.T.H. Sultan, An Overview of Mechanical and Physical Testing of Composite Materials, in: M. Jawaid, M. Thariq, N.B.T.-M. and P.T. of B. Saba Fibre-Reinforced Composites and Hybrid Composites (Eds.), Mech. Phys. Test. Biocomposites, Fibre-Reinforced Compos. Hybrid Compos., Woodhead Publishing, 2019: pp. 1–12. doi:https://doi.org/10.1016/B978-0-08-102292-4.00001-1.

[408] C.E. Misch, Z. Qu, M.W. Bidez, Mechanical properties of trabecular bone in the human mandible: Implications for dental implant treatment planning and surgical placement, J. Oral Maxillofac. Surg. 57 (1999) 700–706. doi:https://doi.org/10.1016/S0278-2391(99)90437-8.

[409] K. Birnbaum, R. Sindelar, J.R. Gärtner, D.C. Wirtz, Material properties of trabecular bone structures, Surg. Radiol. Anat. 23 (2002) 399–407. doi:10.1007/s00276-001-0399-x.

[410] K.L. Winwood, P. Zioupos, J.D. Currey, J.R. Cotton, M. Taylor, The importance of the elastic and plastic components of strain in tensile and compressive fatigue of human cortical bone in relation to orthopaedic biomechanics, J. Musculoskelet. Neuronal Interact. 6 (2006) 134–141.

[411] E. Hearn, Simple Stress and Strain, in: E. Hearn (Ed.), Mech. Mater. 1, 3rd ed., Butterworth-Heinemann, Oxford, 1997: pp. 1–26. doi:https://doi.org/10.1016/B978-075063265-2/50002-5.

[412] M. Unal, O. Akkus, Supplementary Figures: Raman spectral classification of mineral- and collagen-bound water's associations to elastic and post-yield mechanical properties of cortical bone, (2015) 1–4.

[413] J. Conly, B. Johnston, Where are all the new antibiotics? The new antibiotic paradox, Can. J. Infect. Dis. Med. Microbiol. = J. Can. Des Mal. Infect. La Microbiol. Medicale.

16 (2005) 159–160. doi:10.1155/2005/892058.

[414] Z. Kmietowicz, Few novel antibiotics in the pipeline, WHO warns, BMJ. 358 (2017) j4339. doi:10.1136/bmj.j4339.

[415] J.W. White, L.W. Doner, Honey composition and properties. In Beekeeping in the United States, Sci. Educ. Adm. East. Reg. Res. Center, Philadelphia, Pennsylvania. (1980) 82–92.

[416] P.H.S. Kwakman, A.A. Te Velde, L. de Boer, C.M.J.E. Vandenbroucke-Grauls, S.A.J. Zaat, Two major medicinal honeys have different mechanisms of bactericidal activity, PLoS One. 6 (2011) e17709–e17709. doi:10.1371/journal.pone.0017709.

[417] S.B. Almasaudi, A.A.M. Al-Nahari, E.S.M. Abd El-Ghany, E. Barbour, S.M. Al Muhayawi, S. Al-Jaouni, E. Azhar, M. Qari, Y.A. Qari, S. Harakeh, Antimicrobial Effect of Different Types of Honey on Staphylococcus Aureus, Saudi J. Biol. Sci. 24 (2017) 1255–1261. doi:https://doi.org/10.1016/j.sjbs.2016.08.007.

[418] M.S. Dryden, J. Cooke, R.J. Salib, R.E. Holding, T. Biggs, A.A. Salamat, R.N. Allan, R.S. Newby, F. Halstead, B. Oppenheim, T. Hall, S.C. Cox, L.M. Grover, Z. Al-hindi, L. Novak-Frazer, M.D. Richardson, Reactive oxygen: A novel antimicrobial mechanism for targeting biofilm-associated infection, J. Glob. Antimicrob. Resist. 8 (2017) 186–191. doi:10.1016/j.jgar.2016.12.006.

[419] D.J. Candy, Glucose Oxidase and Other Enzymes of Hydrogen Peroxide Metabolism from Cuticle of Schistocerca Americana Gregaria, Insect Biochem. 9 (1979) 661–665. doi:https://doi.org/10.1016/0020-1790(79)90106-9.

[420] J. Duley, R.S. Holmes, A Spectrophotometric Procedure for Determining the Activity of Various Rat Tissue Oxidases, Anal. Biochem. 69 (1975) 164–169. doi:https://doi.org/10.1016/0003-2697(75)90577-1.

[421] V. Mishin, J.P. Gray, D.E. Heck, D.L. Laskin, J.D. Laskin, Application of the Amplex

Red/Horseradish Peroxidase Assay to Measure Hydrogen Peroxide Generation by Recombinant Microsomal Enzymes, Free Radic. Biol. Med. 48 (2010) 1485–1491. doi:10.1016/j.freeradbiomed.2010.02.030.

[422] R.K. Delong, Q. Zhou, Hexokinase and G6PDH Catalyzed Reactions of Glucose Measurement, in: R.K. Delong, Q.B.T.-I.E. on B. and their I. Zhou (Eds.), Introd. Exp. Biomol. Their Interact., Academic Press, Boston, 2015: pp. 45–57. doi:https://doi.org/10.1016/B978-0-12-800969-7.00005-0.

[423] J.I. Peterson, D.S. Young, Evaluation of the Hexokinase/Glucose-6-Phosphate Dehydrogenase Method of Determination of Glucose in Urine, Anal. Biochem. 23 (1968) 301–316. doi:https://doi.org/10.1016/0003-2697(68)90361-8.

[424] J.L. Sepulveda, Challenges in Routine Clinical Chemistry Testing Analysis of Small Molecules, in: A. Dasgupta, J.L.B.T.-A.R. in the C.L. (Second E. Sepulveda (Eds.), Accurate Results Clin. Lab., 2nd ed., Elsevier, 2019: pp. 101–140. doi:https://doi.org/10.1016/B978-0-12-813776-5.00009-1.

[425] S.A. El Sohaimy, S.H.D. Masry, M.G. Shehata, Physicochemical Characteristics of Honey from Different Origins, Ann. Agric. Sci. 60 (2015) 279–287. doi:https://doi.org/10.1016/j.aoas.2015.10.015.

[426] M. Oroian, S. Paduret, S. Amariei, G. Gutt, Chemical Composition and Temperature Influence on Honey Texture Properties, J. Food Sci. Technol. 53 (2016) 431–440. doi:10.1007/s13197-015-1958-1.

[427] J.M.B. de Sousa, E.L. de Souza, G. Marques, M. de T. Benassi, B. Gullón, M.M. Pintado, M. Magnani, Sugar Profile, Physicochemical and Sensory Aspects of Monofloral Honeys Produced by Different Stingless Bee Species in Brazilian Semi-arid Region, LWT - Food Sci. Technol. 65 (2016) 645–651. doi:https://doi.org/10.1016/j.lwt.2015.08.058.

[428] A.T.M.M. Rahman, D.H. Kim, H.D. Jang, J.H. Yang, S.J. Lee, Preliminary Study on Biosensor-Type Time-Temperature Integrator for Intelligent Food Packaging, Sensors. 18 (2018). doi:10.3390/s18061949.

[429] H. Bright, G. Quentin, The Oxidation of L-Deuterated Glucose by Glucose Oxidase, J. Biol. Chem. 242 (1967) 994–1003.

[430] M.K. Weibel, H.J. Bright, The Glucose Oxidase Mechanism: Interpretation of the pH Dependance, J. Biol. Chem. 246 (1971) 2734–2744. http://www.jbc.org/content/246/9/2734.abstract.

[431] M.-H. Schmid-Wendtner, H.C. Korting, The pH of the Skin Surface and Its Impact on the Barrier Function, Skin Pharmacol. Physiol. 19 (2006) 296–302. doi:10.1159/000094670.

[432] B.M. Delavary, W.M. van der Veer, M. van Egmond, F.B. Niessen, R.H.J. Beelen, Macrophages in skin injury and repair, Immunobiology. 216 (2011) 753–762. doi:https://doi.org/10.1016/j.imbio.2011.01.001.

[433] Q.H. Gibson, B.E.P. Swoboda, V. Massey, Kinetics of Action of Glucose, J. Biol. Chem. 239 (1964) 3927–3934.

[434] D.W. Ball, The Chemical Composition of Honey, J. Chem. Educ. 84 (2007) 1643. doi:10.1021/ed084p1643.

[435] P.B. Olaitan, O.E. Adeleke, I.O. Ola, Honey: A Reservoir for Microorganisms and an Inhibitory Agent for Microbes, Afr. Health Sci. 7 (2007) 159–165. doi:10.5555/afhs.2007.7.3.159.

[436] M.A. Fischbach, C.T. Walsh, Antibiotics For Emerging Pathogens Michael, Science (80-.). 325 (2009) 1089–1093. doi:10.1126/science.1176667.Antibiotics.

[437] F.C. Fang, Antimicrobial Actions of Reactive Oxygen Species, MBio. 2 (2011) e00141-11. doi:10.1128/mBio.00141-11.

[438] D. McClements, Food Emulsions: Principles, Practices, and Techniques, Third Edit, CRC Press, 2015.

[439] P. Posocco, A. Perazzo, V. Preziosi, E. Laurini, S. Pricl, S. Guido, Advances Interfacial tension of oil / water emulsions with mixed non-ionic surfactants : comparison between experiments and molecular simulations †, RSC Adv. 6 (2016) 4723–4729. doi:10.1039/C5RA24262B.

[440] T.M. Silva, N.N.P. Cerize, A.M. Oliveira, The Effect of High Shear Homogenization on Physical Stability of Emulsions, Int. J. Chem. 8 (2016) 52. doi:10.5539/ijc.v8n4p52.

[441] Z. Berk, Mixing, in: Z.B.T.-F.P.E. and T. (Third E. Berk (Ed.), Food Process Eng. Technol., 3rd ed., Academic Press, 2018: pp. 193–217. doi:https://doi.org/10.1016/B978-0-12-812018-7.00007-5.

[442] Y. Qin, Antimicrobial Textile Dressings in Managing Wound Infection, in: S.B.T.-A.T. for W.C. Rajendran (Ed.), Adv. Text. Wound Care, Woodhead Publishing, 2009: pp. 179–197. doi:https://doi.org/10.1533/9781845696306.1.179.

[443] M.-S. Kwak, H.-J. Ahn, K.-W. Song, Rheological Investigation of Body Cream and Body Lotion in Actual Application Conditions, Korea-Australia Rheol. J. 27 (2015) 241–251. doi:10.1007/s13367-015-0024-x.

[444] T.F. Tadros, Fundamental Principles of Emulsion Rheology and Their Applications, Colloids Surfaces A Physicochem. Eng. Asp. 91 (1994) 39–55. doi:https://doi.org/10.1016/0927-7757(93)02709-N.

[445] M.C. Adeyeye, A.C. Jain, M.K.M. Ghorab, W.J. Reilly, Viscoelastic Evaluation of Topical Creams Containing Microcrystalline Cellulose/Sodium Carboxymethyl Cellulose as a Stabilizer, AAPS PharmSciTech. 3 (2002) 16–25. doi:10.1208/pt030208.

[446] C.W. Lantman, W.J. MacKnight, R.D. Lundberg, Ionomers, in: G. Allen, J.C.B.T.-C.P.S. and S. Bevington (Eds.), Compr. Polym. Sci. Suppl., Pergamon, Amsterdam,

1989: pp. 755–773. doi:https://doi.org/10.1016/B978-0-08-096701-1.00062-8.

[447] H. Ji, H.M. Lim, Y.W. Chang, H. Lee, Comparison of the viscosity of ceramic slurries using a rotational rheometerand a vibrational viscometer, J. Korean Ceram. Soc. 49 (2012) 542–548. doi:10.4191/kcers.2012.49.6.542.

[448] M.A. Hubbe, P. Tayeb, M. Joyce, P. Tyagi, M. Kehoe, K. Dimic-Misic, L. Pal, Rheology of Nanocellulose-rich Aqueous Suspensions: A Review, Bioresour. Vol 12, No 4. (2017). http://ojs.cnr.ncsu.edu/index.php/BioRes/article/view/BioRes_12_4_9556_Hubbe_Rheology_Nanocellulose_Aqueous_Suspension.

[449] W. Stringer, R. Bryant, Dose uniformity of topical corticosteroid preparations : difluprednate ophthalmic emulsion 0 . 05 % versus branded and generic prednisolone acetate ophthalmic suspension 1 %, J. Clin. Ophthalmol. 4 (2010) 1119–1124. doi:10.2147/OPTH.S12441.

[450] B.P. Binks, S.O. Lumsdon, Pickering Emulsions Stabilized by Monodisperse Latex Particles: Effects of Particle Size, Langmuir. 17 (2001) 4540–4547. doi:10.1021/la0103822.

[451] B.P. Binks, S.O. Lumsdon, Catastrophic Phase Inversion of Water-in-Oil Emulsions Stabilized by Hydrophobic Silica, Langmuir. 16 (2000) 2539–2547. doi:10.1021/la991081j.

[452] C.D. Robinson, Some Factors Influencing Sedimentation, Ind. Eng. Chem. 18 (1926) 869–871. doi:10.1021/ie50200a036.

[453] G.J. Kynch, A theory of sedimentation, Trans. Faraday Soc. 48 (1952) 166–176. doi:10.1039/TF9524800166.

[454] H.A. Barnes, Thixotropy—a review, J. Nonnewton. Fluid Mech. 70 (1997) 1–33. doi:https://doi.org/10.1016/S0377-0257(97)00004-9.

[455] J. Mewis, N.J. Wagner, Thixotropy, Adv. Colloid Interface Sci. 147–148 (2009) 214–227. doi:https://doi.org/10.1016/j.cis.2008.09.005.

[456] C. Acquarone, P. Buera, B. Elizalde, Pattern of pH and electrical conductivity upon honey dilution as a complementary tool for discriminating geographical origin of honeys, Food Chem. 101 (2007) 695–703. doi:10.1016/j.foodchem.2006.01.058.

[457] B.C. Tatar, G. Sumnu, S. Sahin, Rheology of Emulsions, Adv. Food Rheol. Its Appl. 151 (2016) 437–457. doi:10.1016/B978-0-08-100431-9.00017-6.

[458] L.M. Bang, C. Buntting, P. Molan, The Effect of Dilution on the Rate of Hydrogen Peroxide Production in Honey and Its Implications for Wound Healing, J. Altern. Complement. Med. 9 (2003) 267–273. doi:10.1089/10755530360623383.

[459] M.L. Bruschi, ed., Modification of drug release, in: Strateg. to Modify Drug Release from Pharm. Syst., Woodhead Publishing, 2015: pp. 15–28. doi:10.1016/b978-0-08-100092-2.00002-3.

[460] F. Halstead, B. Oppenheim, M. Dryden, The in vitro antibacterial activity of engineered honey (Surgihoney™) against important biofilm-forming burn wound pathogens, Fed. Infect. Soc. Conf. Poster Present. 22 (2014) 19606.

[461] J. Peng, W. Dong, L. Li, J. Xu, D. Jin, X. Xia, Y. Liu, Effect of High-Pressure Homogenization Preparation on Mean Globule Size and Large-Diameter Tail of Oil-in-Water Injectable Emulsions, J. Food Drug Anal. 23 (2015) 828–835. doi:https://doi.org/10.1016/j.jfda.2015.04.004.

[462] N. Querol, C. Barreneche, L.F. Cabeza, Storage Stability of Bimodal Emulsions vs. Monomodal Emulsions, Appl. Sci. 7 (2017). doi:10.3390/app7121267.

[463] P. Ciullo, M. Andersson, Xanthan gum, a clearly better stabilizer, Vanderbilt SOFW J. (2015).

[464] S.-Q. Wang, S. Ravindranath, Y. Wang, P. Boukany, New Theoretical Considerations

in Polymer Rheology: Elastic Breakdown of Chain Entanglement Network, J. Chem. Phys. 127 (2007) 64903. doi:10.1063/1.2753156.

[465] P. Santos, M. Carignano, O. Campanella, Effect of Shear History on Rheology of Time-Dependent Colloidal Silica Gels, Gels. 3 (2017) 45. doi:10.3390/gels3040045.

[466] F. Franks, Freeze-drying of bioproducts: putting principles into practice, Eur. J. Pharm. Biopharm. 45 (1998) 221–229. doi:https://doi.org/10.1016/S0939-6411(98)00004-6.

[467] S. Corveleyn, S. De Smedt, J.P. Remon, Moisture absorption and desorption of different rubber lyophilisation closures, Int. J. Pharm. 159 (1997) 57–65. doi:https://doi.org/10.1016/S0378-5173(97)00263-9.

[468] A. Bhambhani, B. Medi, Selection of Containers/Closures for Use in Lyophilization Applications: Possibilities and Limitations, Am. Pharm. Rev. 13 (2010).

[469] L.J.J. Hansen, R. Daoussi, C. Vervaet, J.-P. Remon, T.R.M. De Beer, Freeze-Drying of Live Virus Vaccines: A Review, Vaccine. 33 (2015) 5507–5519. doi:https://doi.org/10.1016/j.vaccine.2015.08.085.

[470] F.S. de Almeida, A.C.P. Rocha, S.M. Lima, L.H.C. Andrade, Spectral refractive index technique for monitoring the beer mashing process, Appl. Opt. 57 (2018) 4672–4676. doi:10.1364/AO.57.004672.

[471] Z.H. Loh, A.K. Samanta, P.W. Sia Heng, Overview of Milling Techniques for Improving the Solubility of Poorly Water-Soluble Drugs, Asian J. Pharm. Sci. 10 (2015) 255–274. doi:https://doi.org/10.1016/j.ajps.2014.12.006.

[472] X. Fu, D. Huck, L. Makein, B. Armstrong, U. Willen, T. Freeman, Effect of particle shape and size on flow properties of lactose powders, Particuology. 10 (2012) 203–208. doi:10.1016/j.partic.2011.11.003.

[473] M. Simek, V. Grünwaldová, B. Kratochvíl, Comparison of Compression and Material Properties of Differently Shaped and Sized Paracetamols, Powder Part. 2017 (2016).

doi:10.14356/kona.2017003.

[474] J. Lee, H.J. Herrmann, Angle of repose and angle of marginal stability: molecular dynamics of granular particles, J. Phys. A. Math. Gen. 26 (1993) 373–383. doi:10.1088/0305-4470/26/2/021.

[475] Y.C. Zhou, B.D. Wright, R.Y. Yang, B.H. Xu, A.B. Yu, Rolling friction in the dynamic simulation of sandpile formation, Phys. A Stat. Mech. Its Appl. 269 (1999) 536–553. doi:https://doi.org/10.1016/S0378-4371(99)00183-1.

[476] J.T. Carstensen, P.-C. Chan, Relation between particle size and repose angles of powders, Powder Technol. 15 (1976) 129–131. doi:https://doi.org/10.1016/0032-5910(76)80037-X.

[477] Y.C. Zhou, B.H. Xu, A.B. Yu, P. Zulli, An experimental and numerical study of the angle of repose of coarse spheres, Powder Technol. 125 (2002) 45–54. doi:https://doi.org/10.1016/S0032-5910(01)00520-4.

[478] G.E. Amidon, P.J. Meyer, D.M. Mudie, Particle, Powder, and Compact Characterization, in: Y. Qiu, Y. Chen, G.G.Z. Zhang, L. Yu, R.V.B.T.-D.S.O.D.F. (Second E. Mantri (Eds.), Dev. Solid Oral Dos. Forms, 2nd ed., Academic Press, Boston, 2017: pp. 271–293. doi:https://doi.org/10.1016/B978-0-12-802447-8.00010-8.

[479] K. Vowden, P. Vowden, Wound Dressings: Principles and Practice, Surg. 35 (2017) 489–494. doi:https://doi.org/10.1016/j.mpsur.2017.06.005.

[480] D.G. Armstrong, L.A. Lavery, Negative pressure wound therapy after partial diabetic foot amputation: a multicentre, randomised controlled trial, Lancet. 366 (2005) 1704–1710. doi:https://doi.org/10.1016/S0140-6736(05)67695-7.

[481] C.K. Field, M.D. Kerstein, Overview of wound healing in a moist environment, Am. J. Surg. 167 (1994) S2–S6. doi:https://doi.org/10.1016/0002-9610(94)90002-7.

[482] M. Pawlaczyk, M. Lelonkiewicz, M. Wieczorowski, Age-dependent biomechanical

properties of the skin, Postep. Dermatologii i Alergol. 30 (2013) 302–306. doi:10.5114/pdia.2013.38359.

[483] B. Holt, A. Tripathi, J. Morgan, Viscoelastic response of human skin to low magnitude physiologically relevant shear, J. Biomech. 41 (2008) 2689–2695. doi:10.1016/j.jbiomech.2008.06.008.

[484] I. Ogawa, H. Yamano, K. Miyagawa, Rate of swelling of sodium polyacrylate, J. Appl. Polym. Sci. 47 (1993) 217–222. doi:10.1002/app.1993.070470204.

[485] T. Abdelrahman, H. Newton, Wound dressings: principles and practice, Surg. 29 (2011) 491–495. doi:https://doi.org/10.1016/j.mpsur.2011.06.007.

[486] J.M. Harris, C. Reyes, G.P. Lopez, Common causes of Glucose Oxidase Instability In Vivo Biosensing: A Brief Review, J. Diabetes Sci. Technol. 7 (2013) 1030–1038. doi:10.1177/193229681300700428.

[487] M. Bucekova, L. Jardekova, V. Juricova, V. Bugarova, G. Di Marco, A. Gismondi, D. Leonardi, J. Farkasovska, J. Godocikova, M. Laho, J. Klaudiny, V. Majtan, A. Canini, J. Majtan, Antibacterial Activity of Different Blossom Honeys: New Findings, Molecules. 24 (2019). doi:10.3390/molecules24081573.

[488] N.A. Albaridi, Antibacterial Potency of Honey, Int. J. Microbiol. 2019 (2019) 2464507. doi:10.1155/2019/2464507.

[489] K.C. Gulla, M.D. Gouda, M.S. Thakur, N.G. Karanth, Enhancement of Stability of Immobilized Glucose Oxidase by Modification of Free Thiols Generated by Reducing Disulfide Bonds and Using Additives, Biosens. Bioelectron. 19 (2004) 621–625. doi:https://doi.org/10.1016/S0956-5663(03)00258-6.

[490] M. Altikatoglu, Y. Basaran-Elalmis, Protective Effect of Dextrans on Glucose Oxidase Denaturation and Inactivation, Artif. Cells, Blood Substitutes, Biotechnol. 40 (2012) 261–265. doi:10.3109/10731199.2011.644292.

[491] M.K. Dubey, A. Zehra, M. Aamir, M. Meena, L. Ahirwal, S. Singh, S. Shukla, R.S. Upadhyay, R. Bueno-Mari, V.K. Bajpai, Improvement Strategies, Cost Effective Production, and Potential Applications of Fungal Glucose Oxidase (GOD): Current Updates , Front. Microbiol. . 8 (2017) 1032. https://www.frontiersin.org/article/10.3389/fmicb.2017.01032.

[492] G. Puggioni, G. Calia, P. Arrigo, A. Bacciu, G. Bazzu, R. Migheli, S. Fancello, P.A. Serra, G. Rocchitta, Low-Temperature Storage Improves the Over-Time Stability of Implantable Glucose and Lactate Biosensors, Sensors (Switzerland). 19 (2019) 1–14. doi:10.3390/s19020422.

[493] M. Christwardana, D. Frattini, Electrochemical Study of Enzymatic Glucose Sensors Biocatalyst: Thermal Degradation After Long-Term Storage, Chemosensors. 6 (2018). doi:10.3390/chemosensors6040053.

[494] G. Ozyilmaz, S.S. Tukel, O. Alptekin, Activity and Storage Stability of Immobilized Glucose Oxidase onto Magnesium Silicate, J. Mol. Catal. B Enzym. 35 (2005) 154–160. doi:https://doi.org/10.1016/j.molcatb.2005.07.001.

[495] D. Trau, R. Renneberg, Encapsulation of Glucose Oxidase Microparticles within a Nanoscale Layer-by-Layer Film: Immobilization and Biosensor Applications, Biosens. Bioelectron. 18 (2003) 1491–1499. doi:https://doi.org/10.1016/S0956-5663(03)00119-2.

[496] H. Zhu, R. Srivastava, J.Q. Brown, M.J. McShane, Combined Physical and Chemical Immobilization of Glucose Oxidase in Alginate Microspheres Improves Stability of Encapsulation and Activity, Bioconjug. Chem. 16 (2005) 1451–1458. doi:10.1021/bc050171z.

[497] A.H. Holmes, L.S.P. Moore, A. Sundsfjord, M. Steinbakk, S. Regmi, A. Karkey, P.J. Guerin, L.J. V Piddock, Understanding the mechanisms and drivers of antimicrobial

resistance, Lancet. 387 (2016) 176–187. doi:10.1016/S0140-6736(15)00473-0.

[498] M.B. Dreifke, A.A. Jayasuriya, A.C. Jayasuriya, Current wound healing procedures and potential care, Mater. Sci. Eng. C. 48 (2015) 651–662. doi:10.1016/j.msec.2014.12.068.

[499] T. Suehiro, T. Hirashita, S. Araki, T. Matsumata, S. Tsutsumi, E. Mochiki, H. Kato, T. Asao, H. Kuwano, Prolonged antibiotic prophylaxis longer than 24 hours does not decrease surgical site infection after elective gastric and colorectal surgery, Hepatogastroenterology. 55 (2008) 1636–1639. http://europepmc.org/abstract/MED/19102358.

[500] L.D.T. Topoleski, P. Ducheyne, J.M. Cukler, A fractographic analysis of in vivo poly(methyl methacrylate) bone cement failure mechanisms, J. Biomed. Mater. Res. 24 (1990) 135–154. doi:10.1002/jbm.820240202.

[501] M. Takechi, Y. Miyamoto, K. Ishikawa, M. Nagayama, M. Kon, K. Asaoka, K. Suzuki, Effects of added antibiotics on the basic properties of anti-washout-type fast-setting calcium phosphate cement, J. Biomed. Mater. Res. 39 (1998) 308–316. doi:10.1002/(SICI)1097-4636(199802)39:2<308::AID-JBM19>3.0.CO;2-8.

[502] R. Kumar, B. Bhattacharjee, Porosity, pore size distribution and in situ strength of concrete, Cem. Concr. Res. 33 (2003) 155–164. doi:https://doi.org/10.1016/S0008-8846(02)00942-0.

[503] H. Zhao, Q. Xiao, D. Huang, S. Zhang, Influence of pore structure on compressive strength of cement mortar, ScientificWorldJournal. 2014 (2014) 247058. doi:10.1155/2014/247058.

[504] J. Cooke, M. Dryden, T. Patton, J. Brennan, J. Barrett, The Antimicrobial Activity of Prototype Modified Honeys That Generate Reactive Oxygen Species (ROS) Hydrogen Peroxide, BMC Res. Notes. 8 (2015) 20. doi:10.1186/s13104-014-0960-4.

[505] T. Ghassemi, A. Shahroodi, M.H. Ebrahimzadeh, A. Mousavian, J. Movaffagh, A.

Moradi, Current Concepts in Scaffolding for Bone Tissue Engineering, Arch. Bone Jt. Surg. 6 (2018) 90–99.

[506] C.-C. Liang, A.Y. Park, J.-L. Guan, In vitro scratch assay: a convenient and inexpensive method for analysis of cell migration in vitro., Nat. Protoc. 2 (2007) 329–33. doi:10.1038/nprot.2007.30.

[507] N. Mukaida, Pathophysiological roles of interleukin-8/CXCL8 in pulmonary diseases, Am. J. Physiol. Cell. Mol. Physiol. 284 (2003) L566–L577. doi:10.1152/ajplung.00233.2002.

[508] D.J.J. Waugh, C. Wilson, The interleukin-8 pathway in cancer, Clin. Cancer Res. 14 (2008) 6735–6741. doi:10.1158/1078-0432.CCR-07-4843.

[509] P. Demoly, P. Hagedoorn, A.H. de Boer, H.W. Frijlink, The Clinical Relevance of Dry Powder Inhaler Performance for Drug Delivery, Respir. Med. 108 (2014) 1195–1203. doi:https://doi.org/10.1016/j.rmed.2014.05.009.

[510] K.T. Ung, N. Rao, J.G. Weers, A.R. Clark, H.-K. Chan, In Vitro Assessment of Dose Delivery Performance of Dry Powders for Inhalation, Aerosol Sci. Technol. 48 (2014) 1099–1110. doi:10.1080/02786826.2014.962685.

[511] L.M. Grover, M.P. Hofmann, U. Gbureck, B. Kumarasami, J.E. Barralet, Frozen delivery of brushite calcium phosphate cements, Acta Biomater. 4 (2008) 1916–1923. doi:https://doi.org/10.1016/j.actbio.2008.06.003.

Appendix One

Materials Science & Engineering C 103 (2019) 109735

Contents lists available at ScienceDirect

Materials Science & Engineering C

journal homepage: www.elsevier.com/locate/msec

Antimicrobial emulsions: Formulation of a triggered release reactive oxygen delivery system

Thomas J. Hall[a,*], Jessica M.A. Blair[b], Richard J.A. Moakes[a], Edward G. Pelan[a], Liam M. Grover[a], Sophie C. Cox[a]

[a] School of Chemical Engineering, University of Birmingham, Edgbaston, B15 2TT, United Kingdom of Great Britain and Northern Ireland
[b] Institute of Microbiology and Infection, University of Birmingham, Edgbaston, B15 2TT, United Kingdom of Great Britain and Northern Ireland

ARTICLE INFO

Keywords:
Surgihoney
SurgihoneyRO
Honey
Emulsion
Inversion
ROS
AMR
Antimicrobial
Formulation
CPI

ABSTRACT

The enzyme glucose oxidase mediates the oxidation of glucose to produce reactive oxygen species (ROS), such as hydrogen peroxide. This reaction and its products are key to providing honey with its antimicrobial properties. Currently, honey is an adherent, highly viscous product that produces ROS by means of a water-initiated reaction. These properties reduce clinical usability and present a formulation problem for long term stability. This study aims to engineer a water-in-oil emulsion containing an engineered honey (SurgihoneyRO™) that is easy to administer topically and is controllably activated *in-situ*.

Paraffin oil continuous emulsions formulated using the emulsifier polyglycerol polyricinoleate displayed shear-thinning characteristics. Viscosities between 1.4 and 19.3 Pa·s were achieved at a shear rate representative of post-mixing conditions (4.1 s^{-1}) by changing the volume of the dispersed phase (30–60%). Notably, this wide viscosity range will be useful in tailoring future formulations for specific application mechanisms. When exposed to water and shear, these emulsion systems were found to undergo catastrophic phase inversion, evidenced by a change in conductivity from 0 μS in the non-aqueous state, to > 180 μS in the sheared, inverted state. Encouragingly, sheared formulations containing ≥50% SurgihoneyRO™ generated sufficient levels of ROS to inhibit growth of clinically relevant Gram-positive and Gram-negative bacteria.

This study demonstrates an ability to formulate ROS producing emulsions for use as an alternative to current topical antibiotic-based treatments. Promisingly, the ability of this system to release water-sensitive actives in response to shear may be useful for controlled delivery of other therapeutic molecules.

1. Introduction

Bacteria and other resistant pathogens are predicted to kill more people than cancer by 2050, with estimated global deaths in excess of 10 million per year [1,2]. Antimicrobials are key to infection prevention and curative treatments, for example protecting patients exposed to complex wound healing procedures, such as surgery or cancer chemotherapy [3,4]. Therefore, research into novel antimicrobials and systems by which to deliver them is a healthcare priority [5].

With the antibiotic development pipeline running dry, many researchers are continuing to look for inspiration from nature, such as the use of reactive oxygen species (ROS). This includes the use of hydrogen peroxide (H_2O_2) to treat infections. However, due to its reactivity high doses of H_2O_2 are often used (≥3%) to keep the level of ROS above the bactericidal concentration [6]. This can have cytotoxic effects on any surrounding cells [7,8]. To combat this, Zhu et al. concluded that successful delivery of a lower, tailored dose of ROS would be advantageous [9].

The use of ROS to kill bacteria is a defence mechanism found in honey to prevent it from spoiling. Honey has been used for thousands of years for topical wound care applications without the development of resistance [10]. The problem with using natural honey as an antimicrobial is that the effect can differ greatly from batch to batch [11]. This is largely due to the conditions within the beehive, which are

Abbreviations: SHRO, SurgihoneyRO; ROS, reactive oxygen species; AMR, antimicrobial resistance; MRSA, methicillin-resistant *Staphylococcus aureus*; O/W, oil-in-water; W/O, water-in-oil; CPI, critical phase inversion; PGPR, polyglycerol polyricinoleate; LVR, linear viscoelastic region; LB, Luria-Bertani; *S. aureus*, *Staphylococcus aureus*; *E. coli*, *Escherichia coli*; *P. aeruginosa*, *Pseudomonas aeruginosa*

* Corresponding author.
E-mail addresses: txh544@bham.ac.uk (T.J. Hall), j.m.a.blair@bham.ac.uk (J.M.A. Blair), r.j.a.moakes@bham.ac.uk (R.J.A. Moakes), e.pelan@bham.ac.uk (E.G. Pelan), l.m.grover@bham.ac.uk (L.M. Grover), s.c.cox@bham.ac.uk (S.C. Cox).

https://doi.org/10.1016/j.msec.2019.05.020
Received 12 October 2018; Received in revised form 15 March 2019; Accepted 8 May 2019
Available online 09 May 2019
0928-4931/ Crown Copyright © 2019 Published by Elsevier B.V. All rights reserved.

influenced by a variety of environmental factors such as; the weather, accessibility to pollen and humidity [12]. As such, to realise the potential use of honey as an alternative antimicrobial it would be necessary to chemically engineer a product that would deliver a controlled and tailorable amount of ROS over a sustained period.

There are a number of medical grade honeys available for use, including Medihoney manuka honey, Activon manuka honey and engineered SurgihoneyRO™ (SHRO). Promisingly, *in vitro* and *in vivo* studies using SHRO have demonstrated the complete eradication of the infecting bacterial culture [13–17]. This included both Gram positive and negative species as well as drug resistant strains, such as methicillin-resistant *Staphylococcus aureus* (MRSA) and vancomycin-resistant *Enterococcus faecium* [17]. In addition, it has been shown to be effective against fungi and prevented or reduced the seeding of biofilms [14,15]. Furthermore, SHRO has been found to be equally or more efficacious than Medihoney manuka honey and Activon manuka honey as well as two of the most commonly used topical wound care alternatives, iodine and silver [13,16]. Interestingly, in contrast to iodine and silver dressings, SHRO was not shown to elicit cytotoxic effects [13].

SHRO is currently packaged as a raw product in a sachet or tube. This delivery system is clinically non-optimal since it is highly viscous and adherent to surfaces. Therefore, the development of alternative physical formulations, which incorporate SHRO and facilitate an application specific release profile of ROS, is of great interest. When designing such a system it is important to consider the underlying mechanisms of action. In the case of SHRO, the oxidation of glucose to produce ROS is a reaction that requires water (Fig. 1a). SHRO contains 16–20% water but this is bound to sugars and is not free to react [18]. As a consequence, to avoid premature production of ROS before clinical application a non-aqueous vehicle is required. Such a formulation would enable the product to be stored and activated *in-situ*. To improve the ease of handling SHRO, and facilitate controlled release of ROS, this non-aqueous vehicle will require appropriate physical structuring. One such approach may be to create an emulsion that incorporates SHRO into its non-aqueous phase (Fig. 1b). An emulsion can be defined as a dispersion of droplets of one liquid in another, in which it is not soluble or miscible [19].

There are two basic forms of emulsions: (1) oil in water, denoted (O/W) and (2) water in oil (W/O). Emulsions are inherently thermodynamically unstable and systems quickly phase separate after manufacture to reduce the unfavourably high energy states associated with interfacial tension [20]. To improve stability over time, emulsifiers or surfactants have to be used, these lower the tension between the two species allowing the persistence of droplets, which may contain actives, over much longer time scales [21].

Phase inversion is a phenomenon that occurs when the dispersed phase of an emulsion becomes the continuous phase or *vice versa*, during this process surfactants spontaneously change their arrangement [22]. Phase inversion is widely used to formulate emulsions, with many manufacturers using this process in order to create products with increased stability and a small size distribution of droplets within a continuous phase [23]. It can occur due to: the introduction of particular flows (shear induced), changing temperature, alterations in phase volumes (known as catastrophic phase inversion (CPI)), change in pH or the addition of salts [24].

The focus of this study is to formulate an emulsion system that enables easy delivery of ROS producing honey as a novel antimicrobial (Fig. 1). It is hypothesised that by incorporating the SHRO in oil, this will help to protect the agent from premature ROS activation. By optimising the dispersion of SHRO in paraffin oil, shear thinning behaviour could be achieved easing application (Fig. 1). This work aims to use an inversion trigger whereby water and shear are added to the system until the emulsion inversion point is exceeded and CPI occurs. This paper is the first report of an engineered emulsion system to controllably deliver ROS and demonstrates it is capable of eradicating clinically relevant bacteria *in-vitro*.

2. Materials and methods

2.1. Materials

Luria-Bertani (LB) broth, LB broth with agar and analytical grade paraffin oil were supplied by Sigma Aldrich, UK. The other oils used in this study (vegetable, olive and corn) were commercially sourced. Polyglycerol polyricinoleate (PGPR) was provided by Palsgaard, Denmark and SHRO was supplied by Matoke Holdings, UK. All materials were used as delivered and no further purification or modifications were made.

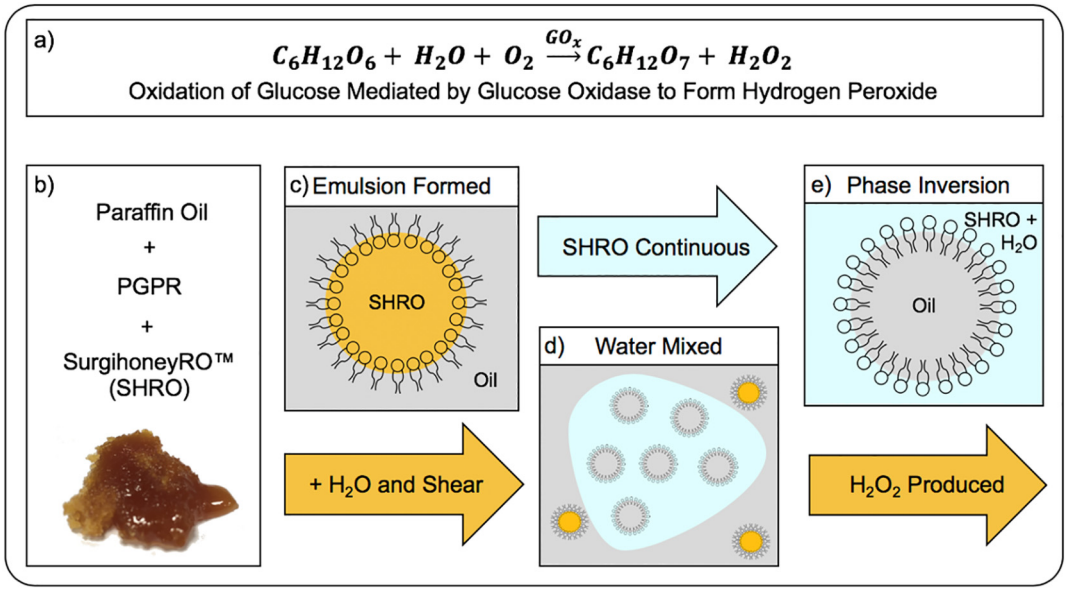

Fig. 1. Schematic highlighting the production of hydrogen peroxide and reactive oxygen species through the aerobic glucose oxidase mediated oxidation reaction of glucose and water (a). The key components of a SurgihoneyRO™ in oil emulsion (b), in which SHRO is the dispersed phase (c). After addition of water and shear (d) phase inversion of the emulsion occurs (e) allowing for the production of hydrogen peroxide and other reactive oxygen species.

2.2. Emulsion formulation

Emulsions were created in a two-step process using a T18 Ultra Turrax® disperser (IKA, UK). The oil phase was combined with PGPR for 1 min at 10,000 rpm. SHRO was then added dropwise, using a 5 mL syringe, to the oil and surfactant mixture. After the SHRO was added, shear was applied at 10,000 rpm until a total time of 10 min had elapsed. The final emulsions were stored in a temperature controlled laboratory set at 21 °C until needed.

Unless otherwise indicated, percentages are denoted as (v/v) and indicate the amount of SHRO present in the formulation. The oil used can be assumed to be paraffin oil with the surfactant volume set at 2% unless otherwise stated.

2.3. Visual characterisation of emulsion stability

Emulsions were formulated according to the method in Section 2.1 and monitored over a 7-day period at 21 °C. At each time point (1, 2, 3 and 7 days) an image was taken of each individual sample. To enable measurement calibration a fixed scale was placed next to the sample during capture. Images were visually assessed to determine if droplet sedimentation or separation of phases occurred. *Image J* software (1.47v National Institutes of Health, USA) was used to calibrate images and obtain a quantitative measurement of separation.

2.4. Rheological characterisation of SHRO in paraffin oil emulsions

An AR-G2 rheometer (TA Instruments, UK) with sandblasted parallel plates (size = 40 mm, gap height = 1 mm) was used to determine the viscoelastic properties of emulsions immediately after manufacture (day 0) and after 7 days of storage at 21 °C. Prior to testing on day 7 the emulsions were shaken for 1 min by hand in order to resuspend the droplets. Viscosity was determined by means of a shear rate sweep from 1.0 to 100.0 s^{-1} conducted over a period of 5 min at 21 °C. From this sweep, a shear rate of 4.1 s^{-1} was used to characterise behaviour prior to storage. This shear rate is representative of a low shear post-mixing state such as that achieved following a shake before use directive [25]. A shear rate of 99.7 s^{-1} was isolated to describe the behaviour under higher shear application such as extrusion from a tube [26].

The linear viscoelastic region (LVR) was identified for all tested emulsions using a strain sweep with frequency set at 1 Hz. This data was used to select a percentage strain value which fell within the LVR. Frequency sweeps were then carried out from 0.1 to 100 Hz at 21 °C and 0.5% strain to obtain storage (G′) and loss (G″) moduli.

It was important to determine the rate of viscosity recovery after simulated application to ensure that the emulsion structure was not altered. Formulations were subjected to 100 s^{-1} for 30 s at 21 °C to mimic extrusion. Shear rate was then reduced to 1.0 s^{-1} and viscosity monitored for 30 s. This process was repeated thrice, and the hysteresis results plotted.

2.5. Size analysis of dispersed SHRO droplets

Laser diffraction measurements were recorded by a Malvern 3000 Mastersizer (Malvern Instruments, UK). Refractive indexes (RI) of 1.487 and 1.473 were used for SHRO and paraffin oil respectively. RI was determined using an ORA-3HA refractometer (Kern-Sohn, Germany) and manufacturer provided values. The software used to calculate size distribution assumed spherical droplets in a uniform media. Size distribution was measured on days 0 and 7 to investigate the occurrence of coalescence. Each emulsion ratio was measured in triplicate and with three readings per experimental run.

2.6. Conductivity measurements

Conductivity was measured using a HI99300 conductivity test meter (Hanna Instruments, UK). Measurements were taken of individual components as well as both prior and post addition of deionised water and shear. Emulsions were diluted with deionised water in a 1:2 ratio and vortexed for 1 min to trigger inversion.

2.7. Hydrogen peroxide release from SHRO emulsions

A fluorescent assay kit (Sigma Aldrich, UK) was used to determine hydrogen peroxide release from SHRO 30, 50 and 60% emulsions. Prior to testing a calibration curve was created using hydrogen peroxide standards 10, 3, 1, 0.3, 0.1, 0.03, 0.01 and 0 μM. A further calibration curve was created using SHRO 2.0, 1.5, 1.0 and 0.5 g/L. This was used to determine the dilution factors used given the concentration limits of the assay. For the assay, 1 mL of each emulsion was diluted with 2 mL of deionised water and vortexed for 10 s. This was then further diluted by adding 0.1 mL to 30 mL of deionised water (1:300) at each time point (1, 3, 6, 12 and 24 h). The manufacturer's instructions were followed, briefly the following standard solutions were made: a master mix containing 50 μL red peroxidase substrate, 200 μL of 20 units/mL peroxidase, 4.75 mL assay buffer, and hydrogen peroxide standards between 0 μM and 10 μM.

50 μL of sample or standard was then added to each well and 50 μL of master mix was added. Wells were mixed by pipetting, protected from light and incubated at room temperature for 30 min. The fluorescence intensity was then measured (λ_{ex} = 540 nm/λ_{em} = 590 nm) using a Tecan Spark plate reader (Tecan Trading AG, Switzerland). Each emulsion was tested in triplicate.

2.8. In-vitro efficacy of SHRO emulsions

LB broth and LB broth with agar was reconstituted with distilled water to concentrations of 20 g/L and 35 g/L respectively, both were sterilised by autoclaving for 20 min at 121 °C and 100 kPa.

Overnight cultures of *Staphylococcus aureus* (*S. aureus* — ATCC 29213), *Escherichia coli* (*E. coli* — MG1655) and *Pseudomonas aeruginosa* (*P. aeruginosa* — NCTC 13437) were prepared by inoculating one colony of each strain into 5 mL of LB broth. The optical density of each overnight culture was then measured at 600 nm using a Spectronic Helios Gamma UV–Vis Spectrophotometer (Thermo Fisher Scientific, UK) and diluted to 0.04.

Agar plates were created from LB broth with agar and inoculated with bacteria. A 10 mm sterile hole borer was then used to create a well in the center of the inoculated agar. 1 mL of each emulsion was diluted with 2 mL of deionised water and vortexed for 1 min in order to trigger the release of ROS. 250 μL of diluted emulsion was then added to the well and incubated at 37 °C for 24 h. Zones of inhibited bacterial growth were then measured, and the bore hole diameter was deducted from the total zone size. Each emulsion formulation and bacterial strain was run in triplicate.

2.9. Statistical analysis

Statistical analysis was performed using GraphPad Prism® 5.0 software. Two-tailed Welch's *t*-tests were used to determine statistical significance. Values of $p < 0.05$ were considered significant. Data is presented as mean ± standard deviation.

3. Results

3.1. Stability of SHRO emulsion

Paraffin oil emulsions containing 30% SHRO and 2% PGPR were found to have a slower sedimentation rate (29.6 ± 8.6%) over 7 days than emulsions formulated with olive (73.9 ± 1.1%), corn (86.0 ± 4.7%) or vegetable oil (78.5 ± 1.1%) (Fig. 2a). With the exception of paraffin oil, the resultant emulsion instabilities were not

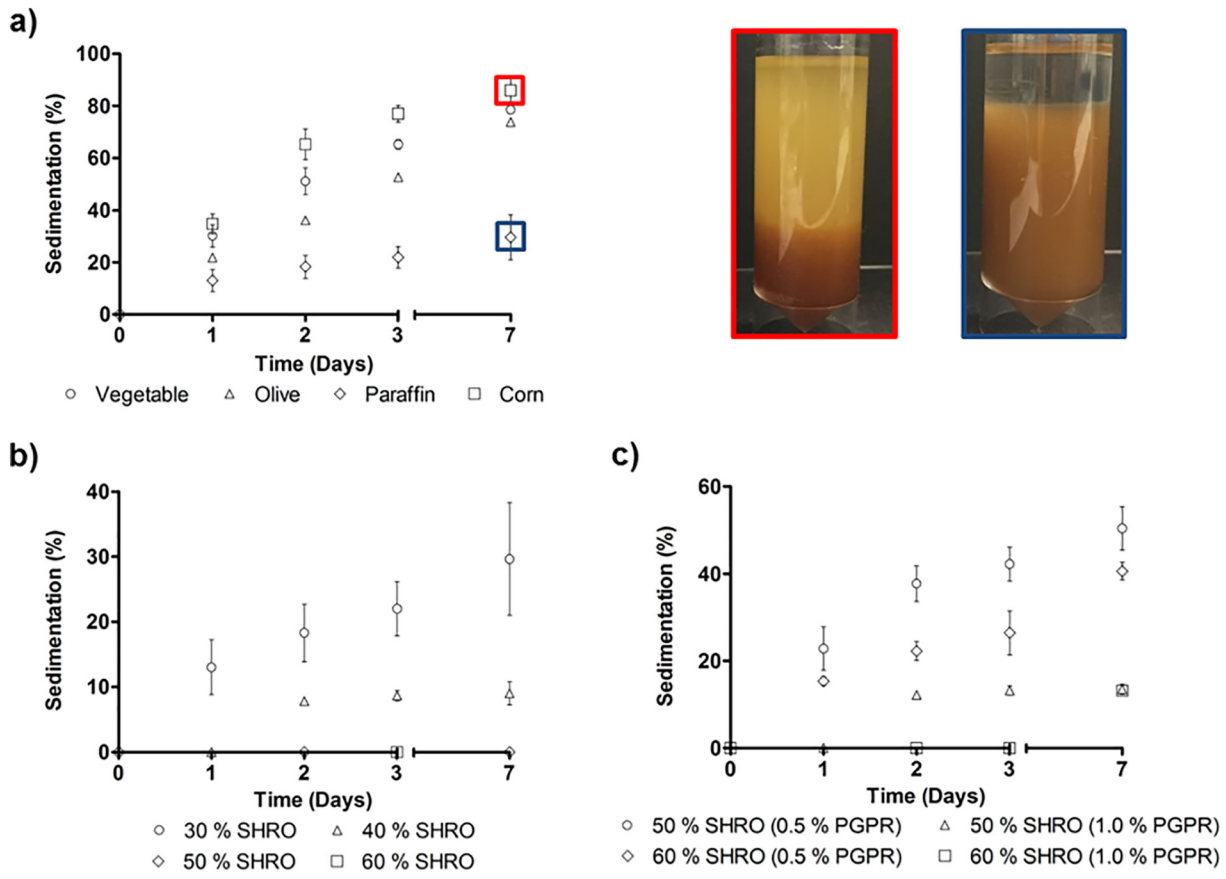

Fig. 2. Rate of droplet sedimentation as a function of the formulation undertaken at room temperature: oil type (a), dispersed phase (SHRO) concentration (b) and emulsifier (PGPR) concentration (c).

reversible by inversion or shaking as phase separation had occurred. Emulsions comprised of paraffin oil maintained the integrity of the SHRO droplets and after initial sedimentation could be re-dispersed by inversion. Coalescence and phase separation did not occur in paraffin oil emulsion systems over the storage periods investigated.

An increase in SHRO concentration for paraffin oil samples resulted in a lower rate of sedimentation. Notably, emulsions containing > 50% SHRO showed no indication of sedimentation over a 7 day period. Emulsions containing 40 and 30% SHRO displayed sedimentation rates of 9.0 ± 1.8 and 29.6 ± 8.6%, respectively over 7 days (Fig. 2b).

Further testing determined that emulsions containing < 2% PGPR sedimented after 7 days. After 24 h sedimentation was observed for both the 60 and 50% SHRO emulsions, which contained 0.5% PGPR with sedimentation rates of 15.3 ± 1.0 and 22.8 ± 5.0%, respectively. Sedimentation progressed and at day 7 was recorded for 60% SHRO emulsions at 40.6 ± 2.0 and 50.4 ± 5.0% for 50% SHRO emulsions (Fig. 2c). With an increase in surfactant to 1%, sedimentation was reduced. After 3 days emulsions containing 60% SHRO still displayed no sedimentation, emulsions that contained 50% SHRO, however sedimented by 3.2 ± 1.1%. After 7 days, 60 and 50% SHRO emulsions containing 1% PGPR showed no significant difference in sedimentation with rates of 13.1 ± 0.3 and 13.5 ± 1.1% respectively (Fig. 2c). For its improved stability 2% PGPR was used for the remainder of the study.

3.2. SHRO emulsion rheology

The ratio of SHRO to paraffin oil within the emulsion significantly alters the overall viscosity (Fig. 3a). An increase in the concentration of SHRO increased viscosity across all shear rates tested (1.0–100 s^{-1}). Apparent viscosities on day 0 and day 7 respectively measured at 19.3 ± 0.2 Pa·s and 13.42 ± 0.2 Pa·s (60%), 9.7 ± 0.3 Pa·s and 6.9 ± 0.5 Pa·s (50%) and 1.4 ± 0.2 Pa·s and 1.8 ± 0.7 Pa·s (30%) at a shear rate of 4.1 s^{-1}. After storage for 7 days at 21 °C there was a 20–35% reduction in viscosity at all tested shear rates between 60 and 50% SHRO emulsions. In contrast, the 30% SHRO emulsion formulation showed no significant difference in viscosity after the 7-day storage period (Fig. 3b).

The apparent viscosity profile of the emulsions differed to that of the control, unprocessed SHRO. At lower shear (4.1 s^{-1}), 60 and 50% SHRO emulsions had a higher viscosity than that of SHRO alone. In contrast, at a higher shear rate (99.7 s^{-1}), it was found that all of the emulsions except 60% SHRO, displayed lower apparent viscosities on day 0 compared to SHRO alone (Fig. 3c).

When SHRO emulsions are rapidly switched from a low (1.0 s^{-1}) to a higher shear (100 s^{-1}) the viscosity reduces but quickly recovers exhibiting shear thinning behaviour (Fig. 3d). The SHRO emulsions did display hysteresis upon application and removal of shear as the recovery viscosity of the formulation is lower than that of the initial measurement (Fig. 3d).

Analysis of the viscoelastic properties of the emulsions determined that higher concentrations of SHRO exhibited higher G′ and G″ values. At 5 Hz, for 60 and 50% SHRO emulsions, the G′ was higher than that of the G″. However, 30% SHRO emulsions exhibited similar G′ and G″ values at 5 Hz. At higher frequencies (30 Hz) G″ exceeded G′ for all formulations. The frequency at which crossover occurred was found increased with increasing SHRO concentration. At day 0 this phenomenon occurred at 63.1 Hz, 50.1 Hz and 1.6 Hz for 60, 50 and 30% SHRO emulsions, respectively and 50.1 Hz, 39.8 Hz and 0.8 Hz on day 7 (Fig. 3f).

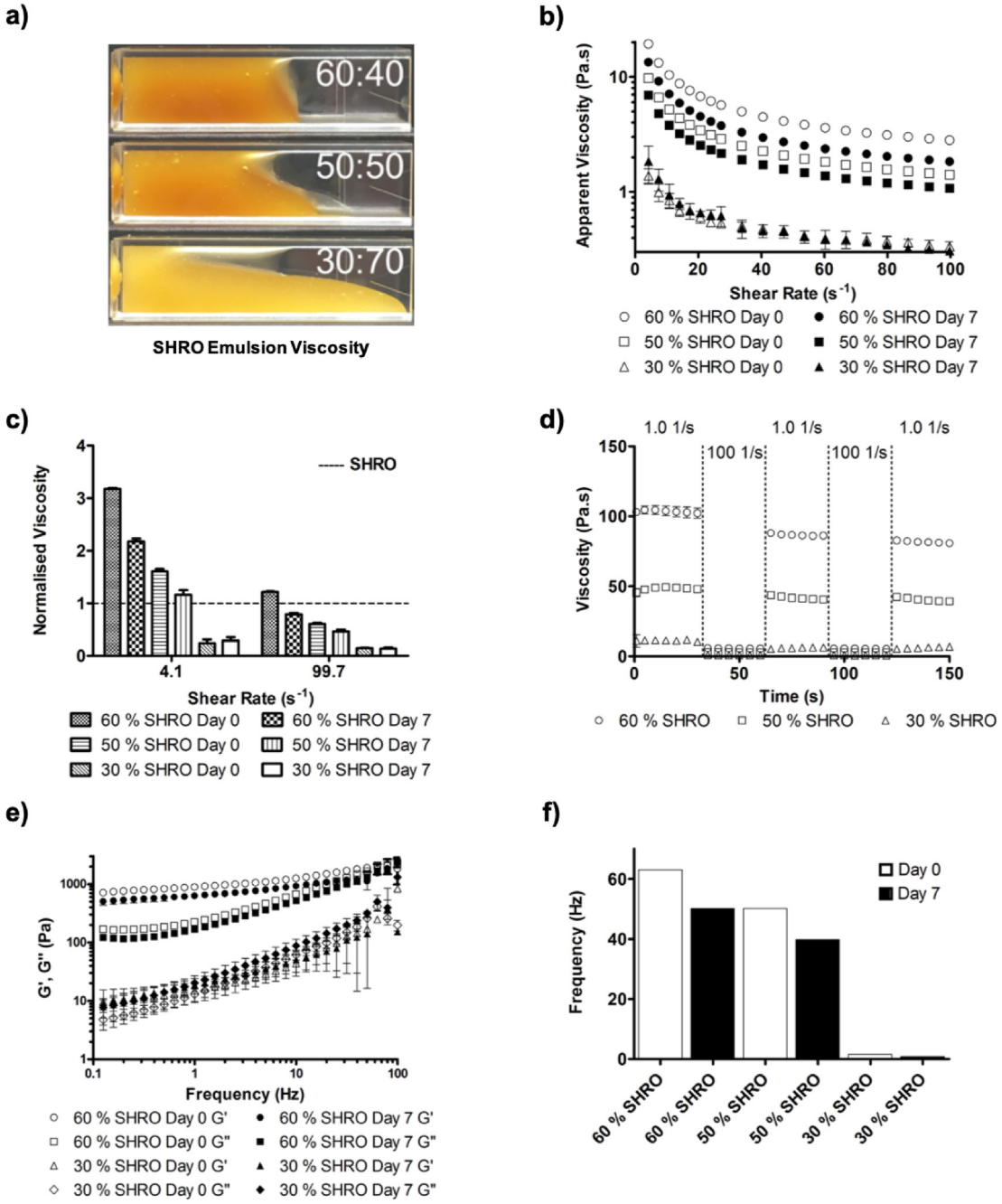

Fig. 3. Visualisation of 60, 50 and 30% SHRO emulsion formulations (a), rheological characterisation of 60, 50 and 30% SHRO emulsions immediately after formulation (day 0) and after 7 days of storage at room temperature highlighting apparent viscosity (b), the viscosity of 60, 50 and 30% SHRO emulsions normalised against SHRO at low (4.1 s^{-1}) and high (99.7 s^{-1}) shear (c), shear thinning behaviour of 60, 50 and 30% SHRO emulsions at shear rates of 1.0 s^{-1} and 100 s^{-1} conducted at 21 °C (d), frequency sweep of 60 and 30% SHRO emulsions conducted at 0.5% strain at 21 °C (e) and the frequency at which G″ is greater than that of G′ for 60, 50 and 30% SHRO emulsions, conducted at 0.5% strain at 21 °C (f). n = 3 and error bars represent standard deviation.

3.3. SHRO emulsion characterisation

The size of the dispersed SHRO droplets was investigated after manufacture (day 0) and following 7 days of storage. The median diameter (D_{50}) of the droplets at day 0 for 30, 50 and 60% SHRO emulsions were found to be 4.92 ± 0.44 μm, 2.09 ± 0.07 μm and 2.07 ± 0.02 μm, respectively. For all samples there was no significant difference found in D_{50} droplet size between day 0 and day 7 (Table 1).

In order to assess the inversion of the emulsion under application of water and shear, conductivity measurements were taken. Neat paraffin oil has no measurable conductivity (0 μS) as such when it is the continuous phase the emulsions, regardless to SHRO concentration, exhibit no conductivity. Following addition of deionised water and applied shear, conductivity measurements showed readings of 219.7 ± 6.7 μS, 204.7 ± 6.7 μS and 181.3 ± 8.4 μS for 60, 50 and 30% SHRO emulsions respectively, indicating CPI (Fig. 4a).

The ability to maintain antimicrobial efficacy of SHRO once formulated into an emulsion is paramount. Therefore, it was important to assess the levels of hydrogen peroxide production following phase inversion of the SHRO emulsions. It was found that the emulsion with the highest ratio of SHRO produced the most hydrogen peroxide; 60% SHRO emulsions produced 595.1 ± 22.1 μM/mL after 24 h and the 50

Table 1
Droplet sizes in 60, 50 and 30% SHRO emulsions at days 0 and 7. A two tailed *t*-test was conducted between D_{50} measurements for day 0 and day 7 in order to assess significance ($p < 0.05$). n = 3, ± standard deviation.

Emulsion	Size (μm)			
	D_{10}	D_{50}	D_{90}	Sig. diff. $p < 0.05$ (Y/N)*
30% SHRO				
Day 0	1.70 ± 0.39	4.92 ± 0.44	11.77 ± 1.48	N
Day 7	1.48 ± 0.21	4.11 ± 0.31	9.88 ± 0.64	
50% SHRO				
Day 0	1.22 ± 0.08	2.09 ± 0.07	3.61 ± 0.09	N
Day 7	1.23 ± 0.03	2.09 ± 0.02	3.48 ± 0.01	
60% SHRO				
Day 0	1.18 ± 0.12	2.07 ± 0.02	41.89 ± 54.4	N
Day 7	1.12 ± 0.09	2.42 ± 0.26	72.13 ± 5.93	

*N = no and Y = yes.

and 30% formulations releasing less at 249.9 ± 3.9 μM and 83.5 ± 3.0 μM respectively (Fig. 4b).

3.4. Antimicrobial efficacy

Unprocessed SHRO controls showed that the bioengineered honey had the potential to be efficacious against *S. aureus*, *P. aeruginosa* and *E. coli* (Fig. 5a). Emulsions with 60, 50 and 30% SHRO were then tested against the same bacterial strains with efficacy compared to neat SHRO diluted in water to the same concentration as would be found within each emulsion. All formulations were shown to inhibit the growth of the Gram-positive bacteria, *S. aureus* (Fig. 5b). However, only 60 and 50% SHRO emulsions produced enough ROS to inhibit the growth of Gram-negative bacteria *P. aeruginosa* and *E. coli* (Fig. 5c and d). No significant difference was identified between the efficacy of the emulsions and their equivalent, neat, SHRO dilution when tested against *S. aureus*. These results were replicated in both Gram-negative bacteria with the exception of the 30% SHRO emulsions which did not inhibit bacterial growth (Fig. 5).

4. Discussion

SHRO is engineered to deliver tailored doses of ROS and does not rely on specific flora or environmental conditions for its antibiotic activity like natural honeys, such as Manuka. Since it is engineered, this means that the level of potency can be controlled. Previous studies looking at the efficacy of SHRO have had promising results, but despite this, there are limitations associated with delivering it to wound sites [13–17,27]. Currently much like commercial honey, it is a concentrated polymer blend which is sticky, viscous and hard to handle. These characteristics make it difficult to apply. This study has demonstrated a method by which to deliver SHRO that enables stable storage whilst maintaining the ability to inhibit bacterial growth when ROS production is trigged. This is achieved by the formulation of emulsions, which undergo CPI when exposed to water and shear.

By creating a SHRO-in-oil emulsion it allows modification of the viscosity, a critical characteristic that may determine how a product may be delivered. In addition, by creating an emulsion devoid of free water there is no premature production of ROS. This is essential for efficacy and shelf life. One of the main challenges when developing an emulsion is addressing the inherent thermodynamic instability of the system. Investigation of SHRO stability within different oil phases showed that paraffin oil produced an emulsion that did not coalesce or show signs of flocculation or creaming. Furthermore, the dispersed SHRO was found to sediment at a slower rate than emulsions formulated with olive, corn or vegetable oil (Fig. 2a). In the cases of the emulsions containing vegetable, olive or corn oil the resultant instability was not reversible by means of inversion and shaking as phase separation had occurred. Although sedimentation is not ideal for this application, since it did not occur immediately and the dispersed droplets could be redistributed easily in paraffin oil, further investigation was deemed necessary. Notably, the need for redistribution of dispersed phases before application is common practice among formulations that contain unstable components. Shaking ensures an even distribution in droplets and therefore administration of a uniform dose, a factor highlighted for its importance by Stringer and Bryant in the formation of corticosteroid emulsions [28]. Promisingly, a comparison of droplet size between days 0 and 7 demonstrated that no coalescence occurred for any of the SHRO paraffin oil emulsions studied (Table 1).

Optimising dispersed phase ratios (30–60%) with a set concentration of PGPR (2%), found that formulations with a higher concentration of SHRO sedimented the least (Fig. 2b). Further, no significant difference in droplet size for the 60% SHRO emulsion was observed over 7 days of storage. This effect is likely due to two factors. Firstly, the droplets formed in the 50 and 60% emulsions are small (around 2 μm) and suffer less from sedimentation compared to the 5 μm droplets of the 30% emulsion, thus reducing sedimentation at higher phase volumes [29]. The second factor is that as more SHRO is added the volume

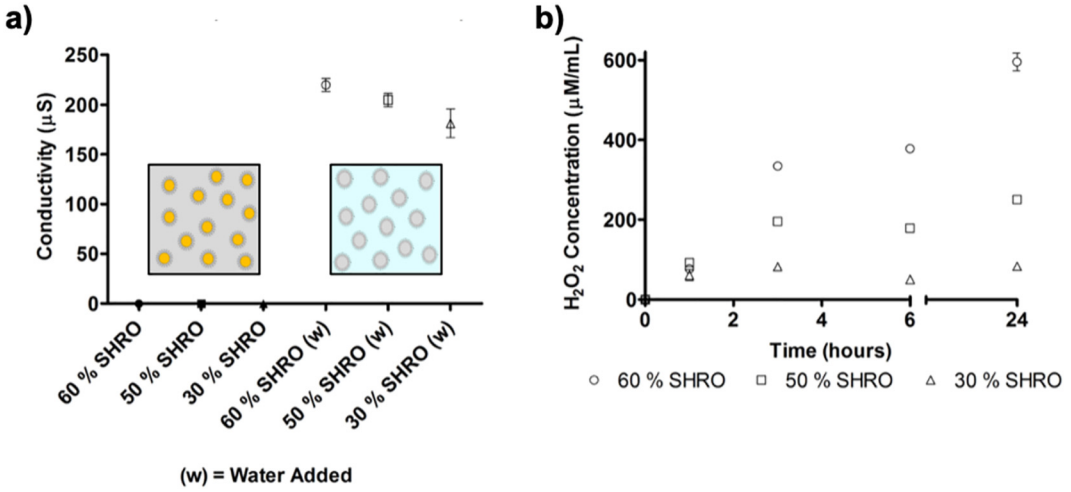

Fig. 4. Conductivity of SHRO emulsions before and after phase inversion (a) and the release of hydrogen peroxide over time (b). n = 3 and error bars represent standard deviation.

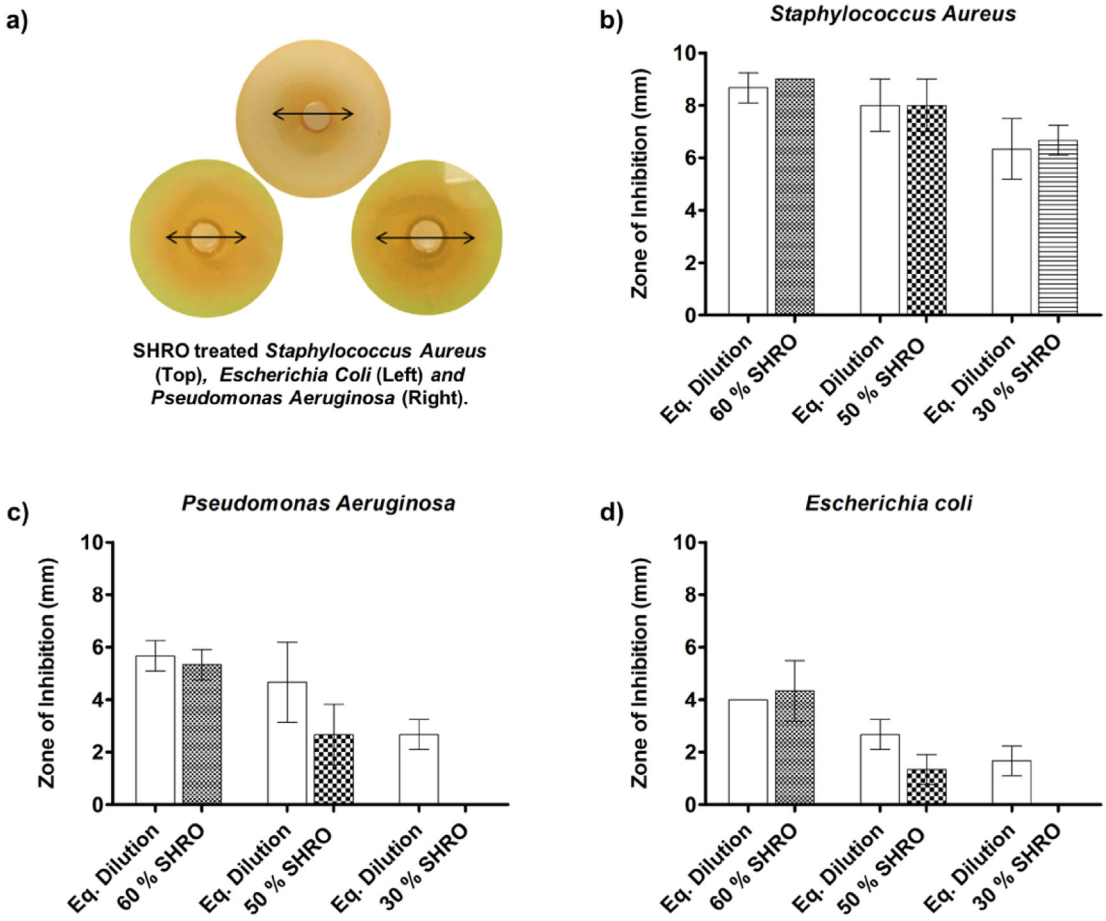

Fig. 5. SHRO treated *Staphylococcus aureus*, *Escherichia coli* and *Pseudomonas aeruginosa* (a), inverted SHRO emulsions and the zones of inhibition by treating *Staphylococcus aureus* (b), *Escherichia coli* (c) and *Pseudomonas aeruginosa* (d). Agar plates were inoculated with bacterial culture (OD_{600} 0.04) at 37 °C for 24 h before treatment. Bore hole size = 10 mm.

occupied by droplets in the system also increases. This higher packing fraction physically prevents sedimentation and results in an increase in viscosity (Fig. 3), which is known to reduce sedimentation speed [30,31]. Notably, both 50 and 60% SHRO emulsions showed no sedimentation over a period of 7 days. The low HLB value (1.5) associated with PGPR clearly aids the stabilisation of the SHRO in oil system greatly. It was determined that 2% was the minimum concentration of PGPR required to stabilise these systems (Fig. 2c).

Promisingly, all of the paraffin oil emulsions displayed shear thinning behaviour (Fig. 3b). This will help to ease delivery, as common methods of administration, such as sprays and creams, often involve the application of shear. After storage for 7 days there was a significant ($p < 0.05$) reduction in viscosity at all tested shear rates for 60 and 50% SHRO, interestingly a phenomenon not apparent in the 30% formulations. The difference between the apparent viscosity of 60 and 50% SHRO emulsions on days 0 and 7 is likely due to an interaction between SHRO droplets, which requires greater shear than that exerted from shaking to mix the emulsion back to its original form [29,30]. This was not the case with the 30% SHRO emulsion; with greater range of movement, due to the lower packing fraction and lower interactions between droplets, viscosities comparable with that of day 0 could be achieved. As demonstrated by the results here and as described by Stokes law, an increase in viscosity slows the rate of sedimentation [30,32,33]. Future applications could use modifiers to increase the viscosity thus avoiding the need to shake before use. This may however prevent the use of delivery systems only suitable for lower viscosity fluids, for example pump spray bottles. This data highlights a trade-off between stability and ease of application; while the 30% emulsion exhibits 29.6 ± 8.6% sedimentation after 7 days it has the lowest viscosity widening the possible administration devices that could be used. That said, it is notable that under high shear all SHRO emulsions exhibited significantly reduced viscosities (Fig. 3c), which will aid delivery and application. Further, it is advantageous that when all formulations were rapidly switched from high to low shear, in the absence of water, viscosity is quickly recovered (Fig. 3d). This means that the viscosity can be reduced in order to deliver the emulsion but then as the shear rate reduces the emulsion quickly becomes more viscous meaning it is more likely to be retained at the site of delivery [34,35]. The SHRO emulsions did display hysteresis, however, since this effect was minimal it is not deemed to affect the final application but warrants further investigation.

Frequency sweeps were also conducted to elucidate the viscoelastic properties and stability of the emulsions. Oscillatory rheology was used to determine the value of the storage (G′) and loss modulus (G″) at low frequency values. This was concluded to be an important assessment of emulsion stability by Tadros [31]. The viscosity profile of the emulsions revealed that both G′ and G″ rapidly increase with frequency (Fig. 3e), with the dependence on frequency considered to be due to the effect of energy dissipation within droplets [36]. The relative values of G′ and G″ are known to be indicative of a change in fluid structure [37]. At 5 Hz, 60 and 50% SHRO emulsions exhibited a higher G′ than G″, which demonstrates they have a greater gel like structure. In contrast, 30% SHRO formulations were observed to have similar G′ and G″ values (28.9 ± 8.7–54.0 ± 17.1 Pa) at this frequency. This correlates with observations that the stability is increased in emulsion formulations with higher concentrations of SHRO as droplets begin to structure and

cause an increase in viscosity [38]. At higher frequencies the emulsions undergo a viscoelastic transition, this is where G″ exceeds that of G′ [39]. This occurred for all samples tested indicating that the droplets within the emulsion interact at a small length scale and as such does not relax quickly. This decreases the elastic behaviour and thus becomes more viscous, or liquid-like [40]. The frequency at which the G′ and G″ crossover increased with rising SHRO concentration. This means that the ease of delivery decreases with increased amount of SHRO as more energy is required to extrude the emulsion from the delivery device.

In addition to easing the delivery of SHRO, this work aimed to create an emulsion that could be triggered to release ROS *in-situ*. Through the addition of water under shear it was possible to cause the developed emulsions to catastrophically phase invert (CPI) leading to activation of SHRO. It is proposed that water may either be co-delivered with the emulsion or media at the wound site could be used in order to trigger release. However, since available moisture will significantly vary at different wound sites it is suggested that co-delivery may be a more reproducible approach [41,42]. In order to confirm that CPI had occurred, conductivity measurements were taken (Fig. 4a). Neat paraffin oil has no measurable conductivity. When SHRO is dissolved in deionised water a current is allowed to flow due to the greater mobility of free ions [39]. Water was added to the emulsion and shear was applied, an increase in conductivity was measured (181.3 ± 14.6–219.7 ± 6.7 μS) with formulations containing higher concentrations of SHRO allowing a greater current to flow. These measurements confirmed that CPI had occurred and that the continuous phase is a combination of SHRO and water.

It is known that the release of ROS, such as hydrogen peroxide is the dominant factor to the antimicrobial efficacy of SHRO [27]. As such, it was critical that SHRO droplets within the emulsion could still be activated to produce ROS after being exposed to water through phase inversion. As expected, it was found that the emulsion with the highest ratio of SHRO (60%) produced the most hydrogen peroxide; 595.0 ± 22.1 μM after 24 h. A controlled and predictable release is critical to ensuring an effective and safe dose is delivered throughout the period of application [43]. Promisingly, release of ROS was observed for the entire time period tested (Fig. 4b). For a topical application, stable release over 24 h would mean that the treatment would only have to be applied at most once daily and therefore makes it more convenient for the patient or healthcare professional applying the product.

Having assessed the viability of ROS production from the formulated SHRO emulsions, clinically relevant bacterial species found in topical wounds [44] were inoculated onto agar plates and the SHRO emulsions ability to inhibit growth was measured. Unprocessed SHRO controls showed that the bioengineered honey had the potential to be efficacious against *S. aureus*, *P. aeruginosa* and *E. coli* (Fig. 5a). This is consistent with previous *in-vitro* evaluations of SHRO [13–16,27,45,46]. Despite releasing different levels of ROS over 24 h, inhibition of Gram-positive bacteria *S. aureus* was achieved for all tested inverted emulsions (Fig. 5b). In contrast, inhibition of *P. aeruginosa* and *E. coli* was only observed for emulsions containing 50 or 60% SHRO. It is known that Gram-negative bacteria are inherently harder to kill as compared with Gram-positive species they contain an extra layer of protection in the form of an outer membrane. Previous studies have demonstrated that higher doses of ROS are necessary to inhibit Gram-negative bacterial growth [47]. The ability to increase the baseline efficacy of SHRO, as reported by Dryden et al., [13] may provide a solution. Working with a batch of SHRO with higher ROS production would enable the lower viscosity characteristics of 30% SHRO emulsions to be exploited to ease application while delivering a dose also capable of killing Gram-negative bacteria.

5. Conclusion

In conclusion this study addresses the need for alternative topical infection treatments to current antibiotics. This is achieved by the successful formulation of an emulsion containing SurgihoneyRO™ (SHRO), which has been engineered to enable triggered release of antimicrobial reactive oxygen species *via* phase inversion. The hypothesis that an oil-based emulsion would protect, store, and release SHRO under shear and dilution with water at the time of application has been demonstrated *in-vitro*. This mechanism could be initiated by added or topical moisture, such as wound exudate and shear produced by hand or a delivery device.

Emulsion composition was optimised to achieve the desired shear thinning behaviour, easing delivery and promoting retention of the active at the site of infection. Stability observations revealed that a small degree of sedimentation did occur, over 7 days, for emulsions containing a dispersed phase of < 50% SHRO, but this was shown to be reversible by shaking. Conveniently this redistributed droplets evenly, which is known to improve dose reproducibility. Hydrogen peroxide measurements indicated that formulations with higher concentrations of SHRO produced greater levels of reactive oxygen species. Emulsions with 30, 50, and 60% SHRO were tested against clinically relevant bacterial species; *Staphylococcus aureus*, *Pseudomonas aeruginosa* and *Escherichia coli*. It was found that 60 and 50% SHRO emulsions were efficacious against all species. In summary, it is demonstrated that emulsion technologies can be used to effectively store and deliver water sensitive products, with triggered release mechanisms to actively combat clinically relevant infections.

Declaration of Competing of Interest

The authors declare no conflict of interest.

Acknowledgements

This research was supported by the EPSRC (Project number 1823302 — novel antimicrobial delivery systems) and undertaken in collaboration with Matoke Holdings Ltd.

References

[1] J. O'Neil, Review on Antimicrobial Resistance. Antimicrobial Resistance: Tackling a Crisis for the Health and Wealth of Nations, (2014), pp. 1–20.
[2] J. O'Neill, Tackling Drug-Resistant Infections Globally: Final Report and Recommendations the Review on Antimicrobial Resistance, (2016), https://doi.org/10.1016/j.jpha.2015.11.005.
[3] A.H. Holmes, L.S.P. Moore, A. Sundsfjord, M. Steinbakk, S. Regmi, A. Karkey, P.J. Guerin, L.J.V. Piddock, Understanding the mechanisms and drivers of antimicrobial resistance, Lancet 387 (2016) 176–187, https://doi.org/10.1016/S0140-6736(15)00473-0.
[4] M.B. Dreifke, A.A. Jayasuriya, A.C. Jayasuriya, Current wound healing procedures and potential care, Mater. Sci. Eng. C 48 (2015) 651–662, https://doi.org/10.1016/j.msec.2014.12.068.
[5] World Health Organization, Global Action Plan on Antimicrobial Resistance, WHO Press, 978 92 4 150976 3, 2015, pp. 1–28.
[6] M. Lu, E.N. Hansen, Hydrogen peroxide wound irrigation in orthopaedic surgery, J. Bone Joint Infect. 2 (2017) 3–9, https://doi.org/10.7150/jbji.16690.
[7] T.A. Wilgus, V.K. Bergdall, L.A. Dipietro, T.M. Oberyszyn, Hydrogen peroxide disrupts scarless fetal wound repair, Wound Repair Regen. 13 (2005) 513–519, https://doi.org/10.1111/j.1067-1927.2005.00072.x.
[8] E.A. O'Toole, M. Goel, D.T. Woodley, Hydrogen peroxide inhibits human keratinocyte migration, Dermatol. Surg. 22 (1996) 525–529 https://journals.lww.com/dermatologicsurgery/Fulltext/1996/06000/Hydrogen_Peroxide_Inhibits_Human_Keratinocyte.4.aspx.
[9] G. Zhu, Q. Wang, S. Lu, Y. Niu, Hydrogen peroxide: a potential wound therapeutic target, Med. Princ. Pract. 26 (2017) 301–308, https://doi.org/10.1159/000475501.
[10] M.D. Mandal, S. Mandal, Honey: its medicinal property and antibacterial activity, Asian Pac. J. Trop. Biomed. 1 (2011) 154–160, https://doi.org/10.1016/S2221-1691(11)60016-6.
[11] P.H.S. Kwakman, A.A. Te Velde, L. de Boer, C.M.J.E. Vandenbroucke-Grauls, S.A.J. Zaat, Two major medicinal honeys have different mechanisms of bactericidal activity, PLoS One 6 (2011) e17709, https://doi.org/10.1371/journal.pone.0017709.
[12] J.W. White, L.W. Doner, Honey composition and properties, Beekeeping in the United States, Sci. Educ. Adm. East. Reg. Res. Center, Philadelphia, Pennsylvania, 1980, pp. 82–92.
[13] M. Dryden, G. Lockyer, K. Saeed, J. Cooke, Engineered honey: in vitro antimicrobial

activity of a novel topical wound care treatment, J. Glob. Antimicrob. Resist. 2 (2014) 168–172, https://doi.org/10.1016/j.jgar.2014.03.006.
[14] M. Dryden, Reactive oxygen therapy: a novel antimicrobial, Int. J. Antimicrob. Agents (2017), https://doi.org/10.1016/j.ijantimicag.2017.08.029.
[15] M. Dryden, J. Cooke, R.J. Salib, R. Holding, S. Pender, J. Brooks, Hot topics in reactive oxygen therapy, J. Glob. Antimicrob. Resist. 8 (2017) 194–198, https://doi.org/10.1016/j.jgar.2016.12.012.
[16] F.D. Halstead, M.A. Webber, M. Rauf, R. Burt, M. Dryden, B.A. Oppenheim, In vitro activity of an engineered honey, medical-grade honeys, and antimicrobial wound dressings against biofilm-producing clinical bacterial isolates, J. Wound Care 25 (2016).
[17] M. Dryden, A. Dickinson, J. Brooks, L. Hudgell, K. Saeed, K.F. Cutting, A multi-centre clinical evaluation of reactive oxygen topical wound gel in 114 wounds, J. Wound Care 25 (2016) 140–146, https://doi.org/10.12968/jowc.2016.25.3.140.
[18] W. Guo, X. Zhu, Y. Liu, H. Zhuang, Sugar and water contents of honey with dielectric property sensing, J. Food Eng. 97 (2010) 275–281, https://doi.org/10.1016/j.jfoodeng.2009.10.024.
[19] D.J. McClements, Critical review of techniques and methodologies for characterization of emulsion stability, Crit. Rev. Food Sci. Nutr. 47 (2007) 611–649, https://doi.org/10.1080/10408390701289292.
[20] D. McClements, Food Emulsions: Principles, Practices, and Techniques, Third ed., CRC Press, 2015.
[21] P. Posocco, A. Perazzo, V. Preziosi, E. Laurini, S. Pricl, S. Guido, Advances interfacial tension of oil/water emulsions with mixed non-ionic surfactants: comparison between experiments and molecular simulations, RSC Adv. 6 (2016) 4723–4729, https://doi.org/10.1039/C5RA24262B.
[22] S. Sajjadi, F. Jahanzad, M. Yianneskis, Catastrophic phase inversion of abnormal emulsions in the vicinity of the locus of transitional inversion, Colloids Surf. A Physicochem. Eng. Asp. 240 (2004) 149–155, https://doi.org/10.1016/j.colsurfa.2004.03.012.
[23] A. Perazzo, V. Preziosi, S. Guido, Phase inversion emulsification: current understanding and applications, Adv. Colloid Interf. Sci. 222 (2015) 581–599, https://doi.org/10.1016/j.cis.2015.01.001.
[24] V. Preziosi, A. Perazzo, S. Caserta, G. Tomaiuolo, S. Guido, Phase inversion emulsification, Chem. Eng. Trans. 32 (2013) 1585–1590.
[25] H. Ji, H.M. Lim, Y.W. Chang, H. Lee, Comparison of the viscosity of ceramic slurries using a rotational rheometer and a vibrational viscometer, J. Korean Ceram. Soc. 49 (2012) 542–548, https://doi.org/10.4191/kcers.2012.49.6.542.
[26] M.A. Hubbe, P. Tayeb, M. Joyce, P. Tyagi, M. Kehoe, K. Dimic-Misic, L. Pal, Rheology of nanocellulose-rich aqueous suspensions: a review, Bioresour. 12 (4) (2017), http://ojs.cnr.ncsu.edu/index.php/BioRes/article/view/BioRes_12_4_9556_Hubbe_Rheology_Nanocellulose_Aqueous_Suspension.
[27] M.S. Dryden, J. Cooke, R.J. Salib, R.E. Holding, T. Biggs, A.A. Salamat, R.N. Allan, R.S. Newby, F. Halstead, B. Oppenheim, T. Hall, S.C. Cox, L.M. Grover, Z. Al-hindi, L. Novak-Frazer, M.D. Richardson, Reactive oxygen: a novel antimicrobial mechanism for targeting biofilm-associated infection, J. Glob. Antimicrob. Resist. 8 (2017) 186–191, https://doi.org/10.1016/j.jgar.2016.12.006.
[28] W. Stringer, R. Bryant, Dose uniformity of topical corticosteroid preparations: difluprednate ophthalmic emulsion 0.05% versus branded and generic prednisolone acetate ophthalmic suspension 1%, J. Clin. Ophthalmol. 4 (2010) 1119–1124, https://doi.org/10.2147/OPTH.S12441.
[29] B.P. Binks, S.O. Lumsdon, Pickering emulsions stabilized by monodisperse latex particles: effects of particle size, Langmuir 17 (2001) 4540–4547, https://doi.org/10.1021/la0103822.
[30] B.P. Binks, S.O. Lumsdon, Catastrophic phase inversion of water-in-oil emulsions stabilized by hydrophobic silica, Langmuir 16 (2000) 2539–2547, https://doi.org/10.1021/la991081j.
[31] T. Tadros, Application of rheology for assessment and prediction of the long-term physical stability of emulsions, Adv. Colloid Interf. Sci. 109 (2004) 227–258, https://doi.org/10.1016/j.cis.2003.10.025.
[32] C.D. Robinson, Some factors influencing sedimentation, Ind. Eng. Chem. 18 (1926) 869–871, https://doi.org/10.1021/ie50200a036.
[33] G.J. Kynch, A theory of sedimentation, Trans. Faraday Soc. 48 (1952) 166–176, https://doi.org/10.1039/TF9524800166.
[34] H.A. Barnes, Thixotropy—a review, J. Non-Newton. Fluid Mech. 70 (1997) 1–33, https://doi.org/10.1016/S0377-0257(97)00004-9.
[35] J. Mewis, N.J. Wagner, Thixotropy, Adv. Colloid Interf. Sci. 147–148 (2009) 214–227, https://doi.org/10.1016/j.cis.2008.09.005.
[36] Y. Otsubo, R.K. Prud'homme, Rheology of oil-in-water emulsions, Rheol. Acta 33 (1994) 29–37, https://doi.org/10.1007/BF00453461.
[37] G. Tabilo-Munizaga, G.V. Barbosa-Cánovas, Rheology for the food industry, J. Food Eng. 67 (2005) 147–156, https://doi.org/10.1016/j.jfoodeng.2004.05.062.
[38] L.G. Torres, R. Iturbe, M.J. Snowden, B.Z. Chowdhry, S.A. Leharne, Preparation of o/w emulsions stabilized by solid particles and their characterization by oscillatory rheology, Colloids Surf. A Physicochem. Eng. Asp. 302 (2007) 439–448, https://doi.org/10.1016/j.colsurfa.2007.03.009.
[39] C. Acquarone, P. Buera, B. Elizalde, Pattern of pH and electrical conductivity upon honey dilution as a complementary tool for discriminating geographical origin of honeys, Food Chem. 101 (2007) 695–703, https://doi.org/10.1016/j.foodchem.2006.01.058.
[40] B.C. Tatar, G. Sumnu, S. Sahin, Rheology of emulsions, Adv. Food Rheol. Its Appl. 151 (2016) 437–457, https://doi.org/10.1016/B978-0-08-100431-9.00017-6.
[41] V. Jones, J.E. Grey, K.G. Harding, Wound dressings, BMJ 332 (2006) 777 LP–780, https://doi.org/10.1136/bmj.332.7544.777.
[42] L.M. Bang, C. Buntting, P. Molan, The effect of dilution on the rate of hydrogen peroxide production in honey and its implications for wound healing, J. Altern. Complement. Med. 9 (2003) 267–273, https://doi.org/10.1089/10755530360623383.
[43] M.L. Bruschi, ed., Modification of drug release, in: Strateg. to Modify Drug Release from Pharm. Syst., Woodhead Publishing, 2015: pp. 15–28. doi:https://doi.org/10.1016/b978-0-08-100092-2.00002-3.
[44] B.A. Lipsky, C. Hoey, Topical antimicrobial therapy for treating chronic wounds, Clin. Infect. Dis. 49 (2009) 1541–1549, https://doi.org/10.1086/644732.
[45] H. Dryden, Cooke, Engineered Honey to Manage Bacterial Bioburden and Biofilm in Chronic Wounds, (n.d.).
[46] F. Halstead, B. Oppenheim, M. Dryden, The in vitro antibacterial activity of engineered honey (Surgihoney™) against important biofilm-forming burn wound pathogens, Fed. Infect. Soc. Conf. Poster Present. 22 (2014) 19606.
[47] M.A. Fischbach, C.T. Walsh, Antibiotics for emerging pathogens Michael, Science 325 (2009) 1089–1093, https://doi.org/10.1126/science.1176667.Antibiotics.